INTERNATIONAL DOCTORAL
SCHOOL OF THE USC

Iria
Rujido Santos

PhD Thesis

Assessment of metal nanoparticles and total metal content in textile products and cosmetics

Santiago de Compostela, 2022

Doctoral Programme in Chemical Science and Technology

TESE DE DOUTORAMENTO

ASSESSMENT OF METAL NANOPARTICLES AND TOTAL METAL CONTENT IN TEXTILE PRODUCTS AND COSMETICS

Iria Rujido Santos

ESCOLA DE DOUTORAMENTO INTERNACIONAL DA UNIVERSIDADE DE SANTIAGO DE COMPOSTELA
PROGRAMA DE DOUTORAMENTO EN CIENCIA E TECNOLOXÍA QUÍMICA

SANTIAGO DE COMPOSTELA
2022

DECLARACIÓN DO AUTOR/A DA TESE

Dna. **Iria Rujido Santos**

Título da tesis: **Assessment of metal nanoparticles and total metal content in textile products and cosmetics**

Presento a miña tese, seguindo o procedemento axeitado ao Regulamento, e declaro que:

1) A tese abarca os resultados da elaboración do meu traballo.
2) De ser o caso, na tese faise referencia ás colaboracións que tivo este traballo.
3) Confirmo que a tese non incorre en ningún tipo de plaxio doutros autores nin de traballos presentados por min para a obtención doutros títulos.
4) A tese é a versión definitiva presentada para a súa defensa e coincide a versión impresa coa presentada en formato electrónico.

E comprométome a presentar o Compromiso Documental de Supervisión no caso de que o orixinal non estea na Escola.

En Santiago de Compostela, 12 de maio de 2022.

AUTORIZACIÓN DO DIRECTOR / TITOR DA TESE

Assessment of metal nanoparticles and total metal content in textile products and cosmetics

D. Antonio Moreda Piñeiro
Dª María del Carmen Barciela Alonso

INFORMAN:

Que a presente tese, correspóndese co traballo realizado por Dna. Iria Rujido Santos, baixo a miña dirección/titorización, e autorizo a súa presentación, considerando que reúne os requisitos esixidos no Regulamento de Estudos de Doutoramento da USC, e que como director desta non incorre nas causas de abstención establecidas na Lei 40/2015.

De acordo co indicado no Regulamento de Estudos de Doutoramento, declara tamén que a presente tese de doutoramento é idónea para ser defendida en base á modalidade de Monográfica con reprodución de publicacións, nos que a participación da doutoranda foi decisiva para a súa elaboración e as publicacións se axustan ao Plan de Investigación.

En Santiago de Compostela, 12 de maio de 2022

ACKNOWLEDGEMENTS

Después de cinco años se termina esta etapa me gustaría darle las gracias a todas las personas que me ha apoyado a lo largo de este camino.

A mi director de tesis, *Antonio*. Me has ayudado desde el día que fui a hablar contigo por un problema administrativo que había tenido con las prácticas del máster, y sin pensarlo me ofreciste la posibilidad de hacer las prácticas en el grupo GETEE, comenzando así mi aventura en el mundo de la investigación. El optimismo que desprendes hace que las cosas sean más fáciles cuando uno se desespera después de experimentos fallidos y muchas horas midiendo con spICP-MS. Gracias por transmitirme tus conocimientos y estar siempre disponible buscando siempre un hueco entre las mil cosas que tenías pendientes por hacer.

A mi tutora, *Maricarmen*, por supervisar mi tesis durante estos años y guiarme durante esta etapa. Gracias por tu calidad humana y por preocuparte siempre por todos mis problemas. Me gustaría también agradecerte tus consejos en esta última etapa de la tesis los cuales fueron de gran ayuda.

A mis compañeros del grupo GETEE, con los que he compartido tantas horas. Me gustaría agradecer a *Paloma* toda la ayuda que me ha ofrecido a lo largo de estos años y a *Pilar* permitirme ser parte del grupo de investigación. Gracias a *Manolo* por animarnos siempre los cafés con un toque de humor y por los apuntes de prácticas, a *Elena* por preocuparte por mi estado de ánimo, a *Raquel* por las mil fotos que nos has hecho en congresos/eventos o en el laboratorio y a *Miguel* por nuestras charlas en los "coffee breaks".

A *Juanjo* y *Ana* por todo el apoyo que me habéis dado en esta última etapa de escritura de la tesis y os deseo mucha suerte en los próximos meses/años, respectivamente. *Cristian* también te deseo suerte en esta recta final. Gracias también a mis excompañeros (*Lucía, Arlene, Blanca, Anis, Vane, Pili*...) por las experiencias vividas con vosotros.

A *Thilini* y a *Kolita* por todos los momentos que hemos disfrutado juntos. Sois unas personas maravillosas y os merecéis todo lo bueno que os pueda pasar. Os echo mucho de menos.

A *Ala*, gracias por todo. Eres una de las mejores personas que he conocido y aunque somos muy diferentes, en el fondo muuuuuuuuy en el fondo sabes que te considero un buen amigo. Echo de menos hacernos fotos en el laboratorio haciendo el tonto, ir a molestarte a tu mesa y nuestros cafés después de comer. Gracias por haber estado a mi lado en momentos complicados de mi vida y por traerme comida al laboratorio cuando estaba encerrada peleándome con mis nanopartículas y single.

A *Eva* e *Bea*, gracias por estar ahí, por todo lo vivido y lo que nos queda…

A *Vero*, gracias por nuestros audios infinitos y por nuestras comidas en el local social.

A todos los compañeros del *Departamento de Química Analítica, Nutrición y Bromatología*, y en particular a todos los miembros del *LIDSA*, a *Mari* y a *Mónica* por todas las conversaciones en el pasillo y comidas prepandemia.

A *Marta Lores* por haberme descubierto mi pasión por la Química Analítica en las clases de Química Analítica III y por haber sido una maravillosa directora de proyecto de fin de carrera.

A *Heidi* por darme la oportunidad de hacer una estancia en LGC y hacer que me sintiera como en casa desde el primer día.

A *Estela* e *Isabel* por toda la ayuda durante la estancia, tanto a nivel profesional como personal. Gracias por las cervezas, los paseos de domingo y por conseguir que no me sintiera sola en medio del caos en el que estaba sumida cuando me fui de estancia. De verdad, sin vosotras no habría sido lo mismo. Gracias también a *Pablo* por aguantarme.

A los miembros (y exmiembros) del *Inorganic Team* del LGC por los "baking days" y los momentos compartidos.

A *Brenda* por compartir conmigo tus conocimientos y ayudarme con mis experimentos.

A *Laura Sarmiento*, *Laura Vázquez*, *Marlene*, *Tamara* y *Ana* por seguir a mi lado después de haber terminado la carrera.

A todos mis familiares y amigos por acompañarme día a día en todos mis proyectos personales y profesionales.

A *Ramón* por ser mi compañero de vida. Gracias por estar a mi lado siempre, entenderme (aunque a veces es complicado) y hacerme feliz.

A mis padres por todos los valores y principios que me han inculcado desde pequeña. En especial, me gustaría darle las gracias a mi madre por haberme ayudado y apoyado siempre. Esta tesis te la dedico a ti…"Oxalá aquí, bótoche de menos mamá!".

Á miña nai

FUNDING

- Xunta de Galicia and European Social Fund (FSE): **Iria Rujido Santos´ pre-doctoral grant ED481A-2018/127**.
- Development of a Strategic Grouping in Materials-AEMAT (grant ED431E2018/08).
- Xunta de Galicia (Grupo de Referencia Competitiva, grant number ED431C2018/19).
- Ministerio de Economía, Industria y Competitividad (project INNOVANANO, reference RT2018-099222-B-100).

INDEX

INDEX

ABBREVIATIONS

ABBREVIATIONS

A

AF4: **A**symmetric **F**low **F**ield-**F**low **F**ractionation

AF4-ICP-MS: **A**symmetric **F**low **F**ield-**F**low **F**ractionation–**I**nductively **C**oupled **P**lasma **M**ass **S**pectrometry

AF4-MALS-ICP-MS: **A**symmetric **F**low **F**ield-**F**low **F**ractionation–**M**ulti **A**ngle **L**ight **S**cattering–**I**nductively **C**oupled **P**lasma **M**ass **S**pectrometry

AF4-UV-ICP-OES: **A**symmetric **F**low **F**ield-**F**low **F**ractionation–**U**ltra**V**iolet spectroscopy–**I**nductively **C**oupled **P**lasma **O**ptical **E**mission **S**pectrometry

AFM: **A**tomic **F**orce **M**icroscopy

AgClNPs: silver chloride nanoparticles

AgNPs: silver nanoparticles

Ag_2SNPs: silver sulphide nanoparticles

AuNPs: gold nanoparticles

C

CE: **C**apillary **E**lectrophoresis

CuONPs: copper oxide NPs

CVAAS: **C**old **V**apour **A**tomic **A**bsorption **S**pectrometry

D

DLLME: **D**ispersive **L**iquid-**L**iquid **M**icro**E**xtraction

DLS: **D**ynamic **L**ight **S**cattering

DOT: **D**i**O**ctyl**T**in

DRC: **D**ynamic **R**eaction **C**ell

E

EDX: **E**nergy-**D**ispersive **X**-ray spectroscopy

F

FAAS: **F**lame **A**tomic **A**bsorption **S**pectrometry

FFF: **F**ield-**F**low **F**ractionation

G

GFAAS: **G**raphite **F**urnace **A**tomic **A**bsorption **S**pectrometry

H

HDC: **H**ydro**D**ynamic **C**hromatography

HG-ICP-MS: **H**ydride **G**eneration **I**nductively **C**oupled **P**lasma **M**ass **S**pectrometry

HRTEM: **H**igh **R**esolution **T**ransmission **E**lectron **M**icroscopy

I

ICP-MS: **I**nductively **C**oupled **P**lasma **M**ass **S**pectrometry

ICP-OES: **I**nductively **C**oupled **P**lasma **O**ptical **E**mission **S**pectrometry

ISO: **I**nternational **O**rganisation for **S**tandardisation

L

LA-ICP-MS: **L**aser **A**blation **I**nductively **C**oupled **P**lasma **M**ass **S**pectrometry

LIBS: **L**aser-**I**nduced **B**reakdown **S**pectroscopy

LOD: **L**imit **O**f **D**etection

LOQ: **L**imit **O**f **Q**uantification

LSPR: **L**ocalised **S**urface **P**lasmon **R**esonance

M

MALS: **M**ulti **A**ngle **L**ight **S**cattering

m/z: mass-to-charge ratio

N

NAA: **N**eutron **A**ctivation **A**nalysis

NMs: nanomaterials

NPs: nanoparticles

P

PDMS: **P**oly**D**i**M**ethyl**S**iloxane (dimethicone)

PET: **P**oly**E**thylene **T**erephthalate

R

ROS: **R**eactive **O**xygen **S**pecies

RP-HPLC: **R**eversed **P**hase **H**igh **P**erformance **L**iquid **C**hromatography

rpm: **r**evolutions **p**er **m**inute

RPq: **R**ejection **P**arameter **q** (adjusts the radiofrequency voltage applied to the reaction cell quadrupole)

RSD: **R**elative **S**tandard **D**eviation

S

SdFFF-ICP-MS: **Sed**imentation **F**ield-**F**low **F**ractionation–**I**nductively **C**oupled **P**lasma **M**ass **S**pectrometry

SDS: **S**odium **D**odecyl **S**ulphate

SEC: **S**ize **E**xclusion **C**hromatography

SEM: **S**canning **E**lectron **M**icroscopy

SiO_2NPs: silica nanoparticles

SPE: **S**olid-**P**hase **E**xtraction

SPF: **S**un **P**rotection **F**actor

spICP-MS: **s**ingle **p**article **I**nductively **C**oupled **P**lasma **M**ass **S**pectrometry

SS-HR-CS-GFAAS: direct **S**olid **S**ampling **H**igh **R**esolution **C**ontinuum **S**ource **G**raphite **F**urnace **A**tomic **A**bsorption **S**pectrometry

STD: **ST**an**D**ard mode (no gas in the collision/cell reaction)

STM: **S**canning **T**unnelling **M**icroscopy

T

TE: **T**ransport **E**fficiency

TEM: **T**ransmission **E**lectron **M**icroscopy

TiO_2NPs: titanium dioxide nanoparticles

TMAH: **T**etra**M**ethyl **A**mmonium **H**ydroxide

ToF-SIMS: **T**ime-**o**f-**F**light **S**econdary **I**on **M**ass **S**pectrometry

U

UPF: **U**ltraviolet **P**rotection **F**actor

UV: **U**ltra**V**iolet

X

XANES: **X**-ray **A**bsorption **N**ear **E**dge **S**tructure spectroscopy

XAS: **X**-ray **A**bsorption **S**pectroscopy

XPS: **X**-ray **P**hotoelectron **S**pectroscopy

XRD: **X**-**R**ay **D**iffraction spectroscopy

XRF: **X**-**R**ay **F**luorescence spectroscopy

Z

ZnONPs: zinc oxide nanoparticles

ABSTRACT

ABSTRACT

The first part of this doctoral thesis focuses on the determination of the total metal content in cosmetics and fabrics due to several metals cause skin lesions and allergic reactions. Furthermore, metals can penetrate through the skin, induce dermal cytotoxicity, and even reach the bloodstream and accumulate in several organs and tissues at long-term exposures. So, the presence of metals in cosmetics and fabrics is regulated by the European Regulations 1223/2009 and 1907/2006, respectively.

Metals can be found in personal care products and fabrics due to accidental contamination and/or intentional addition. In the cosmetic industry, metals are used as pigments (mainly in make-up products), inorganic ultraviolet filters, skin conditioning agents, biocides, emulsion stabilisers, humectants, and opacifiers, among others.

On the other hand, metals are added to fabrics mostly as dyestuffs (metal-complex dyes and pigments), whereas other metals like antimony can appear in fabrics as impurities because of the manufacturing process. Antimony is widely found in polyester fabrics on account of its use as a catalyst in the fabrication of polyethylene terephthalate (PET) which is the most commonly used polyester in the textile industry.

Recently, the cosmetic and textile industries have incorporated the use of inorganic nanoparticles (NPs) to obtain products with new functionalities, increasing thus the interest of consumers. According to the Nanodatabase inventory, silver nanoparticles (AgNPs), titanium dioxide nanoparticles (TiO_2NPs), and zinc oxide nanoparticles (ZnONPs) are the most used inorganic NPs in manufactured products. In addition, based on the information obtained by this inventory, the main human exposure pathway to these inorganic NPs is the dermal contact. So, the second part of this thesis project focuses on the characterisation of AgNPs, TiO_2NPs, and ZnONPs in daily used products which are in direct contact with the skin, such as moisturisers and fabrics.

These NPs have antibacterial properties, so they are added to cosmetics and textiles as biocidal agents, thus avoiding the deterioration of products as well as possible health risks derived from their use or application. In addition to antibacterial properties, AgNPs also have anti-inflammatory properties and are useful in the manufacture of cosmetic products for the treatment of skin lesions caused by diseases such as psoriasis, dermatitis, and acne.

On the other hand, TiO_2NPs and ZnONPs offered ultraviolet shielding since they are semiconductor compounds. Due to this property, TiO_2NPs, and more recently, ZnONPs are widely used in the fabrication of cosmetics and textiles with sun protection factor (SPF) due to ultraviolet radiation exposure generates sunburn, photoaging, immunosuppression, and even carcinogenesis, among other toxic effects. In the cosmetic industry, the use of inorganic sunscreens is booming because TiO_2NPs and ZnONPs do not produce allergic reactions and are photostable, unlike organic filters. However, reactive oxygen species (ROS) [$^{\bullet}O_2^-$,$^{\bullet}OH$, and H_2O_2] are formed on the surface of TiO_2NPs and ZnONPs under ultraviolet radiation. Due to ROS can induce toxicity in dermal cells, TiO_2NPs and ZnONPs used in cosmetics are commonly coated with alumina, aluminium hydroxide, and silica to decrease their photocatalytic activity. The European Regulation 1223/2009 controls the presence of NPs in cosmetic products. NPs addition to cosmetic products shall be notified to European Commission six months prior to the commercialisation of modified cosmetics. All the

ingredients in nano form must be indicated in the list of ingredients followed by the word "nano" in parenthesis. The Regulation 1223/2009 allows the use of TiO_2NPs and ZnONPs as ultraviolet filters, as long as they do not exceed the allowed maximum concentration (25% w/w) and have the physical and chemical properties established by this regulation.
Regarding the textile industry, the photocatalytic activity of TiO_2NPs and ZnONPs avoids the discolouration, yellowing, and strength reduction of fibres caused by ultraviolet radiation. These NPs allow the fabrication of self-cleaning textiles because of the organic matter degradation by the ROS generation under ultraviolet radiation. Furthermore, AgNPs, TiO_2NPs, and ZnONPs are also added to fabrics to obtain water-repellent and antistatic properties, among other applications. Nevertheless, the presence of NPs in textile products is not regulated yet. It is important to determine inorganic NPs in fabrics because they can be released during textile wearing, being a possible risk for humans. NPs can penetrate through the skin due to their small size. Several studies have shown that AgNPs penetrate beyond the *stratum corneum* (outermost layer of skin and responsible for the barrier function), reaching the deepest layers of the skin, while TiO_2NPs and ZnONPs do not. The penetration of NPs can be affected by the health condition of the skin, increasing in the case of damaged skin.
Nevertheless, standardised methodologies for the determination of NPs in manufactured products are not yet available. The development of reliable methodologies for the assessment of physical and chemical properties of NPs (e.g., size, shape, crystal structure, and coating), as well as NPs concentration (mass and number) is therefore required. The existence of nanometrological strategies is very important in the analysis of cosmetic products in order to verify compliance with the Regulation 1223/2009.
The critical step in the determination of NPs in complex matrices is the sample pre-treatment, which must guarantee the stability of these analytes. Organic solvents and surfactants were widely used as extractants of inorganic NPs from cosmetics. Furthermore, several authors used a defatting previous step with hexane. Regarding cosmetic analysis, TiO_2NPs and ZnONPs were mainly quantified in cosmetic products by hyphenation of field-flow fractionation and spectrometric techniques. Nevertheless, the main limitation of these hybrid instrumentations is the long-time consumption. Lately, the use of single particle detection mode inductively coupled plasma mass spectrometry (spICP-MS) in the routine assessment of NPs in cosmetics was proposed by several authors because of its short time of analysis, selectivity (differentiate between dissolved and nanoparticulate analyte), and the information provided (number concentration and size distribution).
In the case of textile products, the majority of available studies simulated the release of NPs from fabrics during home laundering, but detergents affect the integrity of NPs, forming new species such as silver chloride nanoparticles and silver sulphide nanoparticles. In addition, detergents that contain oxidising compounds induce the dissolution of NPs. Other investigations carried out the incubation of nanotextiles with artificial sweat or water. Analytical techniques used for the analysis of leachates from textiles were spectrometric plasma-based techniques such as ICP-MS and inductively coupled plasma optical emission spectrometry (ICP-OES).
These background studies have been considered in the development of methodologies for the assessment of inorganic NPs in moisturising creams and textile products.
This Doctoral thesis is divided into five chapters: quantification of metals in moisturising creams using microwave-assisted acid digestion and ICP-MS (chapter 1), metal content in textile and (nano)textile products (chapter 2), silver nanoparticles assessment in moisturising creams by ultrasound-assisted extraction followed by spICP-MS (chapter 3), spICP-MS assessment of ZnONPs and TiO_2NPs in moisturisers after a tip sonication sample pre-treatment (chapter 4), and spICP-MS characterisation of silver nanoparticles released from textile products (chapter 5).

PART A: DETERMINATION OF TOTAL METAL CONTENT IN MOISTURISERS AND TEXTILES

Chapter 1. Quantification of metals in moisturising creams using microwave-assisted acid digestion and ICP-MS

Moisturising creams (0.2000 g) have been digested (microwave-assisted acid digestion) using 3.0 mL of 69% nitric acid, 1.0 mL of 33% hydrogen peroxide, and 4.0 mL of ultrapure water prior to total metal content assessment by ICP-MS.

ICP-MS analysis has been found to be accurate and precise (analytical recoveries in the range of 91–110% and relative standard deviations below 5%). Furthermore, the obtained limits of quantification (LOQs) ranged from 0.00770 (beryllium) to 3.37 μg g^{-1} (aluminium).

The developed procedure was applied to fourteen moisturising creams and banned metals (European Regulation 1223/2009) such as lead, mercury, cadmium, chromium, and beryllium were quantified in several moisturisers. In addition, nickel, cobalt, and chromium (allergenic metals) were also found in some studied moisturising creams.

Chapter 2. Metal content in textile and (nano)textile products

Microwave-assisted acid digestion was used for fabric decomposition (0.2000 g) using 8.0 mL of 69% nitric acid, 0.5 mL of 33% hydrogen peroxide, 0.5 mL of 37% hydrochloric acid, and 1.0 mL of 40% hydrofluoric acid prior to ICP-MS analysis.

The accuracy of ICP-MS determination has been evaluated by recovery assays at several levels of concentration, and the obtained values varied between 90 and 107%, showing that the ICP-MS was accurate. In addition, the relative standard deviations of eleven measurements of the same diluted acid digest were within the range of 1–3% for all the analysed analytes, which proved that the quantification using this analytical technique was precise. Limits of quantification (LOQs) varied from 0.00427 (beryllium) and 6.33 μg g^{-1} (titanium). The high value of the experimental LOQ for titanium was due to the high dilution required for its analysis.

Commonly metals used in metal-complex dyes (chromium, copper, cobalt, nickel, and iron) or present in pigments (barium, zinc, titanium) were found in several studied fabrics.

Several metals used in catalyst processes during the manufacturing of textile products were also quantified in the textiles studied. As an example, iron and manganese complexes were present in some clothing products and their presence can be due to these compounds are used in the bleaching process of textile fibres and, as a consequence, they may remain in the final fabrics as an impurity. Antimony was also present at high concentrations (up to 218 μg g^{-1}) in polyester fabrics as an impurity attributed to the use of antimony compounds as a catalyst in the manufacture of polyethylene terephthalate (most common polyester used in textile products).

The high concentration of titanium in the studied textiles (156–6223 μg g^{-1}) can be due to titanium is widely used in the textile industry as a whitening colourant (Ti and TiO_2) and a delustering agent (TiO_2).

Latterly, the addition of inorganic NPs is a common practice in the textile industry to obtain fabrics with new functionalities. Zinc, titanium, or silver were quantified in nanotextiles with SPF (contained ZnONPs or TiO_2NPs) and antibacterial properties ("*nanofinishing*" with AgNPs).

PART B: DETERMINATION OF INORGANIC NPS IN MOISTURISERS AND TEXTILES

Chapter 3. Silver nanoparticles assessment in moisturising creams by ultrasound-assisted extraction followed by spICP-MS

Silver nanoparticles have been isolated from moisturisers by ultrasound-assisted extraction (15 cycles of ultrasound treatment for 59 s plus relaxing stage for 59 s applying a 60% of amplitude) using methanol (20 mL) as extractant solvent before spICP-MS determination.

AgNPs commercial standards have been subjected to the developed extraction procedure to evaluate their stability. spICP-MS results proved that AgNPs were stable during the ultrasonication process (invariable AgNPs concentrations and sizes compared with untreated standards).

The calibration used for the assessment of AgNPs sizes by spICP-MS has been carried out by ionic silver standards matched with methanol (matrix effect). In addition, the limits of detection and quantification (LOD and LOQ) obtained were 2.48×10^5 and 8.25×10^5 AgNPs g^{-1}, respectively. The calculated theoretical LOD in size was in the range of 4.5–13.0 nm.

The precision of the whole methodology (ultrasound-assisted extraction and spICP-MS analysis) has been evaluated based on the relative standard deviation (RSD) of eleven methanolic extracts from the same moisturiser. RSDs values were 5% (AgNPs concentration), 11% (AgNPs most frequent size), and 7% (AgNPs mean size), showing that the whole procedure was precise.

The spICP-MS measurements were also accurate (the analytical recoveries obtained were 117±14% for 20 nm AgNPs, 90±1% for 40 nm AgNPs, and 109±2% for 60 nm AgNPs).

Three moisturising creams prescribed for atopic dermatitis which contained silver (previous ICP-MS quantification of total silver after microwave-assisted acid digestion) were subjected to the developed methodology. spICP-MS results showed AgNPs concentrations from 1.83×10^7 to 6.46×10^9 AgNPs g^{-1}, and AgNPs mean sizes in the range of 35–91 nm. The total silver content in digested extracts assessed by ICP-MS (1.4–2352 μg g^{-1}) proved that silver extraction from studied moisturisers was quantitative. Furthermore, the content of nano-silver in these moisturisers varied between 0.24 and 1.1% of the total silver concentration.

TEM and SEM-EDX analysis also confirmed the presence of AgNPs in extracts from moisturising creams after an ultrasound water-bath oxidative procedure with hydrogen peroxide to remove organic matter.

Chapter 4. spICP-MS assessment of ZnONPs and TiO_2NPs in moisturisers after a tip sonication sample pre-treatment

The developed methodology was based on the tip sonication of moisturising creams with SPF in an organic solvent [40 mL of acetone, 40% amplitude, and 5 min using a discontinuous mode (59 s of relaxing afterwards 59 s tip sonication)] followed by spICP-MS assessment of isolated ZnONPs and TiO_2NPs.

Titanium can be quantified without being interfered by calcium (^{48}Ca isobaric interference in a standard mode, no gas) by using ammonia as a reaction gas (RPq=0.2) in instruments with dynamic reaction cell (DRC) technology. Titanium has been successfully quantified by monitoring the $^{48}Ti^{14}NH(^{14}NH_3)_4^+$ adduct (*m/z* ratio of 131) using an ammonia flow rate of 1.0 mL min^{-1}.

In addition, the quantification of zinc in a standard mode (no gas in the collision/reaction cell) can be hindered due to ^{64}Zn and ^{66}Zn isotopes are interfered by polyatomic titanium species ($^{48}Ti^{16}O^+$ and $^{50}Ti^{16}O^+$, respectively). Nevertheless, the sensitivity for zinc in DRC mode was found to be very low and there was an interference in the quantification of zinc (monitoring of

zinc adducts with *m/z* 115 and 117) generated by titanium even at low levels of the interference (5 μg L^{-1} of Ti) using the optimal ammonia conditions obtained for zinc (2.0 mL min^{-1} of ammonia, and RPq value of 0.2). Finally, a study of interferences proved that zinc quantification (monitoring of *m/z* ratio of 66) by ICP-MS can be carried out in a standard mode in samples (extracts or digested samples) containing up to 500 μg L^{-1} of titanium.

In addition, suspensions containing both TiO_2NPs (50 nm) and ZnONPs (50–80 nm) were analysed by spICP-MS to evaluate the possible interference of TiO_2NPs in the determination of ZnONPs (^{66}Zn isotope, standard mode). The analytical recovery of ZnONPs in the suspensions that contained both NPs was 99±10%, proving that there was not an interference using these operational conditions.

Regarding spICP-MS analysis, the theoretical LODs in size were in the ranges of 29–35 nm (ZnONPs) and 28–33 nm (TiO_2NPs), whereas the instrumental LODs and LOQs were 1.15×10^3 and 3.82×10^3 ZnONPs mL^{-1}, and 1.35×10^3 and 4.50×10^3 TiO_2NPs mL^{-1}, respectively.

Analytical recovery percentages of 119±3 % and 102±12% were achieved for TiO_2NPs (50 nm) and ZnONPs (50–80 nm) suspensions, respectively, which proved that the spICP-MS measurements were accurate.

The precision of the whole developed procedure was evaluated by the RSD of eleven extracts prepared using the optimal extraction conditions. RSDs values below 10% were obtained for both TiO_2NPs and ZnONPs number concentrations and sizes, demonstrating that the proposed methodology was repeatable.

The validated methodology was applied to several moisturising creams. The extraction efficiencies were in the ranges of 52–81% and 23–104% for zinc and titanium, respectively. The low extraction efficiencies obtained in two samples can be justified because they contain high content of inorganic ingredients (e.g., alumina and mica) which can hinder the extraction. Particle number concentrations were found to be in the range of 2.37×10^{11}–5.34×10^{12} ZnONPs g^{-1} and 3.32×10^{11}–1.50×10^{13} TiO_2NPs g^{-1}, and mean sizes varied within the 86–175 nm (ZnONPs) and 84–145 nm (TiO_2NPs) ranges.

The percentages of NPs in the analysed moisturisers were up to 2.0% (w/w) for TiO_2NPs [0.2–2.0%] and 2.5% (w/w) for ZnONPs [0.4–2.5%].

Finally, extracts from moisturisers were concentrated and cleaned (Amicon® Ultra-0.5 centrifugal filter devices), and analysed by HRTEM-EDX, which confirmed the presence of both ZnONPs and TiO_2NPs in samples.

Chapter 5. spICP-MS characterisation of silver nanoparticles released from textile products

spICP-MS has been selected as the analytical instrumentation technique for the determination of AgNPs released from fabrics (nanosilver textiles) because of its low limits of detection and the information provided on nanoparticle concentration and size distribution.

AgNPs have been extracted with ultrapure water (10 mL) under orbital-horizontal mechanical shaking (100 rpm, 20°C, 30 min) from textiles (0.4000 g) prior to spICP-MS analysis. After extraction, the leachates from fabrics must be filtered using 5 μm syringe filters to remove textile fluffs. The stability of AgNPs was verified under the extraction and filtration procedures.

The experimental LODs and LOQs obtained were 4.59×10^4 and 1.53×10^5 AgNPs g^{-1}, respectively, while the theoretical LOD value in size was found in the range of 9.8–11.6 nm. Analytical recovery assays using 20 nm, 40 nm, and 60 nm AgNPs standards varied between 102 and 113%, which proved the accuracy of spICP-MS determination. RSDs of the spICP-MS analysis of eleven extracts prepared under the optimised conditions were 14% (AgNPs

concentration) and 6% (AgNPs mean size), indicating that the whole method (extraction and measurement) was repeatable.

The validated methodology was applied to seven commercial textile products modified with silver additives or AgNPs. All the nanosilver fabrics leached quantifiable contents of AgNPs (2.68×10^{5}–1.91×10^{8} AgNPs g^{-1}). Furthermore, two out of four textiles modified with silver additives also released AgNPs ($2.54\times10^{6}\pm1.92\times10^{5}$ and $2.59\times10^{7}\pm3.35\times10^{6}$). The mean sizes of AgNPs in the studied fabrics ranged from 22±2 nm to 40±1 nm.

The presence of AgNPs in one extract from the fabric with the highest AgNPs number concentration was also confirmed by HRTEM-EDX analysis after its clean-up procedure using Amicon® Ultra-0.5 centrifugal filter devices.

However, the percentages of nanosilver leached in aqueous extracts calculated as the ratio between the silver mass concentration estimated from AgNPs number concentration (spICP-MS) and the total silver concentration (microwave-assisted acid digestion followed by ICP-MS) were very low, varying from 0.001 to 0.2%. On the other hand, the percentage of total silver released ranged between 0.3 and 9%, which indicated that the extraction was not quantitative (as in other previously published studies).

Finally, the fabric which exhibited the lowest extraction efficiency was subjected to several consecutive extractions using the same extraction conditions (30 min, 20°C, and 100 rpm). The number of extracted AgNPs was higher when consecutive cycles were carried out. This fact could be explained due to AgNPs are strongly integrated into the fibres and are slowly released during textile washing.

I. INTRODUCTION

I. INTRODUCTION

I.1 DETERMINATION OF TRACE ELEMENTS IN COSMETICS AND TEXTILES

Metals can be present in textiles and cosmetics due to contamination (manufacturing and storage procedures) and/or intentional addition by manufacturers. The addition of metals provides and/or enhances a specific property to manufactured products which can increase consumer interest and boost sales. Nevertheless, metals released from fabrics and cosmetics can be absorbed through the skin and even accumulate in several tissues and organs. In addition, several metals such as nickel are important skin allergens [1].

On the other hand, the release of metals from fabrics during domestic laundering may pose an environmental risk [2].

I.1.1 Total metal content in cosmetics

In Europe, metal compounds authorised in cosmetics are listed in the Annexes III, IV, V, and VI of the Regulation 1223/2009 ("list of substances which cosmetic products must not contain except subject to the restrictions laid down", "list of colourants allowed in cosmetic products", "list of preservatives allowed in cosmetic products", and "list of UV filters allowed in cosmetic products", respectively) [3].

Moreover, the Regulation 1223/2009 prohibits antimony, beryllium, arsenic, cadmium, lead, thallium, zirconium, tellurium, mercury, and their compounds in cosmetic products. Various strontium compounds (lactate, nitrate, and polycarboxylate), and several compounds of potassium, sodium, cobalt, molybdenum, and tin are also not allowed. Furthermore, the addition of barium salts, gold salts, chromium, chromic acid and its salts, nickel and several nickel compounds, divanadium pentaoxide, and indium phosphide to cosmetics is banned.

Nevertheless, according to the Article 17 of the European Regulation 1223/2009, "the non-intended presence of a small quantity of a prohibited substance, stemming from impurities of natural or synthetic ingredients, the manufacturing process, storage, migration from packaging, which is technically unavoidable in good manufacturing practice, shall be permitted". However, the maximum concentration allowed as an impurity is not indicated in this regulation.

There are some exceptions to the mentioned prohibitions. Phenylmercuric salts (as preservatives in eye products up to 0.007% of Hg), barium sulphides (in depilatories, 6% as sulphur), barium colourants listed in the Annex IV, gold (as a colourant, code E175, and purity of 90% or higher [4]), and aluminium zirconium chloride hydroxide complexes and aluminium zirconium chloride hydroxide glycine complexes (in antiperspirants and 5.4% of zirconium as maximum concentration) can be added to cosmetic items (Regulation 1223/2009).

Mineral pigments used as colouring agents are the main source of metallic elements in cosmetics, so most studies focus on the analysis of cosmetics used for make-up [5,6]. Nevertheless, research investigations about the analysis of metal elements in daily used personal care products (e.g., moisturisers and body lotions) are scant [7–12].

X-ray fluorescence (XRF) [13,14], laser-induced breakdown spectroscopy (LIBS) [15], direct solid sampling high resolution continuum source graphite furnace atomic absorption spectrometry (SS-HR-CS-GFAAS) [16–18], and neutron activation analysis (NAA) [19] have been used for direct analysis of cosmetics without sample pre-treatment steps, but the implementation of these techniques in routine analysis is hampered owing to sample heterogeneity and issues attributed to calibration procedures [6].

On the other hand, wet digestion with concentrated acids using microwave or conventional heating has been the most common sample pre-treatment of cosmetic samples. In wet digestion procedures, oxidising agents (nitric acid, sulphuric acid, and hydrogen peroxide) oxidise the organic matter and complexing acids (hydrochloric acid and hydrofluoric acid) solubilise elements associated with the insoluble inorganic fraction, such as lead, cadmium, titanium dioxide and/or silicates, among others [20,21]. The addition of complexing agents is required to achieve the complete digestion of cosmetics with high content of inorganic pigments like lipsticks, eye shadows, and sunscreens. Mixtures of HNO_3/H_2O_2 [22], H_2SO_4/H_2O_2 [23], $HNO_3/H_2O_2/HF$ [24] or $HNO_3/HCl/HF$ [25] have been used for wet digestion of cosmetics.

Dry ashing followed by solubilisation of ash (commonly under acidic conditions) is also an effective method for sample preparation of cosmetics rich in wax and oils [26].

Alkaline solubilisation using tetramethyl ammonium hydroxide (TMAH) [27] and cosmetic solubilisation by sample emulsification procedures [28] are further proposed as cosmetic pre-treatment procedures prior to elemental analysis.

Several authors also suggested the use of solid-phase extraction (SPE) [29] and dispersive liquid-liquid microextraction (DLLME) [30] after cosmetic pre-treatment (e.g., acid digestion and dry ashing) for the separation and preconcentration of analytes before their analysis.

After sample pre-treatment, atomic spectrometric techniques such as flame atomic absorption spectrometry (FAAS) [31], graphite furnace atomic absorption spectrometry (GFAAS) [24], inductively coupled plasma optical emission spectrometry (ICP-OES) [25], and inductively coupled plasma mass spectrometry (ICP-MS) [20,31] have been used for total metal quantification in various types of cosmetic samples (e.g., lipsticks, eye shadows, sunscreens). Cold vapour atomic absorption spectrometry (CVAAS) has been used for mercury determination in facial skin creams [22]. Hydride generation-ICP-MS (HG-ICP-MS) and electrothermal vaporisation-ICP-MS quantify elements such as As, Cd, Sb, Hg, and Pb in nail polish [32].

I.1.2 Total metal content in textiles

The main application of metals in the textile industry is their use as dyestuffs. Metal-complex dyes are synthetised by the coordination of several acid dyes and transition metal ions. The use of metal-complex dyes improves the wash fastness of coloured textile products. Metal is chelated in the dye structure before (premetallised dye) or during the dyeing procedure (mordant dye). Mordant dyes are produced directly on the textile fibres using three different approaches. In the pre-mordanting procedure, the fibres are firstly treated with the metal and then with the dye. The dye and the metal can also be concurrently added in the same bath (meta-mordanting process). Another possibility is the post-mordanting procedure where the metal is applied to the dyed fibres. Metals such as copper, cobalt, nickel, chromium, iron, aluminium, and tin (or their salts) are used in the synthesis of metal-complex dyes [33]. Barium chloride and barium acetate are also used as mordants in the textile industry [34].

Furthermore, fabrics can be coloured by the addition of pigments. Titanium dioxide, lithopone (mixture of barium sulphate and zinc sulphide), lead white (complex salt of lead which contains both carbonate and hydroxide ions), zinc oxide, and zinc sulphate pigments provide white colours. Coloured metallic pigments are cadmium pigments, chromium (III) pigments, lead chromate, and bismuth vanadate, among others [35].

Antimony is commonly found in polyester fibres as a contaminant due to its use as a catalyst in the manufacturing of polyethylene terephthalate (PET) which is the most common type of polyester used in fabrics [36]. In addition, antimony compounds (Sb_2O_3) enhance the flame retardant activity of halogen compounds [37]. Complexes of zirconium or titanium are

added to textile fibres to obtain flame retardant properties (Zirpro process) [38], and zinc and molybdenum compounds (zinc borate, zinc stannate, or ammonium molybdates) are effective smoke suppressant agents [39].

Textile products can also be contaminated with iron or manganese owing to their usage as catalysts in the bleaching process of textile products [40].

Recently, the presence of metals in textile fibres can be due to their modification with inorganic NPs to obtain fabrics with novel properties.

In Europe, the content of several metals in textile products is regulated by the Regulation 1907/2006 [41]. The maximum concentration of lead, cadmium, chromium (VI), and arsenic (and their compounds) in textiles is 1 $\mu g\ g^{-1}$. Furthermore, the impregnation of yarns with mercury compounds is forbidden and the content of dioctyltin (DOT) in fabrics that are in direct contact with the skin shall not exceed 1000 $\mu g\ g^{-1}$.

Few studies have been reported in the literature for the determination of total metal contents in textile samples. ICP-OES and ICP-MS are the most commonly used techniques for total element determination in acid digested textile products. Microwave-assisted acid digestion using nitric acid [42–45], or mixtures of nitric acid and hydrogen peroxide [46] have been used for the digestion of fabrics. Nevertheless, the addition of hydrofluoric acid is necessary to achieve the complete digestion of textiles that contain silicon dioxide or titanium dioxide particles [47,48].

Laser ablation inductively coupled plasma mass spectrometry (LA-ICP-MS) has been used by Gallo et al. (2009) [42] for elemental analysis of cotton fabrics. This technique allows the direct analysis of textile products without previous digestion/solution steps, reducing thus the time of analysis, costs, and exposure to hazardous chemicals.

I.2 Assessment of inorganic nanoparticles in textile products and cosmetics

I.2.1 Introduction to nanotechnology

Owing to the development of nanotechnology, it has been necessary to establish definitions for new concepts such as nanomaterial and nanoparticle. In 2011, the European Commission recommended defining a "nanomaterial" as "a natural, incidental, or manufactured material containing particles, in an unbound state or as an aggregate or as an agglomerate and where, for 50% or more of the particles in the number size distribution, one or more external dimensions is in the size range 1 nm–100 nm. In specific cases and where warranted by concerns for the environment, health, safety or competitiveness the number size distribution threshold of 50% may be replaced by a threshold between 1 and 50%" [49]. Alternative definitions of nanomaterials established by other regulatory institutions worldwide were listed by Boverhof and co-workers [50].

Furthermore, the international organisation for standardisation (ISO) defined a "nanomaterial" as a "material with any external dimension at the nanoscale or with internal structure or surface structure at the nanoscale", and "nanoparticle" as a "nano-object with all three external dimensions in the nanoscale" (nanoscale ranges from 1 to 100 nm) [50].

The physical and chemical properties of nanoparticles (NPs) are different from those provided by bulk particles, thus NPs have novel applications in various industrial sectors and manufactured products like cosmetics, paints, textiles, food products (food packaging, colourants, and additives), electronic devices, medical material (sanitary items and drugs), and so on [51]. Nowadays, nanotechnology is booming owing to its high economic impact. Despite their interesting properties, the potential risk of exposure to NPs is not clear yet due to toxicity studies are scarce. The development of reliable methods for the assessment of NPs in manufactured products is therefore needed.

I.2.2 Inorganic NPs under study

According to the Nanodatabase inventory [52], silver nanoparticles (AgNPs), titanium dioxide nanoparticles (TiO_2NPs), and zinc oxide nanoparticles (ZnONPs) are among the most widely used inorganic NPs in manufactured products (**Figure I.1a**). The number of products modified with these NPs has increased swiftly (2.8 times for AgNPs, 4.7 times for TiO_2NPs, and 2.6 times for ZnONPs during the period 2012–2021, **Figure I.1b**).

According to the Nanodatabase inventory [52], the main route of exposure to these NPs is dermal contact (**Figure I.1c**). Thus, a part of this thesis focuses on the characterisation and quantification of AgNPs, TiO_2NPs, and ZnONPs in products which are in direct and prolonged contact with the skin, such as cosmetics (moisturising creams) and textile products.

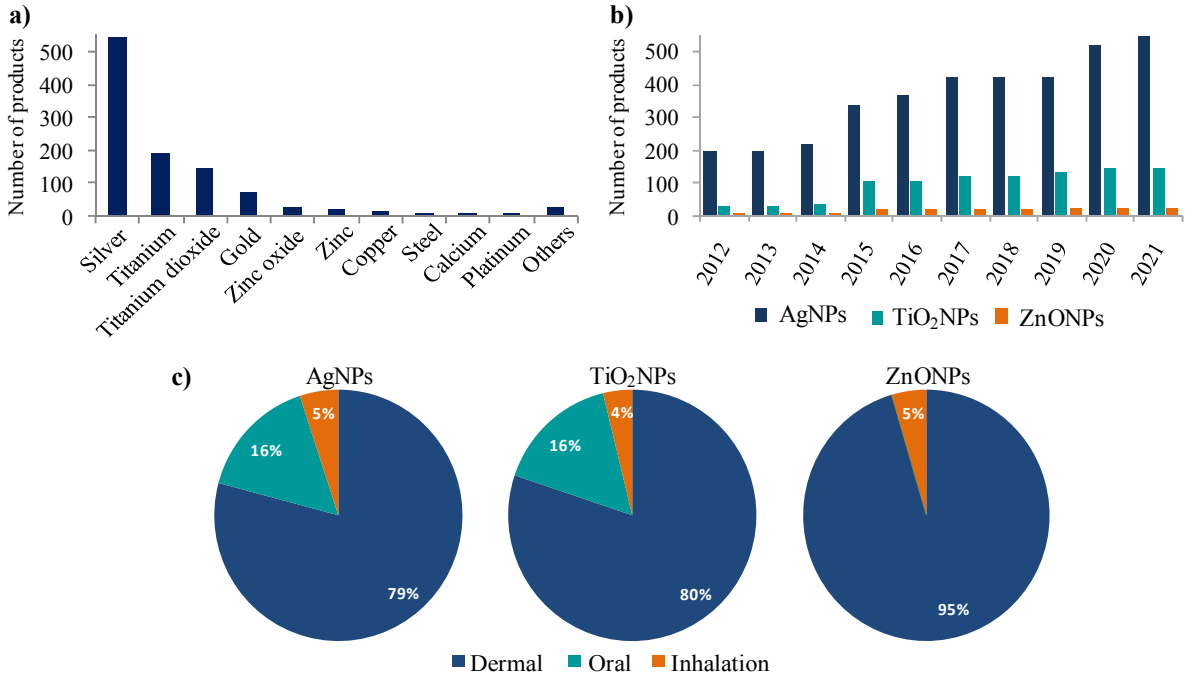

Figure I.1. Number of consumer products modified with inorganic NPs currently inventoried (a). Evolution of the number of manufactured products with AgNPs, TiO_2NPs and ZnONPs over the last years (b). Possible routes of exposure to AgNPs, TiO_2NPs, and ZnONPs (c). [52]

I.2.3 Properties and applications of analysed NPs

I.2.3.1 AgNPs

Drug resistance of several strains of bacteria has been an issue of concern in recent years [53]. A promising alternative is the use of AgNPs to treat infections owing to their antibacterial activity against both Gram-negative and Gram-positive bacteria. Several researchers have shown that Gram-positive bacteria are most resistant to AgNPs [54,55], which is probably because of their cell wall structure [56]. The physical and chemical properties of AgNPs determine their efficacy against bacteria. AgNPs with high specific surface area exhibit greater antibacterial activity [57]. Coating [58] and surface charge of AgNPs [59] also influence their antibacterial effect.

The mechanism of AgNPs antimicrobial activity is not entirely clear. Several studies proved that AgNPs can form pits on the bacterial envelope, leading to leakage of cellular components and subsequent cell death [59,60]. AgNPs can also bind to bacterial proteins and

decrease or even inhibit their activity [61,62]. As a result, AgNPs origin depletion on the activity of respiratory chain enzymes [63] and damage the bacterial cytoskeleton [64]. AgNPs can also induce damage in the bacterial DNA, and even cause its condensation [63].

Moreover, the damage to bacterial biomolecules such as membrane lipids, proteins, and DNA may be attributed to the oxidative stress caused by reactive oxygen species (ROS). Several studies have demonstrated the formation of ROS after bacterial exposure to AgNPs [62].

On the other hand, several authors proposed an antibacterial mechanism for AgNPs based on the action of Ag^+ ions released from AgNPs. Silver ions can also induce the same cytotoxic effects as those generated by AgNPs to bacteria (bacterial membrane damage, interaction with proteins and enzymes, ROS generation, and DNA alterations, among others) [65]. In conclusion, the antibacterial activity of AgNPs may originate from an ion-only mechanism, particle-only mechanism, or combined ion-particle mechanism [66].

Due to their antibacterial properties, AgNPs are widely used in several fields such as the environmental sector (water and air disinfection), the medical sector (medical devices, treatment of hospital-acquired infections, and wound healing), the textile industry, food packaging, and animal husbandry [67]. In addition to their antibacterial properties, AgNPs can be a promising agent in medicine (treatment of diseases caused by fungal or viruses, cancer therapies [68,69], and contrast agents [70,71]). AgNPs are also used in sensors [72], removal of pollutants [73], and colouring of materials (plasmonic properties) [74].

I.2.3.2 TiO_2NPs and ZnONPs

TiO_2 and ZnO are semiconductors, thus after their light irradiation (absorption of a photon with energy greater or equal to its band gap), an electron jumps from the valence band to the empty conduction band, originating an electron-hole pair. Bands gaps are 3.20 eV for anatase, 3.02 eV for rutile, 2.96 eV for brookite (polymorphs of TiO_2), and 3.37 eV for ZnO [75]. These large band gaps cause TiO_2NPs and ZnONPs are only triggered when exposed to ultraviolet (UV) light [75,76]. The generated electron-hole pairs form ROS [75,76], such as $^{\bullet}O_2^-$, $^{\bullet}OH$, and H_2O_2 from oxygen-containing species (O_2, H_2O, and OH^-, respectively) [**Figure I.2**].

The photoactivity depends on the crystal structure. Natural polymorphs of TiO_2 are anatase, rutile, and brookite, but anatase exhibits a higher photocatalytic activity [77]. Photoactivity also relies on crystalline size, specific surface area, and porous structure [78–80]. Therefore, the photoactivity of TiO_2NPs and ZnONPs is greater than their bulk materials owing to their large surface areas (there is a proportional relationship between surface area and photoactivity [79,81]). Moreover, photoactivity depends on nanoarchitecture [82,83]. Recently, TiO_2NPs and ZnONPs have been doped with metals or other compounds to reduce their band gap, extending the light absorption in the visible region and improving their photocatalytic properties [84,85].

Furthermore, TiO_2NPs and ZnONPs can be used as biocidal agents and the antibacterial activity depends on their particle size and concentration [86–88]. The antibacterial activity of TiO_2NPs is mainly caused by their photoactivity due to non-existent [89,90] or low [91,92] bacterial inhibition under dark conditions. However, ZnONPs exhibit antibacterial activity even in absence of light [93,94], though irradiated ZnONPs possess greater antimicrobial properties [94]. Antibacterial mechanisms of TiO_2NPs and ZnONPs are still not clear, as well as in the case of AgNPs. TiO_2NPs and ZnONPs attach to bacteria [93] and cause alterations of morphology and damage to the bacterial envelope, leading to internalisation of NPs and leakage of intracellular components [95,96], which provoke cell death. The main mechanism of antibacterial activity is that irradiated ZnONPs and TiO_2NPs generate ROS [97,98] which damage lipids (cellular membrane), proteins, and DNA [99,100].

Several studies have shown that the antibacterial activity of ZnONPs is attributed to Zn^{2+} ions (formed from ZnONPs dissolution) [101,102], which could explain the bacterial inhibition caused by ZnONPs under dark conditions. The dissolution of ZnONPs depends on the chemistry of the medium and the physical and chemical properties of ZnONPs like shape, particle size, porosity, and concentration [103].

TiO_2NPs and ZnONPs are used as inorganic UV filters in the cosmetic [104] and textile industries [105,106], and have applications in the electronics field, like in the fabrication of sensors [107,108], solar cells [109,110], and light emission devices [111,112]. They are promising agents for the photocatalytic degradation of pollutants [113,114] and also exhibit self-cleaning activity [115,116]. TiO_2NPs and ZnONPs can also be used in the medical field as antiviral and antifungal agents [75,117,118], and as photosensitisers and sonosensitisers (cancer treatment) [119,120]. These NPs are further useful in bioimaging and drug delivery.

On the other hand, the additive E171, which contains ≅ 10–40% of TiO_2NPs [121], is widely used in food and medicinal products as a whitening and opacifying agent. However, the commercialisation of foodstuffs containing E171 will be banned as of 07 August 2022 [122].

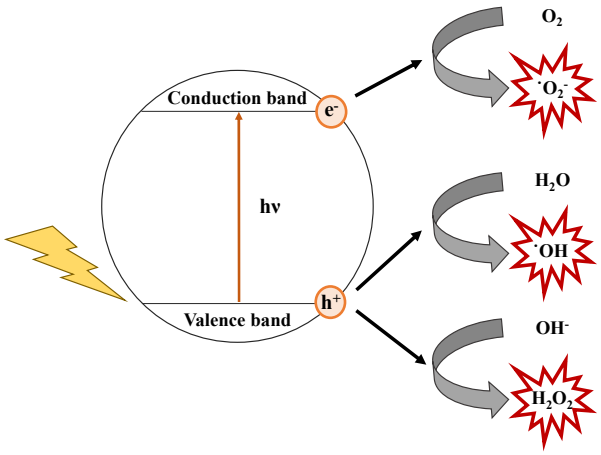

Figure I.2. ROS formation after irradiation of TiO_2NPs or ZnONPs

I.2.3.3 Applications of inorganic NPs in cosmetics

According to the Nanodatabase inventory, 54 cosmetic items with TiO_2NPs, 6 with TiO_2NPs and ZnONPs, 6 with only ZnONPs, and 11 with AgNPs are available in the European market [123].

TiO_2NPs and ZnONPs are increasingly used in the cosmetics industry because they are effective UV blockers. TiO_2NPs and ZnONPs of about 50–100 nm add to cosmetics better transparency and UV protective properties than larger particles [124]. In addition, these NPs are photostable and do not generate allergic reactions (contrary to organic UV filters) [125].

Nevertheless, TiO_2NPs and ZnONPs generate cytotoxic ROS under UV radiation. Thus, TiO_2NPs and ZnONPs used in cosmetic formulations are usually coated with alumina, aluminium hydroxide, or silica to reduce their photocatalytic activity. Furthermore, an additional external layer with stearic acid, dimethicone (polydimethylsiloxane, PDMS), or simethicone (mixture of polydimethylsiloxane and silica gel) improves the dispersion of NPs in the cosmetic formulation [126]. Coating of NPs also prevents their agglomeration and dissolution (agglomeration is more relevant for TiO_2NPs and dissolution for ZnONPs).

ZnONPs can also act as preservatives in cosmetics [127] and are useful in the manufacture of cosmeceuticals for treating cutaneous infections [128] due to their antifungal and antibacterial properties.

AgNPs also avoid microbial spoilage that can affect the quality of cosmetic products. In addition, creams and ointments with AgNPs are useful to treat psoriasis lesions [129] and acne [130,131] due to the antibacterial and anti-inflammatory activity of these NPs.

According to the European Regulation 1223/2009 [3], the commercialisation of cosmetics modified with NPs must be noticed to the Commission six months prior to their introduction into the market. The list of ingredients shall specify all ingredients that are present in the form of nanomaterials. The word 'nano' in parentheses must appear after the names of such substances. The authorised NPs shall not be used in applications that may lead to exposure by inhalation. TiO_2NPs and ZnONPs are allowed UV filters in cosmetic products as long as they have the physical and chemical characteristics indicated by the European Committee. Purity, shape, specific surface area, coating, and size of TiO_2NPs and ZnONPs are regulated criteria. In addition, the allowed crystalline structures are wurtzite (ZnONPs) and rutile or rutile with up to 5% anatase (TiO_2NPs). The solubility of ZnONPs shall not exceed 50 mg L^{-1}, and TiO_2NPs must be photostable in the final formulation. The maximum allowed concentration for both TiO_2NPs and ZnONPs in cosmetics is 25% w/w. If bulk and nano TiO_2 or ZnO are used in cosmetic formulations, the sum of compounds must not exceed the established limits.

I.2.3.4 Applications of inorganic NPs in fabrics

Scouring is an important textile pre-treatment which consists of the removal of natural impurities (e.g, wax, fat, oil, gum, and dust) before bleaching and dyeing processes. Despite the initial process of scouring, colouring matter remains in fibres, causing yellowing and browning. Thus, another step called bleaching is necessary to remove these impurities and produce whiter textiles with a minimal impact on the strength of fibres. TiO_2NPs or ZnONPs can be used in these first steps of textile manufacturing. Thus, ROS formed on the surface of TiO_2NPs or ZnONPs under light irradiation degrade impurities and organic matter. These NPs are hence effective "*nanophotoscouring*" and "*nanophotobleaching*" agents [132,133].

Textile modification with NPs during the chemical finishing step is known as "*nanofinishing*". The addition of NPs allows the manufacture of products with new properties such as water repellence, wrinkle resistance, anti-static activity, UV blocking action, bacterial inhibition, flame retardancy, and self-cleaning, among others [134,135].

Hydrophobicity is important in the case of fibres such as cotton and cellulose which are absorbent and quickly soiled by liquids owing to the abundance of hydroxyl groups on their surface [136,137]. Hydrophobic fabrics are obtained by the immobilisation of inorganic NPs to increase the surface roughness followed by a chemical modification to decrease the surface energy. The surface modification is usually performed by the addition of a silane (non-fluorinated alkyl silane or fluoro silane) or fluorochemicals. Silica nanoparticles (SiO_2NPs) [138], TiO_2NPs [139], ZnONPs [140], and AgNPs [141] can be used in the manufacture of water-repellent textiles.

Photoprotective clothing prevent the sun's dangerous rays from reaching human skin and causing health risks. Furthermore, UV radiation can origin yellowing, discolouration, and strength reduction of fibres [142]. Ultraviolet protection factor (UPF) is a parameter to evaluate the UV protection level of garments and was first established by Australian/New Zealand standard AS/NZS 4399 in 1996 [143]. Thus, fabrics can be classified according to their UPF values: 15 to 24 (good protection), 25 to 39 (very good protection), and 40 to 50 (excellent protection). As an example, an UPF of 50 indicates that only 1/50 of the UV radiation can penetrate through the textile product and reach the skin. This means that 98% of UV light is blocked when wearing a garment with UPF 50 [144].

UV-shielding cotton [145,146], wool [146,147], polyester [148], silk [149], and bamboo [150] fabrics are manufactured by the addition of TiO_2NPs and ZnONPs since they can absorb and scatter UV radiation. Both absorption and scattering processes are dependent on the size of NPs. Thus, UV absorption is greater at lower particle sizes and UV scattering at larger sizes (scattering causes white colours) [151].

On the other hand, textile products are in constant contact with the skin and hence create an excellent environment for the adhesion of skin bacteria that may be transferred from the human skin to fabrics through direct contact or sweat migration [152]. Bacteria proliferate in fabrics under appropriate conditions (high humidity and adequate temperature) and originate unpleasant odours [153]. Furthermore, natural fibres such as cotton, wool, and silk are also rapidly impaired by bacteria, originating loss of strength, discolouration, and even damage to the molecular structure of fibres. Although most synthetic textiles are resistant to biodeterioration, several chemicals used for textile processing and/or finishing are prone to microbial attack [154]. The addition of biocidal NPs to textiles prevents microbial spoilage in these manufactured products. Antibacterial fabrics are obtained by the modification of fibres with AgNPs [155], gold nanoparticles (AuNPs) [156], ZnONPs [157], TiO_2NPs [158], and copper oxide NPs (CuONPs) [159]. An important example is the addition of these biocidal NPs to hospital textiles to avoid the transmission of diseases to patients or hospital staff [160].

Another application of "*nanofinishing*" is the manufacture of self-cleaning garments by chemical modification with TiO_2NPs and ZnONPs. Under UV radiation, these NPs remove stains due to the degradation of organic matter to CO_2 and H_2O by the ROS generated [158,161].

The introduction of AgNPs [74,162] and AuNPs [163] into textile fibres allows the fabrication of colourful fabrics owing to their localised surface plasmon resonance (LSPR). The colour of modified textiles is dependent on the size and shape of NPs.

Inorganic NPs are also used for the manufacture of wrinkle-resistant fabrics. As an example, alcohol groups on adjacent cellulose chains are partially cross-linked to maintain the chains fixed, thus diminishing the potential shrink of cotton fibres [164]. NPs can be used as photocatalysts (TiO_2NPs) or cross-linking agents (AgNPs, ZnONPs, TiO_2NPs, copper/CuONPs) during the cross-linking process [165].

In addition, AgNPs [166], TiO_2NPs [158], and ZnONPs [167] impart antistatic properties to fabrics. These particles dissipate the static electricity of textile fibres due to their conductivity. Antistatic activity is very important in the specific case of synthetic fibres which have a high static charge.

Finally, metallic NPs such as SiO_2, TiO_2, ZnO, and aluminium oxide hydroxide NPs are used in flame-retardant textile finishes [168].

I.2.4 Toxicological risks of inorganic NPs

Interactions of NPs and human skin during textile wearing or cosmetic application must be considered due to their possible toxicological effect. Available studies focus on the penetration of NPs into the skin and the viability of human skin cells under exposure to NPs.

I.2.4.1 Penetration of NPs into the skin

The skin is the largest organ of the human body and represents 10% of the total body mass and is composed of three layers: epidermis, dermis, and hypodermis [169].

The epidermis is divided into *stratum corneum* and viable epidermis. The *stratum corneum* is the outermost layer of the skin, and it is responsible for the skin´s barrier function. Adequate hydration of the *stratum corneum* (water content of 20–50%) is necessary to preserve its integrity and its function as a protective barrier [170].

The viable epidermis is a non-vascular multilayer composed of *stratum lucidum*, *stratum granulosum*, *stratum spinosum*, and *stratum basale* (in contact with the dermis). These layers are established in accordance with the level of keratinisation of the cells. Thus, the keratinocytes of the inner epidermis undergo a process of keratinisation during their migration to the outer layers, which leads to differentiated and dead cells (filled mainly with keratin and keratin-protein complexes). So, the *stratum corneum* is formed of dead cells called corneocytes which are surrounded by a lipid matrix [170,171].

The dermis is mainly composed of collagen and elastin fibres. Regarding its cellular composition, fibroblasts (main cell type), mast cells, and melanocytes are present in this layer. Sweat glands, sebaceous glands, and hair follicles are originated in the dermis. Besides, the skin´s blood supply takes place in this layer.

The innermost layer of skin is the hypodermis which is formed of fat cells that are linked to the dermis through collagen and elastin fibres. The hypodermis attaches the skin to the muscles and reinforces the neuronal and vascular system of the skin [169].

Regarding the mechanism of the penetration, NPs can pass through the *stratum corneum* (defensive barrier) by two possible pathways. NPs can penetrate via transappendageal route (through hair follicles and sweat glands) or transepidermal route [intercellular lipid route (through lipid channels) or transcellular route (through corneocytes and lipids)] [169,170].

Applying a cosmetic formulation by massaging can increase the penetration of NPs through the skin due to the increase in local temperature that causes the fluidisation of the tails of intercorneocyte lipids of the *stratum corneum* [170].

In vivo, *ex vivo*, or *in vitro* approaches using human and porcine skin have been carried out to study skin penetration of NPs. Porcine skin is an adequate model to study human skin penetration due to its similar absorption rates and thickness [172].

Most of the studies have shown that AgNPs penetrate through the *stratum corneum* (defensive function) and reach deeper skin layers (viable epidermis and dermis) [173,174]. Moreover, Larese et al. (2009) [175] demonstrated that silver skin penetration was higher in damaged skin than in intact skin.

On the other hand, several studies on the percutaneous penetration of TiO_2NPs and ZnONPs have shown that these NPs do not penetrate beyond the *stratum corneum* of the skin [176,177].

In the study carried out by Holmes et al. (2016) [178], ZnONPs did not penetrate beyond the *stratum corneum* after topical application of any of the sunscreen formulations tested. Nevertheless, there was an enhancement of zinc ion fluorescence signal in both *the stratum corneum* and the epidermis after the application of ZnONPs in a pH 6 aqueous vehicle (similar pH of the human skin surface). This increased signal was attributed to the dissolution of ZnONPs at pH 6, so zinc ions could reach deeper skin layers and subsequently the circulatory system and urine, being a risk for human health.

Percutaneous penetration of ZnONPs can be affected by skin health as demonstrated by Leite-Silva et al. (2016) [179]. These authors concluded that bare and coated (triethoxycaprylylsilane) ZnONPs do not cross *stratum corneum* in human healthy skin but reach the epidermis in human barrier-impaired skin. This study also showed that skin occlusion does not increase the penetration of these ZnONPs.

I.2.4.2 Viability of human skin cells under exposure to NPs

Toxic effects of NPs on dermal cells should be considered in the case of NPs that can penetrate through the *stratum corneum*. Cytotoxicity depends on the type of NPs, the size of

NPs, the core of NPs, the concentration of NPs, the dermal cell type, the assay used, and the exposure time to NPs.

Regarding the size, smaller NPs usually exhibit greater cytotoxicity. Nevertheless, in the study carried out by Pan et al. (2009) [180], larger TiO_2NPs are more cytotoxic to human dermal fibroblasts due to their crystallographic structure (anatase particles are more deadly for the studied cells than rutile ones). The toxicity of NPs also depends on the coating of NPs [181], the type of dermal cell used [182], exposure time [183,184], and the assay performed [185].

I.2.5 Determination of inorganic NPs in cosmetics and textile products

I.2.5.1 Analysis of inorganic NPs in cosmetics

Standardised methodologies must be developed and validated for the assessment of NPs (size and particle concentration) in cosmetics to ensure law enforcement (European Regulation 1223/2009 [3]). Most investigations have focused on the analysis of TiO_2NPs and ZnONPs in cosmetic samples, especially in sunscreens, due to their widespread use and regulation. Dynamic light scattering (DLS) [23,186,187], transmission electron microscopy coupled to energy-dispersive X-ray spectroscopy (TEM-EDX) [23,188–192], cryogenic TEM-EDX (imaging of frozen samples) [23], scanning electron microscopy coupled to energy-dispersive X-ray spectroscopy (SEM-EDX) [188,191,193], atomic force microscopy (AFM) [189], and X-ray diffraction (XRD) [189,190,192,193] techniques determine the physical and chemical properties such as hydrodynamic diameter, morphology, crystalline structure, and/or size of TiO_2NPs and ZnONPs in cosmetic products.

Regarding quantitative methodologies, Benítez-Martínez et al. (2016) [194] proposed a simple and rapid methodology for quantification of TiO_2NPs in sunscreens using N-doped graphene quantum dots. TiO_2NPs were extracted by liquid-liquid extraction and then analysed by fluorescence spectroscopy (TiO_2NPs induce a quenching effect on the fluorescence of the quantum dots used).

SS-HR-CS-GFAAS was also proposed by García-Mesa et al. (2021) [195] as a valid technique for the quantification of zinc species (Zn^{2+} and ZnONPs) in cosmetic samples.

Most studies have focused on the hyphenation of field-flow fractionation techniques (FFF) and spectrometry to determine both concentration and size distribution of NPs. Sedimentation field-flow fractionation–inductively coupled plasma mass spectrometry (SdFFF-ICP-MS) [196], and asymmetrical flow field-flow fractionation (AF4) coupled to plasma-based techniques (AF4-UV-ICP-OES [197], AF4-ICP-MS [198,199], and AF4-MALS-ICP-MS [186,200]) have been used for the quantification of TiO_2NPs and ZnONPs in cosmetic samples. The main drawback of these hybrid techniques is the long analysis time. However, an important advantage is that they can determine the coating of separated NPs due to the multi-detection capabilities of spectrometry [200]. The coating of NPs can also be assessed by time-of-flight secondary ion mass spectrometry (ToF-SIMS) [23] and electron microscopy coupled to EDX [193].

Recently, spICP-MS has been proposed as a suitable technique for the routine analysis of inorganic NPs in cosmetic samples because of its simplicity and short analysis time. Furthermore, NPs can be quantified by spICP-MS without a previous separation step. This technique provides information about number concentration and sizes of TiO_2NPs and ZnONPs in cosmetic products [186,187,192,200,201].

However, the critical step in the determination of NPs in complex matrices is the sample pre-treatment, which must guarantee the stability of the NPs present in the samples. Several authors diluted commercial sunscreens containing TiO_2NPs and ZnONPs with ethanol [189,190,193] or a mixture of ultrapure water/methanol (1:1) [188] before electron microscopy

analysis. Furthermore, centrifugation of sunscreens using chloroform [193], methanol [191], or several organic solvents of different polarities [192] has been performed prior to electron microscopy analysis to remove the organic matrix of cosmetics, which hinders the characterisation of NPs.

Defatting with hexane has also been proposed for organic component removal before the assessment of TiO_2NPs and ZnONPs in cosmetics. Hexane was added to a portion of the sample, and then the mixture was shaken, sonicated, and allowed to settle. After settling, centrifugation was performed and the supernatant, which contained undesirable organic compounds, was removed. Finally, the solid residue was resuspended in ultrapure water [196,199] or in a mixture of water and hexane (19.5/0.5 or 20/0.5) [186,187,198]. Nischwitz et al. (2012) [198] proved that the hexane added to the precipitate formed after the defatting step aids NPs disaggregation. Furthermore, these authors proved that the addition of hexane to the precipitate formed enhances the extraction efficiency of TiO_2NPs. The percentage of extracted Ti ranged from 64% to 79% for aqueous extracts, while greater extraction efficiencies (68% to 110%) were achieved when 2.5% (v/v) hexane was used in the redispersion of the precipitate. Lower extraction efficiencies in aqueous extracts were due to the adsorption of TiO_2NPs on the tube walls [198]. Nevertheless, the use of hexane can dissolve the dimethicone (PDMS) coating of NPs, especially when a sonication procedure is used [23].

Water/methanol/hexane mixture using 2/2/2 [194] or 20/20/10 [197] proportions were also used for NPs extraction. However, a low percentage of extracted TiO_2NPs [7.83–21.47% (w/w) range] was reported by Contado et al. (2008) [197].

Several studies have proposed the dispersion of sunscreens in 1% sodium dodecyl sulphate (SDS) [187] or 1% Triton X-100 [192,200,201] aqueous solutions to obtain usually 0.1% (w/v) suspensions. The resultant suspensions have been sonicated and diluted with ultrapure water before their analysis by AF4-MALS-ICP-MS or spICP-MS.

De la Calle et al. (2017) [187] obtained different values for the number of particles and sizes of TiO_2NPs measured by spICP-MS, depending on the extraction procedure used (defatting with hexane or dispersion in SDS). This difference could be due to the poor solubility of cosmetics in the SDS solution, the solubilisation of NPs in hexane, or the loss of NPs during the filtration step [the authors filtered (0.45µm) the resuspended precipitate after defatting with hexane]. On the other hand, the particle sizes obtained by spICP-MS of cosmetic suspensions in SDS were in most cases larger than those of defatted samples. This finding could be explained by the matrix effect of SDS. SDS-induced negatively charged droplets can attract cations, resulting in an enrichment of the analyte in aerosol droplets and thus larger TiO_2 particle sizes after ionisation were obtained. Furthermore, the authors suggested that the smaller sizes of TiO_2NPs in defatted cosmetics could be due to a suppression of the analyte signal caused by the organic solvent.

I.2.5.2 Analysis of inorganic NPs in textile products

Several studies reported in the literature focus on the leachate of AgNPs and TiO_2NPs from textiles. The release of NPs from textiles depends on the composition of the washing medium, the conditions of washing, and the methodology used for the incorporation of NPs (surface coating or integration of NPs into fibres). Most of these studies have simulated a washing process in households. The interest of these studies is that the NPs can be released during the washing procedure and discharged into waste-water treatment plants, occasioning environmental hazards [202].

However, NPs can be affected by detergents, as reported by Mitrano et al. (2015) [203] who studied the effect of different commercial detergents on the suspensions of silver standards

under simulated washing procedures. Five detergents were purchased from a local store (grocery) and two industrial detergents from a company. The selected detergents had different ionic composition, oxidant concentration, and physical form (powder or liquid). AgNPs (100 nm, citrate-coated) and $AgNO_3$ standards were added to the washing solutions (detergents diluted with ultrapure water) and analysed by spICP-MS and TEM-EDX to evaluate the stability of these silver standards under washing. AgNPs were formed after the addition of $AgNO_3$ in all powder detergents (grocery and industrial). After the addition of AgNPs into two grocery powder detergents which contained peroxide (all-purpose and oxi powder detergents), STEM-EDX images confirmed that some AgNPs were damaged. In addition, spICP-MS measurements demonstrated that the particle distribution shifted to smaller sizes. On the other hand, the industrial liquid detergent promoted the highest dissolution of AgNPs (only a few particles remained in the washing solution). AgNPs were also damaged in the industrial powder detergent, but to a less extent (increase in the number of smaller particles).

Some studies reported in the literature have also proved changes in metal speciation after washing fabrics with detergents (**Table I.1**). In the study carried out by Mitrano et al. (2014) [47], AgNPs were formed after the addition of an $AgNO_3$ standard (1100 μg L^{-1}) into the laundering liquid used (2.3% of silver was quantified in the nanoparticulate fraction, 10 kDa–100 nm). Silver chloride nanoparticles (AgClNPs) and/or silver sulphide nanoparticles (Ag_2SNPs) were also found in washing liquids [47,204] and on the surface of washed textiles [205,206].

The rate of release is greater in textiles modified with NPs on the surface of the fibres than in the case of textiles with NPs embedded in the fibres [47]. In addition, silver release from textiles during washing procedures with detergents is affected by the coating of AgNPs [206]. This behaviour can be explained by the electrostatic interaction of the capping agent and the binder used for fixing the NPs to textile products.

In several studies, the extraction of NPs from textiles using detergents was not quantitative and the total silver released from fabrics was lower than 40% [47,204,207]. Nevertheless, the extraction percentages of extracted titanium reported by Windler et al. (2012) [208] were even lower. In this study, total titanium released (one washing/rinsing cycle) from textiles was in the range of 0.01–0.06%, except for one sample which leached a percentage corresponding to the 3.4% of total titanium.

Other investigations have focused on the release of NPs from textiles by incubation in artificial sweat solutions (alkaline and acidic sweat). After incubation, the extracted metals in solutions were quantified by ICP-MS [209,210], ICP-OES [211], GFAAS [212], and spICP-MS [210]. The speciation of the metal released from fabrics depends on the pH of the medium. The main silver species found in sweat solutions were dissolved silver [210] and AgClNPs [211] (due to the high content of chloride). On the other hand, titanium was mostly found as particulate in sweat solutions [211].

Finally, other authors proposed the extraction of NPs from textiles using ultrapure water to minimise the possible alterations in the released species. In the study performed by Spielman-Sun et al. (2018) [209], fabric swatches (4 cm^2) were incubated at 37 ºC in 20 mL of ultrapure water for 60 min. The percentage of total silver released from textiles was quantified by ICP-MS and varied between 10 and 30%.

Benn et al. (2008) [213] washed different commercial socks modified with AgNPs in ultrapure water. The socks were agitated in 500 mL of ultrapure water at 50 rpm for either 1 h or 24 h. Silver was determined in the aqueous extracts by ICP-OES. The results obtained showed that two samples were still leaching significant content of silver after four cycles of consecutive 24-h washings. The authors also found that the amount of dissolved silver in

extracts from one sample increased after three consecutive 1-h washing cycles. This could indicate the dissolution of AgNPs after prolonged exposure to water.

Mackevika et al. (2018) [48] also carried out the extraction of TiO_2NPs from textile products by shaking them with water. 400 cm^2 of a fabric was introduced into a polyethylene bottle containing 200 mL of ultrapure water. The sample was bath sonicated for 15 min to facilitate the start of the extraction and then was subjected to shaking for 24 h (150 movements per min). According to spICP-MS results, synthetic textiles released higher contents of TiO_2NPs. However, less than 1% of total titanium content in fabrics was released as TiO_2NPs, which meant that titanium was present as larger particles or strongly bound to fibres.

Table I.1. Extraction of inorganic NPs from fabrics using detergents

Element analysed	Washing procedure	Detergent	Fractionation of washing solutions	Analytical technique	Changes in metal speciation after washing	Reference
Silver	Laboratory washing machine (ISO 105-C06:2010, 40±2 rpm, 40±2 °C, 45 min, 75 mL of washing solution, 5 polyethylene balls, and 4 grams of fabric).	ECE-2 Colour Fastness Test Detergent in ultrapure water (9.8% of sodium sulphate). pH=10.5–10.7.	Yes. 0.45 µm, 0.10 µm, and centrifugal (10 kDa) filtrations.	ICP-MS TEM-EDX	- Oxidation of Ag^+ ions to AgNPs. - Formation of AgClNPs and Ag_2SNPs.	Mitrano et al. (2014) [47]
Silver	Laboratory washing machine (ISO 105-C06:1994, 40±2 rpm, 40±2 °C, 30 min, 120±0.15 mL of washing solution, 10 polyethylene balls, and 8±0.05 grams of textile) followed by two rinsing cycles with tap water.	ECE-77 Colour Fastness Test Detergent in ultrapure water (21% of sodium sulphate). pH=10.6.	Yes. 0.45 µm and centrifugal (30 kDa) filtrations.	ICP-OES STEM-EDX TSEM-EDX	Formation of AgClNPs	Lorenz et al. (2012) [204]
Silver	- Laboratory washing procedure (same conditions as those used by Lorentz et al. [204]). - Machine washing procedure (regular washing machine, commercial washing powder, and textiles were washed with other soiled fabrics).	- Laboratory washing: ECE-2 Colour Fastness Test Detergent. - Machine washing: commercial washing powder.	No. Direct analysis of textile products.	ICP-OES XANES	- Formation of AgNPs (laboratory washing procedure). - Formation of AgClNPs (machine washing procedure).	Lombi et al. (2014) [205]
Silver	Laboratory washing machine (ISO Standard 105-C06:2010, 40±2 rpm, 40±2 °C, 20 mL of washing solution, 0.5 grams of fabric, and 5 polyethylene balls). One washing cycle consisted in a washing step (40 min) and two rinsing steps (ultrapure water for 5 min each).	- Grocery detergents: two liquid detergents ("color" and "all purpose") and three powder detergents ("color","all purpose", and "oxi". - Industrial detergents: one liquid and one powder.	Yes. 10 kDa.	SEM XANES ICP-MS spICP-MS TEM-EDX	- Detergents with oxidising agents promote the dissolution of AgNPs. - Formation of Ag_2SNPs and AgClNPs in several washing solutions.	Mitrano et al. (2016) [206]

Table I.1. (continued)

Element analysed	Washing procedure	Detergent	Fractionation of washing solutions	Analytical technique	Changes in metal speciation after washing	Reference
Silver	- Laboratory washing machine (ISO 105-C06:1997, 40±2 rpm, 40 °C, 30 min, 10 steel balls, textile range of 4.7–27.4 g L^{-1}, and detergent/container volume ratio of 0.279). - Shaking (100-150 rpm) of textiles in a solution with pH 10 (0.1 g L^{-1} SDS, buffered with 0.005M Na_2CO_3). The amount of fabric introduced into the solution ranged from 4.9 to 36.2 g L^{-1}. After 120 min peracetic acid (bleaching agent) was added.	Laboratory washing machine: ECE-98 Colour Fastness Test Detergent (9.8% of sulphate).	Yes. 0.45 µm and centrifugal (30 kDa) filtrations.	ICP-OES	Different silver species depending on the methodology used for the extraction	Geranio et al. (2009) [207]
Silver	Laboratory washing procedure (ISO 105-C06:2010, 40 rpm, 30 min, 50 mL of water with or without detergent, 5 glass beads, and 2 grams of fabric).	American Association of Textile Colourists and Chemists. (Formulation, 2003).	Yes. 30 kDa.	ICP-MS	The percentage of silver released as a dissolved form was greater when fabrics were washed with ultrapure water	Reed et al. (2016) [214]
Titanium	Laboratory washing procedure (ISO 105-C06:1994, 40±2 rpm, 40±2 °C, 30 min, 120±0.15 mL of washing solution, 10 polyethylene balls, and 8±0.05 grams of fabric). The washing cycle was followed by two rinsing cycles (textiles were washed with 20±0.03 mL of tap water for 5 min in each rinsing cycle).	ECE-77 Colour Fastness Test Detergent (pH=10.6).	Yes. 0.45 µm and centrifugal (30 kDa) filtrations.	ICP-OES TSEM-EDX STEM-EDX	Not observed	Windler et al. (2012) [208]

I.2.5.3 spICP-MS: a powerful technique for the analysis of inorganic NPs

Recently, the analysis of inorganic NPs using spICP-MS has been widely studied. This technique provides information on the chemical composition, particle concentration, and particle size. Thus, spICP-MS allows the detection and quantification of NPs and the dissolved form in complex matrices without a prior separation step at concentration levels of ng L^{-1}.

Degueldre et al. (2006) [215] outlined theoretical aspects of spICP-MS, which were recently discussed by Laborda et al. (2014,2016) [216,217].

spICP-MS analysis is based on the different behaviour of ionic and nanoparticulate species of the analyte in the plasma (**Figure I.3**). Ionic forms of analyte are distributed uniformly in the solution and in the aerosol droplets. As a result, the mass of the element entering the plasma per unit time and reaching the detector as ions can be considered constant, generating a stable signal during the acquisition time. On the other hand, the element is not homogeneously distributed and is only present in a small fraction of aerosol droplets after the nebulisation of a suspension of NPs. Each NP is vaporised, atomised, and ionised, forming a pack of ions with a duration in the detector of about 300–500 microseconds (μs). Thus, if an adequate diluted suspension of NPs is introduced into the plasma, the cloud of ions formed from each single particle can be detected as events (transient signals or pulses) [217].

In addition to the concentration requirement, it is necessary to work with sufficiently high data acquisition frequencies ($\geq 10^4$ Hz which corresponds with reading times of ≤100 μs) to record the transient signal generated by each individual NP. However, packs of ions are detected as pulses using lower frequencies [217].

Using the correct dilution factors and acquisition frequencies, each detected event corresponds to a single particle. Thus, the number of events detected (N_P) during an acquisition time (t) is directly proportional to the number concentration of particles (C_P) [**Equation I.1**]:

$$N_P = Q_{sam}\, \eta_{neb}\, t\, C_P \quad (\mathbf{Eq.\, I.\, 1})$$

where Q_{sam} is the sample introduction flow rate and η_{neb} is the nebulisation efficiency.

Furthermore, the intensity of each event (I_P) is directly related to the mass of element per particle (m_P) [**Equation I.2]**:

$$I_P = K_{ICPMS}\, K_M\, m_P \quad (\mathbf{Eq.\, I.\, 2})$$

where K_{ICPMS} is the detection efficiency (ratio of the number of ions detected and the number of atoms introduced), while K_M is related to the element measured and is calculated by the ratio AN_{AV}/M_M (A is the atomic abundance of the isotope analysed, N_{AV} the Avogadro´s number, and M_M the atomic mass of the element).

For a homogeneous, solid, and spherical particle, the **Equation I.2** can be re-written as **Equation I.3**:

$$I_P = \frac{1}{6}\, \pi\, \rho\, f_P\, K_{ICPMS}\, K_M\, d^3 \quad (\mathbf{Eq.\, I.\, 3})$$

where ρ is the particle density, f_P the mass fraction of the element in the particle, and d the particle diameter.

The particle number concentration, the mass of analyte per particle, and the diameter of the particles are therefore calculated using the **Equations I.1**, **I.2** and **I.3**, respectively [217].

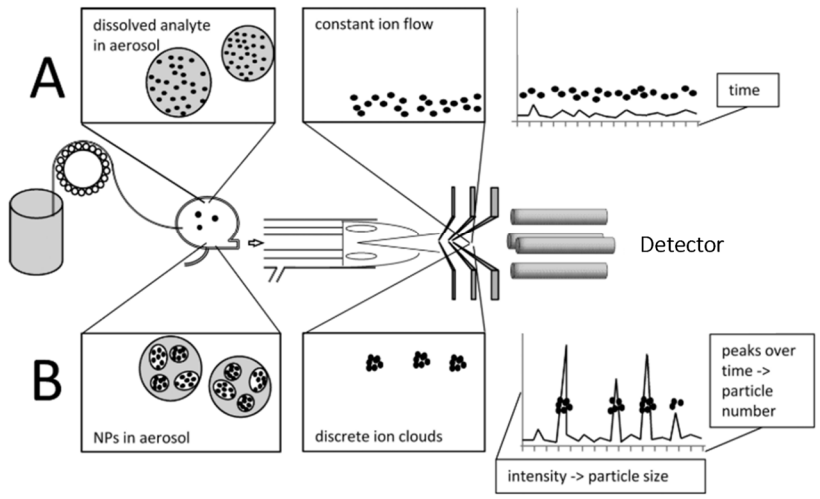

Figure I.3. spICP-MS signals generated by dissolved analyte (A) and nanoparticles (B). Adapted with permission from Witzler et al. (2016) [218] (Copyright © 2016, American Chemical Society)

REFERENCES

[1] M.E. Tu, Y.H. Wu, Multiple allergies to metal alloys, Dermatol. Sin. 29 (2011) 41–43, DOI: 10.1016/j.dsi.2011.05.010.

[2] B.C. Almroth, J. Cartine, C. Jönander, M. Karlsson, J. Langlois, M. Lindström, J. Lundin, N. Melander, A. Pesqueda, I. Rahmqvist, J. Renaux, J. Roos, F. Spilsbury, J. Svalin, H. Vestlund, L. Zhao, N. Asker, G. Ašmonaitė, L. Birgersson, T. Boloori, F. Book, T. Lammel, J. Sturve, Assessing the effects of textile leachates in fish using multiple testing methods: From gene expression to behavior, Ecotoxicol. Environ. Saf. 207 (2021) 111523, DOI: 10.1016/j.ecoenv.2020.111523.

[3] Regulation (EC) N° 1223/2009 of the European Parliament and of the Council of 30 November 2009 on cosmetic products, Official Journal of the European Union, L342 (01 March 2022) 1–392.

[4] Commission Directive 95/45/EC of 26 July 1995 laying down specific purity criteria concerning colours for use in foodstuffs, Official Journal of the European Union, L226 (22 September 1995) 1–45.

[5] B. Bocca, A. Pino, A. Alimonti, G. Forte, Toxic metals contained in cosmetics: A status report, Regul. Toxicol. Pharmacol. 68 (2014) 447–467, DOI: 10.1016/j.yrtph.2014.02.003.

[6] M.F. Mesko, D. La Rosa Novo, V.C. Costa, A.S. Henn, E.M.M. Flores, Toxic and potentially toxic elements determination in cosmetics used for make-up: A critical review, Anal. Chim. Acta 1098 (2020) 1–26, DOI: 10.1016/j.aca.2019.11.046.

[7] B. Bocca, G. Forte, F. Petrucci, A. Cristaudo, Levels of nickel and other potentially allergenic metals in Ni-tested commercial body creams, J. Pharm. Biomed. Anal. 44 (2007) 1197–1202, DOI: 10.1016/j.jpba.2007.04.031.

[8] C.E.R. de Paula, G.F.B. Cruz, C.M.S.P. Rezende, R.J. Cassella, Determination of Cr and Mn in moisturizing creams by graphite furnace atomic absorption spectrometry through direct introduction of the samples in the form of emulsions, Microchem. J. 127 (2016) 1–6, DOI: 10.1016/j.microc.2016.01.017.

[9] Z. Grosser, L. Davidowski, L. Thompson, The Determination of Metals in Cosmetics, Perkin Elmer Appl. Note (2011) 1–6.

[10] Y. Gao, Z. Shi, Q. Zong, P. Wu, J. Su, R. Liu, Direct determination of mercury in cosmetic samples by isotope dilution inductively coupled plasma mass spectrometry after dissolution with formic acid, Anal. Chim. Acta 812 (2014) 6–11, DOI: 10.1016/j.aca.2014.01.002.

[11] W.N. Chen, S.J. Jiang, Y.L. Chen, A.C. Sahayam, Slurry sampling flow injection chemical vapor generation inductively coupled plasma mass spectrometry for the determination of trace Ge, As, Cd, Sb, Hg and Bi in cosmetic lotions, Anal. Chim. Acta 860 (2015) 8–14, DOI: 10.1016/j.aca.2015.01.011.

[12] C.M.A. Iwegbue, F.I. Bassey, G.O. Tesi, S.O. Onyeloni, G. Obi, B.S. Martincigh, Safety evaluation of metal exposure from commonly used moisturizing and skin-lightening creams in Nigeria, Regul. Toxicol. Pharmacol. 71 (2015) 484–490, DOI: 10.1016/j.yrtph.2015.01.015.

[13] F.L. Melquiades, P.S. Parreira, L.Y. Endo, G. dos Santos, L. Wouk, O.P. Filho, Portable EDXRF for Quality Assurance of Cosmetics, Cosmetics 2 (2015) 277–285, DOI: 10.3390/cosmetics2030277.

[14] C.R. Hamann, W. Boonchai, L. Wen, E.N. Sakanashi, C.Y. Chu, K. Hamann, C.P. Hamann, K. Sinniah, D. Hamann, Spectrometric analysis of mercury content in 549 skin-

lightening products: Is mercury toxicity a hidden global health hazard?, J. Am. Acad. Dermatol. 70 (2014) 281–287, DOI: 10.1016/j.jaad.2013.09.050.

[15] M.A. Gondal, Z.S. Seddigi, M.M. Nasr, B. Gondal, Spectroscopic detection of health hazardous contaminants in lipstick using Laser Induced Breakdown Spectroscopy, J. Hazard. Mater. 175 (2010) 726–732, DOI: 10.1016/j.jhazmat.2009.10.069.

[16] A.I. Barros, D.V. de Babos, E.C. Ferreira, J.A. Gomes Neto, Effect of different precursors on generation of reference spectra for structural molecular background correction by solid sampling high-resolution continuum source graphite furnace atomic absorption spectrometry: Determination of antimony in cosmetics, Talanta 161 (2016) 547–553, DOI: 10.1016/j.talanta.2016.09.017.

[17] S. Gunduz, S. Akman, Investigation of lead contents in lipsticks by solid sampling high resolution continuum source electrothermal atomic absorption spectrometry, Regul. Toxicol. Pharmacol. 65 (2013) 34–37, DOI: 10.1016/j.yrtph.2012.10.009.

[18] H. Tinas, N. Ozbek, S. Akman, Method development for the determination of cadmium in lipsticks directly by solid sampling high-resolution continuum source graphite furnace atomic absorption spectrometry, Microchem. J. 138 (2018) 316–320, DOI: 10.1016/j.microc.2018.01.031.

[19] L. Sneyers, L. Verheyen, P. Vermaercke, M. Bruggeman, Trace element determination in beauty products by k_0-instrumental neutron activation analysis, J. Radioanal. Nucl. Chem. 281 (2009) 259–263, DOI: 10.1007/s10967-009-0105-8.

[20] E. Pinto, K. Paiva, A. Carvalhido, A. Almeida, Elemental impurities in lipsticks: Results from a survey of the Portuguese and Brazilian markets, Regul. Toxicol. Pharmacol. 95 (2018) 307–313, DOI: 10.1016/j.yrtph.2018.04.009.

[21] M.F. Mesko, D. La Rosa Novo, F.S. Rondan, R.M. Pereira, V.C. Costa, Sample preparation of lipstick for further Cd and Pb determination by ICP-MS: is the use of complexing acids really necessary?, J. Anal. At. Spectrom. 32 (2017) 1780–1788, DOI: 10.1039/C7JA00139H.

[22] Y.B. Ho, N.H. Abdullah, H. Hamsan, E.S.S. Tan, Mercury contamination in facial skin lightening creams and its health risks to user, Regul. Toxicol. Pharmacol. 88 (2017) 72–76, DOI: 10.1016/j.yrtph.2017.05.018.

[23] A. Philippe, J. Košík, A. Welle, J.M. Guigner, O. Clemens, G.E. Schaumann, Extraction and characterization methods for titanium dioxide nanoparticles from commercialized sunscreens, Environ. Sci. Nano 5 (2018) 191–202, DOI: 10.1039/C7EN00677B.

[24] C. Contado, A. Pagnoni, A new strategy for pressed powder eye shadow analysis: Allergenic metal ion content and particle size distribution, Sci. Total Environ. 432 (2012) 173–179, DOI: 10.1016/j.scitotenv.2012.05.092.

[25] G.A. Zachariadis, E. Sahanidou, Multi-element method for determination of trace elements in sunscreens by ICP-AES, J. Pharm. Biomed. Anal. 50 (2009) 342–348, DOI: 10.1016/j.jpba.2009.05.003.

[26] A. Papadopoulos, N. Assimomytis, A. Varvaresou, Sample Preparation of Cosmetic Products for the Determination of Heavy Metals, Cosmetics 9 (2022) 21, DOI: 10.3390/cosmetics9010021, DOI: 10.3390/cosmetics9010021.

[27] A.R. Soares, C.C. Nascentes, Development of a simple method for the determination of lead in lipstick using alkaline solubilization and graphite furnace atomic absorption spectrometry, Talanta 105 (2013) 272–277, DOI: 10.1016/j.talanta.2012.09.021.

[28] I. Lavilla, N. Cabaleiro, M. Costas, I. de la Calle, C. Bendicho, Ultrasound-assisted emulsification of cosmetic samples prior to elemental analysis by different atomic spectrometric techniques, Talanta 80 (2009) 109–116, DOI: 10.1016/j.talanta.2009.06.036.

[29] G. Daneshvar Tarigh, F. Shemirani, Magnetic multi-wall carbon nanotube nanocomposite as an adsorbent for preconcentration and determination of lead (II) and manganese (II) in various matrices, Talanta 115 (2013) 744–750, DOI: 10.1016/j.talanta.2013.06.018.

[30] K. Sharafi, N. Fattahi, M. Pirsaheb, H. Yarmohamadi, M. Fazlzadeh Davil, Trace determination of lead in lipsticks and hair dyes using microwave-assisted dispersive liquid-liquid microextraction and graphite furnace atomic absorption spectrometry, Int. J. Cosmet. Sci. 37 (2015) 489–495, DOI: 10.1111/ics.12221.

[31] M.G. Volpe, M. Nazzaro, R. Coppola, F. Rapuano, R.P. Aquino, Determination and assessments of selected heavy metals in eye shadow cosmetics from China, Italy, and USA, Microchem. J. 101 (2012) 65–69, DOI: 10.1016/j.microc.2011.10.008.

[32] F.F. Huang, S.J. Jiang, Y.L. Chen, A.C. Sahayam, Chemical vapor generation sample introduction for the determination of As, Cd, Sb, Hg, and Pb in nail polish by inductively coupled plasma mass spectrometry, Spectrochim. Acta B 140 (2018) 84–88, DOI: 10.1016/j.sab.2017.12.010.

[33] J. N. Chakraborty, Metal-complex dyes, in M. Clark (Ed.), *Handbook of Textile and Industrial Dyeing: Principles, Processes and Types of Dyes*, Woodhead Publishing, Cambridge, United Kingdom (2011) 446–465, DOI: 10.1533/9780857093974.2.446.

[34] H.A. Aziz, M.F. Ghazali, Y.T. Hung, L.K. Wang, Toxicity, Source, and Control of Barium in the Environment, in J.P. Chen, L.K. Wang, M.H.S. Wang, Y.T. Hung, N.K. Shammas (Eds.), *Remediation of Heavy Metals in the Environment*, CRC Press, Boca Raton, FL, USA (2016) 463–482, DOI: 10.1201/9781315374536.

[35] A. Gürses, K. Güneş, E. Şahin, Removal of dyes and pigments from industrial effluents, in S. K. Sharma (Ed.), *Green Chemistry and Water Remediation: Research and Applications*, Elsevier, Amsterdam, The Netherlands (2021) 135–187, DOI: 10.1016/B978-0-12-817742-6.00005-0.

[36] M. Biver, A. Turner, M. Filella, Antimony release from polyester textiles by artificial sweat solutions: A call for a standardized procedure, Regul. Toxicol. Pharmacol. 119 (2021) 104824, DOI: 10.1016/j.yrtph.2020.104824.

[37] S. Gaan, V. Salimova, P. Rupper, A. Ritter, H. Schmid, Flame retardant functional textiles, in N. Pan, G. Sun (Eds.), *Functional Textiles for Improved Performance, Protection and Health*, Woodhead Publishing, Cambridge, United Kingdom (2011) 98–130, DOI: 10.1533/9780857092878.98.

[38] R.M. Kozłowski, M. Muzyczek, Improving the flame retardancy of natural fibres, in R.M. Kozłowski, M. Mackiewicz-Talarczyk (Eds.), *Handbook of Natural Fibres. Volume 2: Processing and Applications* (Second Edition), Woodhead Publishing, Cambridge, United Kingdom (2020) 355–391, DOI: 10.1016/B978-0-12-818782-1.00010-9.

[39] S. Posner, Developments in flame retardants for interior materials and textiles, in T. Rowe (Ed.) *Interior textiles. Design and Developments*, Woodhead Publishing, Cambridge, United Kingdom (2009) 211–228, DOI: 10.1533/9781845696870.2.211.

[40] R. Hage, J.W. de Boer, F. Gaulard, K. Maaijen, Manganese and Iron Bleaching and Oxidation Catalysts, in R. van Eldik, C.D. Hubbard (Eds.) *Advances in Inorganic Chemistry. Homogeneous Catalysis*, Academic Press, Cambridge, United Kingdom 65 (2013) 85–116, DOI: 10.1016/B978-0-12-404582-8.00003-1.

[41] Regulation (EC) N° 1907/2006 of the European Parliament and of the Council of 18 December 2006 concerning the Registration, Evaluation, Authorisation and Restriction of Chemicals (REACH), establishing a European Chemicals Agency, amending Directive 1999/45/EC and repealing Council Regulation (EEC) Nº 793/93 and Commission Regulation

(EC) N° 1488/94 as well as Council Directive 76/769/EEC and Commission Directives 91/155/EEC, 93/67/EEC, 93/105/EC and 2000/21/EC, Official Journal of the European Union, L396 (01 March 2022) 1–557.

[42] J.M. Gallo, J.R. Almirall, Elemental analysis of white cotton fiber evidence using solution ICP-MS and laser ablation ICP-MS (LA-ICP-MS), Forensic Sci. Int. 190 (2009) 52–57, DOI: 10.1016/j.forsciint.2009.05.011.

[43] I. Rezić, I. Steffan, ICP-OES determination of metals present in textile materials, Microchem. J. 85 (2007) 46–51, DOI: 10.1016/j.microc.2006.06.010.

[44] I. Rezić, M. Zeiner, I. Steffan, Determination of 28 selected elements in textiles by axially viewed inductively coupled plasma optical emission spectrometry, Talanta 83 (2011) 865–871, DOI: 10.1016/j.talanta.2010.10.031.

[45] E. Matoso, S. Cadore, Determination of inorganic contaminants in polyamide textiles used for manufacturing sport T-shirts, Talanta 88 (2012) 496–501, DOI: 10.1016/j.talanta.2011.11.022.

[46] E.A. Menezes, R. Carapelli, S.R. Bianchi, S.N.P. Souza, W.O. Matos, E.R. Pereira-Filho, A.R.A. Nogueira, Evaluation of the mineral profile of textile materials using inductively coupled plasma optical emission spectrometry and chemometrics, J. Hazard. Mat. 182 (2010) 325–330, DOI: 10.1016/j.jhazmat.2010.06.033.

[47] D.M. Mitrano, E. Rimmele, A. Wichser, R. Erni, M. Height, B. Nowack, Presence of Nanoparticles in Wash Water from Conventional Silver and Nano-silver Textiles, ACS Nano 8 (2014) 7208–7219, DOI: 10.1021/nn502228w.

[48] A. Mackevica, M.E. Olsson, S.F. Hansen, Quantitative characterization of TiO_2 nanoparticle release from textiles by conventional and single particle ICP-MS, J. Nanopart. Res. 20 (2018) 6, DOI: 10.1007/s11051-017-4113-2.

[49] Commission Recommendation of 18 October 2011 on the definition of nanomaterial (2011/696/EU), Official Journal of the European Union, L275 (20 October 2011) 38–40.

[50] D.R. Boverhof, C.M. Bramante, J.H. Butala, S.F. Clancy, M. Lafranconi, J. West, S.C. Gordon, Comparative assessment of nanomaterial definitions and safety evaluation considerations, Regul. Toxicol. Pharmacol. 73 (2015) 137–150, DOI: 10.1016/j.yrtph.2015.06.001.

[51] A. López-Serrano, R.M. Olivas, J.S. Landaluze, C. Cámara, Nanoparticles: A global vision. Characterization, separation, and quantification methods. Potential environmental and health impact, Anal. Methods 6 (2014) 38–56, DOI: 10.1039/C3AY40517F.

[52] The Nanodatabase Inventory (https://nanodb.dk); accessed on 07 April 2021.

[53] G. Taubes, The Bacteria Fight Back, Science 321 (2008) 356–361, DOI: 10.1126/science.321.5887.356.

[54] A.L. Kubo, I. Capjak, I.V. Vrček, O.M. Bondarenko, I. Kurvet, H. Vija, A. Ivask, K. Kasemets, A. Kahru, Antimicrobial potency of differently coated 10 and 50 nm silver nanoparticles against clinically relevant bacteria *Escherichia coli* and *Staphylococcus aureus*, Colloids Surf. B 170 (2018) 401–410, DOI: 10.1016/j.colsurfb.2018.06.027.

[55] X. Zhang, H. Sun, S. Tan, J. Gao, Y. Fu, Z. Liu, Hydrothermal synthesis of Ag nanoparticles on the nanocellulose and their antibacterial study, Inorg. Chem. Commun. 100 (2019) 44–50, DOI: 10.1016/j.inoche.2018.12.012.

[56] Y.N. Slavin, J. Asnis, U.O. Häfeli, H. Bach, Metal nanoparticles: understanding the mechanisms behind antibacterial activity, J. Nanobiotechnol. 15 (2017) 65, DOI: 10.1186/s12951-017-0308-z.

[57] J. Helmlinger, C. Sengstock, C. Groß-Heitfeld, C. Mayer, T.A. Schildhauer, M. Köller, M. Epple, Silver nanoparticles with different size and shape: equal cytotoxicity, but different antibacterial effects, RSC Adv. 6 (2016) 18490–18501, DOI: 10.1039/C5RA27836H.

[58] C.C.S. Batista, L.J.C. Albuquerque, I. de Araujo, B.L. Albuquerque, F.D. da Silva, F.C. Giacomelli, Antimicrobial activity of nano-sized silver colloids stabilized by nitrogen-containing polymers: the key influence of the polymer capping, RSC Adv. 8 (2018) 10873–10882, DOI: 10.1039/C7RA13597A.

[59] A.M. El Badawy, R.G. Silva, B. Morris, K.G. Scheckel, M.T. Suidan, T.M. Tolaymat, Surface Charge-Dependent Toxicity of Silver Nanoparticles, Environ. Sci. Technol. 45 (2011) 283–287, DOI: 10.1021/es1034188.

[60] W.R. Li, X.B. Xie, Q.S. Shi, H.Y. Zeng, Y.S. Ou-Yang, Y.B. Chen, Antibacterial activity and mechanism of silver nanoparticles on *Escherichia coli*, Appl. Microbiol. Biotechnol. 85 (2010) 1115–1122, DOI: 10.1007/s00253-009-2159-5.

[61] N.S. Wigginton, A. De Titta, F. Piccapietra, J. Dobias, V.J. Nesatyy, M.J.F. Suter, R. Bernier-Latmani, Binding of Silver Nanoparticles to Bacterial Proteins Depends on Surface Modifications and Inhibits Enzymatic Activity, Environ. Sci. Technol. 44 (2010) 2163–2168, DOI: 10.1021/es903187s.

[62] X. Yan, B. He, L. Liu, G. Qu, J. Shi, L. Hu, G. Jiang, Antibacterial mechanism of silver nanoparticles in *Pseudomonas aeruginosa*: proteomics approach, Metallomics 10 (2018) 557–564, DOI: 10.1039/C7MT00328E.

[63] W.R. Li, X.B. Xie, Q.S. Shi, S.S. Duan, Y.S. Ouyang, Y.B. Chen, Antibacterial effect of silver nanoparticles on *Staphylococcus aureus*, Biometals 24 (2011) 135–141, DOI: 10.1007/s10534-010-9381-6.

[64] S. Sanyasi, R.K. Majhi, S. Kumar, M. Mishra, A. Ghosh, M. Suar, P.V. Satyam, H. Mohapatra, C. Goswami, L. Goswami, Polysaccharide-capped silver nanoparticles inhibit biofilm formation and eliminate multi-drug-resistant bacteria by disrupting bacterial cytoskeleton with reduced cytotoxicity towards mammalian cells, Sci. Rep. 6 (2016) 24929, DOI: 10.1038/srep24929.

[65] L. Rizzello, P.P. Pompa, Nanosilver-based antibacterial drugs and devices: Mechanisms, methodological drawbacks, and guidelines, Chem. Soc. Rev. 43 (2014) 1501–1518, DOI: 10.1039/C3CS60218D.

[66] L.M. Stabryla, K.A. Johnston, J.E. Millstone, L.M. Gilbertson, Emerging investigator series: it's not all about the ion: support for particle-specific contributions to silver nanoparticle antimicrobial activity, Environ. Sci. Nano 5 (2018) 2047–2068, DOI: 10.1039/C8EN00429C.

[67] S.P. Deshmukh, S.M. Patil, S.B. Mullani, S.D. Delekar, Silver nanoparticles as an effective disinfectant: A review, Mater. Sci. Eng. C 97 (2019) 954–965, DOI: 10.1016/j.msec.2018.12.102.

[68] L. Wei, J. Lu, H. Xu, A. Patel, Z.S. Chen, G. Chen, Silver nanoparticles: synthesis, properties, and therapeutic applications, Drug Discov. Today 20 (2015) 595–601, DOI: 10.1016/j.drudis.2014.11.014.

[69] S.M. Imani, L. Ladouceur, T. Marshall, R. Maclachlan, L. Soleymani, T.F. Didar, Antimicrobial Nanomaterials and Coatings: Current Mechanisms and Future Perspectives to Control the Spread of Viruses Including SARS-CoV-2, ACS Nano 14 (2020) 12341–12369, DOI: 10.1021/acsnano.0c05937.

[70] K.A. Homan, M. Souza, R. Truby, G.P. Luke, C. Green, E. Vreeland, S. Emelianov, Silver Nanoplate Contrast Agents for *in Vivo* Molecular Photoacoustic Imaging, ACS Nano 6 (2012) 641–650, DOI: 10.1021/nn204100n.

[71] R. Karunamuni, P.C. Naha, K.C. Lau, A. Al-Zaki, A.V. Popov, E.J. Delikatny, A. Tsourkas, D.P. Cormode, A.D.A. Maidment, Development of silica-encapsulated silver nanoparticles as contrast agents intended for dual-energy mammography, Eur. Radiol. 26 (2016) 3301–3309, DOI: 10.1007/s00330-015-4152-y.

[72] Z. Khalifa, M. Zahran, M.A.H. Zahran, M.A. Azzem, Mucilage-capped silver nanoparticles for glucose electrochemical sensing and fuel cell applications, RSC Adv. 10 (2020) 37675–37682, DOI: 10.1039/D0RA07359H.

[73] Y. Vicente-Martínez, M. Caravaca, A. Soto-Meca, R. Solana-González, Magnetic core-modified silver nanoparticles for ibuprofen removal: an emerging pollutant in waters, Sci. Rep. 10 (2020) 18288, DOI: 10.1038/s41598-020-75223-1.

[74] B. Tang, J. Li, X. Hou, T. Afrin, L. Sun, X. Wang, Colorful and Antibacterial Silk Fiber from Anisotropic Silver Nanoparticles, Ind. Eng. Chem. Res. 52 (2013) 4556–4563, DOI: 10.1021/ie3033872.

[75] J. Bogdan, J. Zarzyńska, J. Pławińska-Czarnak, Comparison of Infectious Agents Susceptibility to Photocatalytic Effects of Nanosized Titanium and Zinc Oxides: A Practical Approach, Nanoscale Res. Lett. 10 (2015) 309, DOI: 10.1186/s11671-015-1023-z.

[76] Z.F. Yin, L. Wu, H.G. Yang, Y.H. Su, Recent progress in biomedical applications of titanium dioxide, Phys. Chem. Chem. Phys. 15 (2013) 4844–4858, DOI: 10.1039/C3CP43938K.

[77] J. Zhang, P. Zhou, J. Liu, J. Yu, New understanding of the difference of photocatalytic activity among anatase, rutile and brookite TiO_2, Phys. Chem. Chem. Phys. 16 (2014) 20382–20386, DOI: 10.1039/C4CP02201G.

[78] X. Li, V.T. John, G. He, J. Zhan, G. Tan, G. McPherson, Shear Induced Formation of Patterned Porous Titania with Applications to Photocatalysis, Langmuir 25 (2009) 7586–7593, DOI: 10.1021/la900158r.

[79] D.S. Kim, S.J. Han, S.Y. Kwak, Synthesis and photocatalytic activity of mesoporous TiO_2 with the surface area, crystallite size, and pore size, J. Colloid Interface Sci. 316 (2007) 85–91, DOI: 10.1016/j.jcis.2007.07.037.

[80] X. Li, W. Zheng, G. He, R. Zhao, D. Liu, Morphology Control of TiO_2 Nanoparticle in Microemulsion and Its Photocatalytic Property, ACS Sustain. Chem. Eng. 2 (2014) 288−295, DOI: 10.1021/sc400328u.

[81] C.L. Bianchi, S. Gatto, C. Pirola, A. Naldoni, A. Di Michele, G. Cerrato, V. Crocellà, V. Capucci, Photocatalytic degradation of acetone, acetaldehyde and toluene in gas-phase: Comparison between nano and micro-sized TiO_2, Appl. Catal. B 146 (2014) 123–130, DOI: 10.1016/j.apcatb.2013.02.047.

[82] Y. Yu, P. Zhang, L. Guo, Z. Chen, Q. Wu, Y. Ding, W. Zheng, Y. Cao, The Design of TiO_2 Nanostructures (Nanoparticle, Nanotube, and Nanosheet) and Their Photocatalytic Activity, J. Phys. Chem. C 118 (2014) 12727−12733, DOI: 10.1021/jp500252g.

[83] J.S. Chang, J. Strunk, M.N. Chong, P.E. Poh, J.D. Ocon, Multi-dimensional zinc oxide (ZnO) nanoarchitectures as efficient photocatalysts: What is the fundamental factor that determines photoactivity in ZnO?, J. Hazard. Mat. 381 (2020) 120958, DOI: 10.1016/j.jhazmat.2019.120958.

[84] V. Kumaravel, K.M. Nair, S. Mathew, J. Bartlett, J.E. Kennedy, H.G. Manning, B.J. Whelan, N.S. Leyland, S.C. Pillai, Antimicrobial TiO_2 nanocomposite coatings for surfaces, dental and orthopaedic implants, Chem. Eng. J. 416 (2021) 129071, DOI: 10.1016/j.cej.2021.129071.

[85] A.E. Ramírez, M. Montero-Muñoz, L.L. López, J.E. Ramos-Ibarra, J.A.H. Coaquira, B. Heinrichs, C.A. Páez, Signifcantly enhancement of sunlight photocatalytic performance of ZnO by doping with transition metal oxides, Sci. Rep. 11 (2021) 2804, DOI: 10.1038/s41598-020-78568-9.

[86] A. Simon-Deckers, S. Loo, M. Mayne-L'Hermite, N. Herlin-Boime, N. Menguy, C. Reynaud, B. Gouget, M. Carrière, Size-, Composition- and Shape-Dependent Toxicological Impact of Metal Oxide Nanoparticles and Carbon Nanotubes toward Bacteria, Environ. Sci. Technol. 43 (2009) 8423–8429, DOI: 10.1021/es9016975.

[87] N. Padmavathy, R. Vijayaraghavan, Enhanced bioactivity of ZnO nanoparticles - an antimicrobial study, Sci. Technol. Adv. Mater. 9 (2008) 035004, DOI: 10.1088/1468-6996/9/3/035004.

[88] K.R. Raghupathi, R.T. Koodali, A.C. Manna, Size-Dependent Bacterial Growth Inhibition and Mechanism of Antibacterial Activity of Zinc Oxide Nanoparticles, Langmuir 27 (2011) 4020–4028, DOI: 10.1021/la104825u.

[89] T. Tong, A. Shereef, J. Wu, C.T.T. Binh, J.J. Kelly, J.F. Gaillard, K.A. Gray, Effects of Material Morphology on the Phototoxicity of Nano-TiO_2 to Bacteria, Environ. Sci. Technol. 47 (2013) 12486–12495, DOI: 10.1021/es403079h.

[90] T. Tong, C.T.T. Binh, J.J. Kelly, J.F. Gaillard, K.A. Gray, Cytotoxicity of commercial nano-TiO_2 to Escherichia coli assessed by high-throughput screening: Effects of environmental factors, Water Res. 47 (2013) 2352–2362, DOI: 10.1016/j.watres.2013.02.008.

[91] A. Luthfiah, M.D. Permana, Y. Deawati, M.L. Firdaus, I. Rahayu, D.R. Eddy, Photocatalysis of nanocomposite titania–natural silica as antibacterial against *Staphylococcus aureus* and *Pseudomonas aeruginosa*, RSC Adv. 11 (2021) 38528–38536, DOI: 10.1039/D1RA07043F.

[92] F. Achouri, M. BenSaid, L. Bousselmi, S. Corbel, R. Schneider, A. Ghrabi, Comparative study of Gram-negative bacteria response to solar photocatalytic inactivation, Environ. Sci. Pollut. Res. 26 (2019) 18961–18970, DOI: 10.1007/s11356-018-2435-y.

[93] W. Jiang, H. Mashayekhi, B. Xing, Bacterial toxicity comparison between nano- and micro-scaled oxide particles, Environ. Pollut. 157 (2009) 1619–1625, DOI: 10.1016/j.envpol.2008.12.025.

[94] T.P. Dasari, K. Pathakoti, H.M. Hwang, Determination of the mechanism of photoinduced toxicity of selected metal oxide nanoparticles (ZnO, CuO, Co_3O_4 and TiO_2) to *E. coli* bacteria, J. Environ. Sci. 25 (2013) 882–888, DOI: 10.1016/S1001-0742(12)60152-1.

[95] J.M. Radziwill-Bienkowska, P. Talbot, J.B.J. Kamphuis, V. Robert, C. Cartier, I. Fourquaux, E. Lentzen, J.N. Audinot, F. Jamme, M. Réfrégiers, J.K. Bardowski, P. Langella, M. Kowalczyk, E. Houdeau, M. Thomas, M. Mercier-Bonin, Toxicity of Food-Grade TiO_2 to Commensal Intestinal and Transient Food-Borne Bacteria: New Insights Using Nano-SIMS and Synchrotron UV Fluorescence Imaging, Front. Microbiol. 9 (2018) 794, DOI: 10.3389/fmicb.2018.00794.

[96] S.T. Wang, S.P. Li, W.Q. Wang, H. You, The impact of zinc oxide nanoparticles on nitrification and the bacterial community in activated sludge in an SBR, RSC Adv. 5 (2015) 67335–67342, DOI: 10.1039/C5RA07106B.

[97] A. Lipovsky, Z. Tzitrinovich, H. Friedmann, G. Applerot, A. Gedanken, R. Lubart, EPR Study of Visible Light-Induced ROS Generation by Nanoparticles of ZnO, J. Phys. Chem. C 113 (2009) 15997–16001, DOI: 10.1021/jp904864g.

[98] M. Li, J.J. Yin, W.G. Wamer, Y.M. Lo, Mechanistic characterization of titanium dioxide nanoparticle-induced toxicity using electron spin resonance, J. Food Drug Anal. 22 (2014) 76–85, DOI: 10.1016/j.jfda.2014.01.006.

[99] U. Joost, K. Juganson, M. Visnapuu, M. Mortimer, A. Kahru, E. Nõmmiste, U. Joost, V. Kisand, A. Ivask, Photocatalytic antibacterial activity of nano-TiO_2 (anatase)-based thin films: Effects on *Escherichia coli* cells and fatty acids, J. Photochem. Photobiol. B 142 (2015) 178–185, DOI: 10.1016/j.jphotobiol.2014.12.010.

[100] B. Ezraty, A. Gennaris, F. Barras, J.F. Collet, Oxidative stress, protein damage and repair in bacteria, Nat. Rev. Microbiol. 15 (2017) 385–396, DOI: 10.1038/nrmicro.2017.26.

[101] M. Li, L. Zhu, D. Lin, Toxicity of ZnO Nanoparticles to *Escherichia coli*: Mechanism and the Influence of Medium Components, Environ. Sci. Technol. 45 (2011) 1977–1983, DOI: 10.1021/es102624t.

[102] A. Joe, S.H. Park, K.D. Shim, D.J. Kim, K.H. Jhee, H.W. Lee, C.H. Heo, H.M. Kim, E.S. Jang, Antibacterial mechanism of ZnO nanoparticles under dark conditions, J. Ind. Eng. Chem. 45 (2017) 430–439, DOI: 10.1016/j.jiec.2016.10.013.

[103] J. Pasquet, Y. Chevalier, J. Pelletier, E. Couval, D. Bouvier, M.A. Bolzinger, The contribution of zinc ions to the antimicrobial activity of zinc oxide, Colloids Surf. A 457 (2014) 263–274, DOI: 10.1016/j.colsurfa.2014.05.057.

[104] S. Nafisi, H.I. Maibach, Nanotechnology in Cosmetics, in: K. Sakamoto, R.Y. Lochhead, H.I. Maibach, Y. Yamashita (Eds.), *Cosmetic Science and Technology. Theoretical Principles and Applications*, Elsevier, Amsterdam, The Netherlands (2017) 337–369, DOI: 10.1016/B978-0-12-802005-0.00022-7.

[105] M.E. El-Naggar, T.I. Shaheen, S. Zaghloul, M.H. El-Rafie, A. Hebeish, Antibacterial Activities and UV Protection of the in Situ Synthesized Titanium Oxide Nanoparticles on Cotton Fabrics, Ind. Eng. Chem. Res. 55 (2016) 2661–2668, DOI: 10.1021/acs.iecr.5b04315.

[106] L.E. Román, J. Huachani, C. Uribe, J.L. Solís, M.M. Gómez, S. Costa, S. Costa, Blocking erythemally weighted UV radiation using cotton fabrics functionalized with ZnO nanoparticles *in situ*, Appl. Surf. Sci. 469 (2019) 204–212, DOI: 10.1016/j.apsusc.2018.11.047.

[107] J. Bai, B. Zhou, Titanium Dioxide Nanomaterials for Sensor Applications, Chem. Rev. 114 (2014) 10131–10176, DOI: 10.1021/cr400625j.

[108] L.B.V.S. Garimella, T.K. Dhiman, R. Kumar, A.K. Singh, P.R. Solanki, One-Step Synthesized ZnO np-Based Optical Sensors for Detection of Aldicarb via a Photoinduced Electron Transfer Route, ACS Omega 5 (2020) 2552−2560, DOI: 10.1021/acsomega.9b01987.

[109] J. Vinodhini, J. Mayandi, R. Atchudan, P. Jayabal, V. Sasirekha, J.M. Pearce, Effect of microwave power irradiation on TiO_2 nano-structures and binder free paste screen printed dye sensitized solar cells, Ceram. Int. 45 (2019) 4667–4673, DOI: 10.1016/j.ceramint.2018.11.157.

[110] A. Wibowo, M.A. Marsudi, M.I. Amal, M.B. Ananda, R. Stephanie, H. Ardy, L.J. Diguna, ZnO nanostructured materials for emerging solar cell applications, RSC Adv. 10 (2020) 42838–42859, DOI: 10.1039/D0RA07689A.

[111] K. Qasim, J. Chen, Z. Li, W. Lei, J. Xa, Highly-improved performance of TiO_2 nanocrystal based quantum dot light emitting diodes, RSC Adv. 3 (2013) 12104–12108, DOI: 10.1039/C3RA42055H.

[112] E. Moyen, J.H. Kim, J. Kim, J. Jang, ZnO Nanoparticles for Quantum-Dot-Based Light-Emitting Diodes, ACS Appl. Nano Mater. 3 (2020) 5203–5211, DOI: 10.1021/acsanm.0c00639.

[113] K.P. Gopinath, N.V. Madhav, A. Krishnan, R. Malolan, G. Rangarajan, Present applications of titanium dioxide for the photocatalytic removal of pollutants from water: A review, J. Environ. Manage. 270 (2020) 110906, DOI: 10.1016/j.jenvman.2020.110906.

[114] M.T. Islam, A. Dominguez, B. Alvarado-Tenorio, R.A. Bernal, M.O. Montes, J.C. Noveron, Sucrose-Mediated Fast Synthesis of Zinc Oxide Nanoparticles for the Photocatalytic Degradation of Organic Pollutants in Water, ACS Omega 4 (2019) 6560–6572, DOI: 10.1021/acsomega.9b00023.

[115] C. Zhu, J. Shi, S. Xu, M. Ishimori, J. Sui, H. Morikawa, Design and characterization of self-cleaning cotton fabrics exploiting zinc oxide nanoparticle-triggered photocatalytic degradation, Cellulose 24 (2017) 2657–2667, DOI: 10.1007/s10570-017-1289-7.

[116] W.S. Tung, W.A. Daoud, Self-cleaning fibers *via* nanotechnology: a virtual reality, J. Mater. Chem. 21 (2011) 7858–7869, DOI: 10.1039/C0JM03856C.

[117] J. Beer, H. Majmudar, Y. Mishra, D. Shukla, V. Tiwari, Nanoparticles-Mediated Interventions to Prevent Herpes Simplex Virus (HSV) Entry into Susceptible Hosts, in N. Sharma, S. Sahi (Eds.), *Nanomaterial Biointeractions at the Cellular, Organismal and System Levels. Nanomaterial Interactions in Cell Lines and Microorganisms*, Springer Nature Switzerland AG, Gewerbestrasse, Switzerland (2021) 347–370, DOI: 10.1007/978-3-030-65792-5_14.

[118] A. Markowska-Szczupak, K. Ulfig, A.W. Morawski, The application of titanium dioxide for deactivation of bioparticulates: An overview, Catal. Today 169 (2011) 249–257, DOI: 10.1016/j.cattod.2010.11.055.

[119] J. Bogdan, J. Pławińska-Czarnak, J. Zarzyńska, Nanoparticles of Titanium and Zinc Oxides as Novel Agents in Tumor Treatment: a Review, Nanoscale Res. Lett. 12 (2017) 225, DOI: 10.1186/s11671-017-2007-y.

[120] P. Yan, L.H. Liu, P. Wang, Sonodynamic Therapy (SDT) for Cancer Treatment: Advanced Sensitizers by Ultrasound Activation to Injury Tumor, ACS Appl. Bio Mater. 3 (2020) 3456–3475, DOI: 10.1021/acsabm.0c00156.

[121] L. Givelet, D. Truffier-Boutry, L. Noël, J.F. Damlencourt, P. Jitaru, T. Guérin, Optimisation and application of an analytical approach for the characterisation of TiO_2 nanoparticles in food additives and pharmaceuticals by single particle inductively coupled plasma-mass spectrometry, Talanta 224 (2021) 121873, DOI: 10.1016/j.talanta.2020.121873.

[122] Commission Regulation (EU) 2022/63 of 14 January 2022 amending Annexes II and III to Regulation (EC) Nº 1333/2008 of the European Parliament and of the Council as regards the food additive titanium dioxide (E 171), Official Journal of the European Union, L11 (18 January 2022) 1–5.

[123] The Nanodatabase Inventory (https://nanodb.dk); accessed on 16 March 2022.

[124] C.C. Lee, Y.H. Lin, W.C. Hou, M.H. Li, J.W. Chang, Exposure to ZnO/TiO_2 Nanoparticles Affects Health Outcomes in Cosmetics Salesclerks, Int. J. Environ. Res. Public Health 17 (2020) 6088, DOI: 10.3390/ijerph17176088.

[125] E. Gilbert, F. Pirot, V. Bertholle, L. Roussel, F. Falson, K. Padois, Commonly used UV filter toxicity on biological functions: review of last decade studies, Int. J. Cosmet. Sci. 35 (2013) 208–219, DOI: 10.1111/ics.12030.

[126] R. Catalano, A. Masion, F. Ziarelli, D. Slomberg, J. Laisney, J.M. Unrine, A. Campos, J. Labille, Optimizing the dispersion of nanoparticulate TiO_2-based UV filters in a non-polar medium used in sunscreen formulations – The roles of surfactants and particle coatings, Colloids Surf. A 599 (2020) 124792, DOI: 10.1016/j.colsurfa.2020.124792.

[127] J. Pasquet, Y. Chevalier, E. Couval, D. Bouvier, M.A. Bolzinger, Zinc oxide as a new antimicrobial preservative of topical products: Interactions with common formulation ingredients, Int. J. Pharm. 479 (2015) 88–95, DOI: 10.1016/j.ijpharm.2014.12.031.

[128] S. Sonia, H.L.J. Kumari, K. Ruckmani, M. Sivakumar, Antimicrobial and antioxidant potentials of biosynthesized colloidal zinc oxide nanoparticles for a fortified cold cream formulation: A potent nanocosmeceutical application, Mater. Sci. Eng. C 79 (2017) 581–589, DOI: 10.1016/j.msec.2017.05.059.

[129] L. David, B. Moldovan, A. Vulcu, L. Olenic, M. Perde-Schrepler, E. Fischer-Fodor, A. Florea, M. Crisan, I. Chiorean, S. Clichici, G.A. Filip, Green synthesis, characterization and anti-inflammatory activity of silver nanoparticles using European black elderberry fruits extract, Colloids Surf. B 122 (2014) 767–777, DOI: 10.1016/j.colsurfb.2014.08.018.

[130] A.C. Paiva-Santos, F. Mascarenhas-Melo, S.C. Coimbra, K.D. Pawar, D. Peixoto, R. Chá-Chá, A.R.T.S. Araujo, C. Cabral, S. Pinto, F. Veiga, Nanotechnology-based formulations toward the improved topical delivery of anti-acne active ingredients, Expert Opin. Drug Deliv. 18 (2021) 1435–1454, DOI: 10.1080/17425247.2021.1951218.

[131] P. Sathishkumar, J. Preethi, R. Vijayan, A.R.M. Yusoff, F. Ameen, S. Suresh, R. Balagurunathan, T. Palvannan, Anti-acne, anti-dandruff and anti-breast cancer efficacy of green synthesised silver nanoparticles using *Coriandrum sativum* leaf extract, J. Photochem. Photobiol. B 163 (2016) 69–76, DOI: 10.1016/j.jphotobiol.2016.08.005.

[132] M. Montazer, T. Harifi, Nanoscouring, in *Nanofinishing of Textile Materials*, Woodhead Publishing, Cambridge, United Kingdom (2018) 35–50, DOI: 10.1016/B978-0-08-101214-7.00003-0.

[133] M. Montazer, T. Harifi, Nanobleaching, in *Nanofinishing of Textile Materials*, Woodhead Publishing, Cambridge, United Kingdom (2018) 51–64, DOI: 10.1016/B978-0-08-101214-7.00004-2.

[134] A.K. Yetisen, H. Qu, A. Manbachi, H. Butt, M.R. Dokmeci, J.P. Hinestroza, M. Skorobogatiy, A. Khademhosseini, S.H. Yun, Nanotechnology in Textiles, ACS Nano 10 (2016) 3042–3068, DOI: 10.1021/acsnano.5b08176.

[135] P.J. Rivero, A. Urrutia, J. Goicoechea, F.J. Arregui, Nanomaterials for Functional Textiles and Fibers, Nanoscale Res. Lett. 10 (2015) 501, DOI: 10.1186/s11671-015-1195-6.

[136] G.Y. Bae, B.G. Min, Y.G. Jeong, S.C. Lee, J.H. Jang, G.H. Koo, Superhydrophobicity of cotton fabrics treated with silica nanoparticles and water-repellent agent, J. Colloid Interface Sci. 337 (2009) 170–175, DOI: 10.1016/j.jcis.2009.04.066.

[137] G. Gonçalves, P.A.A.P. Marques, T. Trindade, C.P. Neto, A. Gandini, Superhydrophobic cellulose nanocomposites, J. Colloid Interface Sci. 324 (2008) 42–46, DOI: 10.1016/j.jcis.2008.04.066.

[138] J. Li, L. Yan, Y. Zhao, F. Zha, Q. Wang, Z. Lei, One-step fabrication of robust fabrics with both-faced superhydrophobicity for the separation and capture of oil from water, Phys. Chem. Chem. Phys. 17 (2015) 6451–6457, DOI: 10.1039/C5CP00154D.

[139] M.Z. Khan, J. Militky, V. Baheti, J. Wiener, M. Vik, Development of durable superhydrophobic and UV protective cotton fabric via TiO_2/trimethoxy(octadecyl)silane nanocomposite coating, J. Text. Inst. 112 (2021) 1639–1650, DOI: 10.1080/00405000.2020.1834235.

[140] M.Z. Khan, J. Militky, V. Baheti, M. Fijalkowski, J. Wiener, L. Voleský, K. Adach, Growth of ZnO nanorods on cotton fabrics via microwave hydrothermal method: effect of size and shape of nanorods on superhydrophobic and UV-blocking properties, Cellulose 27 (2020) 10519–10539, DOI: 10.1007/s10570-020-03495-x.

[141] X. Zhu, Z. Zhang, J. Yang, X. Xu, X. Men, X. Zhou, Facile fabrication of a superhydrophobic fabric with mechanical stability and easy-repairability, J. Colloid Interface Sci. 380 (2012) 182–186, DOI: 10.1016/j.jcis.2012.04.063.

[142] W. Zhang, D. Zhang, Y. Chen, H. Lin, Hyperbranched Polymer Functional TiO_2 Nanoparticles: Synthesis and Its Application for the anti-UV Finishing of Silk Fabric, Fibers Polym. 16 (2015) 503–509, DOI: 10.1007/s12221-015-0503-1.

[143] Australian/New Zealand Standard: Sun protective clothing–Evaluation and classification, AS/NZS 4399, Standards Australia International Ltd. (1996).

[144] M. Radetić, Functionalization of textile materials with TiO_2 nanoparticles, J. Photochem. Photobiol. C 16 (2013) 62–76, DOI: 10.1016/j.jphotochemrev.2013.04.002.

[145] M.N. Morshed, X. Shen, H. Deb, S. Al Azad, X. Zhang, R. Li, Sonochemical fabrication of nanocryatalline titanium dioxide (TiO_2) in cotton fiber for durable ultraviolet resistance, J. Nat. Fibers 17 (2020) 41–54, DOI: 10.1080/15440478.2018.1465506.

[146] X. Wang, X. Sun, X. Guan, Y. Wang, X. Chen, X. Liu, Tannic interfacial linkage within ZnO-loaded fabrics for durable UV-blocking applications, Appl. Surf. Sci. 568 (2021) 150960, DOI: 10.1016/j.apsusc.2021.150960.

[147] Y. Liang, E. Pakdel, M. Zhang, L. Sun, X. Wang, Photoprotective properties of alpaca fiber melanin reinforced by rutile TiO_2 nanoparticles: A study on wool fabric, Polym. Degrad. Stab. 160 (2019) 80–88, DOI: 10.1016/j.polymdegradstab.2018.12.006.

[148] N. Bouazizi, A. Abed, S. Giraud, A. El Achari, C. Campagne, M.N. Morshed, O. Thoumire, R. El Moznine, O. Cherkaoui, J. Vieillard, F. Le Derf, Development of new composite fibers with excellent UV radiation protection, Physica E 118 (2020) 113905, DOI: 10.1016/j.physe.2019.113905.

[149] X. Xiao, X. Liu, F. Chen, D. Fang, C. Zhang, L. Xia, W. Xu, Highly Anti-UV Properties of Silk Fiber with Uniform and Conformal Nanoscale TiO_2 Coatings via Atomic Layer Deposition, ACS Appl. Mater. Interfaces 7 (2015) 21326–21333, DOI: 10.1021/acsami.5b05868.

[150] G. Zhang, Y. Liu, H. Morikawa, Y. Chen, Application of ZnO nanoparticles to enhance the antimicrobial activity and ultraviolet protective property of bamboo pulp fabric, Cellulose 20 (2013) 1877–1884, DOI: 10.1007/s10570-013-9979-2.

[151] T.A. Egerton, I.R. Tooley, UV absorption and scattering properties of inorganic-based sunscreens, Int. J. Cosmet. Sci. 34 (2012) 117–122, DOI: 10.1111/j.1468-2494.2011.00689.x.

[152] L. Teufel, A. Pipal, K.C. Schuster, T. Staudinger, B. Redl, Material-dependent growth of human skin bacteria on textiles investigated using challenge tests and DNA genotyping, J. Appl. Microbiol. 108 (2010) 450–461, DOI: 10.1111/j.1365-2672.2009.04434.x.

[153] C. Callewaert, E. De Maeseneire, F.M. Kerckhof, A. Verliefde, T. Van de Wiele, N. Boon, Microbial Odor Profile of Polyester and Cotton Clothes after a Fitness Session, Appl. Environ. Microbiol. 80 (2014) 6611–6619, DOI: 10.1128/AEM.01422-14.

[154] J. Szostak-Kotowa, Biodeterioration of textiles, Int. Biodeterior. Biodegrad. 53 (2004) 165–170, DOI: 10.1016/S0964-8305(03)00090-8.

[155] J. Zhou, D. Cai, Q. Xu, Y. Zhang, F. Fu, H. Diao, X. Liu, Excellent binding effect of L-methionine for immobilizing silver nanoparticles onto cotton fabrics to improve the antibacterial durability against washing, RSC Adv. 8 (2018) 24458–24463, DOI: 10.1039/C8RA04401E.

[156] L. Zhou, K. Yu, F. Lu, G. Lan, F. Dai, S. Shang, E. Hu, Minimizing antibiotic dosage through *in situ* formation of gold nanoparticles across antibacterial wound dressings: A facile

approach using silk fabric as the base substrate, J. Clean. Prod. 243 (2020) 118604, DOI: 10.1016/j.jclepro.2019.118604.

[157] P. Petkova, A. Francesko, I. Perelshtein, A. Gedanken, T. Tzanov, Simultaneous sonochemical-enzymatic coating of medical textiles with antibacterial ZnO nanoparticles, Ultrason. Sonochem. 29 (2016) 244–250, DOI: 10.1016/j.ultsonch.2015.09.021.

[158] M.M. Rashid, B. Simončič, B. Tomšič, Recent advances in TiO_2-functionalized textile surfaces, Surf. Interfaces 22 (2021) 100890, DOI: 10.1016/j.surfin.2020.100890.

[159] S. Sathiyavimal, S. Vasantharaj, D. Bharathi, M. Saravanan, E. Manikandan, S.S. Kumar, A. Pugazhendhi, Biogenesis of copper oxide nanoparticles (CuONPs) using *Sida acuta* and their incorporation over cotton fabrics to prevent the pathogenicity of Gram negative and Gram positive bacteria, J. Photochem. Photobiol. B 188 (2018) 126–134, DOI: 10.1016/j.jphotobiol.2018.09.014.

[160] V. Carraro, A. Sanna, A. Pinna, G. Carrucciu, S. Succa, L. Marras, G. Bertolino, V. Coroneo, Evaluation of Microbial Growth in Hospital Textiles Through Challenge Test, in G. Donelli (Ed.), *Advances in Microbiology, Infectious Diseases and Public Health*, Springer Nature Switzerland AG, Gewerbestrasse, Switzerland, 15 (2021) 19–34, DOI: 10.1007/5584_2020_560.

[161] V.H.T. Thi, B.K. Lee, Development of multifunctional self-cleaning and UV blocking cotton fabric with modification of photoactive ZnO coating via microwave method, J. Photochem. Photobiol. A 338 (2017) 13–22, DOI: 10.1016/j.jphotochem.2017.01.020.

[162] B. Tang, M. Zhang, X. Hou, J. Li, L. Sun, X. Wang, Coloration of Cotton Fibers with Anisotropic Silver Nanoparticles, Ind. Eng. Chem. Res. 51 (2012) 12807−12813, DOI: 10.1021/ie3015704.

[163] M. Sivakavinesan, M. Vanaja, G. Annadurai, Dyeing of cotton fabric materials with biogenic gold nanoparticles, Sci. Rep. 11 (2021) 13249, DOI: 10.1038/s41598-021-92662-6.

[164] C.W.M. Yuen, S.K.A. Ku, Y. Li, Y.F. Cheng, C.W. Kan, P.S.R. Choi, Improvement of wrinkle-resistant treatment by nanotechnology, J. Text. Inst. 100 (2009) 173–180, DOI: 10.1080/00405000701661028.

[165] M. Montazer, T. Harifi, Nanocrosslinking, in *Nanofinishing of Textile Materials*, Woodhead Publishing, Cambridge, United Kingdom (2018) 109–125, DOI: 10.1016/B978-0-08-101214-7.00008-X.

[166] F.M. Kelly, J.H. Johnston, Colored and Functional Silver Nanoparticle-Wool Fiber Composites, ACS Appl. Mater. Interfaces 3 (2011) 1083–1092, DOI: 10.1021/am101224v.

[167] F. Zhang, J. Yang, Preparation of Nano-ZnO and Its Application to the Textile on Antistatic Finishing, Int. J. Chem. 1 (2009) 18–22, DOI: 10.5539/ijc.v1n1p18.

[168] M. Montazer, T. Harifi, Flame-retardant textile nanofinishes, in *Nanofinishing of Textile Materials*, Woodhead Publishing, Cambridge, United Kingdom (2018) 163–181, DOI: 10.1016/B978-0-08-101214-7.00011-X.

[169] M.E. Lane, Nanoparticles and the skin–applications and limitations, J. Microencapsul. 28 (2011) 709–716, DOI: 10.3109/02652048.2011.599440.

[170] B. Baroli, Penetration of Nanoparticles and Nanomaterials in the Skin: Fiction or Reality?, J. Pharm. Sci. 99 (2010) 21–50, DOI: 10.1002/jps.21817.

[171] E. Antunes, A. Cavaco-Paulo, Stratum corneum lipid matrix with unusual packing: A molecular dynamics study, Colloids Surf. B 190 (2020) 110928, DOI: 10.1016/j.colsurfb.2020.110928.

[172] M.E. Samberg, S.J. Oldenburg, N.A. Monteiro-Riviere, Evaluation of Silver Nanoparticle Toxicity in Skin in Vivo and Keratinocytes in Vitro, Environ. Health Perspect. 118 (2010) 407–413, DOI: 10.1289/ehp.0901398.

[173] C. Bianco, G. Adami, M. Crosera, F. Larese, S. Casarin, C. Castagnoli, M. Stella, G. Maina, Silver percutaneous absorption after exposure to silver nanoparticles: A comparison study of three human skin graft samples used for clinical applications, Burns 40 (2014) 1390–1396, DOI: 10.1016/j.burns.2014.02.003.

[174] M.E.K. Kraeling, V.D. Topping, Z.M. Keltner, K.R. Belgrave, K.D. Bailey, X. Gao, J.J. Yourick, *In vitro* percutaneous penetration of silver nanoparticles in pig and human skin, Regul. Toxicol. Pharmacol. 95 (2018) 314–322, DOI: 10.1016/j.yrtph.2018.04.006.

[175] F.F. Larese, F. D'Agostin, M. Crosera, G. Adami, N. Renzi, M. Bovenzi, G. Maina, Human skin penetration of silver nanoparticles through intact and damaged skin, Toxicology 255 (2009) 33–37, DOI: 10.1016/j.tox.2008.09.025.

[176] P. Filipe, J.N. Silva, R. Silva, J.L. Cirne De Castro, M. Marques Gomes, L.C. Alves, R. Santus, T. Pinheiro, Stratum Corneum is an Effective Barrier to TiO_2 and ZnO Nanoparticle Percutaneous Absorption, Skin Pharmacol. Physiol. 22 (2009) 266–275, DOI: 10.1159/000235554.

[177] Z. Szikszai, Zs. Kertész, E. Bodnár, I. Borbíró, B. Kiss, A. Angyal, L. Csedreki, E. Furu, Z. Szoboszlai, Á.Z. Kiss, J. Hunyadi, Nuclear microprobe investigation of the penetration of ultrafine zinc oxide into human skin affected by atopic dermatitis, Nucl. Instrum. Methods Phys. Res. B 269 (2011) 2278–2280, DOI: 10.1016/j.nimb.2011.02.055.

[178] A.M. Holmes, Z. Song, H.R. Moghimi, M.S. Roberts, Relative Penetration of Zinc Oxide and Zinc Ions into Human Skin after Application of Different Zinc Oxide Formulations, ACS Nano 10 (2016) 1810–1819, DOI: 10.1021/acsnano.5b04148.

[179] V.R. Leite-Silva, W.Y. Sanchez, H. Studier, D.C. Liu, Y.H. Mohammed, A.M. Holmes, E.M. Ryan, I.N. Haridass, N.C. Chandrasekaran, W. Becker, J.E. Grice, H.A.E. Benson, M.S. Roberts, Human skin penetration and local effects of topical nano zinc oxide after occlusion and barrier impairment, Eur. J. Pharm. Biopharm. 104 (2016) 140–147, DOI: 10.1016/j.ejpb.2016.04.022.

[180] Z. Pan, W. Lee, L. Slutsky, R.A.F. Clark, N. Pernodet, M.H. Rafailovich, Adverse Effects of Titanium Dioxide Nanoparticles on Human Dermal Fibroblasts and How to Protect Cells, Small 5 (2009) 511–520, DOI: 10.1002/smll.200800798.

[181] V. Bastos, J.M.P. Ferreira de Oliveira, D. Brown, H. Jonhston, E. Malheiro, A.L. Daniel-da-Silva, I.F. Duarte, C. Santos, H. Oliveira, The influence of Citrate or PEG coating on silver nanoparticle toxicity to a human keratinocyte cell line, Toxicol. Lett. 249 (2016) 29–41, DOI: 10.1016/j.toxlet.2016.03.005.

[182] P.L. Sanches, W. Souza, S. Gemini-Piperni, A.L. Rossi, S. Scapin, V. Midlej, Y. Sade, A.F.P. Leme, M. Benchimol, L.A. Rocha, R.B.V. Carias, R. Borojevic, J.M. Granjeiro, A.R. Ribeiro, Rutile nano-bio-interactions mediate dissimilar intracellular destiny in human skin cells, Nanoscale Adv. 1 (2019) 2216–2228, DOI: 10.1039/C9NA00078J.

[183] S. Arora, N. Tyagi, A. Bhardwaj, L. Rusu, R. Palanki, K. Vig, S.R. Singh, A.P. Singh, S. Palanki, M.E. Miller, J.E. Carter, S. Singh, Silver nanoparticles protect human keratinocytes against UVB radiation-induced DNA damage and apoptosis: potential for prevention of skin carcinogenesis, Nanomed.-Nanotechnol. Biol. Med. 11 (2015) 1265–1275, DOI: 10.1016/j.nano.2015.02.024.

[184] M. Ramasamy, M. Das, S.S.A. An, D.K. Yi, Role of surface modification in zinc oxide nanoparticles and its toxicity assessment toward human dermal fibroblast cells, Int. J. Nanomed. 9 (2014) 3707–3718, DOI: 10.2147/IJN.S65086.

[185] S.G. Mukherjee, N. O'Claonadh, A. Casey, G. Chambers, Comparative *in vitro* cytotoxicity study of silver nanoparticle on two mammalian cell lines, Toxicol. Vitr. 26 (2012) 238–251, DOI: 10.1016/j.tiv.2011.12.004.

[186] I. de la Calle, M. Menta, M. Klein, B. Maxit, F. Séby, Towards routine analysis of TiO_2 (nano-)particle size in consumer products: Evaluation of potential techniques, Spectrochim. Acta B 147 (2018) 28–42, DOI: 10.1016/j.sab.2018.05.012.

[187] I. de la Calle, M. Menta, M. Klein, F. Séby, Screening of TiO_2 and Au nanoparticles in cosmetics and determination of elemental impurities by multiple techniques (DLS, SPICP-MS, ICP-MS and ICP-OES), Talanta 171 (2017) 291–306, DOI: 10.1016/j.talanta.2017.05.002.

[188] C. Lorenz, K. Tiede, S. Tear, A. Boxall, N. Von Goetz, K. Hungerbühler, Imaging and Characterization of Engineered Nanoparticles in Sunscreens by Electron Microscopy, Under Wet and Dry Conditions, Int. J. Occup. Environ. Health 16 (2010) 406–428, DOI: 10.1179/107735210799160101.

[189] P.J. Lu, S.C. Huang, Y.P. Chen, L.C. Chiueh, D.Y.C. Shih, Analysis of titanium dioxide and zinc oxide nanoparticles in cosmetics, J. Food Drug Anal. 23 (2015) 587–594, DOI: 10.1016/j.jfda.2015.02.009.

[190] P.J. Lu, W.L. Cheng, S.C. Huang, Y.P. Chen, H.K. Chou, H.F. Cheng, Characterizing titanium dioxide and zinc oxide nanoparticles in sunscreen spray, Int. J. Cosmet. Sci. 37 (2015) 620–626, DOI: 10.1111/ics.12239.

[191] M. Sysoltseva, R. Winterhalter, A.S. Wochnik, C. Scheu, H. Fromme, Electron microscopic investigation and elemental analysis of titanium dioxide in sun lotion, Int. J. Cosmet. Sci. 39 (2017) 292–300, DOI: 10.1111/ics.12375.

[192] P.J. Lu, S.W. Fang, W.L. Cheng, S.C. Huang, M.C. Huang, H.F. Cheng, Characterization of titanium dioxide and zinc oxide nanoparticles in sunscreen powder by comparing different measurement methods, J. Food Drug Anal. 26 (2018) 1192–1200, DOI: 10.1016/j.jfda.2018.01.010.

[193] Z.A. Lewicka, A.F. Benedetto, D.N. Benoit, W.W. Yu, J.D. Fortner, V.L. Colvin, The structure, composition, and dimensions of TiO_2 and ZnO nanomaterials in commercial sunscreens, J. Nanopart. Res. 13 (2011) 3607, DOI: 10.1007/s11051-011-0438-4.

[194] S. Benítez-Martínez, A.I. López-Lorente, M. Valcárcel, Determination of TiO_2 nanoparticles in sunscreen using N-doped graphene quantum dots as a fluorescent probe, Microchim. Acta 183 (2016) 781–789, DOI: 10.1007/s00604-015-1696-0.

[195] J.C. García-Mesa, P. Montoro-Leal, A. Rodríguez-Moreno, M.M. López Guerrero, E.I. Vereda Alonso, Direct solid sampling for speciation of Zn^{2+} and ZnO nanoparticles in cosmetics by graphite furnace atomic absorption spectrometry, Talanta 223 (2021) 121795, DOI: 10.1016/j.talanta.2020.121795.

[196] A. Samontha, J. Shiowatana, A. Siripinyanond, Particle size characterization of titanium dioxide in sunscreen products using sedimentation field-flow fractionation-inductively coupled plasma-mass spectrometry, Anal. Bioanal. Chem. 399 (2011) 973–978, DOI: 10.1007/s00216-010-4298-z.

[197] C. Contado, A. Pagnoni, TiO_2 in Commercial Sunscreen Lotion: Flow Field-Flow Fractionation and ICP-AES Together for Size Analysis, Anal. Chem. 80 (2008) 7594–7608, DOI: 10.1021/ac8012626.

[198] V. Nischwitz, H. Goenaga-Infante, Improved sample preparation and quality control for the characterisation of titanium dioxide nanoparticles in sunscreens using flow field-flow fractionation on-line with inductively coupled plasma mass spectrometry, J. Anal. At. Spectrom. 27 (2012) 1084–1092, DOI: 10.1039/C2JA10387G.

[199] I. López-Heras, Y. Madrid, C. Cámara, Prospects and difficulties in TiO_2 nanoparticles analysis in cosmetic and food products using asymmetrical flow field-flow fractionation

hyphenated to inductively coupled plasma mass spectrometry, Talanta 124 (2014) 71–78, DOI: 10.1016/j.talanta.2014.02.029.

[200] B. Bocca, S. Caimi, O. Senofonte, A. Alimonti, F. Petrucci, ICP-MS based methods to characterize nanoparticles of TiO_2 and ZnO in sunscreens with focus on regulatory and safety issues, Sci. Total Environ. 630 (2018) 922–930, DOI: 10.1016/j.scitotenv.2018.02.166.

[201] Y. Dan, H. Shi, C. Stephan, X. Liang, Rapid analysis of titanium dioxide nanoparticles in sunscreens using single particle inductively coupled plasma-mass spectrometry, Microchem. J. 122 (2015) 119–126, DOI: 10.1016/j.microc.2015.04.018.

[202] D. Voelker, K. Schlich, L. Hohndorf, W. Koch, U. Kuehnen, C. Polleichtner, C. Kussatz, K. Hund-Rinke, Approach on environmental risk assessment of nanosilver released from textiles, Environ. Res. 140 (2015) 661–672, DOI: 10.1016/j.envres.2015.05.011.

[203] D.M. Mitrano, Y.A.R. Dasilva, B. Nowack, Effect of Variations of Washing Solution Chemistry on Nanomaterial Physicochemical Changes in the Laundry Cycle, Environ. Sci. Technol. 49 (2015) 9665–9673, DOI: 10.1021/acs.est.5b02262.

[204] C. Lorenz, L. Windler, N. von Goetz, R.P. Lehmann, M. Schuppler, K. Hungerbühler, M. Heuberger, B. Nowack, Characterization of silver release from commercially available functional (nano)textiles, Chemosphere 89 (2012) 817–824, DOI: 10.1016/j.chemosphere.2012.04.063.

[205] E. Lombi, E. Donner, K.G. Scheckel, R. Sekine, C. Lorenz, N. Von Goetz, B. Nowack, Silver speciation and release in commercial antimicrobial textiles as influenced by washing, Chemosphere 111 (2014) 352–358, DOI: 10.1016/j.chemosphere.2014.03.116.

[206] D.M. Mitrano, E. Lombi, Y.A.R. Dasilva, B. Nowack, Unraveling the Complexity in the Aging of Nanoenhanced Textiles: A Comprehensive Sequential Study on the Effects of Sunlight and Washing on Silver Nanoparticles, Environ. Sci. Technol. 50 (2016) 5790–5799, DOI: 10.1021/acs.est.6b01478.

[207] L. Geranio, M. Heuberger, B. Nowack, The Behavior of Silver Nanotextiles during Washing, Environ. Sci. Technol. 43 (2009) 8113–8118, DOI: 10.1021/es9018332.

[208] L. Windler, C. Lorenz, N. von Goetz, K. Hungerbühler, M. Amberg, M. Heuberger, B. Nowack, Release of Titanium Dioxide from Textiles during Washing, Environ. Sci. Technol. 46 (2012) 8181–8188, DOI: 10.1021/es301633b.

[209] E. Spielman-Sun, T. Zaikova, T. Dankovich, J. Yun, M. Ryan, J.E. Hutchison, G.V. Lowry, Effect of silver concentration and chemical transformations on release and antibacterial efficacy in silver-containing textiles, NanoImpact 11 (2018) 51–57, DOI: 10.1016/j.impact.2018.02.002.

[210] S. Wagener, N. Dommershausen, H. Jungnickel, P. Laux, D. Mitrano, B. Nowack, G. Schneider, A. Luch, Textile Functionalization and Its Effects on the Release of Silver Nanoparticles into Artificial Sweat, Environ. Sci. Technol. 50 (2016) 5927–5934, DOI: 10.1021/acs.est.5b06137.

[211] N. von Goetz, C. Lorenz, L. Windler, B. Nowack, M. Heuberger, K. Hungerbühler, Migration of Ag- and TiO_2-(Nano)particles from Textiles into Artificial Sweat under Physical Stress: Experiments and Exposure Modeling, Environ. Sci. Technol. 47 (2013) 9979–9987, DOI: 10.1021/es304329w.

[212] K. Kulthong, S. Srisung, K. Boonpavanitchakul, W. Kangwansupamonkon, R. Maniratanachote, Determination of silver nanoparticle release from antibacterial fabrics into artificial sweat, Part. Fibre Toxicol. 7 (2010) 8, DOI: 10.1186/1743-8977-7-8.

[213] T.M. Benn, P. Westerhoff, Nanoparticle Silver Released into Water from Commercially Available Sock Fabrics, Environ. Sci. Technol. 42 (2008) 4133–4139, DOI: 10.1021/es7032718.

[214] R.B. Reed, T. Zaikova, A. Barber, M. Simonich, R. Lankone, M. Marco, K. Hristovski, P. Herckes, L. Passantino, D.H. Fairbrother, R. Tanguay, J.F. Ranville, J.E. Hutchison, P.K. Westerhoff, Potential Environmental Impacts and Antimicrobial Efficacy of Silver- and Nanosilver-Containing Textiles, Environ. Sci. Technol. 50 (2016) 4018–4026, DOI: 10.1021/acs.est.5b06043.

[215] C. Degueldre, P.Y. Favarger, S. Wold, Gold colloid analysis by inductively coupled plasma-mass spectrometry in a single particle mode, Anal. Chim. Acta 555 (2006) 263–268, DOI: 10.1016/j.aca.2005.09.021.

[216] F. Laborda, E. Bolea, J. Jiménez-Lamana, Single Particle Inductively Coupled Plasma Mass Spectrometry: A Powerful Tool for Nanoanalysis, Anal. Chem. 86 (2014) 2270–2278, DOI: 10.1021/ac402980q.

[217] F. Laborda, E. Bolea, J. Jiménez-Lamana, Single particle inductively coupled plasma mass spectrometry for the analysis of inorganic engineered nanoparticles in environmental samples, Trends Environ. Anal. Chem. 9 (2016) 15–23, DOI: 10.1016/j.teac.2016.02.001.

[218] M. Witzler, F. Küllmer, A. Hirtz, K. Günther, Validation of Gold and Silver Nanoparticle Analysis in Fruit Juices by Single-Particle ICP-MS without Sample Pretreatment, J. Agric. Food Chem. 64 (2016) 4165–4170, DOI: 10.1021/acs.jafc.6b01248.

II. OBJECTIVES

II. OBJECTIVES

The determination of the total metal content in cosmetics and textiles is investigated since several metals cause skin allergies and can even be toxic to humans. Furthermore, the presence of metal compounds in cosmetic products and fabrics is regulated by the European Regulations 1223/2009 and 1907/2006, respectively.

Moreover, the continuous increase of fabrics and cosmetics modified with inorganic NPs requires the development of nanometrological platforms for the characterisation (size, shape, and composition) and quantification of NPs in these complex matrices. The determination of NPs in products in direct and long-term contact with the skin is necessary because studies on their toxicity are scarce. In addition, the assessment of inorganic NPs in cosmetic products must be carried out to ensure law enforcement (Regulation 1223/2009).

The specific objectives of this Doctoral Thesis are:

- Developing microwave-assisted acid digestion procedures for the determination of total metal content in moisturisers and textiles by ICP-MS.

- Optimising ultrasound-assisted methodologies to carry out the extraction of inorganic NPs from moisturising creams using organic solvents as extractants before their quantification by spICP-MS.

- Evaluating the release of inorganic NPs from fabrics by mechanical shaking in ultrapure water under controlled temperature conditions (sample pre-treatment) and spICP-MS (assessment of NPs).

- Developing sample pre-treatments to preconcentrate and clean extracts from moisturisers and fabrics prior to their characterisation by electron microscopic techniques for the qualitative characterisation of NPs (comparative purposes).

III. METHODOLOGY

III. METHODOLOGY

This Doctoral thesis is divided into five chapters:

Chapter 1. Quantification of metals in moisturising creams using microwave-assisted acid digestion and ICP-MS
A microwave-assisted acid digestion procedure using a mixture of nitric acid and hydrogen peroxide was used for the sample pre-treatment of moisturisers prior to their total metal content by ICP-MS.

Chapter 2. Metal content in textile and (nano)textile products
Metal quantification in textiles and textiles modified with inorganic NPs was carried out by ICP-MS after their microwave-assisted acid digestion. The presence of inorganic compounds (mainly titanium and silica) in textile fibres hinders the complete decomposition of several samples. A mixture of oxidising agents (nitric acid and hydrogen peroxide) and complexing agents (hydrochloric acid and hydrofluoric acid) was used to completely digest the studied fabrics.

Chapter 3. Silver nanoparticles assessment in moisturising creams by ultrasound-assisted extraction followed by spICP-MS
An ultrasound-assisted extraction method has been developed for the determination of AgNPs in moisturisers prescribed for atopic dermatitis. Factors affecting the extraction process such as type of extractant, energy (amplitude of ultrasonic probe), time, volume of extractant, and ultrasonication mode (continuous or discontinuous ultrasonication) were evaluated and optimised. The extracts from moisturisers were analysed by spICP-MS for the determination of AgNPs concentration (mass and number concentrations), AgNPs size distribution (mode and mean sizes), and ionic silver content. Extracts from studied creams were also analysed by electron microscopy (SEM-EDX and TEM) after a clean-up procedure based on an ultrasound water-bath oxidative treatment with hydrogen peroxide for comparative purposes.
Moisturisers and extracts were also acid digested using microwave energy to assess their total silver content by ICP-MS.

Chapter 4. spICP-MS assessment of ZnONPs and TiO_2NPs in moisturisers after a tip sonication sample pre-treatment
The proposed methodology was based on the ultrasound-assisted extraction of TiO_2NPs and ZnONPs from moisturising creams using acetone as a solvent prior to spICP-MS assessment (size distribution, NPs concentration, and ionic content). spICP-MS results were compared with total content in the extracts and in the acid digests. HRTEM-EDX analysis of extracts was also carried out for NPs characterisation.

Chapter 5. spICP-MS characterisation of silver nanoparticles released from textile products
AgNPs have been released from fabrics by mechanical shaking under controlled temperature using ultrapure water as an extractant. spICP-MS has been used for AgNPs determination in the aqueous extracts from textiles owing to its low detection limits (ng L^{-1}) and information provided on nanoparticle concentration and size distribution. HRTEM-EDX also confirmed the presence of AgNPs in aqueous extracts from textiles.
Microwave-assisted acid digestion of fabrics was also carried out, followed by ICP-MS analysis to determine the total silver content.

IV. RESULTS AND DISCUSSION

PART A. DETERMINATION OF TOTAL METAL CONTENT IN MOISTURISERS AND TEXTILES

CHAPTER 1. QUANTIFICATION OF METALS IN MOISTURISING CREAMS USING MICROWAVE-ASSISTED ACID DIGESTION AND ICP-MS

CHAPTER 1. QUANTIFICATION OF METALS IN MOISTURISING CREAMS USING MICROWAVE-ASSISTED ACID DIGESTION AND ICP-MS

1.1 ABSTRACT

Metals are present in cosmetics owing to a deliberated addition by manufacturers, contamination of raw materials, and/or contamination during their manufacture or storage. The metal content of cosmetics is regulated by the European Commission (Regulation 1223/2009). Moisturisers have been digested (microwave-assisted acid digestion) and analysed by inductively coupled plasma mass spectrometry (ICP-MS) for metal assessment. The ICP-MS measurement was successfully validated (RSDs lower than 5% and analytical recoveries within the 91–110% range). The proposed methodology was applied to several moisturising creams to assess their total metal content. Banned metals in cosmetics like beryllium, cadmium, mercury, and lead were quantified in several studied moisturisers. Furthermore, nickel, chromium, and cobalt (potential skin allergens) were also found in the analysed creams.

1.2 INTRODUCTION

The colouration of cosmetics can be achieved by the addition of compounds based on metals such as antimony, cadmium, and chromium [1]. Whitening colours, which are preferable in moisturising creams, are obtained by adding aluminium, silver, zinc oxide, and titanium dioxide powders, among others [2]. Moreover, metals modify the surface appearance of cosmetics, providing metal brightness (copper, brass, silver, gold, and aluminium powders), pearled glitter (bismuth oxychloride and mica), or dullness (titanium dioxide) [3]. Inorganic mercury species, like ammoniated mercury, are added to skin lightening creams due to their ability to inhibit the formation of melanin by competing with copper in the enzyme tyrosinase. On the other hand, organic mercury species (phenyl and thiomersal mercury salts) are used to preserve cosmetics [1].

Table S1.1 (Supplementary Information) summarises the properties provided by metal-based compounds to moisturising creams. This table is an adaptation from the European Commission's inventory of ingredients in cosmetics [4], and it has been prepared considering the metal compounds allowed by the Regulation 1223/2009 on cosmetic products [5] and the type of matrix under study (moisturisers).

Nevertheless, metals in cosmetics can penetrate the skin, reaching its deepest layers or even the bloodstream. Thus, metals can be distributed throughout the body and accumulated in several organs and tissues. This risk is enhanced considering the daily use and the prolonged exposure to cosmetic products.

Several studies have demonstrated metal percutaneous penetration and skin lesions caused by metals. Long-term exposure to arsenic has been reported to produce skin lesions such as hyperpigmentation, hyperkeratosis, and basal and squamous cell carcinomas [6,7]. Beryllium salts cause dermal hypersensitivity resulting in dermatitis or even ulcers [8,9], and gold salts are skin allergens [10]. Nickel, cobalt, and chromium also cause contact allergies and *in vitro* experiments have shown that these chemicals can penetrate through the skin [11,12].

Thallium salts, typically used in depilatory products in the 1920s, are now forbidden in cosmetic formulations since these salts cause alopecia, in addition to poisoning symptoms like gastrointestinal disorders, nervous system damage, cardiac diseases, hallucinations, and delirium [13]. Chronic topical exposure to mercury salts leads to bluish/blackish pigmentation of the skin, contact dermatitis, erythroderma, purpura, gingivostomatitis, and acrodynia (the latter disease is common in children) [14]. Zirconium salts can be used in antiperspirants, but their use has been demonstrated to cause granulomas [15]. Compounds of lead and barium are able to penetrate through the skin [16,17], and cadmium causes oxidative stress and DNA damage in the HaCaT cell line (immortalised non-tumoral human keratinocytes) [18]. Bluish-black skin discolouration, scaling and itching of the skin, and inhibition of sweat secretion can be induced by tellurium exposure [19]. Studies on the dermal toxicity of vanadium in humans are not available, but pentavalent vanadium (the most toxic vanadium form) has been shown to accumulate in the lungs and can be distributed throughout the body, causing diseases or even poisoning human organs [20].

Because of these possible hazardous effects, the presence of metals in cosmetic products is regulated by the Regulation 1223/2009 in Europe [5]. This regulation bans antimony, arsenic, beryllium, cadmium, lead, tellurium, thallium, zirconium, mercury, and their compounds in cosmetic products. In addition, the use of barium salts, gold salts, various strontium compounds (lactate, nitrate, and polycarboxylate), chromium, divanadium pentaoxide, indium phosphide, nickel and a lot of nickel compounds, and several compounds of potassium, sodium, cobalt, molybdenum, and tin are not allowed. There are several exceptions to the aforementioned prohibitions, barium sulphides (depilatories, 6% as sulphur), barium colourants listed in the Annex IV, phenylmercuric salts (as preservatives in eye products up to 0.007% Hg), aluminium zirconium chloride hydroxide complexes (antiperspirants products and 5.4% of zirconium as maximum concentration), and gold (colouring purposes, code: E175; purity: 90% or higher [5,21]) can be added to cosmetics. Metal compounds allowed in cosmetic products are listed in the Annexes III, IV, V, and VI of the Regulation 1223/2009 (“list of substances which cosmetic products must not contain except subject to the restrictions laid down”, “list of colourants allowed in cosmetic products”, “list of preservatives allowed in cosmetic products”, and “list of UV filters allowed in cosmetic products”, respectively) [5].

According to the literature, most trace metal analyses in cosmetic matrices focus on coloured make-up products since a lot of pigments contain metal compounds. However, studies about the presence of metals in daily used personal care items, like moisturising creams, are scarce [22–29]. Therefore, this study deals with a simple methodology for metal quantification in moisturisers using microwave-assisted acid digestion followed by inductively coupled plasma mass spectrometry (ICP-MS).

1.3 MATERIAL AND METHODS

1.3.1 Instrumentation

An analytical balance ML 204T (Mettler Toledo, Colombus, OH, USA) was used for weighing reagents and samples. An ETHOS PLUS microwave lab-station (Milestone, Sorisole, Italy) was used for microwave-assisted acid digestion of moisturisers. Quantification of metals was carried out using a NexION® 300X ICP-MS (Perkin Elmer, Waltham, MA, USA) equipped with a SeaFastSC2 DX autosampler (Elemental Scientific, Omaha, NB, USA). Nebulisation was carried out by a Meinhard® nebuliser and a cyclonic spray chamber thermostated by a Peltier refrigerator.

1.3.2 Reagents

69% Nitric acid (Hiperpur) and 33% hydrogen peroxide were from Panreac (Barcelona, Spain). Memory Test 1 Solution (1000 mg L^{-1} Al, Ca, Fe, K, Mg, Na and 20 mg L^{-1}Ag, As, Ba, Be, Cd, Co, Cr, Cu, Mn, Ni, Pb, Se, Tl, V, Zn), NexIon Setup Solution (10 µg L^{-1} of U, Pb, Mg, Li, In, Fe, Ce, Be), and individual standards of Sn, Ge, Rh, and In (1000 mg L^{-1} each) were supplied by Perkin Elmer. Standards of 1000 mg L^{-1} B, Li, Mo, and Sb were purchased from Merck (Darmstadt, Germany). Y and Hg (1000 mg L^{-1} each) were from Panreac and Scharlau (Barcelona, Spain), respectively. Ultrapure water (18 MΩcm) was collected from a Milli-Q® water purification system (Millipore, Bedford, MA, USA).

1.3.3 Samples

The composition of analysed moisturisers is shown in **Table S1.2** (Supplementary Information). These cosmetic samples were purchased from online stores (creams coded as C1, C2, C4, and C5) and from local shops in Santiago de Compostela, Spain (moisturiser C3 was bought in a pharmacy and coded creams from C6 to C14 in cosmetic shops). Before sampling, the upper part of the creams was removed (due to their possible oxidation) and they were homogenised with a plastic spatula. Samples were sealed and kept at 4°C.

1.3.4 Microwave-assisted acid digestion

Moisturising creams (0.2000 g) were placed into a Teflon digestion vessel (100 mL), and 3.0 mL of 69% nitric acid, 1.0 mL of 33% hydrogen peroxide, and 4.0 mL of ultrapure water were then added. The samples were then digested using the microwave operating conditions shown in **Table 1.1**.

Moisturisers were digested in triplicate and one blank was carried out for each set of digestions. Once digestion was completed, samples and blanks were made up to 25 mL with ultrapure water.

Table 1.1. Operating conditions for microwave-assisted acid digestion of moisturising creams

Time (min)	Temperature (°C)
0-2	Room temperature-90
2-7	90-140
7-12	140-200
12-27	200

1.3.5 Quantification of metals by ICP-MS

A solution containing 1 µg L^{-1} of Be, Ce, Fe, ln, Li, Mg, Pb, and U was used for daily adjustment of ICP-MS parameters (torch position, nebulisation flow, and quadrupole voltages) to enhance the sensitivity.

Acid digests were ten-fold diluted with ultrapure water prior to ICP-MS analyses, except for samples coded as C1 and C2, which were five thousand times diluted for zinc assessment and twenty times for the remaining metals.

Table 1.2 shows the ICP-MS parameters used for metal determination, where a longer dwell time (200 ms instead 50 ms) was used for arsenic assessment due to its low sensitivity.

Standard addition calibration was performed to avoid matrix effects. The calibration covered the linear range of 0–100 µg L^{-1}, except for aluminium and iron (0–5000 µg L^{-1}). Polyatomic interferences were minimised using helium as a collision cell gas (variable helium flow rates were used depending on the analyte, **Table 1.2**).

Germanium, yttrium, rhodium, and indium were used as internal standards (10 μg L^{-1} in 1% HNO_3). Internal standards were added to standards and samples using a T-shaped plastic connector before their introduction into the nebuliser.

Table 1.2. ICP-MS parameters for metal determination in moisturisers

Operating parameters	
Radiofrequency power (W)	1600
Plasma gas flow (L min^{-1})	16
Auxiliary gas flow (L min^{-1})	1.2
Nebulisation gas flow (L min^{-1})	0.9 – 1.1
Collision cell gas	He
Acquisition parameters	
Replicates	3
Sweeps / Reading	20
Dwell time per amu (ms)	50 (200 for As)
Integration time (ms)	1000 (4000 for As)
Monitored ions (*m/z*)	
1.0 mL min^{-1} He	^{7}Li, ^{9}Be, ^{55}Mn, ^{63}Cu, ^{98}Mo, ^{107}Ag, ^{111}Cd, ^{138}Ba, ^{202}Hg, ^{208}Pb
4.0 mL min^{-1} He	^{27}Al, ^{51}V, ^{53}Cr, ^{57}Fe, ^{59}Co, ^{60}Ni, ^{66}Zn, ^{75}As, ^{118}Sn, ^{121}Sb
Internal standards	^{74}Ge, ^{89}Y, ^{103}Rh, ^{115}In

1.3.6 Validation

Limit of detection (LOD) and limit of quantification (LOQ) were calculated in terms of $3\sigma/m$ and $10\sigma/m$ criteria, respectively [σ is the standard deviation of eleven measurements of a blank (1% nitric acid) by ICP-MS, and m is the slope of the standard addition calibration). The LODs and LOQs for the studied metals are listed in **Table 1.3**. The lowest LOQ was obtained for beryllium (0.00770 μg g^{-1}) and the highest was for aluminium (3.37 μg g^{-1}).

The precision of ICP-MS determinations was assessed by the relative standard deviation (RSD) of eleven measurements of an acid digest from a moisturising cream. RSDs of the concentrations in the digested creams are shown in **Table 1.3**. The calculated RSDs values were in the range of 1–4% which demonstrated the high precision of ICP-MS assessment.

Due to the lack of certified reference materials, the accuracy of ICP-MS analyses was evaluated by analytical recovery assays after spiking acid digests at several concentration levels (**Table 1.3**). Analytical recoveries at each spiked concentration level were calculated for all analytes after eleven ICP-MS measurements, and the obtained values (91–110%) verified the accuracy of ICP-MS quantification.

Table 1.3. Methodology validation

			Analytical recoveries		
	LOD_{method} (µg g^{-1})	LOQ_{method} (µg g^{-1})	µg L^{-1} added	Mean value (%)	RSD (%)
Li	0.00932	0.0311	0.25, 0.50,1.0	107 ± 3	3
Be	0.00231	0.00770	0.25, 0.50,1.0	106 ± 4	1
Al	1.01	3.37	12.5, 25.0, 50.0	100 ± 6	3
V	0.00602	0.0201	0.25, 0.50,1.0	105 ± 4	3
Cr	0.0266	0.0887	0.25, 0.50,1.0	110 ± 5	3
Mn	0.00623	0.0208	0.25, 0.50,1.0	106 ± 5	1
Fe	0.171	0.571	12.5, 25.0, 50.0	105 ± 4	3
Co	0.00249	0.00829	0.25, 0.50,1.0	106 ± 3	2
Ni	0.0323	0.108	0.50, 1.0	91 ± 3	3
Cu	0.0220	0.0734	0.50, 1.0	105 ± 4	1
Zn	0.0594	0.198	25.0, 50.0	109 ± 4	2
As	0.0235	0.0785	0.25, 0.50, 1.0	104 ± 4	3
Mo	0.00271	0.00905	0.25, 0.50, 1.0	108 ± 6	1
Ag	0.0102	0.0339	0.25, 0.50, 1.0	96 ± 2	2
Cd	0.00663	0.0221	0.25, 0.50, 1.0	99 ± 4	2
Sn	0.00757	0.0252	0.25, 0.50, 1.0	102 ± 6	2
Sb	0.0230	0.0765	0.25, 0.50, 1.0	93 ± 5	4
Ba	0.0152	0.0505	0.25, 0.50, 1.0	104 ± 5	1
Hg	0.0265	0.0885	1.0, 5.0, 10	102 ± 2	3
Pb	0.00866	0.0289	0.25, 0.50,1.0	105 ± 4	2

1.4 RESULTS AND DISCUSSION

Table 1.4 shows the concentrations of metals found in the analysed moisturisers. As mentioned before, compounds or salts of arsenic, antimony, beryllium, cadmium, lead, and mercury are not allowed in cosmetic samples in the European Community [5]. Nevertheless, quantifiable amounts of some of these forbidden metals were found in some moisturising creams. Beryllium was present in samples coded as C1 and C2 (0.00809±0.000838 and 0.0825±0.00455 µg g^{-1}, respectively). Cream C2 was the only sample which contains cadmium (0.0745±0.00958 µg g^{-1}). Lead was quantified in four moisturisers (C1, C2, C6, and C7), and the concentrations ranged between 0.0342 and 0.437 µg g^{-1}. In addition, moisturising creams coded as C2, C3, C4, and C10 were found to contain mercury (within the range of 0.0990–0.180 µg g^{-1}). On the other hand, arsenic and antimony were not detected in any studied cosmetic sample.

Besides, nickel (and a vast number of nickel compounds), chromium, and several cobalt compounds are not allowed due to their allergenic potential. However, chromium was quantified in three creams (codes C2, C3, and C10), cobalt in two (codes C2 and C3), and nickel in six samples (codes C2, C4, C5, C6, C11, and C12), and the concentration ranges were 0.0934–0.303 µg g^{-1}, 0.0178–0.134 µg g^{-1}, and 0.164–0.559 µg g^{-1} for Cr, Co, and Ni, respectively.

Aluminium and aluminium compounds provide whitening colours, and functions like skin conditioning, emulsion stabilising, opacifying, and viscosity controlling, as is indicated in **Table S1.1**. Creams C13 and C14 were found to contain relatively similar aluminium content

(5.10±0.0212 and 7.47±0.162 μg g^{-1}, respectively), while it was quantified at higher levels in samples C2 (2176±257.7 μg g^{-1}) and C8 (31.3±1.72 μg g^{-1}).
The European Commission allows the use of zinc oxide and zinc stearate as whitening colourants, as well as zinc oxide (bulk and nanoparticulate forms) as an UV filter. The maximum concentration of zinc oxide is 25% (w/w), also in the case of combining bulk and nano form [5]. Furthermore, a high number of zinc compounds is used to achieve properties such as skin protecting, skin conditioning, antimicrobial, and opacifying, among others (**Table S1.1**), but the maximum concentration of several of these zinc compounds is regulated as in the case of zinc peroxide (4.0% of H_2O_2, present or released, in skin products) and several water-soluble zinc salts (acetate, chloride, gluconate, and glutamate not exceeding the 1% as zinc) [5].
Nine of the fourteen studied samples contain zinc, and samples C1 and C2 were found to contain very high zinc concentrations (73479±3017 and 25455±1601 μg g^{-1}, respectively). Zinc concentrations in the remaining moisturisers varied from 1.83 to 41.2 μg g^{-1}.
Several manganese compounds are added to cosmetics to obtain skin conditioning and moisturising properties (**Table S1.1**). The results show that twelve moisturisers contained manganese in their formulations within the range of 0.0245–0.0836 μg g^{-1}, except for cream C2 which showed a higher concentration (10.7±0.959 μg g^{-1}).
Several lithium compounds (lithium nickel dioxide, cobalt lithium nickel oxide, and lithium perfluorooctane sulfonate) are banned in the European Community [5]. Creams coded as C2, C12, and C14 contained lithium in their formulations. In particular, the concentration of lithium in the moisturiser C2 (8.35±0.904 μg g^{-1}) was much higher than in the other two samples.
Divanadium pentaoxide and nickel divanadium hexaoxide were the only banned vanadium species [5], and vanadium was solely quantified in moisturising cream C2 (0.173±0.0173 μg g^{-1}).
Copper was quantified in eleven samples and its concentration was below 1.00 μg g^{-1}, except for creams C1 and C2 (5.00±0.694 and 2.55±0.256 μg g^{-1}, respectively). The high number of moisturisers with copper can be attributed to the use of copper compounds that provide properties as skin conditioners, skin protectors, and humectants (**Table S1.1**).
Iron was found in six samples (C2, C3, C10, C11, C13, and C14), and its concentration varied between 0.699 and 1.62 μg g^{-1}, excluding sample C2 which contained the highest concentration (4933±292.2 μg g^{-1}).
Silver can be used as a whitening colourant, antimicrobial agent, preservative, and bulking material (**Table S1.1**). The use of silver chloride as a preservative in cosmetics is restricted, and the maximum allowed concentration is 0.004% (as AgCl) or 20% AgCl (w/w) if it is deposited on titanium dioxide [5]. Silver content in the studied creams varied between 0.0408 and 1.18 μg g^{-1}, with the exception of samples C3 (2329±262.0 μg g^{-1}) and C5 (31.1±3.81 μg g^{-1}). In other studies included in this thesis, it was demonstrated that moisturising creams C3, C4, and C5 contained silver nanoparticles (AgNPs) [30]. Despite the European Regulation 1223/2009 states that cosmetic products containing nanomaterials have to be notified to the Commission and they must be clearly indicated in the list of ingredients (names of such ingredients followed by the word 'nano' in brackets) [5], there was no indication about the presence of AgNPs in the list of ingredients of moisturisers C3, C4, and C5.
Moisturising creams C3 and C11 were the only creams with molybdenum (0.0162±0.00244 and 0.191±0.00957 μg g^{-1}, respectively). The unique molybdenum compound listed in the inventory of ingredients of cosmetic products elaborated by the European Commission is molybdenum aspartate which has skin conditioning properties [4].
There are several stannous compounds banned by the European Commission which are dibutyltin hydrogen borate, nickel stannate, dibutyltin dichloride (DBTC), dimethyltin dichloride, tributyltin

compounds, and dibutyltin dilaurate [5]. Creams coded as C2, C3, C8, C12, and C13 were found to contain tin, and the maximum concentration was 0.483±0.0147 μg g^{-1} (sample C2).
Barium species allowed in cosmetics are barium sulphate (whitening colourant, CI 77120) and other coloured barium pigments (CI 10316, CI 12085, CI 15510, CI 15580, CI 15630, CI 15850, CI 15865, CI 15985, CI 16255, CI 17200, CI 19140, CI 42051, CI 45370, CI 45380, CI 45410, and CI 45430) [5]. Barium was quantified in five samples (C1, C2, C3, C10, and C12), and its concentrations were lower than 0.700 μg g^{-1}, except for moisturiser C2 which contained 4.84±0.384 μg g^{-1} of barium.

Table 1.4. Concentration (μg g^{-1}) of the studied metals in commercial moisturising creams

Sample code	Li	Be	Al	V	Cr	Mn
C1	<LOD	0.00809 ± 0.000838	<LOQ	<LOQ	<LOQ	0.0522 ± 0.00439
C2	8.35 ± 0.904	0.0825 ± 0.00455	2176 ± 257.7	0.173 ± 0.0173	0.303 ± 0.0191	10.7 ± 0.959
C3	<LOD	<LOD	<LOD	<LOD	0.0934 ± 0.00320	0.0595 ± 0.0101
C4	<LOD	<LOD	<LOQ	<LOD	<LOQ	<LOQ
C5	<LOD	<LOD	<LOD	<LOD	<LOQ	0.0412 ± 0.00496
C6	<LOD	<LOD	<LOQ	<LOD	<LOD	0.0353 ± 0.000876
C7	<LOD	<LOD	<LOQ	<LOD	<LOD	<LOQ
C8	<LOD	<LOD	31.3 ± 1.72	<LOD	<LOD	0.0636 ± 0.00143
C9	<LOD	<LOD	<LOQ	<LOD	<LOQ	0.0325 ± 0.00288
C10	<LOQ	<LOD	<LOD	<LOD	0.213 ± 0.00462	0.0836 ± 0.0131
C11	<LOQ	<LOD	<LOQ	<LOD	<LOQ	0.0245 ± 0.00205
C12	1.07 ± 0.0275	<LOQ	<LOQ	<LOD	<LOQ	0.0277 ± 0.00481
C13	<LOD	<LOD	5.10 ± 0.0212	<LOD	<LOQ	0.0418 ± 0.00506
C14	0.0445 ± 0.00493	<LOD	7.47 ± 0.162	<LOD	<LOQ	0.0379 ± 0.00281

Table 1.4. (continued)

Sample code	Fe	Co	Ni	Cu	Zn	Mo
C1	<LOQ	<LOQ	<LOQ	5.00 ± 0.694	73479 ± 3017.4	<LOQ
C2	4933 ± 292.2	0.134 ± 0.000803	0.559 ± 0.0490	2.55 ± 0.256	25455 ± 1600.8	<LOQ
C3	1.44 ± 0.268	0.0178 ± 0.00131	<LOQ	0.283 ± 0.00102	2.22 ± 0.333	0.0162 ± 0.00244
C4	<LOQ	<LOD	0.257 ± 0.0414	<LOD	<LOD	<LOQ
C5	<LOD	<LOD	0.164 ± 0.0184	0.145 ± 0.0217	2.96 ± 0.338	<LOQ
C6	<LOQ	<LOD	0.425 ± 0.0261	<LOD	<LOD	<LOD
C7	<LOQ	<LOD	<LOD	<LOD	<LOD	<LOQ
C8	<LOD	<LOD	<LOD	0.171 ± 0.00868	2.23 ± 0.305	<LOD
C9	<LOD	<LOD	<LOD	0.192 ± 0.0267	41.2 ± 1.36	<LOD
C10	1.01 ± 0.0774	<LOQ	<LOQ	0.102 ± 0.00192	4.07 ± 0.0785	<LOQ
C11	1.62 ± 0.112	<LOD	0.501 ± 0.0800	0.512 ± 0.0815	8.58 ± 0.871	0.191 ± 0.00957
C12	<LOQ	<LOD	0.216 ± 0.0347	0.318 ± 0.0303	1.83 ± 0.0884	<LOQ
C13	1.49 ± 0.205	<LOD	<LOD	0.243 ± 0.0360	<LOD	<LOD
C14	0.699 ± 0.133	<LOD	<LOD	0.251 ± 0.0350	<LOD	<LOD

Table 1.4. (continued)

Sample code	Ag	Cd	Sn	Ba	Hg	Pb
C1	0.380 ± 0.00959	<LOD	<LOQ	0.0601 ± 0.00299	<LOD	0.0509 ± 0.00354
C2	0.0859 ± 0.00888	0.0745 ± 0.00958	0.483 ± 0.0147	4.84 ± 0.384	0.0990 ± 0.00633	0.437 ± 0.0383
C3	2329 ± 262.0	<LOQ	0.0388 ± 0.00427	0.180 ± 0.0140	0.180 ± 0.0281	<LOD
C4	1.18 ± 0.0710	<LOQ	<LOD	<LOD	0.107 ± 0.0119	<LOD
C5	31.1 ± 3.81	<LOQ	<LOD	<LOQ	<LOD	<LOQ
C6	<LOD	<LOD	<LOQ	<LOD	<LOD	0.0342 ± 0.000183
C7	<LOD	<LOD	<LOD	<LOD	<LOD	0.0987 ± 0.0124
C8	<LOD	<LOD	0.108 ± 0.00121	<LOQ	<LOD	<LOD
C9	<LOD	<LOD	<LOD	<LOD	<LOD	<LOD
C10	<LOD	<LOQ	<LOD	0.440 ± 0.0138	0.150 ± 0.0272	<LOD
C11	<LOD	<LOD	<LOD	<LOQ	<LOD	<LOD
C12	0.0408 ± 0.00471	<LOD	0.425 ± 0.0434	0.680 ± 0.0114	<LOD	<LOD
C13	<LOD	<LOD	0.130 ± 0.00610	<LOD	<LOD	<LOD
C14	<LOD	<LOD	<LOD	<LOD	<LOD	<LOD

<LOD: below LOD; <LOQ: below LOQ

1.5 CONCLUSIONS

All the studied metals, except molybdenum, antimony, and arsenic were found in moisturising cream C2. Thus, the selling of this cream, which was purchased from an online store, is not legal in Europe since it contained banned metals such as beryllium, cadmium, mercury, and lead [5]. Furthermore, cream C2 showed quantifiable contents of nickel, cobalt, and chromium which are also banned owing to their allergenic effect on the skin. Similarly, moisturisers C1, C3, C4, C6, C7, and C10 do not comply with the European Regulation 1223/2009 due to the presence of lead (C6 and C7), beryllium and lead (C1), chromium and mercury (C10), and mercury (C3 and C4). Moisturisers C5, C11, and C12 probably do not comply with the regulation since nickel and many nickel salts (potential allergens) are banned in cosmetic products. Regarding barium, its allowed species [barium sulphate (CI 77120) and other barium pigments] were not listed in the ingredients of creams C1, C2, C3, C10, and C12, so the presence of barium in these samples was neither justified nor allowed. Moisturising creams labelled as C3, C4, and C5 contained Ag (as AgNPs according to published studies) but AgNPs presence was not indicated in the list of ingredients, in breach of the European cosmetic regulation.

To conclude, moisturising creams coded as C1, C2, C3, C4, C5, C6, C7, C10, C11, and C12 do not comply with the Regulation 1223/2009 on cosmetic products, and the only moisturiser that fulfils the stated regulation is the sample coded as C9. Furthermore, speciation studies are necessary in the case of samples C8 and C13 (tin speciation) and C14 (lithium speciation) to ensure compliance with the Regulation 1223/2009 (several lithium and stannous compounds are banned by the European Commission).

SUPPLEMENTARY INFORMATION

Table S1.1. Functions of the studied metals in formulations of moisturising creams (adaptation from the European Commission's inventory of ingredients in cosmetic products [4] and considering the metal compounds allowed by the Regulation 1223/2009 on cosmetic products [5])

Compound	Function
ALUMINIUM	
Aluminium capryloyl hydrolysed collagen	Skin conditioning
Aluminium undecylenoyl collagen aminoacids	Skin conditioning
Alumina	Opacifying/viscosity controlling
Aluminium behenate	Opacifying/viscosity controlling
Aluminium silicate	Opacifying/absorbent
Aluminium caprylate	Emulsion stabilising/opacifying/viscosity controlling
Aluminium dilinoleate	Emulsion stabilising/opacifying/viscosity controlling
Aluminium dimyristate	Emulsion stabilising/opacifying/viscosity controlling
Aluminium distearate and aluminium tristearate	Emulsion stabilising/opacifying/viscosity controlling/emollient
Aluminium isostearate	Emulsion stabilising/opacifying/viscosity controlling
Aluminium isostearates/laurates/palmitates	Emulsion stabilising/opacifying/viscosity controlling
Aluminium isostearates/myristates	Emulsion stabilising/opacifying/viscosity controlling
Aluminium isostearates/palmitates	Emulsion stabilising/opacifying/viscosity controlling
Aluminium isostearates/stearates	Emulsion stabilising/opacifying/viscosity controlling
Aluminium myristates/palmitates	Emulsion stabilising/opacifying/viscosity controlling
Aluminium methionate	Viscosity controlling
Aluminium starch octenylsuccinate	Viscosity controlling/absorbent
Aluminium hydroxide	Viscosity controlling/emollient/humectant
Aluminium butoxide	Emulsion stabilising
Aluminium myristate	Emulsion stabilising
Aluminium dicetyl phosphate	Emulsion stabilising
Aluminium/magnesium hydroxide stearate	Emulsion stabilising
Aluminium lanolate	Emulsifying/surfactant
Aluminium hydrogenated tallow glutamate	Surfactant
Aluminium acetate	Antimicrobial
Aluminium benzoate	Antimicrobial
Aluminium diacetate	Antimicrobial
Aluminium formate	Antimicrobial
Aluminium phenolsulphonate	Antimicrobial
Aluminium glycinate	Buffering
Aluminium lactate	Buffering/astringent
Aluminium PCA	Astringent
Aluminium bromohydrate	Astringent
Aluminium chloride	Astringent

Table S1.1. (continued)

Compound	Function
Aluminium chlorohydrate	Astringent
Aluminium chlorohydrex PEG	Astringent
Aluminium chlorohydrex PG	Astringent
Aluminium dichlorohydrate	Astringent
Aluminium dichlorohydrex PEG	Astringent
Aluminium dichlorohydrex PG	Astringent
Aluminium sesquichlorohydrate	Astringent
Aluminium sesquichlorohydrex PEG	Astringent
Aluminium sesquichlorohydrex PG	Astringent
Aluminium citrate	Astringent
Aluminium	Colourant (CI 77000, E 173, white)
Aluminium hydroxide sulphate	Colourant (CI 77002, white)
Natural hydrated aluminium silicate, ($Al_2O_3.2SiO_2.2H_2O$)	Colourant (CI 77004, white)
Aluminium stearate	Colourant (white)
BARIUM	
Barium sulphate	Opacifying, colourant (CI 77120, white)
COBALT	
Cobalt titanium oxide	Skin conditioning
COPPER	
Alanine/histidine/lysine polypeptide copper HCl	Skin conditioning
Copper sulphate	Skin conditioning
Cupric acetate	Skin conditioning
Saccharomyces/copper ferment	Skin conditioning
Copper acetylmethionate	Skin conditioning/moisturising
Copper aspartate	Skin conditioning/skin protecting
Copper gluconate	Skin conditioning/skin protecting
Copper acetyl tyrosinate methylsilanol	Humectant
Copper PCA	Humectant
Copper PCA methylsilanol	Humectant
Copper usnate	Antimicrobial
Disodium cupric citrate	Stabilising
Disodium EDTA-copper	Chelating/astringent
IRON	
Ferric citrate	Skin conditioning
Ferrous aspartate	Skin conditioning
Ferrous glucoheptonate	Skin conditioning
Saccharomyces/iron ferment	Skin conditioning
Ferric chloride	Astringent

Table S1.1. (continued)

Compound	Function
Ferric glycerophosphate	Astringent
Ferrous sulphate	Astringent
Iron hydroxide	Stabilising
LITHIUM	
Lithium gluconate	Skin conditioning
Dilithium oxalate	Chelating
Lithium magnesium silicate	Binding/viscosity controlling/bulking
Lithium magnesium sodium silicate	Viscosity controlling/bulking
Lithium oxidised polyethylene	Film forming/viscosity controlling
Lithium stearate	Opacifying/viscosity controlling/binding
NICKEL	
Nickel gluconate	Humectant
MANGANESE	
Manganese acetylmethionate	Skin conditioning
Manganese aspartate	Skin conditioning
Manganese chloride	Skin conditioning
Manganese gluconate	Skin conditioning
Saccharomyces/manganese ferment	Skin conditioning
Manganese glycerophosphate	Astringent
Manganese PCA	Humectant/skin conditioning/moisturising
MOLYBDENUM	
Molybdenum aspartate	Skin conditioning
SILVER	
Silver chloride	Antimicrobial
Silver acetylmethionate	Antimicrobial
Silver borosilicate	Antimicrobial
Silver sulphate	Antimicrobial
Silver magnesium aluminium phosphate	Bulking
Silver	Colourant (CI 77820, E174, white)
TIN	
Sodium stannate	Viscosity controlling/stabilising
Tin oxide	Viscosity controlling/opacifying
Stannous chloride	Reducing
ZINC	
Zinc oxide	UV filter, colourant (CI 77947, white)
Zinc oxide (nanoparticulate)	UV filter
Zinc stearate	Colourant (white)
Lactobacillus/zinc ferment	Skin protecting
Porphyridium/zinc ferment	Skin protecting
Saccharomyces/zinc ferment	Skin conditioning

Table S1.1. (continued)

Compound	Function
Zinc acetylmethionate	Skin conditioning
Zinc aspartate	Skin conditioning
Zinc DNA	Skin conditioning
Zinc glucoheptonate	Skin conditioning
Zinc gluconate	Skin conditioning
Zinc glutamate	Skin conditioning
Zinc hydrolysed collagen	Skin conditioning
Zinc yeast derivative	Skin conditioning
Zinc pentadecene tricarboxylate	Skin conditioning/surfactant
Zinc PCA	Skin conditioning/humectant
Zinc laurate	Opacifying/viscosity controlling
Zinc myristate	Opacifying/viscosity controlling
Zinc neodecanoate	Opacifying/viscosity controlling
Zinc acetate	Antimicrobial
Zinc sulphate	Antimicrobial
Zinc undecylenate	Antimicrobial/opacifying
Zinc dibutyldithiocarbamate	Antimicrobial/antioxidant
Zinc phenolsulphonate	Antimicrobial/astringent
Zinc borosilicate	Bulking
Zinc carbonate	Opacifying
Zinc ricinoleate	Opacifying
Zinc rosinate	Opacifying/viscosity controlling
Zinc formaldehyde sulphoxylate	Reducing

Table S1.2. Ingredients of analysed moisturising creams

Code	Ingredients
C1	Water, Cyclopentasiloxane, PEG-10 Dimethicone, Methicone, Isododecane, Propane-diol, Caprylic/Capric Triglycerides, Isodecyl Neopenta-noate, Dimethicone/bis Isobutyl PPG-20 Crosspolymer, Octyldodecyl Stearyl Citrate Crosspolymer, Tapioca Starch, Polymethylsilsesquioxane, Glycerin, Isostearic Acid, Polyhydroxystearic Acid, Dimethicone, Isododecane, Phenoxyl-thanol, Benzoic Acid, Ethylhexylglycerin, Glycereth-2 Cocoate, Dicaprylyl ether, Dehydroxanthan Gum, Carthamus Tinctorius (Safflower) Seed Oil, Melanin, Phytosteryl, Octyldodecyl Lauroyl Glutamate, Sodium Hyaluronate Acid, Trimethylated Silica Gel, Tocopheryl Acetate, Dipotassium Glycyrrhizinate, Porphyridium cruentum, Eucalyptus Globulus Leaf Extract, Zingiber Officinale Root Extract, Gaultheria Procumbens Leaf Extract, Avena Sativa Kernel Extract, Allantoin, Ceramide 3, Zinc oxide (9%), Octinoxate (7.5%).
C2	Water, Cyclopentasiloxane, Caprylyl Methicone, Ethylhexyl Palmitate, Dimethicone, Lauryl PEG-8 Dimethicone, Neopentyl Glycol Diheptanoate, Polymethylsilsesquioxane, PEG-12 Dimethicone, PPG-20 Crosspolymer, Titanium dioxide, Glycerin, Dimethicone Crosspolymer, Tribehenin, Dimethicone, Vinyl Dimethicone Crosspolymer, Algae Extract, Hydroxycapric Acid, Hydroxycaprylic Acid, Hydroxycinnamic Acid, Teprenone, Tetrahexyldecyl Ascorbate, Tocopheryl Acetate, Alumina, Butylene Glycol, Calcium Aluminum Borosilicate, Caprylic/Capric Triglyceride, Disodium EDTA, Iron Oxides, PEG-4, Silica, Synthetic Fluorphlogopite, Tin Oxide, Triethoxycaprylylsilane, Xantan Gum, Caprylyl Glycol, Hexylene Glycol, Phenoxyethanol, Titanium dioxide (5.4%), Zinc oxide (2.96%).
C3	Water, Alcohol Denat, C12-15 Alkyl Benzoate, Oenothera Biennis Oil, Simmondsia Chinensis Seed Oil, Isopropyl myristate, Glycerin, Polyglyceryl-3-Methylglucose Distearate, Cetyl Alcohol, Tocopheryl Acetate, Hydrogenated Coco-Glycerides, Cetyl Palmitate, Octyldodecanol, Silver, Cardiospermum Halicacabum Flower/Leaf/Vine Extract, Echium Platagineum Seed Oil, Helianthus Annus Seed Oil Unsaponificables, Xanthan Gum, Pentaerythrityl Tetra-di-t-butyl Hydroxyhydrocinnamate
C4	Water, Petrolatum, Propylene Glycol, Caprilic/Capric Triglyceride, PEG-20-Glyceryl Stearate, Cetyl Alcohol, Hydrogenated Palm Glycerides, Silver.
C5	Water, Caprylic/Capric Triglyceride, Sorbitol, Pentylene Glycol, Glyceryl Stearate, Cetyl Alcohol, Dicaprylyl Ether, Polyglyceryl-3 Methylglucose Distearate, Ginkgo Biloba Leaf Extract, Chamomilla Recutita Flower Extract, Propylene Glycol, Prunus Amygdalus Dulcis Oil, Tocopherol, Panthenol, Silver, Simmondsia Chinensis Seed Oil, Oenothera Biennis Seed Oil, Glycerin, Cera Alba, Xathan Gum.
C6	Water, Caprylic/Capric Triglyceride, Glycerin, Olea Europaea (Olive) Fruit Oil, Isostearyl Isostearate, 1,2-Hexanediol, Cetearyl Alcohol, Panthenol, Butyrospermum Parkii (Shea) Butter, Niacinamide, Glyceryl Stearate Citrate, Alpha-Glucan Oligosaccharide, Limnanthes Alba Seed Oil, Hydrogenated Lecithin, Hippophae Rhamnoides (Sea Buckthorn) Fruit Extract, Tocopheryl Acetate, Xanthan Gum, Sclerotium Gum, Squalane, Tetrasodium Glutamate Diacetate, Ceramide 3, Citric Acid, Rosmarinus Officinalis (Rosemary) Leaf Extract.
C7	Water, Glycerin, Niacinamide, Dimethicone, Paraffinum Liquidum, Caprylic/Capric Triglyceride, Brassica Campestris Oleifera Oil, Dimethiconol, Sodium Hydroxide, Ammonium Polyacryldimethyl Taurate, Disodium EDTA, Caprylyl Glycol, Xanthan Gum, C10-30 Alkyl Acrylate Crosspolymer, Butyrospermum Parkii Butter, Phenoxyethanol.
C8	Water, Glycerin, Ethylhexyl Salicylate, Butyl Methoxydibenzoylmethane, Alcohol Denat, Cetearyl Alcohol, Dibutyl Adipate, Hydrogenated Coco-Glycerides, Phenylbenzimidazole Sulfonic Acid, Methylpropanediol, C12-15 Alkyl Benzoate, Aluminum Starch Octenylsuccinate, Arginine HCl, Bis-Ethyhexyloxyphenol Methoxyphenyl Triazine, Magnolia Officinalis Bark Extract, Pimpinella Anisum Fruit Extract, Sodium Hyaluronate, Methyl Methacrylate Cross-polymer, Carbomer, Sodium Stearoyl Glutamate, Sodium Chloride, Silica Dimethyl Silylate, Dimethicone, Trisodium EDTA, 1,2-Hexanediol, Phenoxyethanol, Parfum.
C9	Water, Glycerin, Tribehenin PEG-20 Esters, Caprylic/Capric Triglyceride, Propanediol, Isostearyl Isostearate, Cyclopentasiloxane, Lecithin, Cyclohexasiloxane, Ammonium Acryloyldimethyltaurate/vp Copolymer, Nicotiana Benthamiana Hexapeptide 40 sh-polypeptide 2, Nicotiana Benthamiana Hexapeptide-40 sh-Oligopeptide-1, Nicotiana Benthamiana Hexapeptide-40 sh-Polypeptide-5, Nicotiana Benthamiana sh-Polypeptide-15 Hexapeptide-40, Alcohol, BHA, BHT, Biotin, Caprylyl Glycol, Carbomer, Citric Acid, Coco-Glucoside, Dimethyl Mea, Dipotassium Phosphate, Disodium EDTA, DL-Alfa Tocopherol Acetato, Ethylhexylglycerin, Glaucine, Glycine Soya Protein, Hydrochloric Acid, Hydrolysed Rice Bran Protein, Hydrolysed Sodium Hyaluronate, Lactic Acid, Methylsilanol Mannuronate, Nicotiana Benthamiana sh-Oligopeptide-2, Nicotiana Benthamiana sh-Polypeptide-45, Nicotiana Benthamiana sh-Polypeptide-7, Parfum, PEG-40 Hydrogenated Castor Oil, Phenoxyethanol, Pistacia Lentiscus Gum, Polysorbate 20, Potassium Phosphate, Potassium Sorbate, Retinal, Retinol, Retinyl Palmitate, Sodium Benzoate, Sodium Chloride, Sodium Cholate, Sodium Citrate, Sodium Dextran Sulphate, Sorbic Acid, Superoxide Dismutase, Tocopherol, Triethanolamine, Tromethamine, Xanthan Gum.

Table S1.2. (continued)

Code	Ingredients
C10	Water, Propylene Glycol, Lecithin, Alcohol, PEG/PPG-20/6 Dimethicone, Polymethyl Methacrylate, PEG-40 Hydrogenated Castor Oil, 4-Butylresorcinol, Azelaic Acid, Retinol, Ascorbyl Glucoside, Niacin, Undecylenoyl Phenylalanine, Glycyrrhetinic Acid, Diacetyl Boldine, Phenoxyethanol, Citronellyl Methylcrotonate, Sodium Cholate, Parfum, Carbomer, Xanthan Gum, Triethanolamine, Tocopheryl Acetate, Polysorbate 20, BHT, Ethylhexylglycerin, Sodium Hydroxide, Caprylic/Capric Triglyceride, Sodium Chloride, BHA, Hydrochloric Acid.
C11	Water, Isostearyl Neopentanoate, Glycerin, Octyldodecanol, Propylene Glycol, Pentylene Glycol, Acrylamide, Sodium Acryloyldimethyltaurate Copolymer, Cetearyl Alcohol, Glycine Soya Oil, Triethanolamine, Isohexadecane, Sodium Hyaluronate, Retinol, Retinyl Linoleate, Adenosine, Capryloyl Salycylic Acid, Caprylyl Glycol, Polysorbate 80, Phenoxyethanol, Parfum.
C12	Water, Glycerin, Dibutyl Adipate, C12-15 Alkyl Benzoate, Cetearyl Alcohol, Dicaprylyl Carbonate, Sodium Acrylate/Sodium Acryloydimethyl Taurate Copolymer, Polyisobutene, Ethylhexyl Triazone, Phenoxyethanol, Panthenol, Cyclopentasiloxane, Tocopheryl Acetate, Disodium EDTA, Diethylamino Hydroxybenzoyl Hexyl Benzoate, Ethylparaben, Methylparaben, Bis-ethylhexyloxyphenol Methoxyphenyl Triazine, Parfum, Dimethicone, Sodium Hydroxide, Allantoin, Benzoic Acid, Acrylates/C10-30 Alkyl Acrylate Crosspolymer, Caprylyl/Capryl Glucoside, Dehydroacetic Acid, Pyrus Malus Fruit Extract, Panicum Miliaceum Extract, Chlorella Vulgaris/Lupinus Albus Protein Ferment, Pectin, Tocopherol, Tannic Acid, CI 42051, Potassium Sorbate, Sodium Sulphate.
C13	Water, Sesamum Indicum Seed Oil, Glycerin, Decyl Oleate, Glyceryl Stearate Citrate, Cetearyl Alcohol, Butyrospermum Parkii Butter, Prunus Amygdalus Dulcis Oil, Sorbitol, Panthenol, Vitis Vinifera Seed Oil, Phenoxyethanol, Parfum, Carbomer, Sodium Lactate, Sodium PCA, Disodium EDTA, Ethylhexylglycerin, Potassium Sorbate, Sodium Hydroxide, Sodium Hyaluronate, Alcohol, Soluble Collagen, Caprylic/Capric Triglyceride, Sodium Benzoate, Pantolactone, Ascorbyl Palmitate, Citric Acid, Fructose, Glycine, Inositol, Lactic Acid, Niacinamide, Urea, Ascorbic Acid.
C14	Water, Caprylic/Capric Triglyceride, Cocoglycerides, Isopropyl Myristate, Hydroxypropyl Starch Phosphate, Candelilla/Jojoba/Rice Bran Polyglyceryl-3 Esters, Glyceryl Stearate, Cetyl Alcohol, Cetearyl Alcohol, Lactic Acid, Sodium Stearoyl Lactylate, Sodium Levulinate, Xanthan Gum, Sodium Hydroxide, Citrus Aurantium Amara Peel Oil, Sodium Benzoate, Limonene.

REFERENCES

[1] B. Bocca, A. Pino, A. Alimonti, G. Forte, Toxic metals contained in cosmetics: A status report, Regul. Toxicol. Pharmacol. 68 (2014) 447–467, DOI: 10.1016/j.yrtph.2014.02.003.

[2] M.F. Mesko, D.L.R. Novo, V.C. Costa, A.S. Henn, E.M.M. Flores, Toxic and potentially toxic elements determination in cosmetics used for make-up: A critical review, Anal. Chim. Acta 1098 (2020) 1–26, DOI: 10.1016/j.aca.2019.11.046.

[3] M.G. Volpe, M. Nazzaro, R. Coppola, F. Rapuano, R.P. Aquino, Determination and assessments of selected heavy metals in eye shadow cosmetics from China, Italy, and USA, Microchem. J. 101 (2012) 65–69, DOI: 10.1016/j.microc.2011.10.008.

[4] Commission Decision of 9 February 2006 amending Decision 96/335/EC establishing an inventory and a common nomenclature of ingredients employed in cosmetic products (2006/257/EC), Official Journal of the European Union, L97 (05 April 2006) 1–528.

[5] Regulation (EC) N° 1223/2009 of the European Parliament and of the Council of 30 November 2009 on cosmetic products, Official Journal of the European Union, L342 (01 March 2022) 1–392.

[6] Q. Zeng, A. Zhang, Assessing potential mechanisms of arsenic-induced skin lesions and cancers: Human and in vitro evidence, Environ. Pollut. 260 (2020) 113919, DOI: 10.1016/j.envpol.2020.113919.

[7] Y. Sun, J. Pi, X. Wang, E.J. Tokar, J. Liu, M.P. Waalkes, Aberrant cytokeratin expression during arsenic-induced acquired malignant phenotype in human HaCaT keratinocytes consistent with epidermal carcinogenesis, Toxicology 262 (2009) 162–170, DOI: 10.1016/j.tox.2009.06.003.

[8] J.M. Berlin, J.S. Taylor, J.E. Sigel, W.F. Bergfeld, R.A. Dweik, Beryllium dermatitis, J. Am. Acad. Dermatol. 49 (2003) 939–941, DOI: 10.1016/S0190-9622(03)01555-X.

[9] G.H. Curtis, Cutaneous hypersensitivity due to beryllium. A Study of Thirteen Cases. Arch. Derm. Syphilol. 64 (1951) 470–482, DOI: 10.1001/archderm.1951.01570100087014.

[10] B. Björkner, M. Bruze, H. Möller, High frequency of contact allergy to gold sodium thiosulfate. An indication of gold allergy?, Contact Dermatitis 30 (1994) 144–151, DOI: 10.1111/j.1600-0536.1994.tb00695.x.

[11] F. Larese, A. Gianpietro, M. Venier, G. Maina, N. Renzi, In vitro percutaneous absorption of metal compounds, Toxicol. Lett. 170 (2007) 49–56, DOI: 10.1016/j.toxlet.2007.02.009.

[12] F. Larese Filon, F. D'Agostin, M. Crosera, G. Adami, M. Bovenzi, G. Maina, *In vitro* percutaneous absorption of chromium powder and the effect of skin cleanser, Toxicol. Vitro 22 (2008) 1562–1567, DOI: 10.1016/j.tiv.2008.06.006.

[13] S. Galván-Arzate, A. Santamaría, Thallium toxicity, Toxicol. Lett. 99 (1998) 1–13, DOI: 10.1016/S0378-4274(98)00126-X.

[14] D.E. Engler, Mercury "bleaching" creams, J. Am. Acad. Dermatol. 52 (2005) 1113–1114, DOI: 10.1016/j.jaad.2005.01.136.

[15] O. Braun-Falco, G. Plewig, H.H. Wolff, W.H.C. Burgdorf, Granulomatous Diseases, in *Dermatology*, Springer, Heidelberg, Germany (2000) 1379–1400, DOI: 10.1007/978-3-642-97931-6_50.

[16] J.L. Stauber, T.M. Florence, B.L. Gulson, L.S. Dale, Percutaneous absorption of inorganic lead compounds, Sci. Total Environ. 145 (1994) 55–70, DOI: 10.1016/0048-9697(94)90297-6.

[17] H.A. Aziz, M.F. Ghazali, Y.T. Hung, L.K. Wang, Toxicity, Source, and Control of Barium in the Environment, in J.P. Chen, L.K. Wang, M.H.S. Wang, Y.T. Hung, N.K. Shammas (Eds.), *Remediation of Heavy Metals in the Environment*, CRC Press, Boca Raton, FL, USA (2016) 463–482, DOI: 10.1201/9781315374536.

[18] Y. Nzengue, R. Steiman, C. Garrel, E. Lefèbvre, P. Guiraud, Oxidative stress and DNA damage induced by cadmium in the human keratinocyte HaCaT cell line: Role of glutathione in the resistance to cadmium, Toxicology 243 (2008) 193–206, DOI: 10.1016/j.tox.2007.10.005.

[19] E.S. Blackadder, W.G. Manderson, Occupational absorption of tellurium: a report of two cases, Br. J. Ind. Med. 32 (1975) 59–61, DOI: 10.1136/oem.32.1.59.

[20] WHO, World Health Organization, Vanadium Pentoxide and Other Inorganic Vanadium Compounds, Geneva (2001).

[21] Commission Directive 95/45/EC of 26 July 1995 laying down specific purity criteria concerning colours for use in foodstuffs, Official Journal of the European Union, L226 (22 September 1995) 1–45.

[22] B. Bocca, G. Forte, F. Petrucci, A. Cristaudo, Levels of nickel and other potentially allergenic metals in Ni-tested commercial body creams, J. Pharm. Biomed. Anal. 44 (2007) 1197–1202, DOI: 10.1016/j.jpba.2007.04.031.

[23] Z. Grosser, L. Davidowski, L. Thompson, The Determination of Metals in Cosmetics, Perkin Elmer Appl. Note (2011) 1–6.

[24] C.E.R. de Paula, G.F.B. Cruz, C.M.S.P. Rezende, R.J. Cassella, Determination of Cr and Mn in moisturizing creams by graphite furnace atomic absorption spectrometry through direct introduction of the samples in the form of emulsions, Microchem. J. 127 (2016) 1–6, DOI: 10.1016/j.microc.2016.01.017.

[25] C.M.A. Iwegbue, F.I. Bassey, G.O. Tesi, S.O. Onyeloni, G. Obi, B.S. Martincigh, Safety evaluation of metal exposure from commonly used moisturizing and skin-lightening creams in Nigeria, Regul. Toxicol. Pharmacol. 71 (2015) 484–490, DOI: 10.1016/j.yrtph.2015.01.015.

[26] Y. Gao, Z. Shi, Q. Zong, P. Wu, J. Su, R. Liu, Direct determination of mercury in cosmetic samples by isotope dilution inductively coupled plasma mass spectrometry after dissolution with formic acid, Anal. Chim. Acta 812 (2014) 6–11, DOI: 10.1016/j.aca.2014.01.002.

[27] W.N. Chen, S.J. Jiang, Y.L. Chen, A.C. Sahayam, Slurry sampling flow injection chemical vapor generation inductively coupled plasma mass spectrometry for the determination of trace Ge, As, Cd, Sb, Hg and Bi in cosmetic lotions, Anal. Chim. Acta 860 (2015) 8–14, DOI: 10.1016/j.aca.2015.01.011.

[28] X. Jia, Y. Han, C. Wei, T. Duan, H. Chen, Speciation of mercury in liquid cosmetic samples by ionic liquid based dispersive liquid–liquid microextraction combined with high-performance liquid chromatography-inductively coupled plasma mass spectrometry, J. Anal. At. Spectrom. 26 (2011) 1380–1386, DOI: 10.1039/C0JA00121J.

[29] L. Sneyers, L. Verheyen, P. Vermaercke, M. Bruggeman, Trace element determination in beauty products by k_0-instrumental neutron activation analysis, J. Radioanal. Nucl. Chem. 281 (2009) 259–263, DOI: 10.1007/s10967-009-0105-8.

[30] I. Rujido-Santos, L. Naveiro-Seijo, P. Herbello-Hermelo, M.C. Barciela-Alonso, P. Bermejo-Barrera, A. Moreda-Piñeiro, Silver nanoparticles assessment in moisturizing creams by ultrasound assisted extraction followed by sp-ICP-MS, Talanta 197 (2019) 530–538, DOI: 10.1016/j.talanta.2019.01.068.

CHAPTER 2. METAL CONTENT IN TEXTILE AND (NANO)TEXTILE PRODUCTS

CHAPTER 2. METAL CONTENT IN TEXTILE AND (NANO)TEXTILE PRODUCTS*

*The results from this chapter have already been published as Iria Rujido-Santos, Paloma Herbello-Hermelo, María Carmen Barciela-Alonso, Pilar Bermejo-Barrera, and Antonio Moreda-Piñeiro, Metal Content in Textile and (Nano)Textile Products, Int. J. Environ. Res. Public Health 19 (2022) 944, DOI: 10.3390/ijerph19020944.

Group of Trace Element, Spectroscopy, and Speciation (GETEE), Institute of Materials iMATUS. Department of Analytical Chemistry, Nutrition, and Bromatology. Faculty of Chemistry. Universidade de Santiago de Compostela. Avenida das Ciencias, s/n 15782, Santiago de Compostela. Spain.

2.1 ABSTRACT

Metals, metallic compounds, and, recently, metallic nanoparticles appear in textiles due to impurities from raw materials, contamination during the manufacturing process, and/or their deliberate addition. However, the presence of lead, cadmium, chromium (VI), arsenic, mercury, and dioctyltin in textile products is regulated in Europe (Regulation 1907/2006). Metal determination in fabrics was performed by inductively coupled plasma mass spectrometry (ICP-MS) after microwave-assisted acid digestion. The ICP-MS procedure has been successfully validated; relative standard deviations were up to 3% and analytical recoveries were within the 90–107% range. The developed method was applied to several commercial textiles, and special attention has been focused on textiles with "*nanofinishing*" (fabrics prepared with metallic nanoparticles for providing certain functionalities). Arsenic content (in textile T4) and lead content (in subsamples T1-1, T1-2, and T3-3) were found to exceed the maximum limits established by the European Regulation 1907/2006. Although impregnation of yarns with mercury compounds is not allowed, mercury was quantified in fabrics T1-2, T5, and T6. Further speciation studies for determining hexavalent chromium species in sample T9 are necessary (hexavalent chromium is the only species of chromium regulated). Some textile products commercialised in Europe included in this study do not comply with European Regulation 1907/2006.

2.2 INTRODUCTION

Textile products can be contaminated with metals during both production and storage. Manufacturers also add intentionally metals or metallic compounds to textile products to achieve or improve specific functionalities. As example, approximately 80% of leathers are chrome-tanned [1,2], while vanadium, chromium, barium, lead, copper, cobalt, and nickel are used in textile dyeing [3,4], and iron and manganese are used in bleaching processes [5,6]. In addition, antimony compounds have been demonstrated to enhance the flame retardant properties of halogen compounds [7,8]. Similarly, titanium can be present in some textile products after the Zirpro process with hexafluorotitanate salts for achieving fire-resistant textiles [8,9]. Furthermore, antimony can be an impurity in polyethylene terephthalate (PET) fibres since antimony compounds are used as catalysts in PET manufacture [10].

Currently, the textile industry pays great attention to the possibilities of using metallic nanoparticles (NPs) to improve the manufacture of fibres and to obtain fabrics with new or

improved properties [11]. A new category has, therefore, been added to textile finishing, called "*nanofinishing*" [12]. The use of titanium dioxide nanoparticles (TiO_2NPs) is an example of "*nanofinishing*" to improve the existing textile manufacturing procedures, specifically the scouring and bleaching processes of fibres ("*nanoscouring*" and "*nanobleaching*"). The photocatalytic activity of TiO_2NPs leads to a fast degradation (oxidation by the photo-generated oxidant radicals $^{\bullet}OH$, $RO^{\bullet}$, and $RO_2^{\bullet}$ formed on the surface of TiO_2NPs under irradiation of light) of natural impurities and pigments in fabrics [13,14].
New functionalities in textiles which incorporate metallic NPs include self-cleaning characteristics (ZnONPs and TiO_2NPs) [15,16], hydrophobicity (SiO_2NPs and ZnONPs) [11,17,18], antibacterial properties (AgNPs, CuONPs, ZnONPs, and TiO_2NPs) [11,19,20], UV blocking activity (TiO_2NPs, ZnONPs, CeO_2NPs, and Al_2O_3NPs) [11,21], and electromagnetic wave shielding (Cu-, Ni-, Fe-, and Co-based NPs) [21], among others.
Information about the composition of fibres is mandatory (European Regulation 1007/2011) [22], and the content of several metals is restricted in textile products in Europe. Maximum legal concentration of lead, cadmium, chromium (VI), and arsenic (and their compounds) in fabrics is 1 $\mu g\ g^{-1}$, except for leather articles coming into contact with skin where chromium (VI) content shall not exceed the level of 3 $\mu g\ g^{-1}$. Dioctyltin (DOT) in textile products which are in direct contact with the skin cannot exceed 1000 $\mu g\ g^{-1}$. In addition, impregnation of yarns with mercury compounds is not allowed [23]. On the other hand, the European Commission (2009/567/EC) establishes the ecological criteria for the award of the Community Ecolabel for textile products [24].
Metals can be released from textile products and can permeate through the skin, reach the bloodstream, and accumulate in several organs or tissues. Counter ion, bond type, valence, pH [25], and dermal health [26] affect the percutaneous absorption of metals. Moreover, recent studies reported possible penetration of metallic NPs through skin, which may pose a risk to human health [27,28]. Besides the potential risk of metals and metallic NPs for humans, the presence of metallic NPs in textiles could imply a risk to the environment since several studies have pointed out their release from fabrics during the laundry [29–34].
Laser ablation inductively coupled plasma mass spectrometry (LA-ICP-MS) and total reflection X-ray fluorescence spectrometry (TXRF) [35,36] allow for fabric analysis without sample decomposition. On the other hand, other methods including ICP-MS and inductively coupled plasma optical emission spectrometry (ICP-OES) [35,37–41] require the application of acid digestion processes for multi-element determinations. Nitric acid has been commonly used in the decomposition of fabrics by microwave-assisted acid digestion [35,37–40] and convective (heating block) digestion [41]. The reported methods demonstrated the ability to digest efficiently common textiles based on cotton, wool, silk, polyester, flax, and hemp [35,38,39,41] but not for new fabrics which contain metallic NPs. Thus, more drastic conditions for microwave-assisted acid digestion (sample pre-treatment) and ICP-MS (analytes determination) have been proposed as a reliable method for multi-element assessment in textile products including new fabrics such those based on metallic NPs.

2.3 MATERIALS AND METHODS

2.3.1 Instrumentation

Samples and reagents were weighed using an analytical balance ML 204T (Mettler Toledo, Columbus, OH, USA). The microwave-assisted acid digestion was performed in 100 mL closed Teflon vessels using an ETHOS PLUS microwave lab-station (Milestone, Sorisole, Italy). The total metal content was assessed using a NexION® 300X ICP-MS (Perkin Elmer, Waltham,

MA, USA) equipped with a SeaFast SC2 DX autosampler (Elemental Scientific, Omaha, NB, USA). The nebulisation system consisted of a Meinhard® nebuliser and a cyclonic spray chamber thermostated by a Peltier refrigerator.

2.3.2 Samples

Type and composition of the studied clothing are listed in **Table 2.1**. The table also shows the number of subsamples for some textiles, as some of them were visually different (made of different fibres).

The textile products studied were bought from online marketplaces except for sample T6 (men's cycling culotte) and sample T9 (compression socks with silver ions for diabetic people) which were purchased from a local shop and a pharmacy, respectively. All studied garments were manufactured in Europe, except T1, T2, and T3 (textile products fabricated in Bangladesh by the same company).

Each garment subsample was cut in pieces (5×5 mm approximately) with ceramic scissors and stored in plastic bags at room temperature in the dark.

Table 2.1. Type of item, number of subsamples, and composition of studied textiles

Code	Subsamples	Type	Manufacturing	Composition
T1	T1-1; T1-2	Long sleeve shirt	Bangladesh	70% Viscose, 30% Cotton; with SOLARSHIELD ZnO® (UPF Index: 40+)
T2	T2-1; T2-2; T2-3	Long sleeve shirt	Bangladesh	65% Polyester, 35% Cotton; with SOLARSHIELD ZnO® (UPF Index: 40+)
T3	T3-1; T3-2; T3-3	Long sleeve shirt	Bangladesh	65% Polyester, 35% Cotton; with SOLARSHIELD ZnO® (UPF Index: 40+)
T4	-- (a)	Socks	Unknown (Europe)	80% Cotton, 13% Polyamide, 5% Silver, 2% Elastane
T5	-- (a)	Men's T-shirt	Spain	100% Polyester with silver ions
T6	-- (a)	Men´s cycling culotte	Romania	82% Polyester, 18% Elastane; product treated with silver chloride (biocide)
T7	-- (a)	Children´s T-shirt	Germany	50% Cotton, 50% Cellulose (ModalSun) (UPF Index: 30)
T8	-- (a)	Children´s T-shirt	Germany	46% Cotton, 46% Cellulose (ModalSun), 8% Elastane (UPF Index: 50+)
T9	-- (a)	Socks	Spain	66% Polyamide, 10% Polyamide with silver ions, 24% Elastane
T10	-- (a)	Headband	Czech Republic	60% Cotton, 32% Polyester (Nanosilver®), 8% Elastane (Lycra®)
T11	-- (a)	Women´s underwear	Czech Republic	52% Polyester (COOLMAX®), 48% Polyester (Nanosilver®)
T12	-- (a)	Men´s underwear	Czech Republic	60% Cotton, 32% Polyester (Nanosilver®), 8% Elastane (Lycra®)
T13	-- (a)	Men´s undershirt	Czech Republic	52% Polyester (COOLMAX®), 44% Polyester (Nanosilver®), 4% Elastane (Lycra®)
T14	T14-1; T14-2; T14-3	Socks	Czech Republic	55% Cotton, 30% Polyester (Nanosilver®), 15% Elastane (Lycra®)

(a) Only one subsample.

2.3.3 Reagents

18 MΩcm ultrapure water was collected from a Milli-Q® water purification system (Millipore, Bedford, MA, USA). 69% Nitric acid (Hiperpur), 33% hydrogen peroxide, 37% hydrochloric acid, and 40% hydrofluoric acid were supplied by Panreac (Barcelona, Spain). NexIon Setup Solution (10 μg L^{-1} of U, Pb, Mg, Li, In, Fe, Ce, and Be) and Memory Test 1

Solution (1000 mg L^{-1} of Al, Ca, Fe, K, Mg, Na and 20 mg L^{-1} of Ag, As, Ba, Be, Cd, Co, Cr, Cu, Mn, Ni, Pb, Se, Tl, V, Zn) were purchased from Perkin Elmer. Standards of Ti, Sn, Ge, Rh, and In (1000 mg L^{-1} each) were also from Perkin Elmer. Standards of B, Li, Mo, and Sb (1000 mg L^{-1} each) were supplied by Merck (Darmstadt, Germany). Y and Hg (1000 mg L^{-1} each) were purchased from Panreac (Barcelona, Spain) and Scharlau (Barcelona, Spain), respectively.

2.3.4 Microwave-assisted acid digestion

Clothing samples (0.2000 g) were placed into PTFE digestion vessels and 8.0 mL of 69% nitric acid, 0.5 mL of 33% hydrogen peroxide, 0.5 mL of 37% hydrochloric acid, and 1.0 mL of 40% hydrofluoric acid were added. Operating conditions of the microwave-assisted acid digestion procedure are detailed in **Table 2.2**. Digested samples and blanks were made up to 25 mL with ultrapure water. The samples were digested in triplicate and one blank was performed at least for each set of digestions.

Table 2.2. Operating conditions of microwave-assisted acid digestion of textiles

Time (min)	Temperature (°C)
0-2	Room temperature-150
2-7	150
7-9	150-170
9-19	170
19-20	170-200
20-40	200

2.3.5 Total metal determination by ICP-MS

Daily adjustment of ICP-MS parameters such as torch position, quadrupole voltages, and nebulisation flow was performed to maximise the sensitivity. This adjustment was carried out before the measurement of samples and using a solution of Be, Ce, Fe, In, Li, Mg, Pb, and U (1 µg L^{-1}). Operating and acquisition parameters of ICP-MS, as well as monitored ions, are listed in **Table 2.3**. Due to the low sensitivity of arsenic, a longer dwell time (200 ms) than that used for the other elements (50 ms) was selected. Polyatomic interferences were minimised using helium as a collision gas (either 1.0 mL min^{-1} or 4.0 mL min^{-1} flow rate depending on the monitored ion, **Table 2.3**). A solution containing 10 µg L^{-1} of internal standards (Ge, Y, Rh, and In) in 1% nitric acid was mixed with standards and samples by a T-shaped plastic piece before their introduction into the nebuliser.

Digested textiles were diluted 10-fold with ultrapure water before analysis except for Zn determination in T1, T2, and T3 samples (and their respective subsamples), and for Ti assessment in all samples (200-fold dilution). Multi-elemental standard addition calibration was performed to avoid matrix effects. The standard addition calibration covered the range of 0–100 µg L^{-1}, except for the quantification of aluminium and iron (range of 0–5000 µg L^{-1}).

Table 2.3. ICP-MS conditions for metal assessment in digested clothing samples

Operating Parameters	
Radiofrequency power (W)	1600
Plasma gas flow (L min^{-1})	16
Auxiliary gas flow (L min^{-1})	1.2
Nebulisation gas flow (L min^{-1})	0.9–1.1
Collision cell gas	He
Acquisition Parameters	
Replicates	3
Sweeps/Reading	20
Dwell time per amu (ms)	50 (200 for As)
Integration time (ms)	1000 (4000 for As)
Monitored Ions (*m/z*)	
1.0 mL min^{-1} He	^{7}Li, ^{9}Be, ^{55}Mn, ^{63}Cu, ^{98}Mo, ^{107}Ag, ^{111}Cd, ^{138}Ba, ^{202}Hg, ^{208}Pb
4.0 mL min^{-1} He	^{49}Ti, ^{51}V, ^{53}Cr, ^{57}Fe, ^{59}Co, ^{60}Ni, ^{66}Zn, ^{75}As, ^{118}Sn, ^{121}Sb
Internal standards	^{74}Ge, ^{89}Y, ^{103}Rh, ^{115}In

2.4 RESULTS

2.4.1 Microwave-assisted acid digestion

Since nitric acid has been found adequate to decompose textiles based on cotton, wool, polyester, flax, and hemp [35,38,39,41], a mixture of 69% nitric acid and 33% hydrogen peroxide was firstly used for microwave-assisted acid digestion of (nano)textiles (**Table 2.1**). However, fine white particles were observed in all digests, which impairs precision of the ICP-MS measurements. Therefore, other mineral acids such as hydrochloric acid and hydrofluoric acid were tested, and clear acid digests were obtained when using small volumes of both acids (0.5 and 1.0 mL of hydrochloric acid and hydrofluoric, respectively). Finally, a mixture of nitric acid/hydrogen peroxide/hydrochloric acid/hydrofluoric acid (8:0.5:0.5:1, volume ratio) was selected, and the microwave operating conditions are listed in **Table 2.2**.

2.4.2 Limit of detection, precision, and analytical recovery assays

The 3σ/m and 10σ/m criteria were applied to calculate the limit of detection (LOD) and the limit of quantification (LOQ), respectively. Using these criteria, σ is the standard deviation of eleven measurements of a blank (1% nitric acid) by ICP-MS, and m is the slope of the standard addition calibration. The LODs and LOQs of developed method referred to the textile sample mass are shown in **Table 2.4**. LOQs ranged between 0.00427 (beryllium) and 6.33 μg g^{-1} (titanium). The high LOQ value for titanium was attributed to the high dilution required (1:200) for its analysis.

The precision of ICP-MS determinations for each element was evaluated by the relative standard deviation (RSD) of eleven measurements of an acid digest. RSDs for metal concentrations were within the range of 1–3% (**Table 2.4**), showing good precision for ICP-MS quantification.

The accuracy of ICP-MS assessments was based on the analytical recovery approach at several concentration levels by spiking acid digests at the selected metal concentrations (**Table 2.4**). Each

spiked digest was analysed eleven times and analytical recoveries ranging from 90 to 107% were obtained (**Table 2.4**), which implies accurate ICP-MS determinations.

Table 2.4. Methodology validation

	LOD_{method} (μg g^{-1})	LOQ_{method} (μg g^{-1})	$(Concentration)_{added}$ (μg L^{-1})	Analytical recovery (%)	RSD (%)
Li	0.00324	0.0108	0.25, 0.50, 1.0	90 ± 3	1
Be	0.00128	0.00427	0.25, 0.50, 1.0	103 ± 6	2
Ti	1.90	6.33	1.0, 5.0, 10	92 ± 6	1
V	0.00322	0.0107	0.25, 0.50, 1.0	97 ± 4	2
Cr	0.0176	0.0588	0.25, 0.50, 1.0	95 ± 6	3
Mn	0.00236	0.00788	0.50, 1.0, 5.0	91 ± 5	1
Fe	0.136	0.455	12.5, 25.0, 50.0	91 ± 6	1
Co	0.00151	0.00505	0.25, 0.50, 1.0	96 ± 4	1
Ni	0.0107	0.0356	0.25, 0.50, 1.0	97 ± 5	2
Cu	0.00977	0.0326	5.0, 10, 25	97 ± 2	1
Zn	0.138	0.459	1.0, 5.0, 10	96 ± 4	1
As	0.0143	0.0476	0.25, 0.50, 1.0	94 ± 6	2
Mo	0.00249	0.00829	0.25, 0.50, 1.0	99 ± 3	1
Ag	0.0119	0.0397	25, 50	106 ± 4	1
Cd	0.00383	0.0128	0.25, 0.50, 1.0	101 ± 3	1
Sn	0.0101	0.0335	1.0, 5.0, 10	104 ± 4	1
Sb	0.0134	0.0447	10, 25, 50	95 ± 3	3
Ba	0.00567	0.0189	1.0, 5.0, 10	101 ± 4	1
Hg	0.0240	0.0800	1.0, 5.0, 10	107 ± 6	2
Pb	0.00479	0.0160	0.25, 0.50, 1.0	99 ± 2	1

2.4.3 Metal content in the analysed textiles

Metal content in the studied textile products assessed by ICP-MS after a microwave-assisted acid digestion is shown in **Table 2.5**.

Table 2.5. Metal concentration (μg g^{-1}) in the studied fabrics measured by ICP-MS

Sample Code	Li	Be	Ti	V	Cr	Mn
T1-1	0.699 ± 0.114	<LOQ	<LOD	0.0687 ± 0.00612	<LOQ	5.82 ± 0.143
T1-2	<LOD	<LOQ	156 ± 11.8	0.0613 ± 0.00897	0.272 ± 0.0206	4.25 ± 0.106
T2-1	<LOD	0.0112 ± 0.000754	<LOD	<LOD	0.189 ± 0.0193	4.00 ± 0.216
T2-2	<LOD	<LOD	1020 ± 9.127	0.0859 ± 0.0136	0.156 ± 0.00830	1.56 ± 0.0612
T2-3	<LOD	0.00789 ± 0.00128	1085 ± 16.01	0.0609 ± 0.00913	0.528 ± 0.000931	6.17 ± 0.634
T3-1	<LOD	0.0108 ± 0.000574	<LOD	0.0491 ± 0.00500	0.369 ± 0.0600	7.20 ± 0.0225
T3-2	<LOD	<LOD	1154 ± 57.01	0.0518 ± 0.00281	0.363 ± 0.0229	3.02 ± 0.0876
T3-3	0.422 ± 0.0842	0.0237 ± 0.00400	1262 ± 24.85	0.0366 ± 0.00356	0.369 ± 0.0266	5.24 ± 0.300
T4	<LOD	<LOD	567 ± 31.1	0.123 ± 0.0167	1.03 ± 0.00260	25.0 ± 1.10
T5	<LOD	<LOD	1706 ± 5.244	0.0603 ± 0.00956	0.451 ± 0.0507	0.243 ± 0.0323
T6	<LOD	0.0101 ± 0.000414	6223 ± 12.07	0.256 ± 0.0294	1.03 ± 0.0983	85.1 ± 3.76
T7	<LOD	<LOD	2590 ± 20.28	<LOD	0.318 ± 0.0154	0.171 ± 0.0269
T8	<LOD	<LOD	2949 ± 67.23	0.0525 ± 0.000177	0.359 ± 0.0165	0.187 ± 0.0112
T9	<LOD	<LOQ	2946 ± 50.77	0.143 ± 0.0000797	974 ± 6.01	1.93 ± 0.0188
T10	0.109 ± 0.0122	<LOD	464 ± 4.31	0.0325 ± 0.00263	0.995 ± 0.0323	0.726 ± 0.0336
T11	0.186 ± 0.0255	<LOQ	1501 ± 24.28	0.0160 ± 0.00161	0.469 ± 0.0357	0.186 ± 0.0207
T12	0.628 ± 0.102	0.0164 ± 0.000190	781 ± 11.6	0.0574 ± 0.0102	0.480 ± 0.0266	0.451 ± 0.0608
T13	0.401 ± 0.0851	<LOD	2018 ± 57.69	0.0452 ± 0.00349	0.698 ± 0.0568	2.97 ± 0.0231
T14-1	0.344 ± 0.0352	0.0235 ± 0.00459	887 ± 4.74	0.0471 ± 0.00227	0.358 ± 0.0233	3.97 ± 0.0658
T14-2	0.263 ± 0.0618	0.0250 ± 0.000731	937 ± 10.1	0.0427 ± 0.00368	0.253 ± 0.0214	3.90 ± 0.00414
T14-3	0.425 ± 0.0651	0.0202 ± 0.000320	426 ± 14.8	0.0486 ± 0.00737	0.206 ± 0.0104	0.823 ± 0.00837

Table 2.5. (continued)

Sample Code	Fe	Co	Ni	Cu	Zn	As	Mo
T1-1	28.8 ± 1.49	0.0521 ± 0.00355	0.341 ± 0.0456	0.970 ± 0.00471	835 ± 27.3	<LOD	0.441 ± 0.0848
T1-2	30.7 ± 2.24	0.532 ± 0.00365	0.202 ± 0.0159	0.832 ± 0.0381	741 ± 12.7	<LOD	<LOD
T2-1	28.5 ± 0.0131	0.0143 ± 0.00143	0.265 ± 0.0147	0.818 ± 0.0470	458 ± 5.59	<LOQ	0.332 ± 0.0282
T2-2	27.7 ± 3.56	0.0572 ± 0.00801	0.142 ± 0.0224	2.75 ± 0.539	280 ± 0.591	<LOD	<LOD
T2-3	30.8 ± 3.91	0.496 ±0.0400	0.152 ± 0.0107	0.870 ± 0.106	518 ± 24.4	0.143 ± 0.0159	<LOD
T3-1	20.6 ± 1.38	0.0615 ± 0.00735	0.321 ± 0.0534	1.15 ± 0.127	873 ± 1.54	<LOD	0.306 ± 0.00300
T3-2	18.4 ± 0.0570	0.0825 ± 0.00596	<LOQ	15.6 ± 0.953	556 ± 5.06	0.0556 ± 0.0103	0.454 ± 0.0888
T3-3	31.7 ± 3.21	0.246 ± 0.0225	0.262 ± 0.0173	15.6 ± 0.619	713 ± 0.763	0.162 ± 0.00802	0.428 ± 0.0832
T4	57.1 ± 3.67	<LOD	0.334 ± 0.0454	41.1 ± 1.47	5.19 ± 0.368	15.8 ± 0.920	0.564 ± 0.0365
T5	15.3 ± 2.14	0.0583 ± 0.00152	<LOQ	0.373 ± 0.0375	1.01 ± 0.0974	<LOD	<LOQ
T6	27.8 ± 2.95	ND	0.262 ± 0.000818	0.747 ± 0.0609	5.68 ± 0.931	<LOD	<LOD
T7	5.20 ± 0.0757	0.00561 ±0.0000629	<LOQ	0.474 ± 0.00851	<LOD	<LOD	<LOD
T8	8.58 ± 0.23	<LOQ	0.166 ± 0.0246	2.46 ± 0.0794	ND	<LOD	0.257 ± 0.0516
T9	17.4 ± 2.36	0.127 ± 0.0129	0.179 ± 0.00262	1.61 ± 0.0418	5.45 ± 0.0912	<LOD	<LOD
T10	11.7 ± 0.0844	0.0846 ± 0.00339	<LOD	0.547 ± 0.0439	0.668 ± 0.00414	<LOD	0.223 ± 0.0205
T11	7.85 ± 1.12	3.21 ± 0.0895	0.0383 ± 0.000555	0.361 ± 0.0392	1.65 ± 0.0297	0.250 ± 0.00116	0.558 ± 0.0749
T12	25.6 ± 2.54	0.0275 ± 0.00144	0.151 ± 0.0252	0.415 ± 0.0256	<LOD	<LOD	0.0782 ± 0.0141
T13	18.7 ± 3.17	0.989 ± 0.0127	0.142 ± 0.00306	0.475 ± 0.0571	<LOD	<LOQ	0.266 ± 0.0224
T14-1	10.4 ± 0.371	0.0309 ± 0.00266	<LOD	0.559 ± 0.00213	1.73 ± 0.198	0.159 ± 0.0219	0.136 ± 0.0160
T14-2	14.2 ± 2.64	0.0328 ± 0.00407	<LOD	0.441 ± 0.0386	1.62 ± 0.0920	<LOD	<LOD
T14-3	11.9 ± 0.462	0.0233 ± 0.00183	<LOD	5.39 ± 0.146	0.819 ± 0.124	0.250 ± 0.0133	<LOD

Table 2.5. (continued)

Sample Code	Ag	Cd	Sn	Sb	Ba	Hg	Pb
T1-1	0.960 ± 0.154	0.301 ± 0.0120	<LOQ	0.649 ± 0.0181	3.20 ± 0.350	<LOD	1.04 ± 0.0584
T1-2	<LOD	0.276 ± 0.0130	<LOQ	22.0 ± 0.619	12.2 ± 0.498	0.375 ± 0.0462	1.20 ± 0.179
T2-1	0.959 ± 0.0906	0.189 ± 0.00272	<LOQ	0.463 ± 0.00564	5.90 ± 0.327	<LOQ	0.618 ± 0.0273
T2-2	<LOD	0.120 ± 0.00787	<LOQ	118 ± 1.61	1.28 ± 0.119	<LOD	0.552 ± 0.0490
T2-3	ND	0.244 ± 0.0260	0.162 ± 0.00119	133 ± 2.86	53.9 ± 4.82	<LOD	0.971 ± 0.0747
T3-1	<LOD	0.319 ± 0.00241	<LOQ	0.301 ± 0.0261	6.53 ± 0.334	<LOQ	0.888 ± 0.0415
T3-2	<LOD	0.186 ± 0.0104	0.0568 ± 0.00345	139 ± 4.86	1.92 ± 0.00587	<LOD	0.967 ± 0.0853
T3-3	<LOD	0.247 ± 0.00951	0.199 ± 0.0242	148 ± 1.70	6.45 ± 0.143	<LOD	1.39 ± 0.0751
T4	7.48 ± 0.235	<LOD	5.34 ± 0.199	8.12 ± 0.557	5.47 ± 0.698	<LOD	<LOD
T5	31.2 ± 1.64	0.103 ± 0.00833	0.105 ± 0.00907	109 ± 0.458	1.15 ± 0.149	0.0818 ± 0.00544	<LOD
T6	0.489 ± 0.0236	<LOQ	0.179 ± 0.0185	218 ± 15.9	ND	0.157 ± 0.00597	ND
T7	<LOD	<LOD	0.125 ± 0.000988	<LOD	ND	<LOD	<LOD
T8	<LOD	<LOD	0.255 ± 0.0482	<LOD	2.02 ± 0.357	<LOD	0.184 ± 0.0140
T9	5.83 ± 0.0668	<LOQ	1.26 ± 0.0630	16.1 ± 0.288	<LOD	<LOD	<LOD
T10	1.52 ± 0.0665	<LOQ	0.104 ± 0.00110	63.5 ± 0.961	<LOD	<LOD	<LOD
T11	0.436 ± 0.0260	<LOD	0.0556 ± 0.00472	143 ± 1.43	4.50 ± 0.511	<LOQ	0.657 ± 0.0237
T12	1.20 ± 0.171	<LOQ	0.0571 ± 0.00882	67.3 ± 2.80	ND	<LOQ	<LOD
T13	8.31 ± 0.137	<LOQ	0.0680 ± 0.00948	130 ± 0.935	0.758 ± 0.117	<LOD	<LOD
T14-1	6.40 ± 0.466	<LOD	0.136 ± 0.00799	33.7 ± 0.300	4.65 ± 0.766	<LOD	0.489 ± 0.0647
T14-2	6.02 ± 0.929	<LOD	0.133 ± 0.00236	34.3 ± 0.573	0.816 ± 0.142	<LOD	0.165 ± 0.0138
T14-3	3.47 ± 0.138	<LOQ	0.0760 ± 0.00782	15.3 ± 0.313	4.29 ± 0.568	<LOD	<LOD

<LOD: lower than limit of detection; <LOQ: lower than limit of quantification; ND: not determined.

2.5 DISCUSSION

Despite the fact that the fabrics were manufactured in several European countries and some of them (T1, T2, and T3) in Bangladesh, most of the metal levels were found to be similar in all textile samples. The presence of some metals can be directly related to their use (or their compounds´ usage) during fabrics production and/or functionalisation. However, some metals such as beryllium, mercury, and cadmium were detected at trace levels in some samples even though they have not been reported to have a specific role in the textile industry. Beryllium (concentrations lower than 0.0300 μg g^{-1}), mercury (concentrations between 0.0818 and 0.375 μg g^{-1}), and cadmium (concentrations from 0.103 to 0.319 μg g^{-1}) were found, and their presence in some garments could imply contamination during the manufacturing, storage and/or selling of textiles. Beryllium concentrations in the analysed samples were lower than those reported by Rezyć et al. [38] in samples processed in the Croatian textile industry.

The presence of other metals in textiles can be related to their use in some stages of the production. This is the case of lithium (concentrations within the range of 0.109–0.699 μg g^{-1}) since lithium grease is one of the most widely used lubricants in industry worldwide, and the use of lithium grease in mechanical devices during the manufacturing of garments could contaminate textiles with this metal.

2.5.1 Metals used in the dyeing process

The presence of metals in textiles can be directly related to the dyeing process. That is the case of vanadium, since vanadium compounds are used as catalysts in the production of aniline black dye (CI 50440) [42,43]. Vanadium was detected in most of samples, and the range of concentrations was 0.0160–0.256 μg g^{-1} where samples made of black fibres showed the highest vanadium content [T4 (0.123±0.0167 μg g^{-1}), T6 (0.256±0.0294 μg g^{-1}), and T9 (0.143±0.0000797 μg g^{-1})]. Another example is chromium, because several chromium-based dyes, such as chrome complexes with salicylic acid-based dyes (Mordant Yellow 1 and Mordant Yellow 5) give rise to mainly yellow and orange colours. In addition, Mordant Red 7, Mordant Red 19, Mordant Black 3, Mordant Black 9, Mordant Black 11, and Mordant Blue 13 dyestuffs, obtained by chroming aryl azo compounds, are also used in the textile industry [3,44]. Chromium was, therefore, quantified in all samples, except T1-1, and chromium concentration was within the range of 0.156–1.03 μg g^{-1}, except in textile coded as T9, which showed a very high chromium content (974±6.01 μg g^{-1}). Except for this sample (T9), similar concentrations were obtained by Menezes et al. [37] in textile samples produced in Brazil and China.

In addition, barium sulphate (whitening colourant) and barium pigments can be used in the textile industry. Most of the analysed samples were found to contain barium, such as textiles T2-3 (53.9±4.82 μg g^{-1}) and T13 (0.758±0.117 μg g^{-1}) that contained the highest and lowest concentrations, respectively. Similarly, lead white and lead chromate pigments are also used in the textile industry [45]. Lead concentrations varied between 0.165 and 1.39 μg g^{-1}.

Other metals such as copper, cobalt, and nickel are also used during the dyeing process as mordants [3]. This is the case of cobalt and nickel chlorides, as well as copper (I, II) sulphates [46]. These elements were in the studied samples at the concentration ranges as follows: cobalt from 0.00561 to 3.21 μg g^{-1}, nickel between 0.0383 and 0.341 μg g^{-1}, and copper in the range of 0.361–41.1 μg g^{-1}. The concentrations of these elements were lower than those previously reported in the literature [37–39]. Similarly, stannous chloride is also used as a mordant in dyeing procedures [46], and certain organotin species have been reported as biocides in textile products [47]. Sixteen studied samples were found to contain tin which ranged from 0.0556 to 0.255 μg g^{-1}, except for textile T4 (5.34±0.199 μg g^{-1}) and textile T9 (1.26±0.0630 μg g^{-1}).

2.5.2 Metals used in the bleaching process

Iron can be used to form metal-complex dyes [3,46,48] but it is also used as a catalyst in the bleaching process [5,6] (hydrophobic components removal guarantees an optimum further dyeing). All studied textile samples have been found to contain iron, and textile T4 was the one with the highest level (57.1±3.67 μg g^{-1}). Furthermore, the presence of manganese in textiles is also related to the bleaching stage since several manganese complexes are used as catalysts to enhance this process [6]. Regarding manganese, textile samples coded as T6 and T4 showed the highest concentrations (85.1±3.76 and 25.0±1.10 μg g^{-1}, respectively). The concentration of manganese in the remaining samples was in the range of 0.171–7.20 μg g^{-1}.

2.5.3 Metallic NPs in the textile industry

Titanium dioxide is broadly used as delustering agent in synthetic fibres to reduce the lustre and transparency of yarns [49]. Furthermore, hexafluorotitanate salts [8,9,50] and TiO_2NPs [51,52] can be used to achieve anti-flammable textiles. Besides, TiO_2NPs provide self-cleaning [16,53–56], ultraviolet protection [56,57], and antibacterial activity [56–58] to fabrics. In addition, titanium and titanium dioxide (bulk and nanoparticulate) are whitening colourants. In general, titanium concentrations in the studied textiles ranged between 156 (T1-2) and 6223 (T6) μg g^{-1}.

Samples coded as T7 and T8 were purchased from the same manufacturer (e-market) who specified that TiO_2NPs were added to these textile products (children's T-shirt) to obtain protection against ultraviolet radiation (**Table 2.1**). It was found that titanium concentrations were 2590±20 and 2949±67 μg g^{-1} for T7 and T8, respectively.

The manufacturers of the remaining samples did not specify the addition of titanium, which could mean that titanium was used to enhance fire retardation or opacity of fibres. Moreover, titanium could be present in these samples since they contain totally or partially white fibres (bulk titanium dioxide and TiO_2NPs provide brightness and opacifying characteristics). Samples T10, T11, T12, T13, and T14 (T14-1, T14-2, and T14-3) were all-white clothes. Sample T6 was the sample with highest concentration of titanium, and it was half white and half black (one colour in each side of the piece of garment). In addition, titanium was present in T1-2, T2-2, T2-3, T3-2, and T3-3 which were subsamples that contain white fibres mixed with coloured fibres.

Regarding zinc, textiles coded as T1, T2, and T3 were purchased from the same manufacturer who specified that these garments contained ZnONPs (**Table 2.1**) to provide UV protection [59]. Therefore, these textiles showed very high zinc concentrations, ranging from 280 to 873 μg g^{-1}. Zinc content in the remaining textiles was slightly lower than those levels found in samples T1 to T3, varying between 0.668 and 5.68 μg g^{-1}.

Finally, several manufacturers of the studied textiles have specified the presence of silver ions or AgNPs in the garments since silver compounds offer biocide properties to the textiles [60]. In accordance with textile compositions given by the manufacturers, silver ions were present in the samples T4, T5, T6, and T9, whereas AgNPs were added to textiles T10, T11, T12, T13, and T14 (T14-1, T14-2, and T14-3) (**Table 2.1**). Silver concentrations in the above-mentioned samples ranged between 0.436 (T11) and 31.2 μg g^{-1} (T5). In addition, another two samples (T1-1 and T2-1) were found to contain silver, although silver ions/NPs were not listed in the textile composition.

2.5.4 Other uses of metals in the textile industry

The presence of metals such as molybdenum and antimony is related to their use in flame retardant formulations [7,8,61]. Molybdenum was quantified in twelve samples at concentrations lower than 0.600 μg g^{-1}. The levels of Mo in the samples were lower than those reported by

Rezyć et al. [38] whose found Mo concentrations between 0.04 and 9.93 μg g^{-1} in textile samples. However, antimony was present at high concentrations (0.301 to 218 μg g^{-1}). As previously commented, high antimony concentrations in polyester fibres can be due to its use in the fabrication of polyethylene terephthalate (the most common type of polyester used in garments) [10]. A direct relationship was found between the presence of antimony and the percentage of polyester in the samples, and samples with higher polyester percentages than 50% (**Table 2.1**) were those with the highest antimony levels (higher than 100 μg g^{-1}, samples T2-2, T2-3, T3-2, T3-3, T5, T6, T11, and T13).

Arsenic compounds are effective insecticides and herbicides and the use of organoarsenicals is a common practice to control weeds in cotton fields and as defoliants of cotton plants [62]. Arsenic was, therefore, found in six cotton-based textile samples (T2-3, T3-2, T3-3, T4, T14-1, and T14-3) and in one non-cotton-based fabric (T11) (**Table 2.1**). The concentration of arsenic in the studied textiles varied between 0.0556 and 0.250 μg g^{-1}, except for sample T4 (15.8±0.920 μg g^{-1}), where high arsenic levels could be associated with high cotton percentage (80%) in the garment.

2.6 CONCLUSIONS

A microwave-assisted acid digestion procedure using a mixture of nitric acid, hydrogen peroxide, hydrochloric acid, and hydrofluoric acid has found adequate for decomposing a vast variety of textiles and (nano)textiles. ICP-MS multi-element determinations were found to be accurate (analytical recoveries within the range of 90–107%) and precise (RSDs varied between 1 and 3%).

The content of cadmium, lead, chromium (VI), arsenic, mercury, and dioctyltin in fabrics is regulated in Europe (Regulation 1907/2006). The concentration of arsenic found in textile T4 (15.8±0.920 μg g^{-1}) exceeded the maximum legal concentration of arsenic in textile products manufactured in Europe (1 μg g^{-1}). Subsamples T1-1, T1-2, and T3-3 showed concentrations of lead which were close to the maximum legal limit or over it, 1 μg g^{-1} (1.04±0.0584, 1.20±0.179, and 1.39±0.0751 μg g^{-1}, respectively). Impregnation of yarns with mercury compounds is not allowed, but mercury was found in fabrics T1-2 (0.375±0.0462 μg g^{-1}), T5 (0.0818±0.00544 μg g^{-1}), and T6 (0.157±0.00597 μg g^{-1}).

On the other hand, speciation studies are necessary in the analysis of chromium. Hexavalent chromium is the only chromium species regulated in textile products, and its maximum allowable concentration is 1 μg g^{-1}. Total concentrations of chromium in textiles T4 and T6 were just in the maximum legal limit of hexavalent chromium, whereas sample T9 was over it (974±6.01 μg g^{-1}).

Regarding metals such as silver, titanium, and zinc, which are mainly added as NPs (AgNPs, TiO_2NPs, and ZnONPs) in functionalised (nano)textiles, high levels have been found in some garments which were reported to contain NPs by the manufacturers. Further studies would be welcome in order to characterise the particle size distribution as well as the release of these metallic NPs under conventional washing (laundry) conditions.

REFERENCES

[1] I. Anderie, K. Schulte, Chromate Testing in Leather: EN ISO 17075, in J.K. Chen, J.P. Thyssen (Eds.), *Metal Allergy. From Dermatitis to Implant and Device Failure*, Springer International Publishing AG, Gewerbestrasse, Switzerland (2018) 31–38, DOI: 10.1007/978-3-319-58503-1_4.

[2] J. Zhang, W. Chen, A faster and more effective chrome tanning process assisted by microwave, RSC Adv. 10 (2020) 23503–23509, DOI: 10.1039/D0RA04189K.

[3] J.N. Chakraborty, Metal-complex dyes, in M. Clark (Ed.), *Handbook of Textile and Industrial Dyeing: Principles, Processes and Types of Dyes*, Woodhead Publishing, Cambridge, United Kingdom (2011) 446–465, DOI: 10.1533/9780857093974.2.446.

[4] M. Shahid, Shahid-ul-Islam, F. Mohammad, Recent advancements in natural dye applications: A review, J. Clean Prod. 53 (2013) 310–331, DOI: 10.1016/j.jclepro.2013.03.031.

[5] D. Yu, M. Wu, J. Lin, Establishment of an effective activated peroxide system for low-temperature cotton bleaching using synthesized tetramido macrocyclic iron complex, Fibers Polym. 18 (2017) 1741–1748, DOI: 10.1007/s12221-017-7023-0.

[6] R. Hage, J.W. de Boer, F. Gaulard, K. Maaijen, Manganese and Iron Bleaching and Oxidation Catalysts, in R. van Eldik, C.D. Hubbard (Eds.), *Advances in Inorganic Chemistry, Homogeneous Catalysis*, Academic Press, Cambridge, United Kingdom 65 (2013) 85–116, DOI: 10.1016/B978-0-12-404582-8.00003-1.

[7] S. Gaan, V. Salimova, P. Rupper, A. Ritter, H. Schmid, Flame retardant functional textiles, in N. Pan, G. Sun (Eds.), *Functional Textiles for Improved Performance, Protection and Health*, Woodhead Publishing, Cambridge, United Kingdom (2011) 98–130, DOI: 10.1533/9780857092878.98.

[8] W.D. Schindler, P.J. Hauser, Flame-retardant finishes, in *Chemical Finishing of Textiles*, Woodhead Publishing, Cambridge, United Kingdom (2004) 98–116, DOI: 10.1533/9781845690373.98.

[9] R.M. Kozłowski, M. Muzyczek, Improving the flame retardancy of natural fibres, in R.M. Kozłowski, M. Mackiewicz-Talarczyk (Eds.), *Handbook of Natural Fibres. Volume Two: Processing and Applications* (Second Edition), Woodhead Publishing, Cambridge, United Kingdom (2020) 355–391, DOI: 10.1016/B978-0-12-818782-1.00010-9.

[10] M. Biver, A. Turner, M. Filella, Antimony release from polyester textiles by artificial sweat solutions: A call for a standardized procedure, Regul. Toxicol. Pharmacol. 119 (2021) 104824, DOI: 10.1016/j.yrtph.2020.104824.

[11] A.K. Yetisen, H. Qu, A. Manbachi, H. Butt, M.R. Dokmeci, J.P. Hinestroza, M. Skorobogatiy, A. Khademhosseini, S.H. Yun, Nanotechnology in Textiles, ACS Nano 10 (2016) 3042–3068, DOI: 10.1021/acsnano.5b08176.

[12] M. Montazer, T. Harifi, Introduction: Textile finishing, in *Nanofinishing of Textile Materials*, Woodhead Publishing, Cambridge, United Kingdom (2018) 1–17, DOI: 10.1016/B978-0-08-101214-7.00001-7.

[13] M. Montazer, T. Harifi, Nanobleaching, in *Nanofinishing of Textile Materials*, Woodhead Publishing, Cambridge, United Kingdom (2018) 51–64, DOI: 10.1016/B978-0-08-101214-7.00004-2.

[14] M. Montazer, T. Harifi, Nanoscouring, in *Nanofinishing of Textile Materials*, Woodhead Publishing, Cambridge, United Kingdom (2018) 35–50, DOI: 10.1016/B978-0-08-101214-7.00003-0.

[15] C. Zhu, J. Shi, S. Xu, M. Ishimori, J. Sui, H. Morikawa, Design and characterization of self-cleaning cotton fabrics exploiting zinc oxide nanoparticle-triggered photocatalytic degradation, Cellulose 24 (2017) 2657–2667, DOI: 10.1007/s10570-017-1289-7.

[16] W.S. Tung, W.A. Daoud, Self-cleaning fibers *via* nanotechnology: A virtual reality, J. Mater. Chem. 21 (2011) 7858–7869, DOI: 10.1039/C0JM03856C.

[17] M. Montazer, T. Harifi, Water-repellent textile nanofinishes, in *Nanofinishing of Textile Materials*, Woodhead Publishing, Cambridge, United Kingdom (2018) 183–195, DOI: 10.1016/B978-0-08-101214-7.00012-1.

[18] P.J. Rivero, A. Urrutia, J. Goicoechea, F.J. Arregui, Nanomaterials for Functional Textiles and Fibers, Nanoscale Res. Lett. 10 (2015) 501, DOI: 10.1186/s11671-015-1195-6.

[19] R. Dastjerdi, M. Montazer, A review on the application of inorganic nano-structured materials in the modification of textiles: Focus on anti-microbial properties, Colloids Surf. B 79 (2010) 5–18, DOI: 10.1016/j.colsurfb.2010.03.029.

[20] Y. Zhang, Q. Xu, F. Fu, X. Liu, Durable antimicrobial cotton textiles modified with inorganic nanoparticles, Cellulose 23 (2016) 2791–2808, DOI:10.1007/s10570-016-1012-0.

[21] M. Montazer, T. Harifi, Nanofinishes for protective textiles, in *Nanofinishing of Textile Materials*, Woodhead Publishing, Cambridge, United Kingdom (2018) 265–294, DOI: 10.1016/B978-0-08-101214-7.00018-2.

[22] Regulation (EU) N° 1007/2011 of the European Parliament and of the Council of 27 September 2011 on textile fibre names and related labelling and marking of the fibre composition of textile products and repealing Council Directive 73/44/EEC and Directives 96/73/EC and 2008/121/EC of the European Parliament and of the Council, Official Journal of the European Union, L272 (15 February 2018), 1–81.

[23] Regulation (EC) N° 1907/2006 of the European Parliament and of the Council of 18 December 2006 concerning the Registration, Evaluation, Authorisation and Restriction of Chemicals (REACH), establishing a European Chemicals Agency, amending Directive 1999/45/EC and repealing Council Regulation (EEC) Nº 793/93 and Commission Regulation (EC) N° 1488/94 as well as Council Directive 76/769/EEC and Commission Directives 91/155/EEC, 93/67/EEC, 93/105/EC and 2000/21/EC, Official Journal of the European Union, L396 (01 October 2021), 1–552.

[24] Commission Decision (EU) 2017/1392 of 25 July 2017 amending Decision 2014/350/EU establishing the ecological criteria for the award of the EU Ecolabel for textile products, Official Journal of the European Union, L195 (27 July 2017) 36–45.

[25] J.J. Hostynek, Factors determining percutaneous metal absorption, Food Chem. Toxicol. 41 (2003) 327–345, DOI: 10.1016/S0278-6915(02)00257-0.

[26] F. Larese Filon, F. D'Agostin, M. Crosera, G. Adami, M. Bovenzi, G. Maina, In vitro absorption of metal powders through intact and damaged human skin, Toxicol. Vitr. 23 (2009) 574–579, DOI: 10.1016/j.tiv.2009.01.015.

[27] M.E.K. Kraeling, V.D. Topping, Z.M. Keltner, K.R. Belgrave, K.D. Bailey, X. Gao, J.J. Yourick, In vitro percutaneous penetration of silver nanoparticles in pig and human skin, Regul. Toxicol. Pharmacol. 95 (2018) 314–322, DOI: 10.1016/j.yrtph.2018.04.006.

[28] F. Filon Larese, F. D'Agostin, M. Crosera, G. Adami, N. Renzi, M. Bovenzi, G. Maina, Human skin penetration of silver nanoparticles through intact and damaged skin, Toxicology 255 (2009) 33–37, DOI: 10.1016/j.tox.2008.09.025.

[29] T.M. Benn, P. Westerhoff, Nanoparticle Silver Released into Water from Commercially Available Sock Fabrics, Environ. Sci. Technol. 42 (2008) 4133–4139, DOI: 10.1021/es7032718.

[30] L. Geranio, M. Heuberger, B. Nowack, The Behavior of Silver Nanotextiles during Washing, Environ. Sci. Technol. 43 (2009) 8113–8118, DOI: 10.1021/es9018332.

[31] C. Lorenz, L. Windler, N. von Goetz, R.P. Lehmann, M. Schuppler, K. Hungerbühler, M. Heuberger, B. Nowack, Characterization of silver release from commercially available functional (nano)textiles, Chemosphere 89 (2012) 817–824, DOI: 10.1016/j.chemosphere.2012.04.063.

[32] D.M. Mitrano, E. Rimmele, A. Wichser, R. Erni, M. Height, B. Nowack, Presence of Nanoparticles in Wash Water from Conventional Silver and Nano-silver Textiles, ACS Nano 8 (2014) 7208–7219, DOI: 10.1021/nn502228w.

[33] D.M. Mitrano, E. Lombi, Y.A.R. Dasilva, B. Nowack, Unraveling the Complexity in the Aging of Nanoenhanced Textiles: A Comprehensive Sequential Study on the Effects of Sunlight and Washing on Silver Nanoparticles, Environ. Sci. Technol. 50 (2016) 5790–5799, DOI: 10.1021/acs.est.6b01478.

[34] D.M. Mitrano, Y.A.R. Dasilva, B. Nowack, Effect of Variations of Washing Solution Chemistry on Nanomaterial Physicochemical Changes in the Laundry Cycle, Environ. Sci. Technol. 49 (2015) 9665–9673, DOI: 10.1021/acs.est.5b02262.

[35] J.M. Gallo, J.R. Almirall, Elemental analysis of white cotton fiber evidence using solution ICP-MS and laser ablation ICP-MS (LA-ICP-MS), Forensic Sci. Int. 190 (2009) 52–57, DOI: 10.1016/j.forsciint.2009.05.011.

[36] M. Doğan, M. Soylak, L. Elçi, A. von Bohlen, Application of Total Reflection X-Ray Fluorescence Spectrometry in the Textile Industry, Mikrochim. Acta 138 (2002) 77–82, DOI: 10.1007/s006040200012.

[37] E.A. Menezes, R. Carapelli, S.R. Bianchi, S.N.P. Souza, W.O. Matos, E.R. Pereira-Filho, A.R.A. Nogueira, Evaluation of the mineral profile of textile materials using inductively coupled plasma optical emission spectrometry and chemometrics, J. Hazard. Mater. 182 (2010) 325–330, DOI: 10.1016/j.jhazmat.2010.06.033.

[38] I. Rezić, I. Steffan, ICP-OES determination of metals present in textile materials, Microchem. J. 85 (2007) 46–51, DOI: 10.1016/j.microc.2006.06.010.

[39] I. Rezić, M. Zeiner, I. Steffan, Determination of 28 selected elements in textiles by axially viewed inductively coupled plasma optical emission spectrometry, Talanta 83 (2011) 865–871, DOI: 10.1016/j.talanta.2010.10.031.

[40] E. Matoso, S. Cadore, Determination of inorganic contaminants in polyamide textiles used for manufacturing sport T-shirts, Talanta 88 (2012) 496–501, DOI: 10.1016/j.talanta.2011.11.022.

[41] T. Nguyen, M.A. Saleh, Exposure of women to trace elements through the skin by direct contact with underwear clothing, J. Environ. Sci. Health A 52 (2017) 1–6, DOI: 10.1080/10934529.2016.1221212.

[42] J.N. Chakraborty, Dyeing with oxidation black, in *Fundamentals and Practices in Colouration of Textiles*, Woodhead Publishing India, New Delhi, India (2010) 151–158, DOI: 10.1533/9780857092823.151.

[43] T.I. Fortoul, M. Rojas-Lemus, V. Rodriguez-Lara, A. Gonzalez-Villalva, M. Ustarroz-Cano, G. Cano-Gutierrez, S.E. Gonzalez-Rendon, L.F. Montaño, M. Altamirano-Lozano, Overview of environmental and occupational vanadium exposure and associated health outcomes: An article based on a presentation at the 8th International Symposium on Vanadium Chemistry, Biological Chemistry, and Toxicology, Washington DC, August 15–18, 2012, J. Immunotoxicol. 11 (2014) 13–18, DOI: 10.3109/1547691X.2013.789940.

[44] N. Sekar, Acid dyes, in M. Clark (Ed.), *Handbook of Textile and Industrial Dyeing: Principles, Processes and Types of Dyes*, Woodhead Publishing, Cambridge, United Kingdom (2011) 486–514, DOI: 10.1533/9780857093974.2.486.

[45] A. Gürses, K. Güneş, E. Şahin, Removal of dyes and pigments from industrial effluents, in S.K. Sharma (Ed.), *Green Chemistry and Water Remediation: Research and Applications*, Elsevier, Amsterdam, The Netherlands (2021) 135–187, DOI: 10.1016/B978-0-12-817742-6.00005-0.

[46] M. Feiz, H. Norouzi, Dyeing studies of wool fibers with madder (*Rubia tinctorum*) and effect of different mordants and mordanting procedures on color characteristics of dyed samples, Fibers Polym. 15 (2014) 2504–2514, DOI: 10.1007/s12221-014-2504-x.

[47] P. Manickam, D. Vijay, Chemical hazards in textiles, in S.S. Muthu (Ed.), *Chemical Management in Textiles and Fashion*, Woodhead Publishing, Cambridge, United Kingdom (2021) 19–52, DOI: 10.1016/B978-0-12-820494-8.00002-2.

[48] S.M. Burkinshaw, N. Kumar, The mordant dyeing of wool using tannic acid and $FeSO_4$, Part 1: Initial findings, Dyes Pigm. 80 (2009) 53–60, DOI: 10.1016/j.dyepig.2008.05.008.

[49] A.F. Richards, Nylon fibres, in J.E. McIntyre (Ed.), *Synthetic Fibres: Nylon, Polyester, Acrylic, Polyolefin*, Woodhead Publishing, Cambridge, United Kingdom (2005) 20–94, DOI: 10.1533/9781845690427.20.

[50] P. Joseph, S. Tretsiakova-McNally, Chemical modification of natural and synthetic textile fibres to improve flame retardancy, in F.S. Kilinc (Ed.), *Handbook of Fire Resistant Textiles*, Woodhead Publishing, Cambridge, United Kingdom (2013) 37–67, DOI: 10.1533/9780857098931.1.37.

[51] X.W. Cheng, J.P. Guan, X.H. Yang, R.C. Tang, Improvement of flame retardancy of silk fabric by bio-based phytic acid, nano-TiO_2, and polycarboxylic acid, Prog. Org. Coat. 112 (2017) 18–26, DOI: 10.1016/j.porgcoat.2017.06.025.

[52] M. Montazer, T. Harifi, Flame-retardant textile nanofinishes, in *Nanofinishing of Textile Materials*, Woodhead Publishing, Cambridge, United Kingdom (2018) 163–181, DOI: 10.1016/B978-0-08-101214-7.00011-X.

[53] F.A. Sadr, M. Montazer, In situ sonosynthesis of nano TiO_2 on cotton fabric, Ultrason. Sonochem. 21 (2014) 681–691, DOI: 10.1016/j.ultsonch.2013.09.018.

[54] A. Bozzi, T. Yuranova, I. Guasaquillo, D. Laub, J. Kiwi, Self-cleaning of modified cotton textiles by TiO_2 at low temperatures under daylight irradiation, J. Photochem. Photobiol. A 174 (2005) 156–164, DOI: 10.1016/j.jphotochem.2005.03.019.

[55] A. Bozzi, T. Yuranova, J. Kiwi, Self-cleaning of wool-polyamide and polyester textiles by TiO_2-rutile modification under daylight irradiation at ambient temperature, J. Photochem. Photobiol. A 172 (2005) 27–34, DOI: 10.1016/j.jphotochem.2004.11.010.

[56] M.M. Rashid, B. Simonĉiĉ, B. Tomŝiĉ, Recent advances in TiO_2-functionalized textile surfaces, Surf. Interfaces 22 (2021) 100890, DOI: 10.1016/j.surfin.2020.100890.

[57] M.E. El-Naggar, T.I. Shaheen, S. Zaghloul, M.H. El-Rafie, A. Hebeish, Antibacterial Activities and UV Protection of the in Situ Synthesized Titanium Oxide Nanoparticles on Cotton Fabrics, Ind. Eng. Chem. Res. 55 (2016) 2661–2668, DOI: 10.1021/acs.iecr.5b04315.

[58] K. Kowal, P. Cronin, E. Dworniczek, J. Zeglinski, P. Tiernan, M. Wawrzynska, H. Podbielska, S.A.M. Tofail, Biocidal effect and durability of nano-TiO_2 coated textiles to combat hospital acquired infections, RSC Adv. 4 (2014) 19945–19952, DOI: 10.1039/C4RA02759K.

[59] A. Becheri, M. Dürr, P. Lo Nostro, P. Baglioni, Synthesis and characterization of zinc oxide nanoparticles: Application to textiles as UV-absorbers, J. Nanopart. Res. 10 (2008) 679–689, DOI: 10.1007/s11051-007-9318-3.

[60] M. Rai, A. Yadav, A. Gade, Silver nanoparticles as a new generation of antimicrobials, Biotechnol. Adv. 27 (2009) 76–83, DOI: 10.1016/j.biotechadv.2008.09.002.

[61] S. Posner, Developments in flame retardants for interior materials and textiles, in T. Rowe (Ed.), *Interior Textiles. Design and Developments*, Woodhead Publishing, Cambridge, United Kingdom (2009) 211–228, DOI: 10.1533/9781845696870.2.211.

[62] A.J. Bednar, J.R. Garbarino, J.F. Ranville, T.R. Wildeman, Presence of Organoarsenicals Used in Cotton Production in Agricultural Water and Soil of the Southern United States, J. Agric. Food Chem. 50 (2002) 7340–7344, DOI: 10.1021/jf025672i.

PART B. DETERMINATION OF INORGANIC NPs IN MOISTURISERS AND TEXTILES

CHAPTER 3. SILVER NANOPARTICLES ASSESSMENT IN MOISTURISING CREAMS BY ULTRASOUND-ASSISTED EXTRACTION FOLLOWED BY spICP-MS

CHAPTER 3. SILVER NANOPARTICLES ASSESSMENT IN MOISTURISING CREAMS BY ULTRASOUND-ASSISTED EXTRACTION FOLLOWED BY spICP-MS*

*The results from this chapter have already been published as Iria Rujido-Santos, Lucía Naveiro-Seijo, Paloma Herbello-Hermelo, María Carmen Barciela-Alonso, Pilar Bermejo-Barrera, and Antonio Moreda-Piñeiro, Silver nanoparticles assessment in moisturizing creams by ultrasound assisted extraction followed by sp-ICP-MS, Talanta 197 (2019) 530–538, DOI: 10.1016/j.talanta.2019.01.068.

Group of Trace Element, Spectroscopy, and Speciation (GETEE), Strategic Grouping in Materials (AEMAT). Department of Analytical Chemistry, Nutrition, and Bromatology. Faculty of Chemistry. Universidade de Santiago de Compostela. Avenida das Ciencias, s/n 15782, Santiago de Compostela. Spain.

3.1 ABSTRACT

Advances on nanometrology require reliable sample pre-treatment methods for extracting/isolating nanoparticles from complex samples. The current development deals with a discontinuous ultrasonication method (60% amplitude, 15 cycles of ultrasound treatment for 59 s plus relaxing stage for 59 s, 20 mL of methanol) for a fast and quantitative extraction of silver nanoparticles (AgNPs) from moisturising creams. Possibilities offered by modern inductively coupled plasma mass spectrometry (ICP-MS), which allows 'single particle' assessment (spICP-MS) have been used for AgNPs assessment (AgNPs concentration and Ag size distribution). The relative standard deviation (RSD) of the overall procedure (AgNPs concentration in eleven extracts from a same cream) was found to be 5%; whereas, the analytical recovery for spiking experiments with AgNPs of 20, 40, and 60 nm was found to be within the 90–109% range. The limit of quantification in AgNPs concentration was established at 8.25×10^5 AgNPs g^{-1}, whereas the limit of detection in size was found to be within the 5–13 nm range (several equations were used for the calculation). Finally, moisturising creams prescribed for atopic dermatitis and also regular moisturising creams were analysed for total Ag, and for AgNPs characterisation (AgNPs concentration and AgNPs size distribution) by spICP-MS. Electronic microscopy was also used for comparative (qualitative) purposes.

3.2 INTRODUCTION

The first scientific publication on nanomaterials (NMs) dates back to the 1950s. However, the production and use of NMs has increased drastically in recent years [1]. Based on the existing European Commission recommendation of nanomaterial definition, a nanomaterial can be described as a natural, incidental or manufactured material which contains at least 50% of particles with one or more dimensions between 1 and 100 nm [2]. This definition is also encompassed in the specific European Commission regarding cosmetic products monitoring [3]. NMs can be classified according to parameters such as chemical structure (organic or inorganic NMs), source (natural or engineered NMs), size, and application, among other criteria [4,5].

Physical and chemical properties of NMs are different from those found in bulk material. The high specific surface exhibited by NMs is responsible for their high reactivity and their potential use as catalysts [6]. Differences from bulk materials are also found in mechanical (hardness and elasticity) and optical properties of NMs [5,7], the latter attributed to electronic confinement, which changes light absorption properties due to plasmon resonance. Plasmon resonance occurs when electromagnetic radiation impacts on a metal nanoparticle that causes the oscillation of the free conduction electrons with the same frequency of the incidental field [8]. In addition, electron confinement also makes certain metallic nanoparticles such as quantum dots (QDs) exhibit fluorescent properties [7].

The innovative properties of NMs make them appealing materials for a large number of applications: food industry (additives and food packaging), coatings, explosives, electronics (fuel cells, batteries, light sources), catalysts, bioremediation, paints, cosmetics, textiles [5], medicine (diagnosis, imaging [9], and drug delivery [10]), and wastewater treatment [11]. Silver nanoparticles (AgNPs) are among the most widely used nanoparticles in several sectors of industry mainly because of their antiseptic properties against bacteria, [12] fungi [13], and viruses [14], making them useful in foodstuffs, food packaging, nutritional supplements, textiles, medical products and devices (breathing masks, catheters, bandages), personal care products, disinfectants, coatings for refrigerators, detergents, air cleaners, among others [15–17]. According to the "The Nanodatabase" [18] and the European Union Observatory of Nanomaterials (EUON) [19] inventories, there are currently 3035 consumer products containing NPs available in the European market, and 379 products are modified with AgNPs.

The modification of cosmetics with NPs must be reported to the European Commission six months prior to being placed on the market (Article 16, EC/1223/2009 [3]). According to this regulation, the use of AgNPs in cosmetics is forbidden. Elemental silver (E174) used as colourant, and silver chloride, combined with titanium dioxide, used as preservative [maximum concentration of 0.004% (w/w)], are the allowed silver species (Annex IV and Annex V, EC/1223/2009 [3]). There are, however, creams in which the presence of AgNPs is allowed, and they are prescribed as medicaments for treating bacterial infections in atopic dermatitis [20]. Total silver determination in moisturising creams is therefore not enough to verify the absence of AgNPs since ionic silver is allowed to be present in cosmetics [3]. Reliable methodologies for AgNPs assessment (AgNPs concentration and size distribution) in cosmetics are needed for verifying if the products comply with the regulation.

Electron microscopy (scanning and transmission electron microscopy, SEM and TEM), atomic force microscopy (AFM), scanning tunnelling microscopy (STM), dynamic light scattering (DLS), and X-ray spectroscopy (X-ray absorption, X-ray fluorescence, X-ray diffraction, and X-ray photoelectron spectroscopy, XAS, XRF, XRD, and XPS) provide qualitative information (physical properties and chemical composition) of NPs [5]. However, quantitative information can only be assessed with techniques such as inductively coupled plasma mass spectrometry (ICP-MS), graphite furnace atomic absorption spectroscopy (GFAAS), and inductively coupled plasma optical emission spectroscopy (ICP-OES) [5]. Nevertheless, these techniques do not distinguish between dissolved species and nanoparticles of a certain metal. Metallic speciation can be achieved by coupling these detectors with separation techniques such as asymmetric flow field-flow fractionation (AF4), size exclusion chromatography (SEC), hydrodynamic chromatography (HDC), reversed phase high performance liquid chromatography (RP-HPLC), and capillary electrophoresis (CE) [5]. Single particle inductively coupled plasma mass spectrometry (spICP-MS) is a promising technique for analysing complex samples that contain NPs without a previous separation step. The theoretical basis of spICP-MS was outlined by Deguelde et al. [21–25], and recently reviewed

by Laborda et al. [26]. Single particle-ICP-MS provides metallic NP size distributions and information about NP concentration [27]. The possibilities of spICP-MS using modern instrumentation allowing short dwell times for data acquisition (lower than 100 µs) [28] have been investigated in the current work for AgNPs assessment in moisturising creams. Special attention has focused on performing a reliable and fast sample pre-treatment for AgNPs isolation, guaranteeing the integrity of the targets.

3.3 EXPERIMENTAL

3.3.1 Instrumentation

An Inductively Coupled Plasma Mass Spectrometry NexION® 300X model (Perkin Elmer, Waltham, MA, USA) equipped with a Meinhard® nebuliser and a cyclonic spray chamber, and a SeaFast SC2 DX autosampler (Elemental Scientific, Omaha, NB, USA) was used for total Ag determination. The same instrument was also used for AgNPs assessment using the Syngistix™ Nano Application software version 1.1. A VCX 130 model ultrasonic probe (net power output of 130W and frequency of 20 kHz) from Vibra-Cell™ (Sonics & Materials Inc., Newtown, CT, USA) was used for achieving a rapid extraction of AgNPs from cosmetic samples. An Ethos Plus microwave lab-station (Milestone, Sorisole, Italy) with 100 mL closed Teflon vessels and Teflon covers, HTC adapter plate and HTC safety springs (Milestone) was used for assisting the acid digestion procedure of moisturising creams. A JSM 6400 scanning electron microscope (SEM) and a JEM 1010 transmission electron microscope (TEM) from JEOL (Tokyo, Japan) were used for comparative purposes (SEM/TEM images and microanalysis). A Nevir 6223MG domestic microwave oven (Madrid, Spain), programmable for time and a maximum microwave power of 700 W, was used for methanol extract acid digestion in laboratory-made poly(tetrafluorethylene) (PTFE) bombs hermetically sealed (low-pressure acid digestion). A Raypa UCI–150 ultrasonic cleaner water-bath (ultrasound frequencies of 17 and 35 kHz, 325 W) from R. Espinar S.L. (Barcelona, Spain) was used for assisting extract oxidation before SEM/TEM analysis.

3.3.2 Reagents

Ultrapure water of 18 MΩcm resistivity was obtained from a Milli-Q® water purification system (Millipore, Bedford, MA, USA). Certified reference material NIST 8013 of gold nanoparticles of 60 nm nominal diameter was purchased from National Institute of Standards and Technology (Gaithersburg, MD, USA). Certified reference materials of silver nanoparticles of 20 nm (0.02 g L^{-1}, 4.5×10^{14} NPs L^{-1}), 40 nm (0.02 g L^{-1}, 5.7×10^{13} NPs L^{-1}), and 60 nm (0.02 g L^{-1}, 1.7×10^{13} NPs L^{-1}) nominal diameters in aqueous (sodium citrate buffer) were supplied by Sigma-Aldrich (San Louis, MO, USA). 99.5% Glycerol was also from Sigma Aldrich. Methanol (Chromasolv LC-MS) and isopropanol were supplied by Riedel-de Haën (Seelze, Germany) and Merck (Darmstadt, Germany), respectively. Nitric acid (Hiperpur, 69%), and 33% hydrogen peroxide were from Panreac (Barcelona, Spain). NexIon Setup Solution (10 µg L^{-1} of Be, Ce, Fe, In, Li, Mg, Pb, and U in 1% HNO_3), and NexION Setup Solution (1 µgL^{-1} of Be, Ce, Fe, In, Li, Mg, Pb, and U in 1% HNO_3) were purchased from Perkin Elmer. Rhodium internal standard (1000 mg L^{-1} in 5% HNO_3) and Ag stock standard solution (1000 mg L^{-1} in 0.5 M HNO_3) were from Merck.

3.3.3 Moisturising cream samples

Samples used in the current study consist of three creams prescribed for atopic dermatitis (coded as MC1, MC2, and MC3), one of them bought in a pharmacy, and two purchased online. The remaining samples (coded as MC4 to MC13) were moisturising creams purchased from

local shops in Santiago de Compostela. Composition of samples regarding base compounds was quite similar in all of them, and water, glycerine and/or glycerine derivatives, and seed oils were present (concentrations were not available in the labels). However, other several organic compounds were quite different in the analysed samples. The three creams prescribed for atopic dermatitis listed the presence of silver in the composition, although there was not information regarding the nature (nano and/or bulk) of silver.

To avoid errors derived from possible AgNPs oxidation and/or degradation, and as previously recommended when determining TiO_2NPs in sunscreens [29], the upper surface of the cream was removed before each sampling stage (before each opening of the bottle or jar). In addition, samples were hermetically sealed and kept at 4°C after they were opened.

3.3.4 Microwave-assisted acid digestion of moisturising creams

Moisturising creams (approximately 0.2000 g) were weighed into a PTFE digestion vessel, and 4.0 mL of ultrapure water, 3.0 mL of 69% nitric acid, and 1.0 mL of 33% hydrogen peroxide were added to each vessel. The digested cosmetic samples (microwave operating conditions can be found in **Table 3.1**) were diluted to 25 mL with ultrapure water. Each cream sample was subjected to the microwave-assisted acid digestion process in triplicate, and at least two blanks were prepared in each microwave-assisted acid digestion set.

Similarly, microwave-assisted acid digestion (use of a domestic microwave oven and low-pressure reactors) was applied to the methanolic extracts obtained from moisturising creams after applying the proposed ultrasound-assisted extraction procedure (verification if the extractions of AgNPs were quantitative). In this case, volumes of 0.5 mL of the methanolic extracts were mixed with 1.0 mL of 69% nitric acid, and 0.5 mL of 33% hydrogen peroxide, and subjected to microwave treatment (300 W) in six cycles of 1 min of irradiation plus 5 min of cooling. The digests were further diluted to 5 mL with ultrapure water before ICP-MS determination.

Table 3.1. Microwave-assisted acid digestion program

Moisturising cream samples			
Step	**Time (min)**	**Temperature (°C)**	**Power (W)**
1	0-2	Room temperature-90	1000
2	2-7	90-140	1000
3	7-12	140-200	1000
4	12-27	200	1000

3.3.5 Ultrasound probe-assisted AgNPs extraction from moisturising creams

Approximately 0.1000 g of sample was mixed with 20 mL of methanol into 50 mL plastic tubes. The tubes were then placed in an ice-bath, and ultrasonication (power of the sonicator set at 60% amplitude) was performed for 15 min using discontinuous sonication (15 cycles of ultrasound treatment for 59 s plus a relaxing stage for 59 s). After AgNPs extraction/sample solubilisation, the extracts were kept in amber glass bottles at 4°C. Samples (or each set of experiments) were performed in triplicate, and two different blanks were performed for each set of samples and extraction conditions. The proposed sample pre-treatment was found efficient (clear extracts) for most creams under study, except for sample coded as MC3, which required a centrifugation stage for insoluble residue removal.

3.3.6 Total Ag determination in digests from moisturising creams by ICP-MS

Acid digests from moisturising creams were diluted (1:10 dilution) with ultrapure water before ICP-MS determination. The adjustment of the torch position, the nebulisation flow, the optic lens, and the quadrupole voltages were performed before measurements. Determinations (^{107}Ag *m/z* ratio) were carried out by using the standard addition method covering Ag concentrations within the 0–200 μg L^{-1} range, and ^{103}Rh (10 μg L^{-1}) was used as an internal standard. The helium flux in the collision cell was 1.0 mL min^{-1} for minimising the polyatomic interferences. Other ICP-MS operating conditions are listed in **Table 3.2**.

The limit of detection (LOD) and limit of quantification (LOQ) were calculated based on the 3σ/10σ criteria (σ is the standard deviation of eleven measurements of a blank), using the standard addition slope to obtain LOD/LOQ as Ag concentrations. Values were 0.019 and 0.063 μg g^{-1} for LOD and LOQ, respectively.

Table 3.2. ICP-MS operating conditions for total Ag determination in acid digests and methanolic extract digests from moisturising creams

Operating ICP-MS conditions		
Radiofrequency power		1600 W
Gas flows	Nebulisation	0.84 L min^{-1}
	Auxiliary	1.2 L min^{-1}
	Plasma	16 L min^{-1}
KED	Cell gas A (He)	1.0 mL min^{-1}
m/z ratio	Ag	106.905
	Rh (internal standard)	102.906

3.3.7 Assessment of AgNPs in moisturising creams by spICP-MS

Instrumental ICP-MS parameters were adjusted using a tuning solution containing 10 μg L^{-1} of silver together with Be, Ce, Fe, In, Li, Mg, Pb, and U (1 μg L^{-1}). The flow rate and the transport efficiency (TE%) were further calculated, the latter automatically given by the Syngistix™ Nano Application software after introducing an Au (60 nm) suspension of 518 ng L^{-1} particle number concentration (prepared from NIST 8013). TE% calculation was based on the particle frequency method developed by Pace et al. [30], by measuring the pulse frequency of a nanoparticle suspension, and knowing previously the particle number concentration of the suspension and the sample flow rate. Valid values of TE% were within the 2–3% range.

A dissolved (ionic) silver aqueous calibration within the 0–20 μg L^{-1} range was performed using standard solutions. As pointed out by Pace et al. [30], aqueous calibration for assessing metallic NPs can be used when TE% and the sample flow rate are previously known. Methanolic extracts were 1:40 diluted with 1.0% (w/v) glycerol, and solutions were subjected to ultrasound energy (ultrasound water-bath, 45 kHz, 120 W) for 5 min before spICP-MS measurements (operating conditions summarised in **Table 3.3**).

Table 3.3. spICP-MS operating conditions for AgNPs determination in methanolic extracts from moisturising creams

Operating ICP-MS conditions		
Radiofrequency power		1600 W
Gas flows	Nebulisation	0.87 L min^{-1}
	Auxiliary	1.2 L min^{-1}
	Plasma	16 L min^{-1}
Operating parameters regarding single particle measurements		
Analyte		Ag
m/z ratio		106.905
Density		10.49 g cm^{-3}
Mass fraction		100%
Ionisation efficiency		100%
Sample flow rate		0.45–0.49 mL min^{-1}
Dwell time		100 µs
Sampling time		100 s
Mode		Standard
Cell gas		0 mL min^{-1}
RPa		0
RPq		0.5
Number of scanning		1
Number of readings		1000000
Replicates		3

3.3.8 Ultrasound water-bath oxidative treatment of methanol extracts from moisturising creams for SEM/TEM analysis

Co-extracted organic matter from moisturising cream samples was removed/diminished by applying a digestion procedure with hydrogen peroxide. The procedure consisted of treating 4.0 mL of methanolic extracts from moisturising creams with 0.3 mL aliquots of 33%(v/v) hydrogen peroxide under ultrasounds (ultrasound water-bath) for 15 min. The procedure was repeated eight times by adding fresh 33% (w/v) hydrogen peroxide (0.3 mL) each time. Clean extracts were then subjected to SEM/TEM analysis.

Because of this treatment could change the particle size distribution of extracted AgNPs, studies regarding the effect of hydrogen peroxide and ultrasounds were carried out by subjecting AgNPs solutions (40 nm AgNPs, 2.5 µg L^{-1} as Ag) and methanolic extracts from a moisturising cream (MC3) to the proposed procedure in triplicate. Solutions before and after hydrogen peroxide treatment were further analysed by spICP-MS. AgNPs size distribution (mean size and most frequent size), as well as AgNPs concentration (AgNPs per mL), and ionic Ag concentrations, are displayed in Supplementary Information. Results (**Figure S3.1**, Supplementary Information) have shown similar AgNPs concentrations and mean size for treated and untreated moisturisers, although ionic Ag increased slightly in methanolic extracts after the oxidative process (from 1.7±0.06 µg L^{-1} in untreated samples to 2.4±0.48 µg L^{-1} in treated samples). Regarding 40 nm AgNPs standards, similar AgNPs mean sizes were observed for untreated and treated aqueous standards. However, ultrasound-hydrogen peroxide oxidation implied a slight reduction (approximately 12%) of AgNPs concentration (from $1.5\times10^{9}\pm2.7\times10^{8}$ AgNPs mL^{-1} in untreated samples to $9.4\times10^{8}\pm8.7\times10^{7}$ AgNPs mL^{-1} in treated samples).

Although the AgNPs concentration has been found to change, the proposed ultrasound/ hydrogen peroxide treatment for organic matter removal has been needed for obtaining clean extracts for SEM/TEM analysis. These image-based techniques have been found to be useful for verifying the presence and nature of NPs in the methanolic extracts from moisturisers under study.

3.3.9 SEM/TEM analysis

Regarding SEM, a drop (10 µL) of clean methanol extracts was deposited onto a carbon-coated copper grid, wicked using filter paper, and air-dried at room temperature. Particle sizes and shapes were analysed at acceleration voltage of 200 kV, dwell time of 5 µs, and magnifications of 10×10^3 to 35×10^3. Elemental compositions were determined by energy-dispersive X-ray spectroscopy (EDX).

Similarly, methanol drops (10 µL) was deposited on carbon-coated grids and allowed to dry at room temperature before TEM-EDX assessment (operating voltage of 80 kV).

3.4 RESULTS

3.4.1 Selection of extraction/solubilisation solvent

Preliminary experiments were performed to select the best solvent for the treatment of moisturising cream samples. Water [29,31] and organic solvents such as methanol [32], ethanol [31,33], hexane [29,34], and chloroform [31] have been proposed for TiO_2NPs extraction from sunscreens. Some procedures involve ultrasonication [29], although most developments are based on mechanical shaking and/or sonication [34] and direct dilution [33]. The extracts were found to be adequate for TiO_2NPs assessment by microscopy-based techniques [31–33] and also by AF4 [29,34].

First attempts consisted of using methanol as a solvent, and mechanical stirring and sonication in a water-bath for assisting the extraction process. However, turbid extracts were obtained, even using treatment times of 60 min, which meant the use of a further centrifugation stage. Quite less turbid extracts were obtained when using the ultrasound probe as an assistance method.

Therefore, the use of ultrasonication was fully studied for AgNPs extraction in creams by testing methanol, and also water and isopropanol as solvents. The best preliminary results were obtained when using methanol. Water did not allow an efficient sample solubilisation, and a centrifugation step was needed to remove insoluble residues. Regarding methanol and isopropanol, preliminary experiments in duplicate showed measured AgNPs concentrations of $6.20\times10^7\pm1.43\text{x}10^6$ and $4.74\times10^6\pm2.23\text{x}10^6$ AgNPs g^{-1} in extracts, respectively. In addition to the slightly higher AgNPs concentrations extracted when using methanol, most of organic compounds present in the samples were conveniently dissolved with this solvent (isopropanol led to turbid extracts). Moreover, high ionic (dissolved) silver concentrations and worse repeatability were obtained when using isopropanol. Methanol was therefore chosen for further optimisation.

3.4.2 Optimisation of sample pre-treatment method

Ultrasonication variables [amplitude of ultrasonic probe, ultrasonication time, and ultrasound operation mode (continuous or pulses mode)], and the extractant (methanol) volume were optimised by performing experiments in triplicate from 0.1000 g aliquots of a cream sample (cream sample code as MC1). For all cases, extracts were further diluted (1:40) with 1% (w/v) glycerol before spICP-MS measurements. Two blanks were performed for each set of operating conditions.

3.4.2.1 Amplitude

By fixing a methanol volume of 40 mL and an ultrasonication time of 10 min, several subsamples were subjected to continuous ultrasonication at amplitudes of 20%, 30%, 40%, 50%, and 60% of the ultrasonic probe (130 W power and 20 kHz frequency). Results (size distributions in **Figure S3.2**, Supplementary Information) show that most of AgNPs in MC1

exhibit sizes smaller than 100 nm. AgNPs size distribution was found to be similar when using the highest ultrasonication amplitudes, and mean sizes of 52±7, 64±2, and 57±5 nm were measured for 40, 50 and 60%, respectively (**Figure S3.2** and **Figure 3.1a**). Most frequent sizes were also smaller when using low ultrasound amplitudes (14±4 and 24±8 for amplitudes of 20 and 30%, respectively, versus 39±6 nm, 30±2, and 34±3 nm for amplitudes of 40, 50, and 60%, respectively). In addition, better performance (higher amount of extracted AgNPs, **Figure 3.2a**) was obtained at the highest amplitudes (50 and 60%) of the ultrasound probe. Ionic (dissolved) Ag was found to be negligible in all experiments. An amplitude of 60% was therefore selected as the most convenient value for further experiments.

3.4.2.2 Ultrasound time

Ultrasonication (continuous mode) times of 5, 10, 15, and 20 min were investigated by fixing the amplitude at 60%, and using 40 mL of methanol as an extractant. AgNPs concentrations are plotted in **Figure 3.2b**, which shows that the best extraction was obtained when using ultrasonication times higher than 10 min. Moreover, and as shown in **Figure 3.1b**, ultrasonication time did not affect AgNPs size distribution, and the most frequent sizes (and also mean sizes) were similar under different ultrasonication times. Invariable size distribution was verified by applying an ANOVA test (confidence interval of 95%, data not given) after observing that the standard deviations were statistically significantly similar to the Cochran C test for variance comparison (also at 95% confidence interval). Regarding ionic Ag, negligible concentrations were detected at ultrasonication times of 5 and 10 min; whereas, concentrations lower than 1.0 μg L^{-1} were observed when increasing the extraction time. Based on the theory of counting and sizing NPs by spICP-MS [30], a low dissolved silver concentration in the extracts is required for removing any contribution from the dissolved species to the total AgNPs pulse signal. The dissolved silver concentrations measured are lower than 5.0 μg L^{-1}, which is the maximum dissolved metal concentration specified by the manufacturer so that Syngistix™ Nano software could perform an adequate counting/sizing performance (efficient dissolved metal subtraction). Therefore, an ultrasonication time of 15 min was finally selected.

3.4.2.3 Methanol volume

Continuous ultrasonication (60% amplitude and 15 min) was tested by using several methanol volumes (10 mL, 20 mL, 30 mL, and 40 mL). **Figure 3.2c** shows that the highest AgNPs concentrations were achieved when using methanol volumes higher than 20 mL. In addition, the most frequent sizes (and also mean sizes) were found to be statistically significant similar (ANOVA, 95% confidence interval, data not given) for all the methanol volumes tested (data in **Figure 3.1c)**. Ionic Ag was found to be lower than 5.0 μg L^{-1} (within the 0.7–1.8 μg L^{-1} range) in all experiments, which means an efficient counting/sizing performance**.** Therefore, a methanol volume of 20 mL was finally selected.

3.4.2.4 Continuous/discontinuous ultrasonication

Ultrasonication mode (continuous or discontinuous/pulses) was finally tested. After fixing the remaining parameters at the optimised/selected values, continuous ultrasonication (15 min), and pulses ultrasonication (15 cycles of ultrasound treatment for 59 s plus relaxing stage for 59 s) were applied. **Figure 3.2d** shows an increase on the concentration of extracted AgNPs under discontinuous ultrasonication. Regarding AgNPs size distribution, mean sizes as well as most frequent sizes were similar under both ultrasonication modes (**Figure 3.1d**). Finally, dissolved Ag concentrations were found to be similar under both ultrasonication modes and lower than 5.0 μg L^{-1}. Discontinuous (pulses) ultrasonication was finally selected.

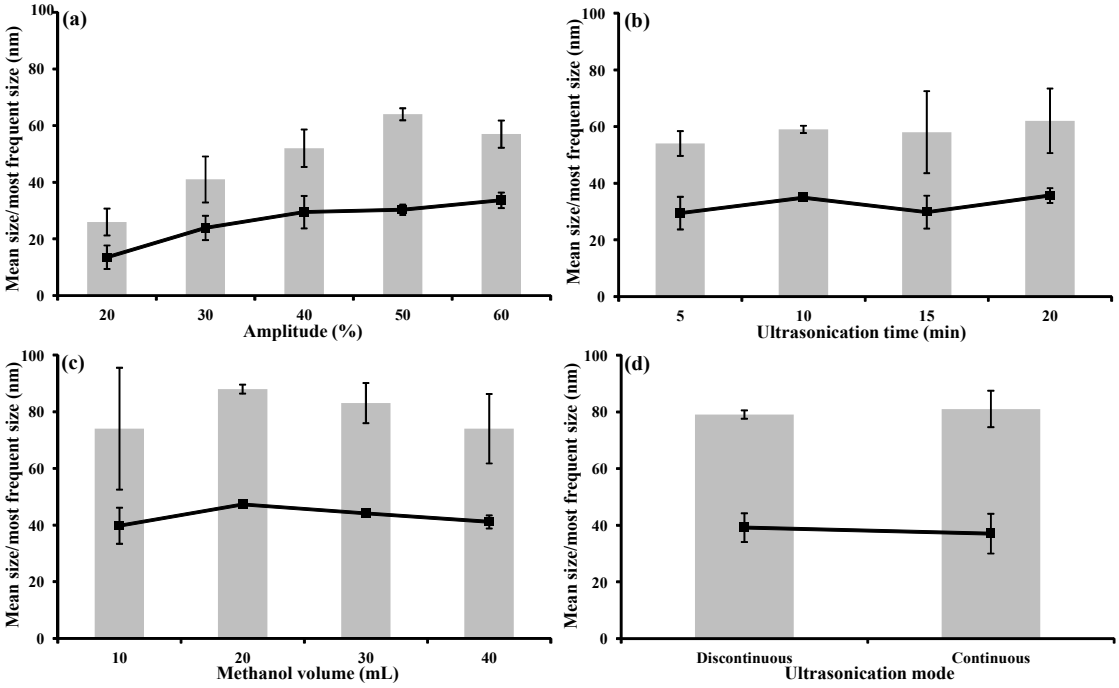

Figure 3.1. Effects of amplitude (a), ultrasonication time (b), methanol volume (c), and ultrasonication mode (d) on AgNPs most frequent size (bars) and mean size (dots)

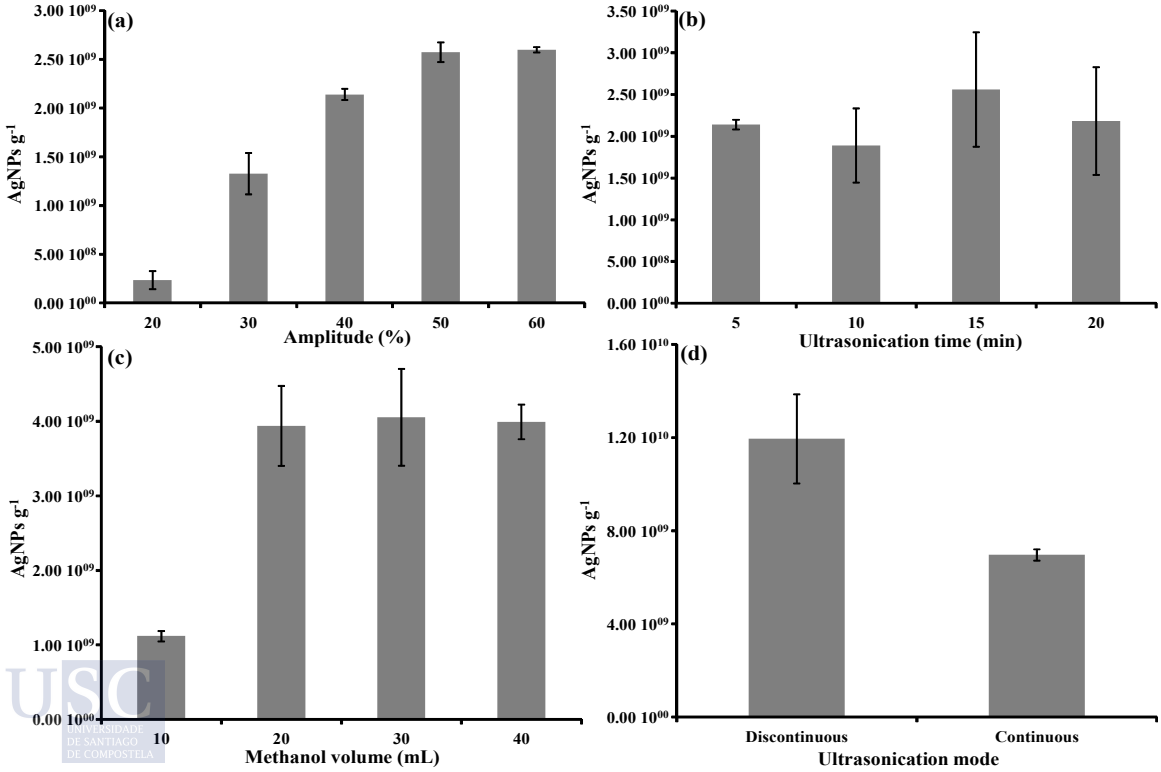

Figure 3.2. Effects of amplitude (a), ultrasonication time (b), methanol volume (c), and ultrasonication mode (d) on AgNPs concentration

3.4.3 AgNPs stability

A series of AgNPs standards of 40 nm were subjected to the optimised extraction procedure in triplicate before spICP-MS determination (each extract measured also in triplicate, n=9). The same AgNPs standards (three 40 nm AgNPs standards) were directly analysed by spICP-MS in triplicate (n=9) for comparison purposes. A mean diameter of 41±1 nm (most frequent size of 35±1 nm) was obtained when analysing 40 nm AgNPs standards subjected to the proposed procedure. These values were quite similar to those obtained when directly analysing the same 40 nm AgNPs standards (mean diameter of 40±0.5 nm, and most frequent size of 35±0.5 nm). These findings show that AgNPs were stable during the ultrasonication process.

3.4.4 Analytical performances

3.4.4.1 Calibration, limit of detection and limit of quantification

Calibration has been performed by using aqueous Ag standards and Ag standards matched with methanol [1:40 dilution in 1% (w/v) glycerol], both at 1, 5, 10, 15, and 20 μg L^{-1}. Slopes of both calibrations (3.75±0.46 and 5.34±0.095 L μg^{-1} cps^{-1} for aqueous and matched calibrations, respectively, n=5) were found to be statistically different [ANOVA test for means comparison (p-value of 0.001< 0.005), 95% confidence interval]. Matrix effect has been found to be present, and methanol [1:40 dilution in 1% (w/v) glycerol] matched calibration was selected for AgNPs assessment in methanolic extracts from moisturising creams.

Regarding AgNPs concentration, the limit of detection (LOD) and the limit of quantification (LOQ) were obtained by preparing and measuring by spICP-MS eleven blanks (20 mL of methanol subjected to the ultrasound-assisted solubilisation procedure, and 1:40 diluted with 1% (w/v) glycerol). Three times (LOD) or ten times (LOQ) the standard deviation (n=11) of the measurements were divided by the mean slope of the calibration graph. The calculated LOD and LOQ, referring to the moisturising cream sample and expressed as AgNPs g^{-1} were 2.48×10^5 and 8.25×10^5, respectively.

The limit of detection for AgNPs size has been calculated according to Lee et al. [35] and Donovan et al. [36] (three times and/or five times criteria) as follows:

$$D_{min} = \sqrt[3]{\frac{6 \times 3\sigma_{DI}}{\mathrm{R} \times f_a \times \rho \times \pi}}$$

where $3\sigma_{DI}$ (or $5\sigma_{DI}$) is three or five times the standard deviation of counts of ultrapure water blanks, R is the sensitivity of the detector (slope of the calibration curve of ionic standard solutions) for the measured element (Ag), f_a is the mass fraction of analysed metallic element in the nanoparticles, and ρ is the density of the AgNPs.

The LOD in size was 4.5 nm using the 3σ criteria; whereas, the application of 5σ criteria gave a LOD size of 5.3 nm. Calculated values were quite similar than those obtained by applying the blank value method and the dissolved calibration method as described by Witzler et al. [37], 11.8 and 13.0 nm, respectively.

3.4.4.2 Precision and analytical recovery

The precision of the whole procedure (sample pre-treatment and spICP-MS measurement) has been established through the relative standard deviation (RSD) after preparing eleven methanolic extracts from a moisturising cream sample (ultrasonication using the optimal extraction conditions), and measuring each methanolic extract three times. Regarding AgNPs concentration, RSD obtained was 5% (AgNPs concentrations of $2.34\times10^9\pm1.28\times10^8$ AgNPs g^{-1}). The RSD values for AgNPs size were 11% (most frequent

size: 39±4 nm) and 7% (mean size: 78±9 nm). Results show that the proposed methodology was repeatable.

Because of the absence of certified reference materials for AgNPs (size distribution and concentration), the accuracy of the spICP-MS measurement was assessed through analytical recovery assays. Analytical recovery values were calculated after performing spICP-MS measurements of spiked and unspiked methanolic extracts from a moisturising cream sample, and also by measuring the AgNPs solution used for spiking experiments. Therefore, methanolic extracts from a single sample spiked with AgNPs of 20, 40, and 60 nm [three extracts for each AgNPs size, spiking concentrations of 5.63×10^{10}, 7.13×10^{9}, 8.50×10^{8} (as AgNPs) for 20, 40, and 60 nm, respectively] were analysed by spICP-MS. In addition, unspiked extracts, and AgNPs (20, 40, and 60 nm) solutions, used for performing the spiking experiments, were also analysed. After all measurements (each solution was measured in triplicate), the AgNPs concentrations found in the unspiked extracts were subtracted from the AgNPs concentrations found in the spiked extracts for assessing the "AgNPs concentration found". Analytical recovery was assessed by dividing the "AgNPs concentration found" by the mean AgNPs concentrations found in the aqueous AgNPs solution used for spiking ("AgNPs added") and multiplying by 100. The analytical recoveries obtained (n=9) were 117±14% for 20 nm AgNPs, 90±1% for 40 nm AgNPs, and 109±2% for 60 nm AgNPs. These values show that the spICP-MS technique was accurate.

3.4.5 Application

Thirteen moisturising creams were subjected in triplicate to microwave-assisted acid digestion and ICP-MS analysis for assessing total Ag contents. Total Ag concentrations higher than the LOQ of the method were only obtained for moisturising creams prescribed for atopic dermatitis (samples denoted as MC1, MC2, and MC3 in **Table 3.4**). Total Ag content in sample MC1 was quite higher than the total Ag contents in the other two creams for atopic dermatitis. This sample was bought in a pharmacy and give information regarding the presence of 'micro silver' in the composition. However, total silver concentration is not given by the manufacturer. Although the presence of Ag is shown in the composition of samples MC2 and MC3, the total Ag contents were quite smaller than in MC1. Other ten moisturising creams (cosmetics) included in the study showed total Ag contents below than the LOD of the method.

Samples containing detectable total Ag contents were subjected to the ultrasound-assisted solubilisation method following by spICP-MS measurement (dilutions varied from 1:10 for MC2 and MC3 to 1:40 for MC1). **Table 3.4** also lists the obtained AgNPs concentrations as well as mean sizes and most frequent sizes. MC1 showed the highest AgNPs concentration; whereas AgNPs levels in MC2 and MC3 were low. AgNPs size distribution was also quite different in the analysed samples, and mean particles sizes varied from 35±5 nm in MC2 to 91±4 nm in MC1.

Figure 3.3 shows the AgNPs size distributions for each sample (the histograms indicate that AgNPs size distribution follow a lognormal distribution [38]). The high frequencies of AgNPs of small size are in good agreement with data from signal frequency distributions (**Figure 3.3**), which means that the highest frequencies were obtained for small intensities (small intensities derived from AgNPs of small sizes).

Total Ag contents were also assessed in methanolic extracts from samples MC1, MC2, and MC3 by ICP-MS to verify that the extraction/solubilisation process was quantitative. The methanolic extracts were subjected to the microwave-assisted acid digestion method as described in section 3.3.4, and further analysed by ICP-MS after acid digest dilution. Total Ag concentrations found after the optimised ultrasound-assisted procedure are listed in **Table 3.4**. Total Ag concentrations in moisturising creams after microwave-assisted acid

digestion and ultrasound-assisted methanolic extraction were not statistically significant different at a confidence interval of 95% (ANOVA, data not given). It can therefore be concluded that the proposed extraction procedure is quantitative.

Considering the number of AgNPs per gram and the size distributions in each sample (**Table 3.4**), an estimative calculation was performed to know the amount (concentration) of silver derived from the isolated AgNPs. These calculations assume a density of 10.49 g cm^{-3} for each AgNP, as well as that all AgNPs exhibit a spherical shape (solid spheres). Results (expressed as μg g^{-1}) are also listed in **Table 3.4**, and it can be seen that the amount of nano silver in the creams under study is quite small, approximately 1.1% of the total Ag concentration in creams MC1, and lower than 1.0% in creams MC2 and MC3. These findings imply the presence of bulk silver (ionic silver) as a major Ag component in these samples.

Finally, extracts from moisturising creams containing AgNPs were also analysed by TEM and SEM-EDX for comparative purposes after an ultrasound water-bath oxidative procedure with hydrogen peroxide (section 3.3.8). TEM images (**Figure 3.4**) of moisturising creams show the presence of AgNPs with sizes ranging from 19 to 30 nm in MC1, and around 30 nm in MC2. AgNPs were quite disperse in these extracts, and MC1 showed a higher number of AgNPs. Regarding MC3, AgNPs sizes ranged from 30 to 45 nm, although AgNPs agglomeration was found in all the TEM images taken. This could be attributed to the presence of organic matter in the extracts that acts as a binder (not removed organic matter is also observed in TEM images from extracts from MC1 and MC2).

A SEM image and EDX microanalysis of several NPs in extracts from MC1 are given in **Figure S3.3** (Supplementary Information). As shown in EDX spectra, NPs are composed of Ag (76.5 and 60.99% in the selected spots). EDX analysis also reveals the presence of C (19.58 and 32.66% in the selected spots) which confirms the presence of organic matter around the AgNPs.

Table 3.4. Total Ag contents, AgNPs concentration, and AgNPs size distribution in creams prescribed for atopic dermatitis

						AgNPs size distribution [c]	
	[Ag] μg g^{-1} [a]	[Ag] μg g^{-1} [b]	[Ag] μg g^{-1} [c,d]	Nano Ag percentage % [e]	AgNPs g^{-1} [c]	Mean size nm	Range size nm
MC1	2329 ± 262	2352 ± 82	26.7 ± 2.1	1.15	$6.46\times10^{9} \pm 5.02\times10^{8}$	91 ± 4	17–211
MC2	1.1 ± 0.1	1.4 ± 0.1	0.0043 ± 0.0007	0.39	$1.83\times10^{7} \pm 2.77\times10^{6}$	35 ± 5	14–168
MC3	31 ± 4	29 ± 1	0.074 ± 0.0055	0.24	$9.62\times10^{7} \pm 7.62\times10^{6}$	52 ± 5	19–177

(a) microwave-assisted acid digestion procedure and ICP-MS; (b) ultrasound-assisted methanol extraction and ICP-MS; (c) ultrasound-assisted methanol extraction and spICP-MS; (d) Ag concentration derived from AgNPs; (e) Ag percentage as nano silver

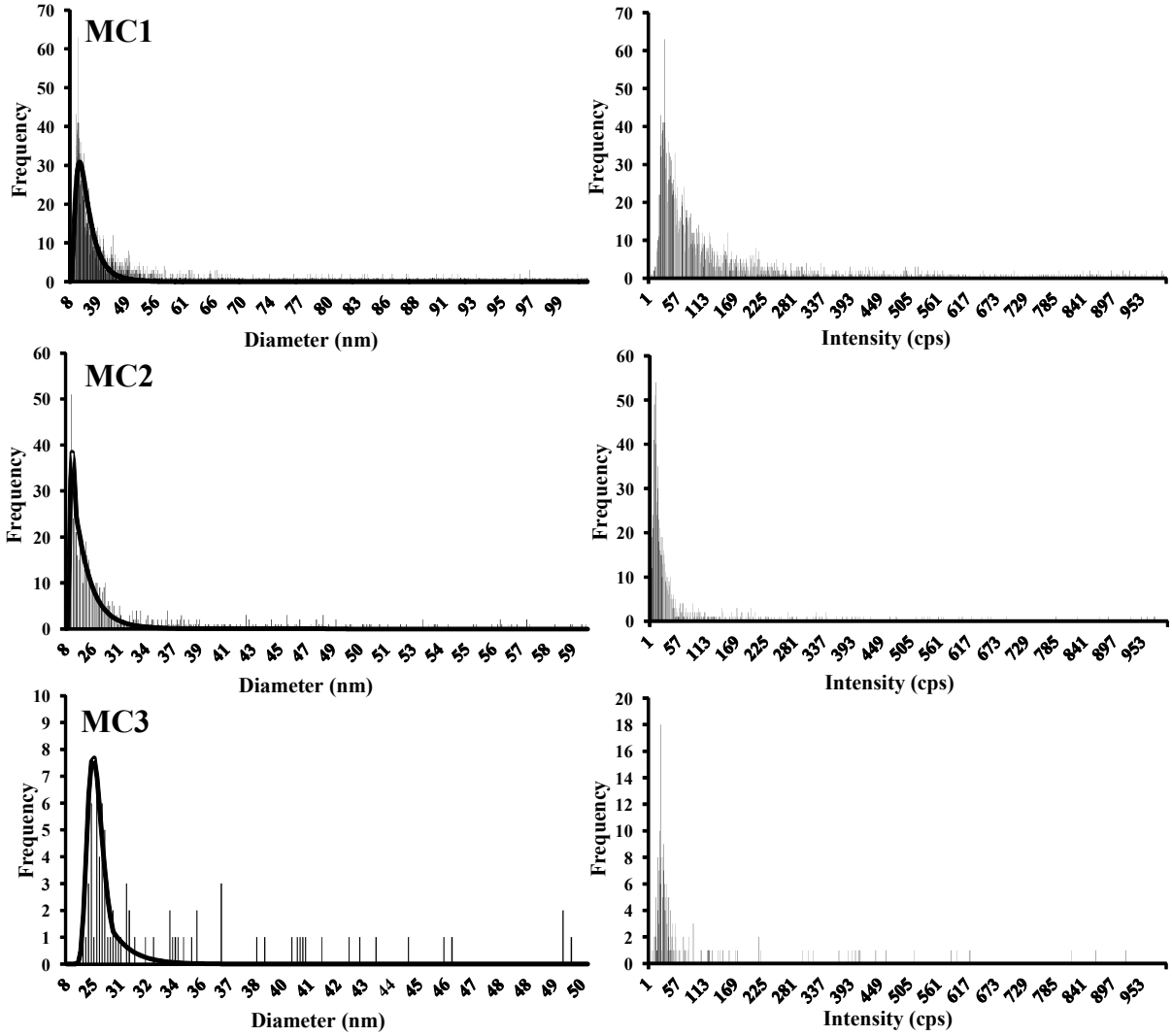

Figure 3.3. AgNPs size distribution and signal (intensity) frequency distribution in moisturising cream samples

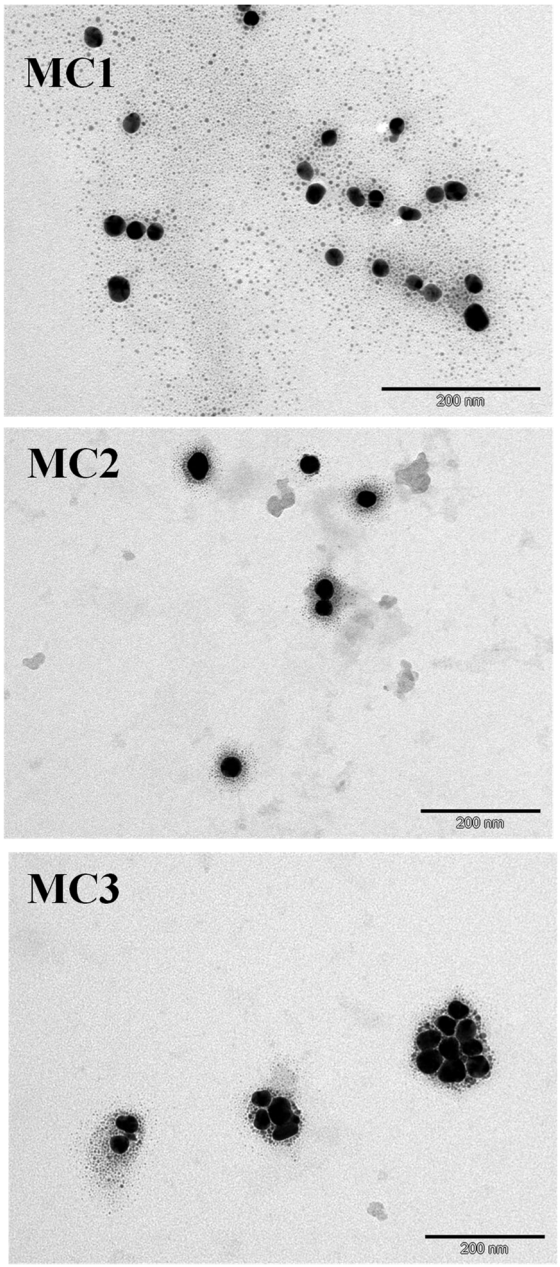

Figure 3.4. TEM images of treated methanolic extracts from moisturising cream MC1

3.5 CONCLUSIONS

A reliable and simple sample pre-treatment method, based on using ultrasonication and methanol as an extractant followed by spICP-MS has been proposed for AgNPs assessment (concentrations and size distribution) in moisturising creams. The high sensitivity inherent to ICP-MS combined with fast acquisition (low dwell times) in modern ICP-MS instrumentation have allowed the determination of AgNPs of small size (smaller than 40 nm) in complex samples such as moisturising creams. spICP-MS measurements have been demonstrated to be accurate and precise in AgNPs concentration and AgNPs size distribution. Only moisturising creams prescribed for atopic dermatitis were found to contain AgNPs (AgNPs concentrations from 1.83×10^{7} to 6.46×10^{9} AgNPs g^{-1}, and AgNPs most frequent size within the 19–26 nm range).

SUPPLEMENTARY INFORMATION

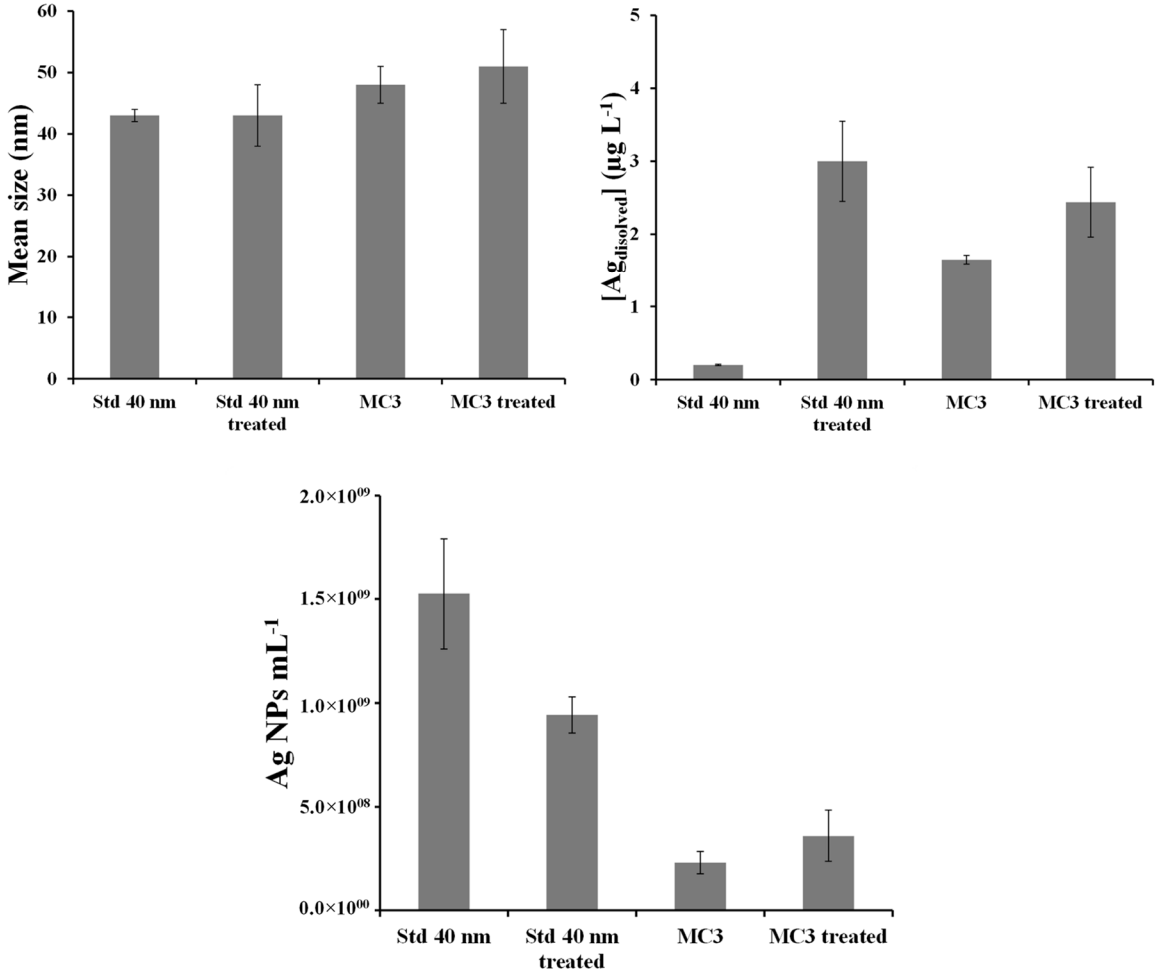

Std 40 nm: standard AgNPs 40 nm
Std 40 nm treated: standard AgNPs 40 nm after oxidative treatment
MC3: moisturising cream 3
MC3 treated: moisturising cream 3 after oxidative treatment

Figure S3.1. AgNPs concentration, AgNPs mean size, and dissolved Ag concentration in AgNPs (40 nm) standards and extracts from moisturising cream MC3 before and after hydrogen peroxide ultrasound-assisted oxidation

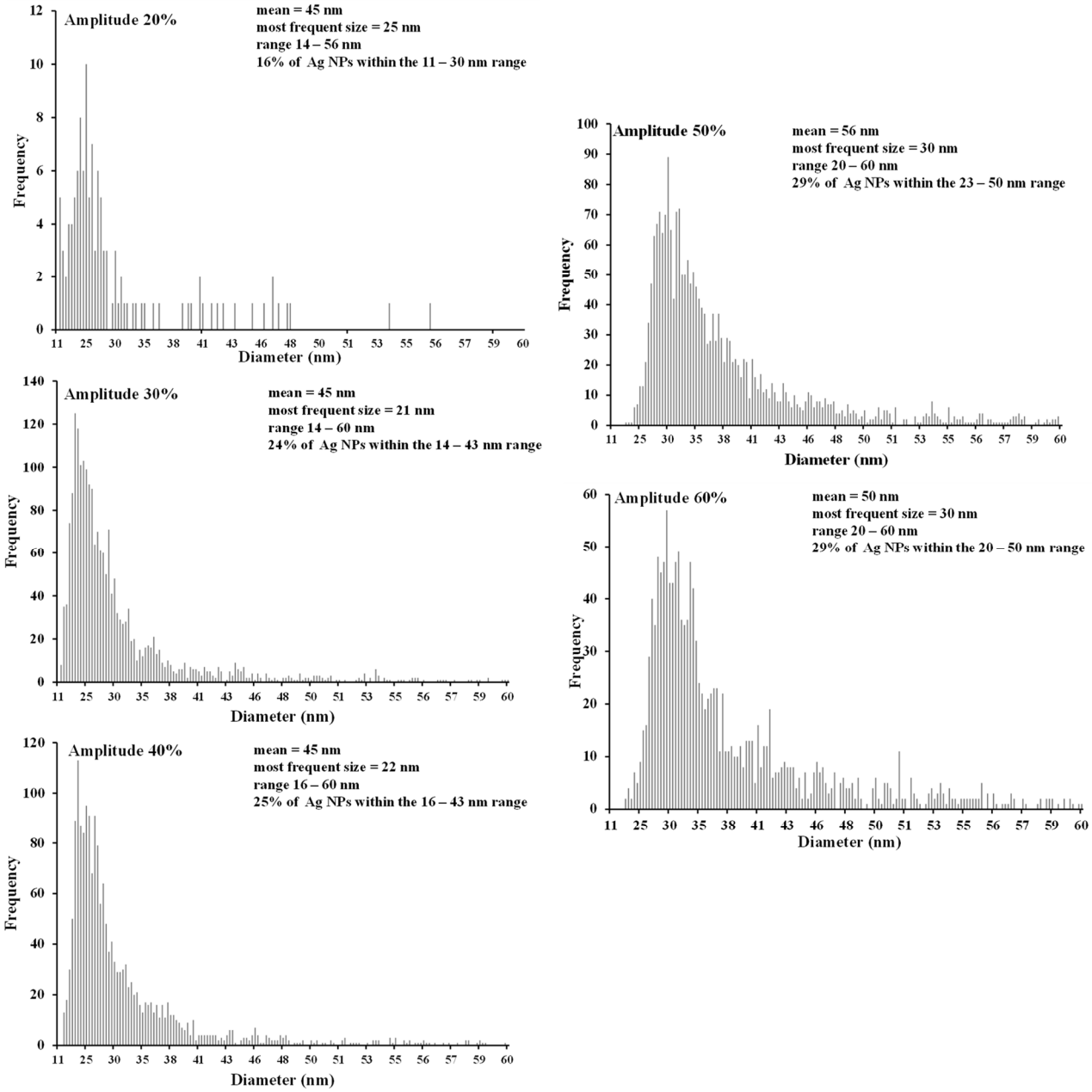

Figure S3.2. AgNPs size distribution in a methanolic extract from moisturising cream MC1 after ultrasound treatment at different ultrasound amplitudes

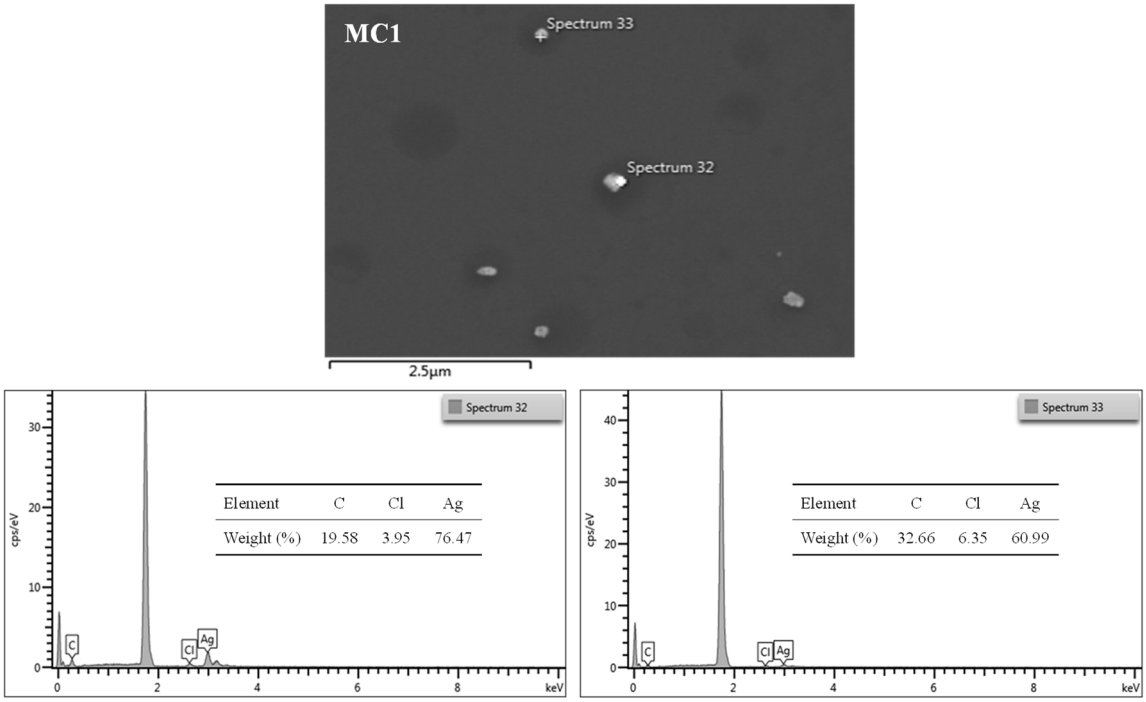

Figure S3.3. SEM images and EDX microanalysis of a treated methanolic extract from moisturising cream sample MC1

REFERENCES

[1] J.R. Peralta-Videa, L. Zhao, M.L. Lopez-Moreno, G. de la Rosa, J. Hong, J.L. Gardea-Torresdey, Nanomaterials and the environment: A review for the biennium 2008–2010, J. Hazard. Mater. 186 (2011) 1–15, DOI: 10.1016/j.jhazmat.2010.11.020.

[2] Commission Recommendation of 18 October 2011 on the definition of nanomaterial (2011/696/EU), Official Journal of the European Union, L275 (20 October 2011) 38–40.

[3] Regulation (EC) Nº 1223/2009 of the European Parliament and of the Council of 30 November 2009 on cosmetic products, Official Journal of the European Union L342 (10 August 2016) 1–345.

[4] I. de la Calle, M. Menta, F. Séby, Current trends and challenges in sample preparation for metallic nanoparticles analysis in daily products and environmental samples: A review, Spectrochim. Acta B 125 (2016) 66–96, DOI: 10.1016/j.sab.2016.09.007.

[5] A. López-Serrano, R. Muñoz-Olivas, J. Sanz-Landaluze, C. Cámara, Nanoparticles: a global vision. Characterization, separation, and quantification methods. Potential environmental and health impact, Anal. Methods 6 (2014) 38–56, DOI: 10.1039/C3AY40517F.

[6] Z. Zhu, J. Wang, A. Munir, H. S. Zhou, Electrocatalytic activity of Pt nanoparticles on bamboo shaped carbon nanotubes for ethanol oxidation, Electrochim. Acta 55 (2010) 8517–8520, DOI: 10.1016/j.electacta.2010.07.058.

[7] H. Kuang, Y. Zhao, W. Ma, L. Xu, L. Wang, C. Xu, Recent developments in analytical applications of quantum dots, Trends Anal. Chem. 30 (2011) 1620–1636, DOI: 10.1016/j.trac.2011.04.022.

[8] R. Bindhu, M. Umadevi, Surface plasmon resonance optical sensor and antibacterial activities of biosynthesized silver nanoparticles, Spectrochim. Acta A 121 (2014) 596–604, DOI: 10.1016/j.saa.2013.11.019.

[9] Y. Ju, H. Zhang, J. Yu, S. Tong, N. Tian, Z. Wang, X. Wang, X. Su, X. Chu, J. Lin, Y. Ding, G. Li, F. Sheng, Y. Hou, Monodisperse Au–Fe_2C Janus Nanoparticles: An Attractive Multifunctional Material for Triple-Modal Imaging-Guided Tumor Photothermal Therapy, ACS Nano 11 (2017) 9239–9248, DOI: 10.1021/acsnano.7b04461.

[10] J. Li, Y. Wang, R. Liang, X. An, K. Wang, G. Shen, Y. Tu, J. Zhu, J. Tao, Recent advances in targeted nanoparticles drug delivery to melanoma, Nanomed.-Nanotechnol. Biol. Med. 11 (2015) 769–794, DOI: 10.1016/j.nano.2014.11.006.

[11] Y.R. Zhang, S.Q. Wang, S.L. Shen, B.X. Zhao, A novel water treatment magnetic nanomaterial for removal of anionic and cationic dyes under severe condition, Chem. Eng. J. 233 (2013) 258–264, DOI: 10.1016/j.cej.2013.07.009.

[12] N. Durán, M. Durán, M. Bispo de Jesús, A. B. Seabra, W. J. Fávaro, G. Nakazato, Silver nanoparticles: A new view on mechanistic aspects on antimicrobial activity, Nanomed.-Nanotechnol. Biol. Med. 12 (2016) 789–799, DOI: 10.1016/j.nano.2015.11.016.

[13] I. Ocsoy, A. Demirbas, E. S. McLamore, B. Altinsoy, N. Ildiz, A. Baldemir, Green synthesis with incorporated hydrothermal approaches for silver nanoparticles formation and enhanced antimicrobial activity against bacterial and fungal pathogens, J. Mol. Liq. 238 (2017) 263–269, DOI: 10.1016/j.molliq.2017.05.012.

[14] K. Juarez-Moreno, C.H. Mejía-Ruiz, F. Díaz, H. Reyna-Verdugo, A.D. Re, E.F. Vazquez-Felix, E. Sánchez-Castrejón, J.D. Mota-Morales, A. Pestryakov, N. Bogdanchikova, Effect of silver nanoparticles on the metabolic rate, hematological

response, and survival of juvenile white shrimp *Litopenaeus vannamei*, Chemosphere 169 (2017) 716–724, DOI: 10.1016/j.chemosphere.2016.11.054.

[15] J. Liu, S. Yu, Y. Yin, J. Chao, Methods for separation, identification, characterization and quantification of silver nanoparticles, Trends Anal. Chem. 33 (2012) 95–106. DOI: 10.1016/j.trac.2011.10.010.

[16] T. Bartłomiejczyk, A. Lankoff, M. Kruszewski, I. Szumiel, Silver nanoparticles – allies or adversaries?, Ann. Agric. Environ. Med. 20 (2013) 48–54.

[17] E. McGillicuddy, I. Murray, S. Kavanagh, L. Morrison, A. Fogarty, M. Cormican, P. Dockery, M. Prendergast, N. Rowan, D. Morris, Silver nanoparticles in the environment: Sources, detection and ecotoxicology, Sci. Total Environ. 575 (2017) 231–246, DOI: 10.1016/j.scitotenv.2016.10.041.

[18] Inventory "The Nanodatabase", http://nanodb.dk/, accessed on 14 January 2019.

[19] European Union Observatory of Nanomaterials (EUON), https://euon.echa.europa.eu/es/home, accessed on 14 January 2019.

[20] C. Bianco, M.J. Visser, O.A. Pluut, V. Svetliĉić, G. Pletikapić, I. Jakasa, C. Riethmuller, G. Adami, F. Larese Filon, D. Schwegler-Berry, A.B. Stefaniak, S. Kezic, Characterization of silver particles in the stratum corneum of healthy subjects and atopic dermatitis patients dermally exposed to a silver-containing garment, Nanotoxicology 10 (2016) 1480–1491, DOI: 10.1080/17435390.2016.1235739.

[21] C. Degueldre, P.Y. Favarger, Colloid analysis by single particle inductively coupled plasma-mass spectroscopy: a feasibility study, Colloids Surf. A 217 (2003) 137–142, DOI: 10.1016/S0927-7757(02)00568-X.

[22] C. Degueldre, P.Y Favarger, Thorium colloid analysis by single particle inductively coupled plasma-mass spectrometry, Talanta 62 (2004) 1051–1054, DOI: 10.1016/j.talanta.2003.10.016.

[23] C. Degueldre, P.Y. Favarger, C. Bitea, Zirconia colloid analysis by single particle inductively coupled plasma–mass spectrometry, Anal. Chim. Acta 518 (2004) 137–142, DOI: 10.1016/j.aca.2004.04.015.

[24] C. Degueldre, P.Y. Favarger, S. Wold, Gold colloid analysis by inductively coupled plasma-mass spectrometry in a single particle mode, Anal. Chim. Acta 555 (2006) 263–268, DOI: 10.1016/j.aca.2005.09.021.

[25] C. Degueldre, P.Y. Favarger, R. Rossé, S. Wold, Uranium colloid analysis by single particle inductively coupled plasma-mass spectrometry, Talanta 68 (2006) 623–628, DOI: 10.1016/j.talanta.2005.05.006.

[26] F. Laborda, E. Bolea, J. Jiménez-Lamana, Single Particle Inductively Coupled Plasma Mass Spectrometry: A Powerful Tool for Nanoanalysis, Anal. Chem. 86 (2014) 2270−2278, DOI: 10.1021/ac402980q.

[27] F. Laborda, J. Jiménez-Lamana, E. Bolea, J.R. Castillo, Critical considerations for the determination of nanoparticle number concentrations, size and number size distributions by single particle ICP-MS, J. Anal. At. Spectrom. 28 (2013) 1220–1232, DOI: 10.1039/C3JA50100K.

[28] I. Abad-Álvaro, E. Peña-Vázquez, E. Bolea, P. Bermejo-Barrera, J.R. Castillo, F. Laborda, Evaluation of number concentration quantification by single-particle inductively coupled plasma mass spectrometry: microsecond vs. millisecond dwell times, Anal. Bioanal. Chem. 408 (2016) 5089–5097, DOI: 10.1007/s00216-016-9515-y.

[29] V. Nischwitz, H. Goenaga-Infante, Improved sample preparation and quality control for the characterisation of titanium dioxide nanoparticles in sunscreens using flow field-flow

fractionation on-line with inductively coupled plasma mass spectrometry, J. Anal. At. Spectrom. 27 (2012) 1084–1092, DOI: 10.1039/C2JA10387G.

[30] H.E. Pace, N.J. Rogers, C. Jarolimek, V.A. Coleman, C.P. Higgins, J.F. Ranville, Determining Transport Efficiency for the Purpose of Counting and Sizing Nanoparticles via Single Particle Inductively Coupled Plasma Mass Spectrometry, Anal. Chem. 83 (2011) 9361–9369, DOI: 10.1021/ac201952t.

[31] Z.A. Lewicka, A.F. Benedetto, D.N. Benoit, W.W. Yu., J.D. Fortner, V.L. Colvin, The structure, composition, and dimensions of TiO_2 and ZnO nanomaterials in commercial sunscreens, J. Nanopart. Res. 13 (2011) 3607, DOI: 10.1007/s11051-011-0438-4.

[32] M. Sysoltseva, R. Winterhalter, A.S. Wochnik, C. Scheu, H. Fromme, Electron microscopic investigation and elemental analysis of titanium dioxide in sun lotion, Int. J. Cosmetic Sci. 39 (2017) 292–300, DOI: 10.1111/ics.12375.

[33] P.J. Lu, S.C. Huang, Y.P. Chen, L.C. Chiueh, D.Y.C. Shih, Analysis of titanium dioxide and zinc oxide nanoparticles in cosmetics, J. Food Drug Anal. 23 (2015) 587–594, DOI: 10.1016/j.jfda.2015.02.009.

[34] I. López-Heras, Y. Madrid, C. Cámara, Prospects and difficulties in TiO_2 nanoparticles analysis in cosmetics and food products using asymmetrical flow field-flow fractionation hyphenated to inductively coupled plasma mass spectrometry, Talanta 124 (2014) 71–78, DOI: 10.1016/j.talanta.2014.02.029.

[35] S. Lee, X. Bi, R.B. Reed, J.F. Ranville, P. Herckes, P. Westerhoff, Nanoparticle Size Detection Limits by Single Particle ICP-MS for 40 Elements, Environ. Sci. Technol. 48 (2014) 10291–10300, DOI: 10.1021/es502422v.

[36] A.R. Donovan, C.D. Adams, Y. Ma, C. Stephan, T. Eichholz, H. Shi, Single particle ICP-MS characterization of titanium dioxide, silver, and gold nanoparticles during drinking water treatment, Chemosphere 144 (2016) 148–153, DOI: 10.1016/j.chemosphere.2015.07.081.

[37] M. Witzler, F. Küllmer, A. Hirtz, K. Günther, Validation of Gold and Silver Nanoparticle Analysis in Fruit Juices by Single-Particle ICP-MS without Sample Pretreatment, J. Agric. Food Chem. 64 (2016) 4165–4170, DOI: 10.1021/acs.jafc.6b01248.

[38] F. Laborda, J. Jiménez-Lamana, E. Bolea, J.R. Castillo, Selective identification, characterization and determination of dissolved silver(I) and silver nanoparticles based on single particle detection by inductively coupled plasma mass spectrometry, J. Anal. At. Spectrom. 26 (2011) 1362–1371, DOI: 10.1039/C0JA00098A.

CHAPTER 4. spICP-MS ASSESSMENT OF ZnONPs AND TiO_2NPs IN MOISTURISERS AFTER A TIP SONICATION SAMPLE PRE-TREATMENT

CHAPTER 4. spICP-MS ASSESSMENT OF ZnONPs AND TiO_2NPs IN MOISTURISERS AFTER A TIP SONICATION SAMPLE PRE-TREATMENT

4.1 ABSTRACT

The use of zinc oxide nanoparticles (ZnONPs) and titanium dioxide nanoparticles (TiO_2NPs) in cosmetic formulations to obtain protection against the sun's UV radiation has become a common practice owing to their high photostability and the absence of allergic reactions induced by these nanoparticles. The manufacturing of cosmetics modified with nanoparticles has been regulated in Europe since 2009. Nevertheless, methodologies for sample pre-treatment and characterisation (quantification and size assessment) of nanoparticles from complex matrices are scarce and still in development.

The proposed methodology was based on the tip sonication of moisturisers in an organic solvent [40 mL of acetone, 40% amplitude, 5 min, and discontinuous mode (59 s of relaxing after 59 s tip sonication)] followed by spICP-MS, which provides information about concentration and size of the NPs. The whole methodology was repeatable (RSDs lower than 10% for size and concentration values of ZnONPs and TiO_2NPs) and accurate (analytical recoveries of 102±12% and 119±3% for ZnONPs and TiO_2NPs standards, respectively).

The overall procedure was applied to several commercial moisturisers with sun protection factor. spICP-MS results were compared with the total content of analyte in the extracts and in the acid digested samples. Finally, transmission electron microscopy coupled to energy-dispersive X-ray spectroscopy analysis of extracts from moisturising creams was carried out as comparative (qualitative) assessment.

4.2 INTRODUCTION

Skin exposure to UV radiation causes erythema (sunburn), immunosuppression, premature photoaging, and carcinogenesis, among other toxic effects [1–3]. Due to the carcinogenic properties of UV rays, the use of UV filters in the cosmetic industry is a common practice. There are twenty-nine UV filters allowed in the European Union, and only two of them are inorganic UV filters (zinc oxide and titanium dioxide, both in bulk and nanoparticulate forms) [4]. Inorganic filters reflect and scatter UV rays, while organic filters absorb them [5,6].

The use of TiO_2NPs and ZnONPs in cosmetic formulations has recently increased because these filters do not generate allergic skin reactions and offer a broader UV protection range than that obtained from organic UV filters [7–10]. Nevertheless, inorganic filters pose the disadvantage of reactive oxygen species (ROS) generation under UV light irradiation [10,11], but this drawback can be overcome by coating the surface of inorganic nanoparticles with chemicals such as alumina, silica and poly (methyl methacrylate) [5,12].

ZnONPs also have antimicrobial properties [13,14], so they can be used as UV filters and preservatives in cosmetic lotions, thus diminishing production costs.

According to the European regulation of cosmetic products, the maximum legal concentration of ZnONPs and TiO_2NPs in ready-to-use preparations is 25% (w/w), with the exception that they cannot be used in those applications that endanger the safety of the user by inhalation. The European Commission regulates the physical and chemical properties (purity, size distribution

and coating) of ZnONPs and TiO_2NPs used in cosmetic products. In addition, water solubility of ZnONPs added to cosmetics is also regulated (EU 2016/621 [15], EU 2016/1143 [16] and EU 2019/1857 amendments [17]).
The manufacturing of cosmetic products modified with TiO_2NPs and ZnONPs is in continuous growth. Nevertheless, the analytical techniques available for the assessment of NPs in complex samples are scarce. Thus, the development of nanometrological strategies is necessary for ensuring compliance with established legislation. Transmission electron microscopy (TEM) is the most often used technique for qualitative analysis of ZnONPs and/or TiO_2NPs in cosmetic products [12,18–20]. TEM provides information on the size of NPs and, if it is combined with energy-dispersive X-ray spectroscopy, on the chemical NPs composition. Regarding quantitative analysis, inorganic UV blockers in cosmetic products can be assessed by field-flow fractionation (FFF) techniques hyphenated to inductively coupled plasma–mass spectrometry (ICP-MS) [21–24]. Field-flow fractionation separates NPs according to their size, which are later identified and quantified by ICP-MS. Nevertheless, these hyphenated techniques require tedious optimisation of FFF separation and long analysis time, which reduces their use in routine analysis.
Several studies have focused on single particle inductively coupled mass spectrometry (spICP-MS) for the determination of metallic NPs since this technique provides information about NPs concentration and size distribution without previous separation of the dissolved metallic analyte (and other chemicals) from the sample´s matrix [25,26]. Recent studies reported in the literature used spICP-MS for TiO_2NPs and ZnONPs determination in water samples [27–31], plants [32], sunscreens and cosmetics [18,19,33,34], food packaging materials [35], food products [19,36,37], and textile products [38].
This study aims to develop an analytical method for the determination of TiO_2NPs and ZnONPs in moisturising creams by spICP-MS.

4.3 MATERIALS AND METHODS

4.3.1 Instrumentation

Weighing of samples was done using an ML 204T model analytical balance (Mettler Toledo, Columbus, OH, USA). Acid digestion of samples was performed in an ETHOS PLUS microwave lab-station with 100 mL closed Teflon vessels, HTC safety springs and HTC adapter plates (Milestone, Sorisole, Italy). A VCX 130 ultrasonic probe (net power output of 130W and frequency of 20 kHz) supplied by Vibra-Cell™ (Sonics & Materials Inc., Newtown, CT, USA) was used for performing the extraction of ZnONPs and TiO_2NPs from moisturising creams. A Raypa UCI-150 model Ultrasonic Cleaner (R. Espinar S.L, Barcelona, Spain) and a vortex D91126 Reax Top (Heidolph, Schwabach, Germany) were used for the homogenisation of samples and extracts.

Total Ti and Zn determination was carried out using a NexION® 2000C ICP-MS (Perkin Elmer) equipped also with a Meinhard® nebuliser and a cyclonic spray chamber thermostated by a Peltier cooler. TiO_2NPs and ZnONPs were determined by spICP-MS using the Syngistix™ Nano Application software version 2.5.

Clean-up of cosmetic extracts was performed using Amicon® Ultra-0.5 Centrifugal Filter Devices (Merck, Darmstadt, Germany) and a Laborcentrifugen 2K15 centrifuge (Sigma, Osterode, Germany). A HRTEM Zeiss Libra 200FE (Oberkochen, Germany) was used for qualitative analysis of NPs in extracts.

4.3.2 Reagents

Methanol (≥99.8%), acetonitrile (≥99.9%), and 2–propanol (isopropanol, ≥99.8%) were supplied by Merck. 99.5% (w/v) Acetone, 69% (w/v) Hiperpur nitric acid, and 33% (w/v) hydrogen peroxide were purchased from Panreac (Barcelona, Spain). Hydrofluoric acid (TraceSELECT™, 47–51%) was from Fluka™ (Charlotte, NC, USA). Ultrapure water (18 MΩcm resistivity) was obtained from a Milli-Q® water purification system (Millipore, Bedford, MA, USA). NexION Setup Solution (10 μg L^{-1} of Be, In, Ce, U, Pb, Mg, Li, and Fe in 1% HNO_3), germanium internal standard (10 mg L^{-1}, 0.16% F^-) and titanium standard (1000 mg L^{-1}, 0.24% F^-) were supplied by Perkin Elmer. Zn standard, 1000 mg L^{-1} in 0.5 mol L^{-1} HNO_3, was from Merck. Certified reference material of 50 nm Ultra Uniform Gold Nanospheres coated by PEG carboxyl (9.89×10^6 particles per mL) was from Perkin Elmer. ZnONPs in ethanol dispersion (40% (w/w), 50–80nm) and TiO_2NPs in ethanol dispersion (15% (w/w), 50 nm) were purchased from US Research Nanomaterials Inc. (Houston, TX, USA).

4.3.3 Cosmetic samples

Four moisturising creams with sun protection factor (SPF) of 30 (sample C1), 50+ (sample C2), and 50 (samples C3 and C4) were purchased from online stores. According to the specifications of the manufacturers, ZnONPs were present in all formulations, whereas only creams C1, C2, and C3 contained TiO_2NPs. Other ingredients of the studied moisturisers are shown in **Table S4.1** (Supplementary Information).

To prevent cosmetic oxidation (possible modification of NPs), bottles of moisturisers were hermetically sealed and stored at 4 ºC before analysis. The upper surface layer of the cream was removed before sample weighing.

4.3.4 Microwave-assisted acid digestion procedure for total Ti and Zn determination

A mass of 0.1000 g of moisturiser cream was weighed into a PTFE vessel where 2.5 mL of 69% nitric acid, 2.5 mL of 33% hydrogen peroxide, 0.5 mL of hydrofluoric acid, and 2.5 mL of ultrapure water were added. Closed vessels were subjected to the microwave temperature program consisting of four steps. In this program, the temperature was first increased linearly from room temperature to 90ºC with increasing the power up to 1000 W for 2 min. The temperature was then increased to 140ºC at 1000 W in 5 min, followed by the third increase in temperature up to 180ºC in 5 min. Finally, this temperature was maintained for 30 min. The samples were digested in triplicate and at least one blank was performed for each digestion set. Finally, samples and blanks were diluted to 25 mL with ultrapure water. Hydrofluoric acid was required to achieve the complete digestion of titanium and silicon present in the cosmetic formulations studied (**Table S4.1**, Supplementary Information).

4.3.5 Ultrasound-assisted TiO_2NPs and ZnONPs extraction procedure

A mass of sample (0.2000 g) was introduced into a polyethylene tube and 40 mL of acetone was added. The mixture was homogenised by vortexing for 2 min and sonicated, using an ultrasonic probe, at 40% amplitude for 5 min in pulse mode (59 s relaxing period followed by 59 s tip sonication period). During the sonication, the sample was placed into an ice bath to avoid sample heating and possible damage to nanoparticles. Samples were prepared in triplicate with at least two blanks for each set of experiments. Finally, the extracts were sonicated in an ultrasonic bath (35kHz, for 5 min) before their dilution and analysis to avoid NPs agglomeration.

4.3.6 Total Ti and Zn determination by ICP-MS

Total contents of titanium and zinc were determined in acid digested samples by ICP-MS. The digested samples were diluted with ultrapure water before the analysis using the dilution factors listed in **Table S4.2**. The instrumental conditions used for titanium and zinc determination by ICP-MS are summarised in **Table 4.1**. Zinc assessment was performed in standard mode by monitoring the ^{66}Zn isotope (*m/z* ratio of 66) and using germanium (22.5 μg L^{-1}) as an internal standard. Titanium was quantified using the DRC mode (1.0 mL min^{-1} ammonia) by monitoring the $^{48}Ti^{14}NH(^{14}NH_3)_4^+$ adduct (mass shift mode, *m/z* ratio of 131). The standard addition calibration (0–10 μg L^{-1}) was carried out for the determination of both analytes to avoid possible matrix effects.

The limit of detection (LOD) and limit of quantification (LOQ) for total zinc and titanium contents were estimated using the $3\sigma/m$ and $10\sigma/m$ criteria, where σ is the standard deviation of eleven measurements of a blank of digestion by ICP-MS, and m is the slope of the standard addition calibration. Instrumental LODs and LOQs were 0.03 and 0.11 μg L^{-1} for zinc quantification, and 0.04 and 0.14 μg L^{-1} for titanium determination, respectively.

Table 4.1. Instrumental conditions of ICP-MS

ICP-MS INSTRUMENTAL CONDITIONS		
Sample flow rate	0.39 – 0.43 mL min^{-1}	
Nebulisation system	Meinhard nebuliser, cyclonic spray chamber	
Plasma parameters	RF Power = 1600 W Plasma gas flow = 15 L min^{-1} Auxiliary gas flow = 1.2 L min^{-1} Nebuliser gas flow = 1.10-1.20 L min^{-1}	
Analyte	**Zn**	**Ti**
m/z	65.926	130.905 (Xenon)
Mode	Standard (STD) mode	Dynamic reaction cell (DRC) mode
Cell gas flow	0	1.0 mL min^{-1} (NH_3)
SYNGISTIX NANO APP		
Software version	2.5	
Dwell time	100 μs	100 μs
Acquisition time	60 s	60 s
Number of scanning	1	1
Density	5.61 g cm^{-3}	4.23 g cm^{-3}
Mass fraction	80.34%	60%
Ionisation efficiency	100%	100%

4.3.7 TiO_2NPs and ZnONPs determination by spICP-MS

Operating conditions for the analysis of TiO_2NPs and ZnONPs are listed in **Table 4.1**. Data acquisition/treatment was performed using the Syngistix™ Nano Application software and parameters such as the sample flow rate and the transport efficiency are required before the analysis. The sample flow rate was calculated considering the mass of water introduced into the nebulisation system per minute. Transport efficiency (TE) was automatically calculated by Syngistix™ nano Application after measuring a suspension of 50 nm AuNPs certified material prepared in ultrapure water (1.0×10^5 particles mL^{-1}, particle frequency method [39]). Sample flow rate within the 0.39–0.43 mL min^{-1} range and TE values of 6.0±1% were assessed.

TiO_2NPs and ZnONPs analysis by spICP-MS were carried using aqueous calibrations of titanium and zinc in a concentration range from 0 to 5 μg L^{-1}.

4.3.8 Analysis of extracts from moisturisers by transmission electron microscopy

Cosmetic extracts were also measured by high resolution transmission electron microscopy coupled to energy-dispersive X-ray spectroscopy (HRTEM-EDX). Using this technique, the analysis requires a clean-up/pre-concentration step before analysis. The clean-up procedure consisted of filtration with Amicon® Ultra-0.5 centrifugal filter devices. Therefore, 500 μL aliquot of the diluted extracts (acetone damages filters) were ultracentrifuged at 14,000 g and 4°C for 20 min, leading to an extract volume of approximately 17 μL. The pre-concentrated extracts were further cleaned by adding 500 μL of ultrapure water to the filter and performing a new ultracentrifugation step (14,000 g, 4°C, 20 min). This cleaning step was repeated eleven times. A final cleaning step (same ultracentrifugation rate and temperature, but for 10 min) was performed to allow the collection of a clean extract of approximately 23 μL. After cleaning-up steps, filter devices were placed upside down in a clean microcentrifuge tube, and centrifugation at 1,000 g for 2 min was carried out to transfer the concentrated extract from the filter device to the collecting tube. This procedure was also applied to aqueous suspensions of ZnONPs (50–80 nm) and TiO_2NPs (50 nm) to ensure that NPs are not lost during the treatment.

Finally, 10 μL of the concentrated and clean extract was placed on a copper grid and allowed to air-dry at room temperature before HRTEM-EDX analysis.

4.4 Results and discussion

4.4.1 Study of interferences for Ti and Zn determination by ICP-MS

The main interferences that could affect the determination of zinc and titanium by ICP-MS are listed in **Table 4.2** [40,41]. The isobaric interference with calcium (^{48}Ca isotope) prevents the quantification of titanium by monitoring the most abundant ion (^{48}Ti isotope, 74% abundance). Nevertheless, titanium can be quantified free of ^{48}Ca isobaric interference by using ammonia as a reaction gas (RPq=0.2) in instruments with dynamic reaction cell (DRC) technology. By setting the ammonia flow rate at 1.0 mL min^{-1}, titanium can be successfully quantified by monitoring the $^{48}Ti^{14}NH(^{14}NH_3)_4^+$ adduct (*m/z* ratio of 131) [42,43].

Several polyatomic species from sulphur, titanium, phosphorous, calcium, and argon can interfere in zinc quantification by ICP-MS when using the *m/z* ratio of 64 (**Table 4.2**). In addition, there is an isobaric interference with nickel (^{64}Ni) under these operational conditions that can affect the analytical signal. Therefore, the effect of these interferences on the determination of Zn must be investigated. The use of ammonia as a reactive gas in DRC technology with the NexION® 2000C ICP-MS was tested (some scarce reports can be found regarding the use of ammonia as a reaction gas for dissolved zinc assessment [44,45]).

Mass scans (within the *m/z* 40–150 range) of an aqueous zinc standard (5 μg L^{-1} in 1% HNO_3) were performed in standard (STD) mode and DRC mode with ammonia (10% NH_3 in He, several flow rates and RPq values using the on-mass and mass-shift approaches). The best results using the DRC mode were obtained using 2.0 mL min^{-1} of ammonia and a RPq value of 0.2 (**Table 4.3**). However, the sensitivity for zinc was found to be very low and there was an interference in the determination of zinc (monitoring of zinc adducts with *m/z* 115 and 117) generated by titanium even at low levels of the interference (5 μg L^{-1} of Ti) using these ammonia conditions. Thus, the use of ammonia as reactive gas in the determination of zinc was discarded.

Table 4.2. Interferences in the determination of zinc and titanium by ICP-MS

Isotope	Abundance (%)	Isobaric interferences	Polyatomic interferences
^{46}Ti	7.99	^{46}Ca	$^{32}S^{14}N^+$, $^{14}N^{16}O_2^+$, $^{15}N_2{}^{16}O^+$
^{47}Ti	7.32	--	$^{32}S^{14}N^1H^+$, $^{30}Si^{16}O^1H^+$, $^{32}S^{15}N^+$, $^{33}S^{14}N^+$, $^{15}N^{16}O_2^+$, $^{14}N^{16}O_2{}^1H^+$, $^{12}C^{35}Cl^+$, $^{31}P^{16}O^+$
^{48}Ti	73.98	^{48}Ca	$^{32}S^{16}O^+$, $^{34}S^{14}N^+$, $^{33}S^{15}N^+$, $^{14}N^{16}O^{18}O^+$, $^{14}N^{17}N_2^+$, $^{12}C_4^+$, $^{36}Ar^{12}C^+$
^{49}Ti	5.46	--	$^{32}S^{17}O^+$, $^{32}S^{16}O^1H^+$, $^{35}Cl^{14}N^+$, $^{34}S^{15}N^+$, $^{33}S^{16}O^+$, $^{14}N^{17}O_2{}^1H^+$, $^{14}N^{35}Cl^+$, $^{36}Ar^{13}C^+$, $^{36}Ar^{12}C^1H^+$, $^{12}C^{37}Cl^+$, $^{31}P^{18}O^+$
^{50}Ti	5.25	^{50}V, ^{50}Cr	$^{32}S^{18}O^+$, $^{32}S^{17}O^1H^+$, $^{36}Ar^{14}N^+$, $^{35}Cl^{15}N^+$, $^{36}S^{14}N^+$, $^{33}S^{17}O^+$, $^{34}S^{16}O^+$, $^1H^{14}N^{35}Cl^+$, $^{34}S^{15}O^1H^+$
^{64}Zn	48.89	^{64}Ni	$^{32}S^{16}O_2^+$, $^{48}Ti^{16}O^+$, $^{31}P^{16}O_2{}^1H^+$, $^{48}Ca^{16}O^+$, $^{32}S_2^+$, $^{31}P^{16}O^{17}O^+$, $^{34}S^{16}O_2^+$, $^{36}Ar^{14}N_2^+$
^{66}Zn	27.81	--	$^{50}Ti^{16}O^+$, $^{34}S^{16}O_2^+$, $^{33}S^{16}O_2{}^1H^+$, $^{32}S^{16}O^{18}O^+$, $^{32}S^{17}O_2^+$, $^{33}S^{16}O^{17}O^+$, $^{32}S^{34}S^+$, $^{33}S_2^+$
^{67}Zn	4.11	--	$^{35}Cl^{16}O_2^+$, $^{33}S^{34}S^+$, $^{34}S^{16}O_2{}^1H^+$, $^{32}S^{16}O^{18}O^1H^+$, $^{33}S^{34}S^+$, $^{34}S^{16}O^{17}O^+$, $^{33}S^{16}O^{18}O^+$, $^{32}S^{17}O^{18}O^+$, $^{33}S^{17}O_2^+$, $^{35}Cl^{16}O_2^+$
^{68}Zn	18.57	--	$^{36}S^{16}O_2^+$, $^{34}S^{16}O^{18}O^+$, $^{40}Ar^{14}N_2^+$, $^{35}Cl^{16}O^{17}O^+$, $^{34}S_2^+$, $^{36}Ar^{32}S^+$, $^{34}S^{17}O_2^+$, $^{33}S^{17}O^{18}O^+$, $^{32}S^{18}O_2^+$, $^{32}S^{36}S^+$
^{70}Zn	0.62	^{70}Ge	$^{35}Cl^{35}Cl^+$, $^{40}Ar^{14}N^{16}O^+$, $^{35}Cl^{17}O^{18}O^+$, $^{37}Cl^{16}O^{17}O^+$, $^{34}S^{18}O_2^+$, $^{36}S^{16}O^{18}O^+$, $^{36}S^{17}O_2^+$, $^{34}S^{36}S^+$, $^{36}Ar^{34}S^+$, $^{38}Ar^{32}S^+$

Table 4.3. Effect of ammonia on ICP-MS signal intensity, isotopes ratios and bias of the studied zinc isotopes

STD mode (no gas)			
m/z	Mean intensity (counts)	Isotope ratio	Bias (%)
64	34741	0.59 [a]	3
66	20614		
DRC mode (2.0 mL min^{-1} NH_3, RPq=0.2)			
m/z	Mean intensity (counts)	Isotope ratio	Bias (%)
64	1012	0.64 [a]	11
66	645		
98	131	0.60 [b]	5
100	79		
115	2599	0.60 [c]	5
117	1562		

Isotope's ratio: ratio of intensities [a] 66/64; [b] 100/98; [c] 117/115
***m/z* 98**: $^{64}Zn(^{14}NH_3)_2^+$; ***m/z* 100**: $^{66}Zn(^{14}NH_3)_2^+$
***m/z* 115**: $^{64}Zn(^{14}NH_3)_3^+$; ***m/z* 117**: $^{66}Zn(^{14}NH_3)_3^+$

On the other hand, using STD mode, ^{64}Zn and ^{66}Zn isotopes are interfered by polyatomic titanium species such as $^{48}Ti^{16}O^+$ and $^{50}Ti^{16}O^+$, respectively (**Table 4.2**). Therefore, a study to evaluate the level of interference of Ti in Zn (*m/z* 64 and 66) determination has been carried out. The experiment was performed with several solutions containing 1 µg L^{-1} of zinc in 1% HNO_3 and increasing titanium concentrations (5, 10, 25, 50, 100, 250, 500, and 1000 µg L^{-1}). Results showed that titanium concentrations higher than 100 µg L^{-1} interfere in Zn determination when *m/z* 64 was monitored (analytical recovery of 153%). However, analytical recoveries using the ^{66}Zn isotope were 90, 86, 86, 90, 92, 111, 122, and 164% for titanium

concentrations of 5, 10, 25, 50, 100, 250, 500, and 1000 μg L^{-1}, respectively. This means that zinc quantification (*m/z* ratio of 66) can be performed in a standard mode in samples (extracts or digested samples) containing up to 500 μg L^{-1} of titanium.

Furthermore, suspensions containing both 10 μg L^{-1} TiO_2NPs (50 nm) and 2 μg L^{-1}ZnONPs (50–80 nm) were measured by spICP-MS to evaluate the possible interference of TiO_2NPs in the assessment of ZnONPs (^{66}Zn isotope, STD mode). The particle number concentration of these suspensions was compared with control suspensions containing only ZnONPs (2.0 μg L^{-1}), and the analytical recovery of ZnONPs in the suspensions that contained both NPs was 99±10%. The mean size of ZnONPs in the suspension was 59±6 nm (spICP-MS experimental value) which was in accordance with the manufacturer's specifications.

Considering the results obtained in this study, Zn was analysed in the samples using STD mode by monitoring the *m/z* 66 and Ti using DRC mode (using ammonia) at *m/z* 131.

4.4.2 Extraction of nanoparticles from moisturisers

A study has been developed for ZnONPs extraction from moisturisers. The influence of parameters such as type and volume of extractant and sonication mode, in the extraction procedure, has been evaluated.

4.4.2.1 Selection of extractant solvent and sonication mode

Surfactant aqueous solutions, mainly Triton X-100 (0.1–1% concentration range) [18,20,34] and 1% sodium dodecyl sulphate [33], have been proposed by several researchers as extractants for the isolation of TiO_2NPs and ZnONPs from sunscreens. Nevertheless, Philippe et al. [20] have reported poor NPs dispersion in surfactant solutions in some cases. On other occasions, a defatting step with hexane before sunscreen dispersion has also been proposed [19–24,33,46], and hexane has been reported to aid TiO_2NPs disaggregation [23]. Other authors have outlined the use of organic solvents or organic solvent/water mixtures as extractants for NPs isolation from cosmetics [23,47].

Our preliminary study on the extraction of ZnONPs from moisturisers was carried out by testing several organic solvents miscible with water (methanol, acetonitrile, acetone, and isopropanol) as extractants. The experiments were based on subjecting a mixture of 0.2000 g of the moisturiser coded as C4 and 20 mL of the organic extractant to ultrasound (water-bath sonication, 35 kHz, 30 min). The extracts obtained using the different solvents were diluted with water and analysed by spICP-MS. Results showed that the concentration of ZnONPs was lower than the limit of detection of the spICP-MS method when using methanol, acetonitrile, and isopropanol as solvents. However, extracts performed in acetone showed detectable ZnONPs concentrations, therefore, acetone was selected as the most suitable solvent.

Regarding the technique for cosmetic sample dispersion, shaking [20], water-bath sonication [18,19,22,23,33,34,46] and tip sonication [23,47] procedures have been described in the literature. Ultrasonic energy was selected in our study to improve extraction efficiency. Therefore, experiments were carried out, using 0.2000 g of sample and 20 mL of acetone as solvent extractant, and using bath sonication (35 kHz, 30 min) and tip sonication (60% amplitude, 10 min). Experiments were carried out in triplicate in both sonication modes and blanks of extraction were also prepared. The results obtained showed that concentrations of ZnONPs per gram of cream were 180 times higher when using the tip sonication procedure than those obtained after water-bath sonication. Furthermore, the ZnONPs size distribution was found to be similar using both sonication modes. Therefore, tip sonication was selected for further studies.

4.4.2.2 Selection of tip sonication conditions

The effect of the amplitude (20, 40, 60, and 80%) of the tip sonication was studied by fixing the amount of sample (0.2000 g of moisturiser C4) and the volume of acetone (20 mL). The extraction procedure was performed by sonication in continuous mode for 10 min. ZnONPs concentrations in the extracts are shown in **Figure 4.1a**, which implies an inefficient extraction/dispersion when using the lowest amplitude (20%). The number of extracted/dispersed ZnONPs was found to increase at higher amplitudes, but the use of amplitudes of 60 and 80% led to lower ZnONPs concentration than those found at 40%. The values of ionic zinc in the diluted extracts were 0.56±0.044, 0.69±0.028 and 1.4±0.15 μg L^{-1} for tip sonication amplitude of 40%, 60%, and 80%, respectively. Therefore, the decrease of the ZnONPs concentration at higher amplitudes could be attributed to ZnONPs dissolution. Considering these results, 40% amplitude of tip sonication was selected as the optimum value.

After fixing the amplitude at 40%, a set of experiments was carried out under the same conditions as those shown above, but varying the extraction time (5, 10, 15, and 20 min). As shown in **Figure 4.1b**, the highest ZnONPs concentration was achieved when performing the tip sonication for 5 min. The decrease of ZnONPs concentration at higher times could be attributed to the dissolution of nanoparticles.

Regarding the tip sonication mode (continuous/discontinuous sonication), **Figure 4.1c** shows that a discontinuous mode (five cycles of 59 s of tip sonication followed by 59 s of relaxing, total pre-treatment time of 10 min) provided higher extraction of ZnONPs compared to a continuous mode (tip sonication for 5 min). A discontinuous sonication mode was therefore selected.

4.4.2.3 Optimisation of the volume of acetone

After the selection of the sonication conditions, experiments have been carried out to study the influence of the extractant volume on the NPs extraction. The study was performed using a sample mass of 0.2000 g and volumes of acetone of 10, 20, 30, and 40 mL. The experiments were carried out in triplicate for each acetone volume. The results obtained are shown in **Figure 4.1d**. It can be seen that the extraction of ZnONPs was enhanced with increasing acetone volume, and a volume of 40 mL was finally selected.

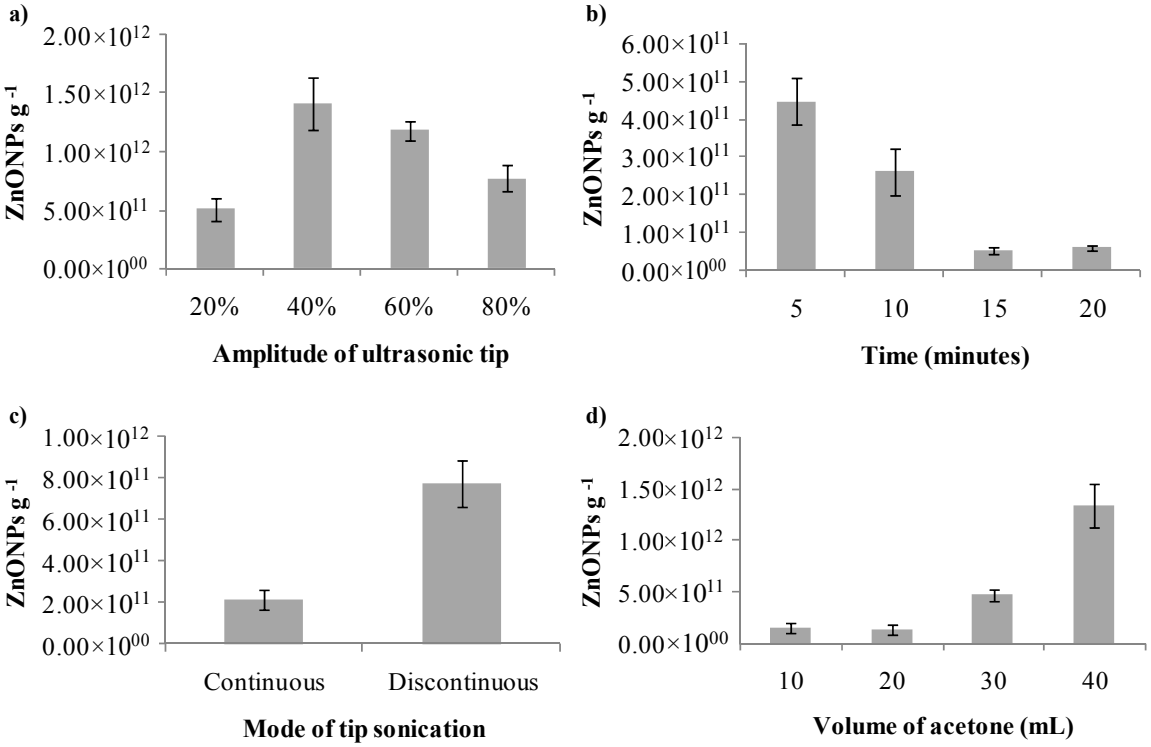

Figure 4.1. Effect of ultrasonication amplitude (a), time (b), and mode (c); and acetone volume (d) on the extraction of ZnONPs from moisturisers based on tip sonication using acetone as extractant solvent before spICP-MS assessment

4.4.3 Analytical performances for TiO_2NPs and ZnONPs determination by spICP-MS

Although the extraction method was optimised for ZnONPs, the proposed methodology was validated for ZnONPs and TiO_2NPs assessments to evaluate the possible quantitative co-extraction of both NPs.

The limit of detection (LOD) and the limit of quantification (LOQ) of ZnONPs and TiO_2NPs number concentrations were calculated through the $3\sigma/m$ and $10\sigma/m$ criteria. Three times or ten times the standard deviation (LOD or LOQ, respectively) of eleven measurements of the blanks of extraction were divided by the slope of the ionic calibration (m). The instrumental LODs and LOQs were 1.15×10^3 and 3.82×10^3 ZnONPs mL^{-1}; and 1.35×10^3 and 4.50×10^3 TiO_2NPs mL^{-1}, respectively.

The LOD in size was obtained by the 3σ and 5σ criteria proposed by Lee et al. [48]. LODs for ZnONPs determination were 29 nm (3σ criterion) and 35 nm (5σ criterion). In the case of TiO_2NPs the LODs were 28 and 33 nm for the 3σ and 5σ criterion, respectively.

The precision of the overall method (including the extraction and spICP-MS analysis) was evaluated through repeatability after preparing eleven extracts from a moisturiser (moisturiser C3 containing TiO_2NPs and ZnONPs). The extracts were diluted with ultrapure water (**Table S4.2**, Supplementary Information) and analysed in triplicate by spICP-MS. RSD values of 9% for ZnONPs g^{-1} of moisturiser, and 3% for determination of the mean size of ZnONPs were obtained. Regarding TiO_2NPs, RSD value of 5% was obtained for both number concentration (per gram of cream) and mean size. These results indicated that the developed methodology was repeatable for the quantification of ZnONPs and TiO_2NPs in moisturisers.

The accuracy of the spICP-MS measurements was assessed by the analytical recovery approach. Extracts from sample C3 were spiked with a concentration of 2.0 µg L^{-1} ZnONPs (50–80 nm) or 10 µg L^{-1} TiO_2NPs (50 nm). Unspiked extracts, spiked extracts, and

ZnONPs/TiO_2NPs suspensions used for spiking (control standards) were prepared in triplicate and measured by spICP-MS in triplicate. The "NPs concentration found" was calculated as the subtraction between the concentration of the spiked extracts and the concentration of the unspiked extracts. The analytical recoveries were assessed as the ratio between the "NPs concentration found" and the NPs concentration of the suspensions used for carrying out the spiking procedures (experimental value). Recovery percentages of 119±3 % and 102±12% were obtained for TiO_2NPs (50 nm) and ZnONPs (50-80 nm) suspensions, respectively. These results demonstrated that the spICP-MS quantification of ZnONPs and TiO_2NPs was accurate.

4.4.4 Application

The proposed methodology was applied for the determination of TiO_2NPs and ZnONPs in commercial moisturisers with SPF (ingredients listed in **Table S4.1**, Supplementary Information). Total zinc and titanium concentrations found in the samples (microwave-assisted acid digestion and dilution according to **Table S4.2**, Supplementary Information) are listed in **Table 4.4**. Zinc concentrations were found to be within the 26.37–109.1 mg g^{-1} range (creams C1 and C2 containing the lowest and the highest zinc concentrations, respectively); whereas titanium concentrations varied from 15.67 to 35.59 mg g^{-1} (moisturisers C1 and C3 containing the lowest and the highest titanium concentrations, respectively).

Cosmetic extracts prepared by the developed extraction procedure were also diluted with ultrapure water (**Table S4.2**, Supplementary Information) and analysed by ICP-MS (assessment of total titanium and total zinc in the extract) and by spICP-MS (TiO_2NPs and ZnONPs quantification). Total titanium and zinc concentrations in the extracts, and TiO_2NPs and ZnONPs concentrations, are also listed in **Table 4.4**.

The comparison between total concentrations in acid digests and extracts obtained by ICP-MS shows that extraction efficiencies were 52% (C1), 53% (C2), 64% (C3) and 81% (C4) for zinc, and 23% (C1), 40% (C2) and 104% (C3) for titanium. Regarding these results, quantitative extractions were only obtained for the moisturisers coded as C3 (titanium) and C4 (zinc). The low extraction efficiencies obtained for creams C1 and C2 could be justified by the precipitation of solid particles at the bottom of the extract that appeared after several hours of performing the extraction. This fact could be due to the presence of inorganic ingredients such as iron oxides, mica, synthetic fluorphlogopite (synthetic mica), tin oxide (cream C1) and alumina (both C1 and C2) [cosmetic formulations are listed in the **Table S4.1**, Supplementary Information]. The higher content in inorganic compounds of cream C1 could also explain why this moisturiser exhibited the lowest extraction efficiencies. On the other hand, the low extraction rate of zinc in moisturiser C3 could be due to the presence of silica which can hinder the extraction. Nevertheless, the extraction of titanium from cream C3 was quantitative. This finding could indicate a different interaction of zinc and titanium with silica particles in this sample.

Regarding spICP-MS analysis, the particle number concentration of ZnONPs was within the 2.37×10^{11}–5.34×10^{12} ZnONPs g^{-1} range (moisturising creams C1 and C3, respectively). On the other hand, concentrations of TiO_2NPs varied from 3.32×10^{11} (cream C1) to 1.50×10^{13} TiO_2NPs g^{-1} (cream C3). Furthermore, spICP-MS provided information about the size distribution of extracted NPs (**Table 4.4**). ZnONPs showed the smallest mean size of 86±1 nm in sample C4, and the largest mean size of 175±5 nm in sample C1. Mean sizes of TiO_2NPs varied within the 84–145 nm range. Size distributions of TiO_2NPs and ZnONPs in the moisturiser coded as C3 can be seen as histograms in **Figure 4.2**.

Particle number concentration can be transformed into mass concentration assuming spherical shape and solid nature of NPs (mean size of NPs was used to carry out these calculations). Estimated mass concentrations of NPs obtained are also shown in **Table 4.4**. It must

be mentioned that the sum of these estimated mass concentration and the ionic concentration (provided by the Syngistix Nano Application) in the studied samples usually agree with the total concentration measured in the extract by ICP-MS (**Table 4.4**). The estimated mass concentrations of the extracted NPs were up to 2.5% (w/w) for ZnONPs [0.4% (C1), 1.8% (C2), 2.5% (C3) and 0.8% (C4)], and up to 2.0%(w/w) for TiO_2NPs [0.2% (C1), 0.6% (C2) and 2.0% (C3)], values lower than the maximum concentration of ZnONPs and TiO_2NPs in ready-to-use preparations [25% (w/w)] set by the European regulation [15–17].

Finally, HRTEM images and energy-dispersive X-ray spectrums confirmed the presence of both ZnONPs and TiO_2NPs in the extracts prepared from moisturising creams coded as C2 and C3 (**Figure 4.3 and Figure 4.4**, respectively). Nevertheless, the size assessment of these NPs was not carried out because most of them were agglomerated on the copper grids. Standards of ZnONPs and TiO_2NPs were also analysed by HRTEM-EDX (**Figure 4.5**), which verified that the proposed clean-up procedure guarantees the NPs integrity.

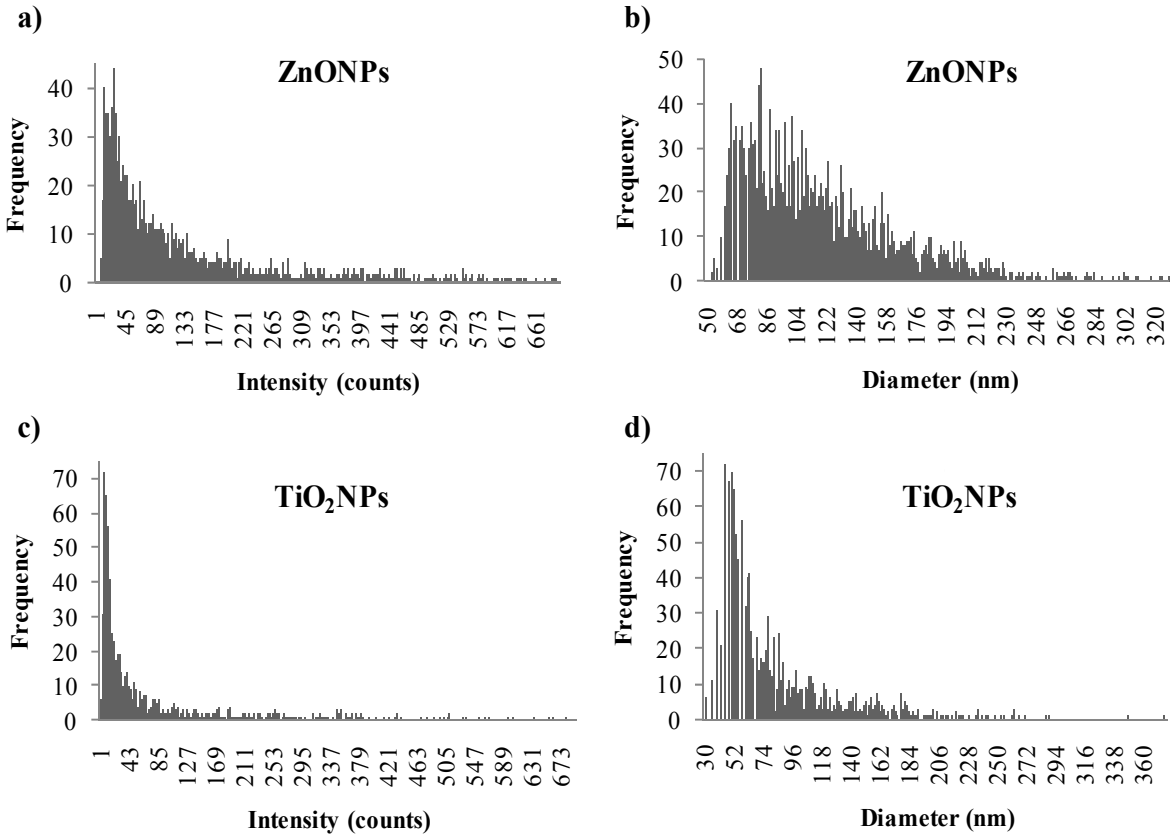

Figure 4.2. Signal distribution (a,c) and size distribution histograms (b,d) of ZnONPs and TiO_2NPs in extracts from moisturiser C3

Table 4.4. Concentrations of zinc, ZnONPs, titanium and TiO_2NPs in the studied moisturisers

	Zn and ZnONPs								
	ICP-MS Total zinc determination		spICP-MS (ionic Zn and ZnONPs determination)				Size distribution (nm)		
	Digest (mg g^{-1})	Extract (mg g^{-1})	mg g^{-1} Zn (ionic)	ZnONPs g^{-1}	mg g^{-1} ZnO (nano) [a]	mg g^{-1} ZnO (ionic +nano)	Mode	Mean	Range
C1	26.4 ± 0.634	13.7 ± 1.14	10.5 ± 0.645	$2.37\times10^{11} \pm 2.25\times10^{10}$	3.75	14.3	129 ± 18	175 ± 5	84 – 445
C2	109 ± 10.1	57.3 ± 5.61	46.2 ± 5.21	$1.47\times10^{12} \pm 5.54\times10^{10}$	17.8	64.0	116 ± 16	160 ± 6	77 – 465
C3	83.4 ± 4.98	53.2 ± 7.14	19.2 ± 1.80	$4.28\times10^{12} \pm 4.26\times10^{11}$	25.4	44.6	79 ± 8	126 ± 2	57 – 369
C4	63.8 ± 2.78	51.9 ± 1.96	36.4 ± 1.26	$4.43\times10^{12} \pm 6.11\times10^{11}$	8.39	44.8	68 ± 5	86 ± 1	46 – 278
	Ti and TiO_2NPs								
	ICP-MS Total titanium determination		spICP-MS (ionic Ti and TiO_2NPs determination)				Size distribution (nm)		
	Digest (mg g^{-1})	Extract (mg g^{-1})	mg g^{-1} Ti (ionic)	TiO_2NPs g^{-1}	mg g^{-1} TiO_2 (nano) [a]	mg g^{-1} TiO_2 (ionic +nano)	Mode	Mean	Range
C1	15.7 ± 2.16	3.62 ± 0.263	2.40 ± 0.231	$3.32\times10^{11} \pm 5.40\times10^{10}$	1.36	4.66	56 ± 6	145 ± 10	38 – 491
C2	26.3 ± 3.30	10.6 ± 2.68	3.41 ± 0.778	$1.01\times10^{12} \pm 1.09\times10^{11}$	3.45	9.17	74 ± 10	137 ± 6	49 – 650
C3	35.6 ± 4.05	37.2 ± 6.96	26.1 ± 0.987	$1.50\times10^{13} \pm 6.90\times10^{11}$	11.7	45.7	49 ± 3	84 ± 3	30 – 391
C4	<LOD	-- [b]	-- [b]	-- [b]	-- [b]	-- [b]	-- [b]	-- [b]	-- [b]

[a] Estimated mass concentration of NPs considering the particle concentration and size distribution of NPs and assuming spherical shape and solid nature of them
[b] Not assessed

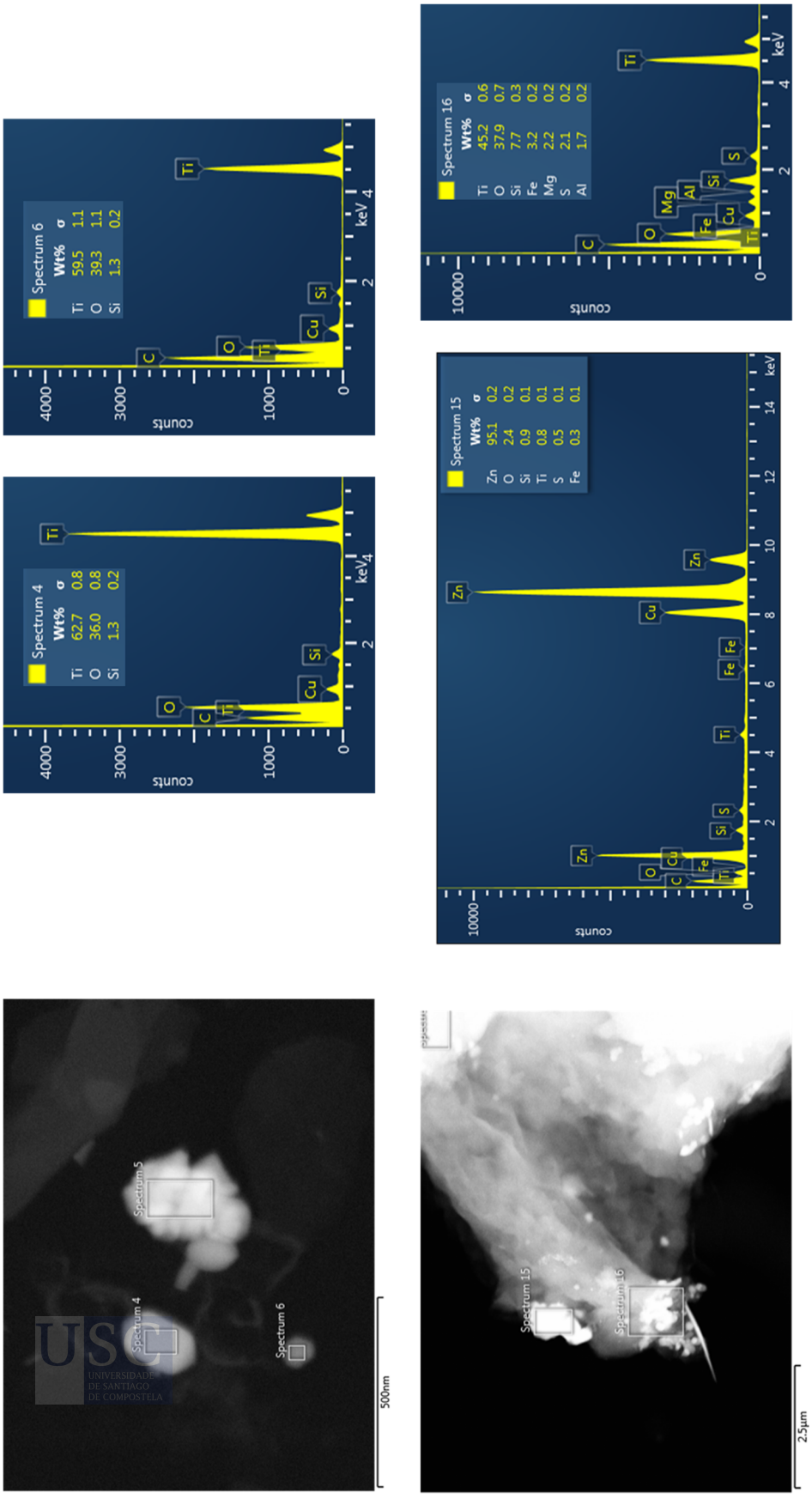

Figure 4.3. HRTEM images and energy-dispersive X-ray spectrums of extracts from moisturiser C2

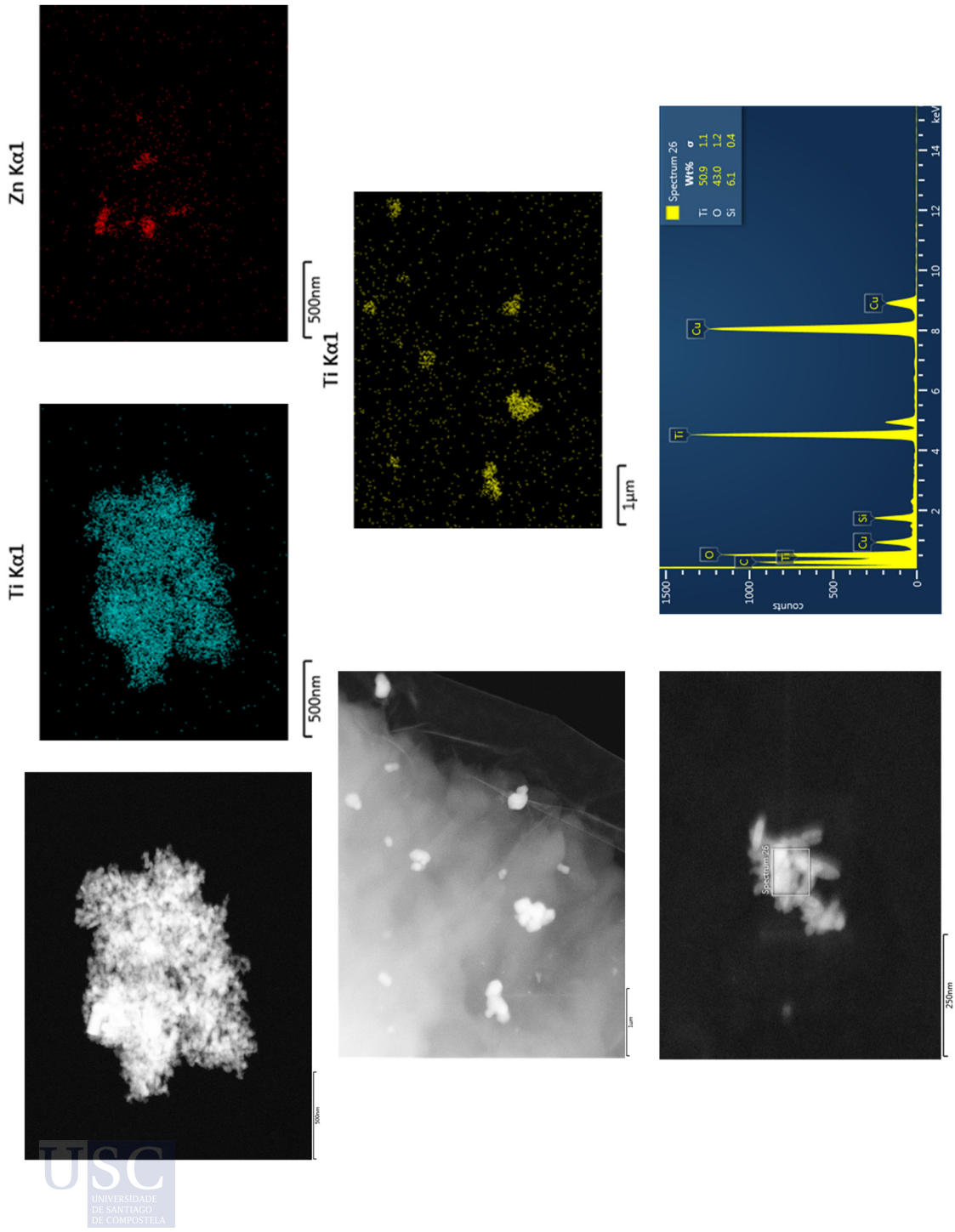

Figure 4.4. HRTEM images and energy-dispersive X-ray spectrums of extracts from moisturiser C3

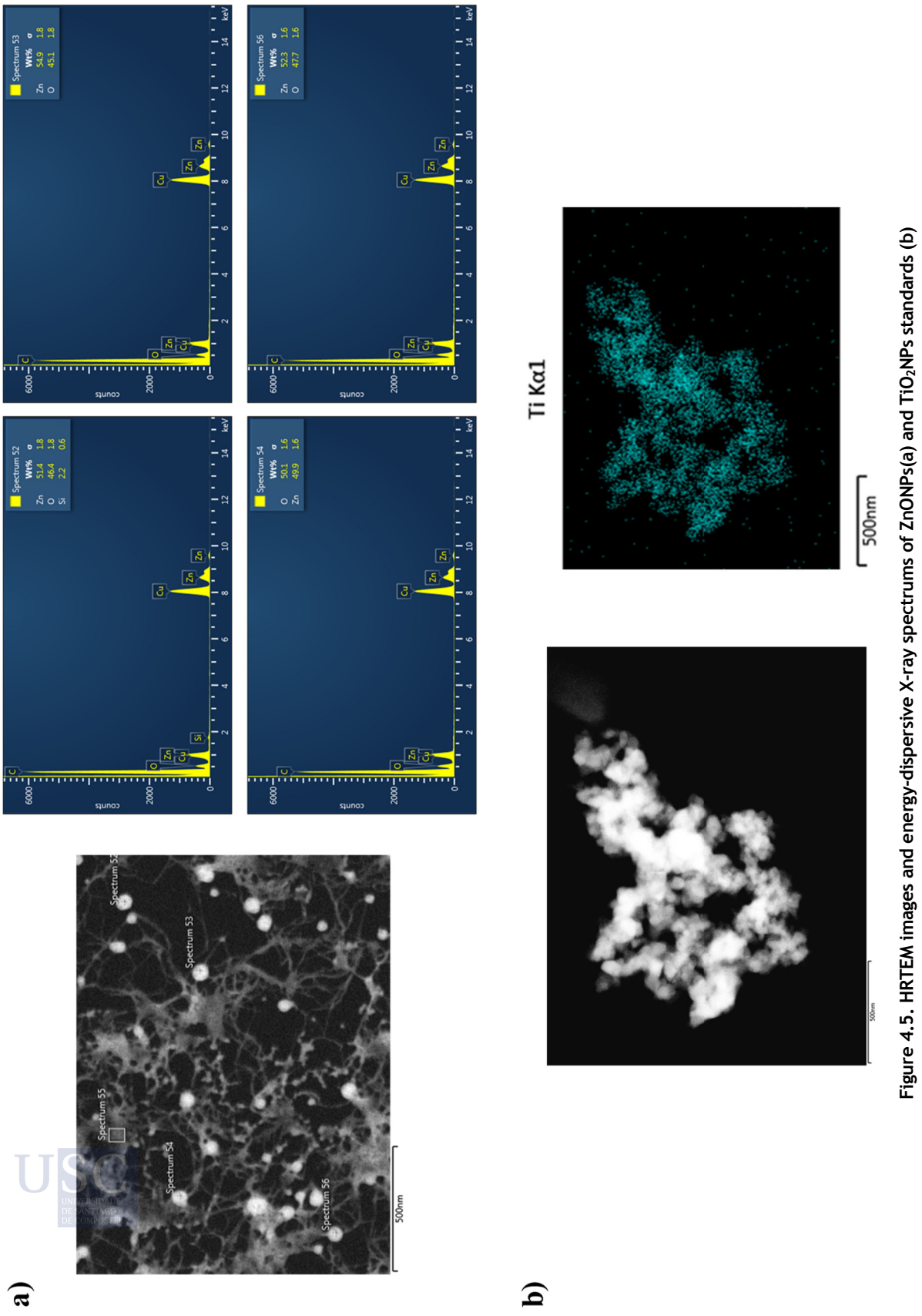

Figure 4.5. HRTEM images and energy-dispersive X-ray spectrums of ZnONPs(a) and TiO_2NPs standards (b)

4.5 CONCLUSIONS

Tip sonication using acetone as an extractant before spICP-MS analysis has been found to be advantageous for isolating ZnONPs and TiO_2NPs from complex samples such as moisturisers. The extraction efficiency was found to be highly dependent on the formulations' components. Particle number concentrations were within the 2.37×10^{11}–4.43×10^{12} ZnONPs g^{-1} and 3.32×10^{11}–1.50×10^{13} TiO_2NPs g^{-1} ranges. The mean sizes varied from 86 to 175 nm for ZnONPs, and within the 84–145 nm range for TiO_2NPs. The presence of ZnONPs and TiO_2NPs in the extracts from moisturisers was also confirmed by HRTEM-EDX analysis. spICP-MS is an useful technique for ZnONPs and TiO_2NPs assessment in moisturisers, but further improvements on sample pre-treatment are required to ensure quantitative extractions without the influence of the sample's matrix.

SUPPLEMENTARY INFORMATION

Table S4.1. Ingredients of analysed moisturising creams

Code	Ingredients
C1	Water, Cyclopentasiloxane, Caprylyl Methicone, Ethylhexyl Palmitate, Dimethicone, Lauryl PEG-8 Dimethicone, Neopentyl Glycol Diheptanoate, Polymethylsilsesquioxane, PEG-12 Dimethicone, PPG-20 Crosspolymer, Titanium dioxide, Glycerin, Dimethicone Crosspolymer, Tribehenin, Dimethicone/Vinyl Dimethicone Crosspolymer, Algae Extract, Hydroxycapric Acid, Hydroxycaprylic Acid, Hydroxycinnamic Acid, Teprenone, Tetrahexyldecyl Ascorbate, Tocopheryl Acetate, Alumina, Butylene Glycol, Calcium Aluminum Borosilicate, Caprylic/Capric Triglyceride, Disodium EDTA, Iron Oxides, Mica, PEG-4, Silica, Synthetic Fluorphlogopite, Tin Oxide, Triethoxycaprylylsilane, Xantan Gum, Caprylyl Glycol, Hexylene Glycol, Phenoxyethanol, Titanium Dioxide (nanoparticulated, 5.40%), Zinc Oxide (nanoparticulated, 2.96%).
C2	Zinc Oxide (nano), Avene Thermal Spring Water, Titanium Dioxide (nano), Cococaprylate/Caprate, Isocetyl Stearoyl Stearate, Isopropyl Palmitate, Isodecyl Neopentanoate, Isododecane, Isohexadecane, PTFE, Triethylhexanoin, Dicaprylyl Ether, PEG-30 Dipolyhydroxystearate, Alumina, Stearic Acid, Caprylyl Glycol, PEG-45/Dodecyl Glycol Copolymer, Silica, Benzoic Acid, Caprylic/Capric Triglyceride, Disodium EDTA, Disteardimonium Hectorite, Glyceryl Behenate, Glyceryl Dibehenate, Heliantus Annuus Seed Oil, Pentaerythrityl Tetra-Di-T-Butyl Hydroxyhydrocinnamate, Polyamide-3, Sodium Chloride, Tocopherol, Tocopheryl Glucoside, Tribehenin, Triethoxycaprylylsilane, Water.
C3	Water, Titanium Dioxide (nano), Diethylhexyl Carbonate, Propylene Glycol Dicaprylate/Dicaprate, Zinc Oxide (nano), Dibutyl Adipate, Dicaprylyl Carbonate, Alcohol Denat, Dimethicone, Butylene Glycol, Trimethylpentanediol/Adipic Acid/Glycerin Crosspolymer, PEG-30 Dipolyhydroxystearate, Silica, Polyglyceryl-6 Polyricinoleate, Butyloctyl Salicylate, Allantoin, Sodium Hyaluronate, Polyglyceryl-2 Isostearate, Panthenol, Tocopheryl Acetate, Magnesium Sulphate, Phenylpropanol, Disteardimonium Hectorite, Propanediol, Caprylyl Glycol, Triethoxycaprylylsilane, Glyceryl Stearate, PEG-8, Dimethicone Crosspolymer, Tocopherol, Ascorbyl Palmitate, Ascorbic Acid, Citric Acid.
C4	Water, Cyclopentasiloxane, PEG-10 Dimethicone, Methicone, Isododecane, Propane-diol, Caprylic/Capric Triglycerides, Isodecyl Neopenta-noate, Dimethicone/bis Isobutyl PPG-20 Crosspolymer, Octyldodecyl Stearyl Citrate Crosspolymer, Tapioca Starch, Polymethylsilsesquioxane, Glycerin, Isostearic Acid, Polyhydroxystearic Acid, Dimethicone, Isododecane, Phenoxyl-thanol, Benzoic Acid, Ethylhexylglycerin, Glycereth-2 Cocoate, Dicaprylyl ether, Dehydroxanthan Gum, Carthamus Tinctorius (Safflower) Seed Oil, Melanin, Phytosteryl, Octyldodecyl Lauroyl Glutamate, Sodium Hyaluronate Acid, Trimethylated Silica Gel, Tocopheryl Acetate, Dipotassium Glycyrrhizinate, Porphyridium cruentum, Eucalyptus Globulus Leaf Extract, Zingiber Officinale Root Extract, Gaultheria Procumbens Leaf Extract, Avena Sativa Kernel Extract, Allantoin, Ceramide 3, Zinc Oxide (9%), Octinoxate (7.5%).

Table S4.2. Dilution factors used for ICP-MS and spICP-MS analyses of acid digests and extracts from moisturisers (dilution with ultrapure water)

	Digests (ICP-MS analysis)		Extracts (ICP-MS/spICP-MS analysis)	
	Zn	Ti	Zn total/ZnONPs	Ti total/TiO_2NPs
C1	1:100,000	1:460,000	1: 24,000	1: 24,000
C2	1:420,000	1:475,000	1: 100,000	1: 60,000
C3	1:350,000	1:475,000	1: 300,000	1: 1,300,000
C4	1:230,000	-- [(a)]	1: 300,000	-- [(a)]

[(a)] Not measured

REFERENCES

[1] A. Kammeyer, R.M. Luiten, Oxidation events and skin aging, Ageing Res. Rev. 21 (2015) 16–29, DOI: 10.1016/j.arr.2015.01.001.

[2] G.P. Pfeifer, A. Besaratinia, UV wavelength-dependent DNA damage and human non-melanoma and melanoma skin cancer, Photochem. Photobiol. Sci. 11 (2012) 90–97, DOI: 10.1039/c1pp05144j.

[3] L.R. Sklar, F. Almutawa, H.W. Lim, I. Hamzavi, Effects of ultraviolet radiation, visible light, and infrared radiation on erythema and pigmentation: a review, Photochem. Photobiol. Sci. 12 (2013) 54–64, DOI: 10.1039/C2PP25152C.

[4] Regulation (EC) N° 1223/2009 of the European Parliament and of the Council of 30 November 2009 on cosmetic products, Official Journal of the European Union, L342 (01 March 2022) 1–392.

[5] M. Åhlén, O. Cheung, M. Strømme, Amorphous Mesoporous Magnesium Carbonate as a Functional Support for UV-Blocking Semiconductor Nanoparticles for Cosmetic Applications, ACS Omega 4 (2019) 4429–4436, DOI: 10.1021/acsomega.8b03498.

[6] D.R. Sambandan, D. Ratner, Sunscreens: An overview and update, J. Am. Acad. Dermatol. 64 (2011) 748–758, DOI: 10.1016/j.jaad.2010.01.005.

[7] C.H. Tan, S. Rasool, G.A. Johnston, Contact dermatitis: Allergic and irritant, Clin. Dermatol. 32 (2014) 116–124, DOI: 10.1016/j.clindermatol.2013.05.033.

[8] S. Onoue, Y. Seto, H. Sato, H. Nishida, M. Hirota, T. Ashikaga, A.M. Api, D. Basketter, Y. Tokura, Chemical photoallergy: photobiochemical mechanisms, classification, and risk assessments, J. Dermatol. Sci. 85 (2017) 4–11, DOI: 10.1016/j.jdermsci.2016.08.005.

[9] S. Afonso, K. Horita, J.P. Sousa e Silva, I.F. Almeida, M.H. Amaral, P.A. Lobão, P.C. Costa, M.S. Miranda, J.C.G. Esteves da Silva, J.M. Sousa Lobo, Photodegradation of avobenzone: Stabilization effect of antioxidants, J. Photochem. Photobiol. B 140 (2014) 36–40, DOI: 10.1016/j.jphotobiol.2014.07.004.

[10] J. Kockler, M. Oelgemöller, S. Robertson, B.D. Glass, Photostability of sunscreens, J. Photochem. Photobiol. C 13 (2012) 91–110, DOI: 10.1016/j.jphotochemrev.2011.12.001.

[11] W. He, H. Jia, J. Cai, X. Han, Z. Zheng, W.G. Wamer, J.J. Yin, Production of Reactive Oxygen Species and Electrons from Photoexcited ZnO and ZnS Nanoparticles: A Comparative Study for Unraveling their Distinct Photocatalytic Activities, J. Phys. Chem. C 120 (2016) 3187–3195, DOI: 10.1021/acs.jpcc.5b11456.

[12] K.R. Millington, M.J. Osmond, M.J. McCall, Detecting free radicals in sunscreens exposed to UVA radiation using chemiluminescence, J. Photochem. Photobiol. B 133 (2014) 27–38, DOI: 10.1016/j.jphotobiol.2014.02.018.

[13] J. Pasquet, Y. Chevalier, E. Couval, D. Bouvier, G. Noizet, C. Morlière, M.A. Bolzinger, Antimicrobial activity of zinc oxide particles on five micro-organisms of the Challenge Tests related to their physicochemical properties, Int. J. Pharm. 460 (2014) 92–100, DOI: 10.1016/j.ijpharm.2013.10.031.

[14] J. Pasquet, Y. Chevalier, E. Couval, D. Bouvier, M.A. Bolzinger, Zinc oxide as a new antimicrobial preservative of topical products: Interactions with common formulation ingredients, Int. J. Pharm. 479 (2015) 88–95, DOI: 10.1016/j.ijpharm.2014.12.031.

[15] Commission Regulation (EU) 2016/621 of 21 April 2016 amending Annex VI to Regulation (EC) Nº 1223/2009 of the European Parliament and of the Council on cosmetic products, Official Journal of the European Union, L106 (22 April 2016) 4–6.

[16] Commission Regulation (EU) 2016/1143 of 13 July 2016 amending Annex VI to Regulation (EC) N° 1223/2009 of the European Parliament and of the Council on cosmetic products, Official Journal of the European Union, L189 (14 July 2016) 40–43.

[17] Commission Regulation (EU) 2019/1857 of 6 November 2019 amending Annex VI to Regulation (EC) Nº 1223/2009 of the European Parliament and of the Council on cosmetic products, Official Journal of the European Union, L286 (07 November 2019) 3–6.

[18] P.J. Lu, S.W. Fang, W.L. Cheng, S.C. Huang, M.C. Huang, H.F. Cheng, Characterization of titanium dioxide and zinc oxide nanoparticles in sunscreen powder by comparing different measurement methods, J. Food Drug Anal. 26 (2018) 1192–1200, DOI:10.1016/j.jfda.2018.01.010.

[19] I. de la Calle, M. Menta, M. Klein, B. Maxit, F. Séby, Towards routine analysis of TiO_2 (nano-)particle size in consumer products: Evaluation of potential techniques, Spectrochim. Acta Part B 147 (2018) 28–42, DOI: 10.1016/j.sab.2018.05.012.

[20] A. Philippe, J. Košík, A. Welle, J.M. Guigner, O. Clemens, G.E. Schaumann, Extraction and characterization methods for titanium dioxide nanoparticles from commercialized sunscreens, Environ. Sci. Nano 5 (2018) 191–202, DOI: 10.1039/C7EN00677B.

[21] M. Velimirovic, S. Wagner, F.A. Monikh, T. Uusimäki, R. Kaegi, T. Hofmann, F. von der Kammer, Accurate quantification of TiO_2 nanoparticles in commercial sunscreens using standard materials and orthogonal particle sizing methods for verification, Talanta 215 (2020) 120921, DOI: 10.1016/j.talanta.2020.120921.

[22] I. López-Heras, Y. Madrid, C. Cámara, Prospects and difficulties in TiO_2 nanoparticles analysis in cosmetic and food products using asymmetrical flow field-flow fractionation hyphenated to inductively coupled plasma mass spectrometry, Talanta 124 (2014) 71–78, DOI: 10.1016/j.talanta.2014.02.029.

[23] V. Nischwitz, H. Goenaga-Infante, Improved sample preparation and quality control for the characterisation of titanium dioxide nanoparticles in sunscreens using flow field-flow fractionation on-line with inductively coupled plasma mass spectrometry, J. Anal. At. Spectrom. 27 (2012) 1084–1092, DOI: 10.1039/C2JA10387G.

[24] A. Samontha, J. Shiowatana, A. Siripinyanond, Particle size characterization of titanium dioxide in sunscreen products using sedimentation field-flow fractionation–inductively coupled plasma–mass spectrometry, Anal. Bioanal. Chem. 399 (2011) 973–978, DOI: 10.1007/s00216-010-4298-z.

[25] F. Laborda, E. Bolea, J. Jiménez-Lamana, Single Particle Inductively Coupled Plasma Mass Spectrometry: A Powerful Tool for Nanoanalysis, Anal. Chem. 86 (2014) 2270–2278, DOI: 10.1021/ac402980q.

[26] B. Meermann, V. Nischwitz, ICP-MS for the analysis at the nanoscale–a tutorial review, J. Anal. At. Spectrom. 33 (2018) 1432–1468, DOI: 10.1039/C8JA00037A.

[27] L. Fréchette-Viens, M. Hadioui, K.J. Wilkinson, Quantification of ZnO nanoparticles and other Zn containing colloids in natural waters using a high sensitivity single particle ICP-MS, Talanta 200 (2019) 156–162, DOI: 10.1016/j.talanta.2019.03.041.

[28] A.R. Donovan, C.D. Adams, Y. Ma, C. Stephan, T. Eichholz, H. Shi, Detection of zinc oxide and cerium dioxide nanoparticles during drinking water treatment by rapid single particle ICP-MS methods, Anal. Bioanal. Chem. 408 (2016) 5137–5145, DOI: 10.1007/s00216-016-9432-0.

[29] A.R. Donovan, C.D. Adams, Y. Ma, C. Stephan, T. Eichholz, H. Shi, Fate of nanoparticles during alum and ferric coagulation monitored using single particle ICP-MS, Chemosphere 195 (2018) 531–541, DOI: 10.1016/j.chemosphere.2017.12.116.

[30] J. Vidmar, R. Milačič, J. Ščančar, Sizing and simultaneous quantification of nanoscale titanium dioxide and a dissolved titanium form by single particle inductively coupled plasma mass spectrometry, Microchem. J. 132 (2017) 391–400, DOI: 10.1016/j.microc.2017.02.030.

[31] A.K. Venkatesan, R.B. Reed, S. Lee, X. Bi, D. Hanigan, Y. Yang, J.F. Ranville, P. Herckes, P. Westerhoff, Detection and Sizing of Ti-Containing Particles in Recreational Waters Using Single Particle ICP-MS, Bull. Environ. Contam. Toxicol. 100 (2018) 120–126, DOI: 10.1007/s00128-017-2216-1.

[32] J. Wojcieszek, J. Jiménez-Lamana, K. Bierla, M. Asztemborska, L. Ruzik, M. Jarosz, J. Szpunar, Elucidation of the fate of zinc in model plants using single particle ICP-MS and ESI tandem MS, J. Anal. At. Spectrom. 34 (2019) 683–693, DOI: 10.1039/C8JA00390D.

[33] I. de la Calle, M. Menta, M. Klein, F. Séby, Screening of TiO_2 and Au nanoparticles in cosmetics and determination of elemental impurities by multiple techniques (DLS, SPICP-MS, ICP-MS and ICP-OES), Talanta 171 (2017) 291–306, DOI: 10.1016/j.talanta.2017.05.002.

[34] Y. Dan, H. Shi, C. Stephan, X. Liang, Rapid analysis of titanium dioxide nanoparticles in sunscreens using single particle inductively coupled plasma–mass spectrometry, Microchem. J. 122 (2015) 119–126, DOI: 10.1016/j.microc.2015.04.018.

[35] B. Gomez-Gomez, M.T. Perez-Corona, Y. Madrid, Using single-particle ICP-MS for unravelling the effect of type of food on the physicochemical properties and gastrointestinal stability of ZnONPs released from packaging materials, Anal. Chim. Acta 1100 (2020) 12–21, DOI: 10.1016/j.aca.2019.11.063.

[36] I. de la Calle, M. Menta, M. Klein, F. Séby, Study of the presence of micro- and nanoparticles in drinks and foods by multiple analytical techniques, Food Chem. 266 (2018) 133–145, DOI: 10.1016/j.foodchem.2018.05.107.

[37] S. Candás-Zapico, D.J. Kutscher, M. Montes-Bayón, J. Bettmer, Single particle analysis of TiO_2 in candy products using triple quadrupole ICP-MS, Talanta 180 (2018) 309–315, DOI: 10.1016/j.talanta.2017.12.041.

[38] A. Mackevica, M.E. Olsson, S.F. Hansen, Quantitative characterization of TiO_2 nanoparticle release from textiles by conventional and single particle ICP-MS, J. Nanopart. Res. 20 (2018) 6, DOI: 10.1007/s11051-017-4113-2.

[39] H.E. Pace, N.J. Rogers, C. Jarolimek, V.A. Coleman, C.P. Higgins, J.F. Ranville, Determining Transport Efficiency for the Purpose of Counting and Sizing Nanoparticles via Single Particle Inductively Coupled Plasma Mass Spectrometry, Anal. Chem. 83 (2011) 9361–9369, DOI: 10.1021/ac201952t.

[40] T.W. May, R.H. Wiedmeyer, A Table of Polyatomic Interferences in ICP-MS, At. Spectrosc. 19 (1998) 150–155.

[41] International Union Of Pure and Applied Chemistry (IUPAC), Isotopic compositions of the elements 1989, Pure Appl. Chem. 63 (1991) 991–1002, DOI: 10.1351/pac199163070991.

[42] C. Suárez-Oubiña, P. Herbello-Hermelo, P. Bermejo-Barrera, A. Moreda-Piñeiro, Single-particle inductively coupled plasma mass spectrometry using ammonia reaction gas as a reliable and free-interference determination of metallic nanoparticles, Talanta 242 (2022) 123286, DOI: 10.1016/j.talanta.2022.123286.

[43] C. Suárez-Oubiña, P. Herbello-Hermelo, P. Bermejo-Barrera, A. Moreda-Piñeiro, Exploiting dynamic reaction cell technology for removal of spectral interferences in the assessment of Ag, Cu, Ti, and Zn by inductively coupled plasma mass spectrometry, Spectrochim. Acta B 187 (2022) 106330, DOI: 10.1016/j.sab.2021.106330.

[44] L. Fu, S. Shi, X. Chen, H. Xie, Analysis of impurity elements in high purity cobalt powder by inductively coupled plasma tandem mass spectrometry, Microchem. J. 139 (2018) 236–241, DOI: 10.1016/j.microc.2018.03.002.

[45] C. Walkner, R. Gratzer, T. Meisel, S.N.H. Bokhari, Multi-element analysis of crude oils using ICP-QQQ-MS, Org. Geochem. 103 (2017) 22–30, DOI: 10.1016/j.orggeochem.2016.10.009.

[46] V. Sogne, F. Meier, T. Klein, C. Contado, Investigation of zinc oxide particles in cosmetic products by means of centrifugal and asymmetrical flow field-flow fractionation, J. Chromatogr. A 1515 (2017) 196–208, DOI: 10.1016/j.chroma.2017.07.098.

[47] C. Contado, A. Pagnoni, TiO_2 in Commercial Sunscreen Lotion: Flow Field-Flow Fractionation and ICP-AES Together for Size Analysis, Anal. Chem. 80 (2008) 7594–7608, DOI: 10.1021/ac8012626.

[48] S. Lee, X. Bi, R.B. Reed, J.F. Ranville, P. Herckes, P. Westerhoff, Nanoparticle Size Detection Limits by Single Particle ICP-MS for 40 Elements, Environ. Sci. Technol. 48 (2014) 10291–10300, DOI: 10.1021/es502422v.

CHAPTER 5. spICP-MS CHARACTERISATION OF SILVER NANOPARTICLES RELEASED FROM TEXTILE PRODUCTS

CHAPTER 5. spICP-MS CHARACTERISATION OF SILVER NANOPARTICLES RELEASED FROM TEXTILE PRODUCTS

5.1 ABSTRACT

The low detection limits and information regarding the concentration and size distribution of nanoparticles provided by single particle inductively coupled plasma mass spectrometry (100 µs dwell time) has been useful for assessing silver nanoparticles in textiles (nanosilver textiles). Silver nanoparticles have been first extracted with ultrapure water (10 mL) under orbital-horizontal shaking (100 rpm, 20°C) for 30 min. Silver nanoparticles have been found to be stable (silver nanoparticle concentration and size distribution) under optimised extraction conditions. The developed method has shown excellent analytical performance. The limit of quantification for silver nanoparticles concentration was set at 1.53×10^5 silver nanoparticles per gram of textile and the limit of detection in size at 12 nm. The repeatability of the overall procedure was 14% (silver nanoparticles concentration) and 6% (mean silver nanoparticle size). Similarly, analytical recovery assays using standard silver nanoparticles of 20, 40, and 60 nm led to recoveries within the 102–113% range. The method has finally been applied to several nanosilver textile products commercialised in local stores and in the electronic market.
In addition, the application of consecutive extraction cycles to assess the silver release pattern from nanosilver fabrics has also been evaluated.

5.2 INTRODUCTION

Silver species such as metallic silver, silver sulfadiazine, and silver nitrate have been used since centuries for treating bacterial infections, wounds, and burns [1]. Similarly, silver nanoparticles (AgNPs) also exhibit antibacterial activity, and they are widely used as an alternative to antibiotics [2]. AgNPs also have antifungal [3] and antiviral [4] properties, which make them useful in several industrial sectors such as medicine or agriculture.
AgNPs are promising compounds used in the medical industry for manufacturing wound dressings for ulcers and burns, bone cement, catheters, hand gels, and surgical drains [5] due to their antibacterial properties. Furthermore, AgNPs are also useful in anticancer treatments [6] and as contrast agents [7].
In addition, AgNPs are used in water filtration [8], food packaging [9], cosmetics [10], appliances [11], paints [12], and textiles [13] because of their bacterial inhibition. On the other hand, AgNPs also offer excellent properties for catalysis [14] and can be useful in the fabrication of electronic devices [15].
Regarding the textile industry, fibres are modified with AgNPs mainly to obtain fabrics with antibacterial properties [16,17]. Humidity, appropriate temperature, sweat, skin dead cells, and finishing agents of textiles enhance bacterial growth on the textile surface [18]. Bacteria can discolour fibres, generate bad odour, and even deteriorate textiles [19]. The growth of bacteria in textiles can also be a risk to human health due to their possible propagation between textile products and human skin. This risk is minimised by textile modification with AgNPs. Furthermore, AgNPs can be used to dye fibres such as wool [20], cotton [21], silk [22], and viscose [23] based on AgNPs localised surface plasmon resonance (LSPR). The colour of

fabrics is dependent on the shape and size of AgNPs. Thus, AgNPs can replace synthetic azo dyes (carcinogenic agents) which are the most used dyes in the textile industry [24].
Several immobilisation procedures by chemical modification of textiles with AgNPs have been described, mainly grouped as *ex situ* and *in situ* treatments. *Ex situ* treatments imply the textile to be soaked in an AgNPs suspension; whereas, *in situ* approaches require a first silver salt integration in the textile yarns and a further *in situ* formation of AgNPs using a reducing agent. In both cases, stabilising agents are used to prevent AgNPs aggregation [25].
The main drawback of textile modification with AgNPs is the lack of stability of the nanoparticles in the fibres, so AgNPs are released during fabric washing. Certain organic polymers, used as linkers between AgNPs and the fibre surface, have been proposed to enhance AgNPs durability in textile products [19].
AgNPs could be a serious risk to humans due to the possible penetration of these particles through the skin. Kraelinga et al. [26] performed *in vitro* experiments to test the penetration of coated AgNPs into human skin. These authors have concluded that less than 10% of the silver dose can be absorbed by the skin, and this small amount was located mostly in the *stratum corneum* of the epidermis, which is responsible for the protective function of the skin. However, detectable concentrations were also found in the deepest layers of skin (dermis). In addition, some *in vitro* findings suggest that AgNPs penetration into human damaged skin is higher than into healthy skin [27].
Research regarding the presence AgNPs on textiles is therefore needed. The available analytical methodology is scarce and the literature deals with experiments that simulate the AgNPs lixiviation from textiles during home laundering [28–33]. Electron microscopy coupled to energy-dispersive X-ray spectroscopy (EDX) was used in several published studies for analysing the washing solutions of fabrics (AgNPs determination/characterisation) [28,29,33]. On the other hand, total silver released from textile products was assessed by inductively coupled plasma mass spectrometry (ICP-MS) or inductively coupled plasma optical emission spectrometry (ICP-OES) after acid digestion of washing solutions or washed textiles [28–33]. Furthermore, X-ray absorption near edge structure spectroscopy (XANES) was used for the direct analysis of textile solid samples (unwashed and/or washed) [30,33]. Recently, ICP-MS operating in the so-called ‘single particle’ mode (spICP-MS) has also been used by Mitrano et al. [33] for AgNPs assessment in the simulated laundry washing wastes.
The aim of the current work has been the development of reliable analytical procedures for the assessment of AgNPs released from fabrics (extraction and characterisation). Sample pre-treatment strategies based on mechanical lixiviation have been investigated for AgNPs isolation from textiles; whereas, spICP-MS has been used for providing information about AgNPs concentration and size distribution.

5.3 MATERIALS AND METHODS

5.3.1 Instrumentation

A NexION® 300X ICP-MS (Perkin Elmer, Waltham, MA, USA) with a nebulisation system composed of a Meinhard® nebuliser and a cyclonic spray chamber thermostated by a Peltier refrigerator was used to analyse digested fabrics (total Ag content) and determine/characterise AgNPs in the aqueous extracts. A SeaFast SC2 DX autosampler (Elemental Scientific, Omaha, NB, USA) was used to introduce digested samples in the ICP-MS when assessing total Ag contents. A Syngistix™ Nano Application software version 1.1 was used to perform AgNPs determination (concentration and size distribution). A HRTEM Zeiss Libra 200FE (Oberkochen, Germany) coupled to EDX spectroscopy was used for the

characterisation of AgNPs in aqueous extracts from fabrics for comparative purposes. An analytical balance ML 204T (Mettler Toledo, Colombus, OH, USA) was used for weighing reagents and samples. A Boxcult temperature-controlled incubation chamber (Stuart Scientific, Surrey, UK) equipped with a Rotabit orbital-rocking platform shaker (J.P. Selecta, Barcelona, Spain) was used to carry out the mechanical extraction of AgNPs. A VibraCell VCx 130 ultrasound probe from Sonics (Newtown, CT, USA) was used to assist AgNPs extraction from textiles. A Laborcentrifugen 2K15 centrifuge (Sigma, Osterode, Germany) was used for the removal of fluffs in textile aqueous extracts. A Raypa UCI-150 Ultrasonic Cleaner (R. Espinar S.L, Barcelona, Spain) with programmable temperature and time was used to sonicate the extracts and avoid AgNPs agglomeration. An ETHOS PLUS microwave lab-station (Milestone, Sorisole, Italy) with 100 mL closed Teflon vessels and Teflon covers was used to perform acid digestion of textile samples.

5.3.2 Reagents

Ultrapure water (18 MΩcm resistivity) was obtained from a Milli-Q® water purification system (Millipore, Bedford, MA, USA). 37% hydrochloric acid, 69% Hiperpur nitric acid, 33% hydrogen peroxide, and ethanol were from Panreac (Barcelona, Spain). 48% hydrofluoric acid was supplied by BDH (Poole, United Kingdom). Glycerol (99.5%), D-lactose monohydrate (99.5%), and 1-butyl-3-methylimidazolium bromide (BMIMBr)>97% were purchased from Sigma Aldrich (San Louis, MO, USA). NexIon Setup Solution (10 μg L^{-1} of U, Pb, Mg, Li, In, Fe, Ce, and Be in 1% HNO_3) was from Perkin Elmer. Silver (1000 mg L^{-1} in 0.5 M HNO_3) and rhodium (1000 mg L^{-1} in 5% HNO_3) stock standard solutions were supplied by Merck (Darmstadt, Germany). 0.02 g L^{-1}AgNPs standards (aqueous suspensions with sodium citrate as a stabiliser) of 60 nm, 40 nm, and 20 nm were purchased from Sigma-Aldrich and NanoComposix (San Diego, CA, USA). The reference material RM 8013 of gold nanoparticles (aqueous suspension with citrate as a stabiliser) of 60 nm nominal diameter was supplied by National Institute of Standards and Technology (Gaithersburg, MD, USA). Other consumables were cellulose acetate 0.22 μm and 0.45 μm syringe filters (Labbox Labware S.L., Barcelona, Spain), Minisart® NML surfactant-free cellulose acetate 5 μm syringe filters (Sartorius, Goettingen, Germany), and 10 mL sterile disposable syringes (Dispomed, Gelnhausen, Germany).

5.3.3 Textile samples

Samples analysed in the current study consisted of T-shirts (two samples), socks (three samples), underwear (one sample), and sportswear (one sample), as shown in **Table 5.1**. Textiles coded as T1 (men´s cycling culotte) and T3 (socks) were bought in local stores in Santiago de Compostela (Spain); whereas, the remaining textiles were purchased in the online market. According to the manufacturer's specifications, studied textiles contain silver (**Table 5.1**). A visual examination of textiles showed that two of them (T1 and T6) were made of fibres with different appearances. In these cases, fabrics were divided into several subsamples (**Table 5.1**). Each textile subsample was cut into small pieces (5×5 mm) with ceramic scissors, and textile pieces were kept in plastic bags at room temperature and protected from light.

Table 5.1. Brief description of analysed textiles

Sample	Subsamples	Type	Composition
T1	T1-1 T1-2	Cycling sportswear	82% polyester, 18% elastane (product containing **silver**)
T2	-	Socks	80% cotton, 13% polyamide, 5% **silver**, 2% elastane
T3	-	Socks	66% polyamide, 24% elastane, 10% polyamide with **silver**
T4	-	Men's T-shirt	100% polyester with **silver**
T5	-	Men´s T-shirt	52% Coolmax® (polyester), 44% **Nanosilver®** (polyester), 4% Lycra® (elastane)
T6	T6-1 T6-2	Socks	55% cotton, 30% **Nanosilver®** (polyester), 15% Lycra® (elastane)
T7	-	Men´s underwear	60% cotton, 32% **Nanosilver®** (polyester), 8% Lycra® (elastane)

- Only one subsample

5.3.4 Microwave-assisted acid digestion of textile samples

Clothing pieces (0.2000g) were placed into PTFE digestion vessels, and 8.0 mL of 69% nitric acid, 0.5 mL of 37% hydrochloric acid, 0.5 mL of 33% hydrogen peroxide, and 1.0 mL of 48% hydrofluoric acid were added. Each vessel was closed and subjected to microwave irradiation (using the microwave temperature program shown in **Table 5.2**). The digestion procedure was performed in triplicate for each sample (or subsamples according to **Table 5.1**), and at least one blank was prepared in each digestion set. Finally, acid digests were diluted to 25 mL with ultrapure water and kept in polyethylene sealed bottles at room temperature.

Table 5.2. Microwave temperature program for acid digestion of textiles

Time (min)	Temperature (°C)
0 - 2	Room temperature - 150
2 - 7	150
7 - 9	150 - 170
9 - 19	170
19 - 20	170 - 200
20 - 40	200

5.3.5 Total Ag determination by ICP-MS

Acid digests from textiles were diluted with ultrapure water before their ICP-MS analysis. The adjustment of the ICP-MS parameters (nebulisation gas flow, torch position, optical lens, and quadrupole voltages) was daily performed. The *m/z* ratio monitored was ^{107}Ag, and ^{103}Rh (10 μg L^{-1}) was used as an internal standard. The addition standard calibration (0–100 μg L^{-1} range) was used to make up for matrix effects. Polyatomic interferences were reduced by introducing a helium flux (1.0 mL min^{-1}) in the collision cell. All operating conditions used for ICP-MS assessment are listed in **Table 5.3**. The limit of detection (LOD) and the limit of quantification (LOQ) were calculated by the $3\sigma/m$ and $10\sigma/m$ criteria, respectively, where σ is the standard deviation of eleven measurements of a blank and m is the slope of the standard addition calibration. LOD and LOQ values of 0.0063 and 0.0208 μgAg g^{-1} were obtained, respectively.

Table 5.3. ICP-MS and spICP-MS instrumental parameters for total silver and AgNPs determination

ICP-MS operating conditions for total Ag assessment	
Plasma gas flow (L min^{-1})	16
Auxiliary gas flow (L min^{-1})	1.2
Nebulisation gas flow (L min^{-1})	0.9 – 1.1
Radiofrequency power (W)	1600
Collision gas (He) cell (mL min^{-1})	1.0
Analyte	Ag (*m/z* 106.905)
Internal standard	Rh (*m/z* 102.906)
spICP-MS operating conditions and SYNGISTIX™ NANO application parameters for AgNPs assessment	
Plasma gas flow (L min^{-1})	16
Auxiliary gas flow (L min^{-1})	1.2
Nebulisation gas flow (L min^{-1})	0.85 – 0.90
Radiofrequency power (W)	1600
Sample flow rate (mL min^{-1})	0.40 – 0.45
Analyte	Ag (*m/z* 106.905)
Mode	Standard
Density (g cm^{-3})	10.49
Mass fraction (%)	100
Ionisation efficiency (%)	100
Dwell time (µs)	100
Sampling time (s)	100
Number of scanning	1
Number of readings	1000000

5.3.6 AgNPs isolation from textiles

AgNPs isolation from textiles was performed by mixing 0.4000 g of textile pieces with 10 mL of ultrapure water into a plastic tube, followed by mechanical extraction at controlled temperature (20°C) for 30 min at 100 revolutions per minute (rpm) orbital-horizontal shaking. The procedure was carried out in triplicate for each sample, and two blanks were performed at least for each extraction condition. Several aqueous extracts required their dilution prior to their measurement by spICP-MS. Extracts were sonicated for 1 min before their dilution and analysis to avoid AgNPs agglomeration.

Furthermore, consecutive extractions from one studied fabric were performed to evaluate the AgNPs release pattern from textiles. Therefore, 0.4000 g of textile T5 was subjected to six extraction cycles using the optimised extraction conditions (10 mL of water, 30 min, 20°C, and 100 rpm). The extracts were filtered (5 µm filter) and analysed by spICP-MS.

5.3.7 AgNPs determination/characterisation by spICP-MS

Aqueous extracts containing AgNPs were analysed by spICP-MS. AgNPs extracts were sonicated for 5 min at 35 kHz before their dilution and measurement to avoid nanoparticle agglomeration. ICP-MS adjustment and the assessment of sample introduction flow rate were daily performed. Transport efficiency (TE%) determination (particle frequency method described by Pace et al. [34]) by using AuNPs aqueous suspension (particle concentration of

518 ng L^{-1} and 60 nm nominal diameter) was also daily carried out before spICP-MS (Syngistix™ Nano Application software). Obtained TE% values were close to 5%. An ionic silver aqueous calibration (0–5 µg L^{-1}) was performed for the AgNPs particle size distribution assessment; whereas, the NPs concentration was calculated by the frequency of NPs events [34,35]. **Table 5.3** shows spICP-MS instrumental conditions used for AgNPs determination.

5.3.8 AgNPs determination/characterisation by HRTEM-EDX

An aqueous extract from fabric T6-1 (only one extraction cycle, 20°C, 30 min, and 100 rpm) was also analysed by high resolution transmission electron microscopy coupled to energy-dispersive X-ray spectroscopy (HRTEM-EDX) for comparative purposes. Due to the limit of detection of HRTEM-EDX (mg L^{-1}), a preliminary sample preconcentration step was therefore required. Preconcentration (and also clean-up) of the aqueous extract was carried out using an Amicon® Ultra-0.5 centrifugal filter device. 500 µL aliquot of the aqueous extract (textile T6-1) was introduced in an Amicon device and ultracentrifuged at 14,000 g and 4°C for 20 min, which led an extract volume of approximately 17 µL. The pre-concentrated extracts were further cleaned by adding 500 µL of ultrapure water to the filter and performing a new ultracentrifugation step (14,000 g, 4°C, and 20 min). This cleaning step with water was repeated five times. The final cleaning step was performed using the same ultracentrifugation rate and temperature, but for 10 min to allow the collection of a sample´s volume of approximately 23 µL. After the cleaning steps, the filter device was placed upside down in a clean microcentrifuge tube, and centrifugation at 1,000 g for 2 min was performed to transfer the concentrated and clean extract from the filter device to the collecting tube prior to analysis by HRTEM-EDX.

5.4 RESULTS

5.4.1 Preliminary studies: Selection of the extraction solvent and the extraction technique

Studies on the release of nanoparticles from fabrics have focused on the simulation of home laundering as a way to assess the possible presence of nanomaterials in wastewaters and thus in the environment. Nevertheless, changes in the speciation of silver species released during textile washing procedure with detergents were proved by several authors. Mitrano et al. [28] demonstrated that AgNPs were formed after the addition of an $AgNO_3$ standard into the washing solution used. AgNPs were also formed as a consequence of the laboratory washing procedure in the study carried out by Lombi et al. [30]. In addition, characterisation studies by electron microscopy coupled to EDX confirmed the formation of silver chloride nanoparticles (AgClNPs) and/or silver sulphide nanoparticles (Ag_2SNPs) [28,29] in washing solutions containing detergents. XANES analysis of fabrics also proved the formation of AgClNPs and/or Ag_2SNPs on the textile surface of washed fabrics [30,33].

Furthermore, detergents with oxidising agents induced damage to AgNPs, size distribution alterations, and dissolution of AgNPs [33,36]. So, detergents were not considered in our study due to the numerous modifications or damages they can cause to AgNPs integrity.

Solvents such as water, and aqueous solutions of glycerol, lactose, and BMIMBr (1.0% w/v) were therefore evaluated as potential extractants. Few articles used water as an extractant of metallic NPs from fabrics [32,37–40]. The remaining solvents were selected due to several published articles demonstrated that ionic liquids, poly-alcohols, and carbohydrates are stabilising agents of NPs, which can prevent their agglomeration [41–43].

Ultrasonication (60% of amplitude and continuous mode for 15 min) was used for assisting the extraction (0.4000 g of textile and 10 mL of solvent) before spICP-MS assessment. Test

tubes were placed into an ice bath during extraction to avoid sample´s heating which could damage AgNPs. Number concentrations of AgNPs extracted are shown in **Figure 5.1a** for experiments in triplicate and after subtracting values derived from solvent blanks analysis. Results (**Figure 5.1b**) showed that extracted AgNPs in BMIMBr exhibited larger size distribution than those observed for the other tested solvents, which implies that BMIMBr enhanced AgNPs agglomeration. Water, glycerol, and lactose solutions led to AgNPs size distributions in which the average size and the most frequent size were quite similar. In addition, as shown in **Figure 5.1a**, higher extraction efficiencies (higher AgNPs concentration) have been obtained when using water as an extracting solution. However, high relative standard deviations (within the 16–44% range) have been found when assessing AgNPs concentrations with all extracting solutions. This may occur as a consequence of the wrapping of textile pieces around the tip of the ultrasonic probe, which hindered the extraction and even could damage the tip.

Extraction assistance by mechanical shaking was therefore tested and compared with ultrasonication assistance in order to improve repeatability (n=3). Ultrasonication conditions were the same as those used in the first experiments, and mechanical shaking consisted of orbital-horizontal shaking at 190 rpm and room temperature for 12 h (0.4000 g of textile and 10 mL of solvent). Aqueous extracts and blanks were measured in triplicate by spICP-MS. AgNPs concentration, expressed as number of AgNPs per gram, was found to be higher when applying mechanical shaking (10 times higher as shown in **Figure 5.1c**). **Figure 5.1d** shows that nanoparticle size distributions were similar. Mechanical shaking under controlled temperature using water as an extractant has been therefore selected for further experiments.

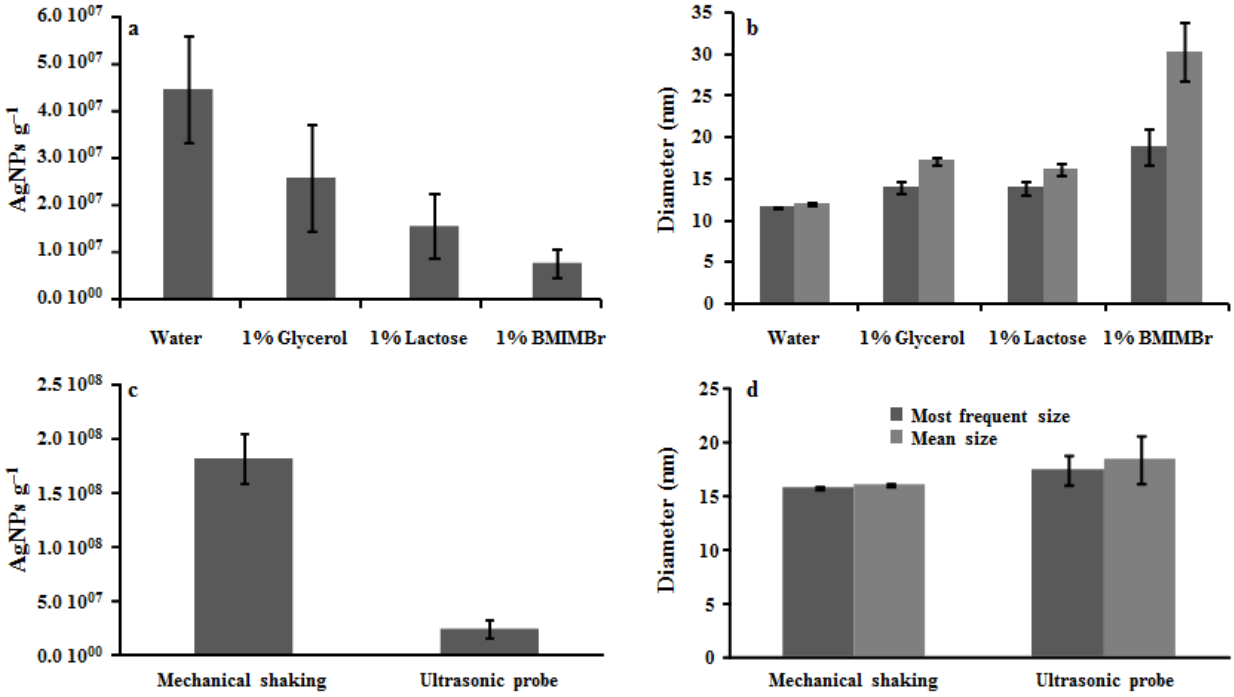

Figure 5.1. Effect of the extraction solvent (continuous ultrasound extraction at 60% amplitude for 15 min) on AgNPs concentration (a) and size distribution (b); and effect of ultrasound assistance (water as a solvent, continuous ultrasound extraction at 60% amplitude for 15 min) and mechanical shaking (water as a solvent, shaking speed at 190 rpm for 12 h) on AgNPs concentration (c) and size distribution (d)

5.4.2 Mechanical shaking parameters

Parameters such as shaking time, temperature, and shaking speed were optimised. All extraction sets were performed in triplicate using 0.4000g of a textile sample coded as T1-1.

Two blanks were prepared for each extracting condition. Finally, the aqueous extracts were analysed in triplicate by spICP-MS.

5.4.2.1 Shaking time

Several textile subsamples were stirred using 10 mL of water at 190 rpm and room temperature for times within the range 0.5–18 h. Results (**Figure 5.2a**) show that there were re-adsorption and/or interaction of the release AgNPs with the textile pieces and other extracted compounds when using large shaking times since the highest AgNPs concentrations were achieved after extraction for short times (from 30 min to 2 h). Another possibility of this behaviour could be due to AgNPs dissolution at longer extraction times (a slight enhancement of ionic contents at longer times was observed, data not shown). AgNPs size distribution has been found to be quite similar for all extracting times (mean sizes from 22 to 26 nm) as also shown in **Figure 5.2a**. In conclusion, a shaking time of 30 min was chosen for further experiments.

5.4.2.2 Temperature

The effect of temperature on the AgNPs release was tested by fixing the extractant volume at 10 mL, the orbital-horizontal shaking speed at 190 rpm, and the time at 30 min. **Figure 5.2b** shows that temperature did not affect AgNPs release from textiles, and AgNPs concentrations were quite similar (ANOVA test, 95% confidence interval) when varying the temperature within the 20–50°C range. Similar conclusions can be attained regarding the size distribution of the extracted AgNPs, which mean sizes were quite similar under all tested temperatures. A temperature of 20°C was therefore selected for further experiments.

5.4.2.3 Shaking speed

Several orbital-horizontal shaking speeds (50, 100, 190, and 240 rpm) were evaluated by applying the selected shaking temperature and time, and using 10 mL of water as an extractant. Results (**Figure 5.2c**) show a slight increase in the extracted AgNPs at high shaking speeds (100, 190, and 240 rpm). Regarding AgNPs size distributions, mean sizes when using high shaking speed were also found to be similar, which allows the selection of 100 rpm as an adequate operating value.

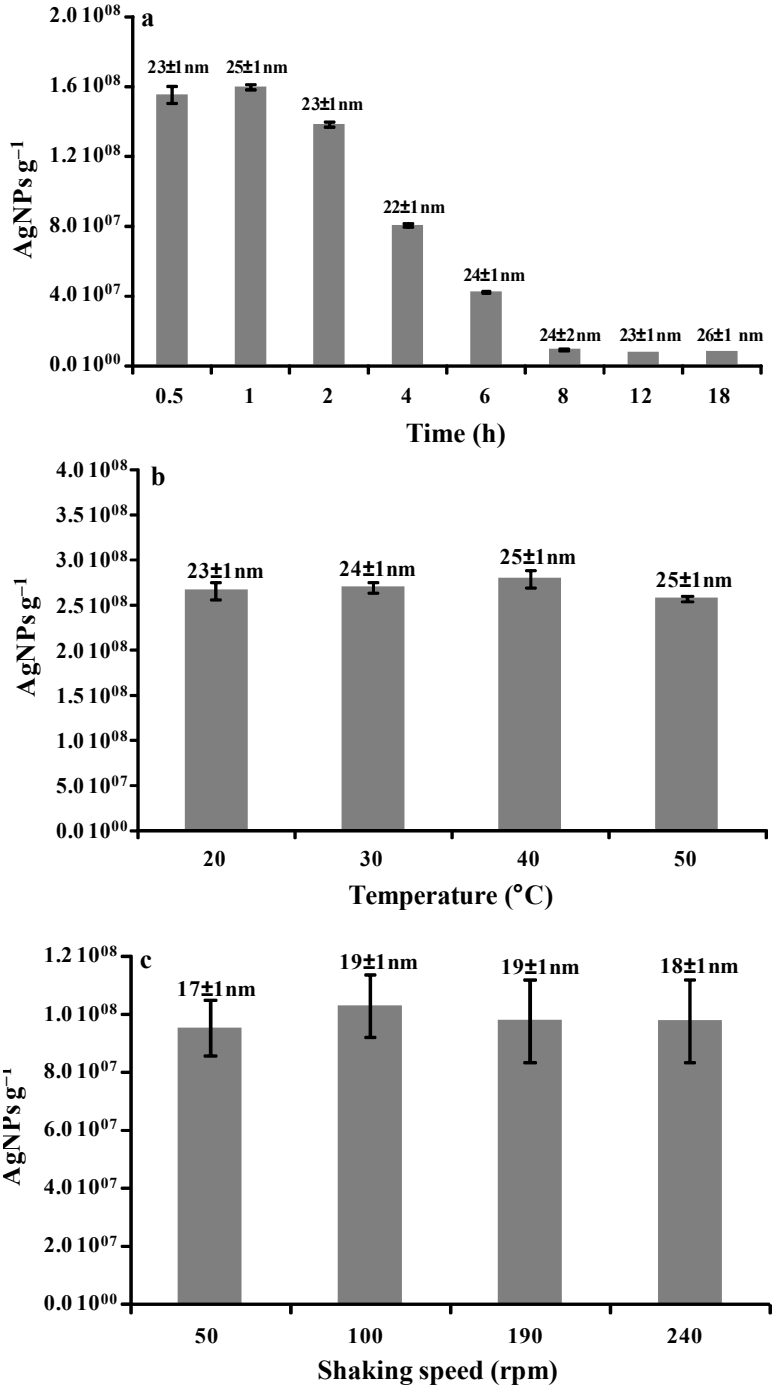

Figure 5.2. Effect of mechanical shaking time (a), temperature (b), and shaking speed (c) on the AgNPs concentration [mean sizes (AgNPs size distribution) are listed onto the top of the bars]

5.4.3. AgNPs stability studies

5.4.3.1 AgNPs stability during filtration (0.22 μm and 0.45 μm filters)

After extraction, some aqueous extracts could contain fluffs from clothing pieces, and attempts based on filtration (mixed cellulose ester syringe filters, 0.22 μm and 0.45 μm) for fluffs removal before spICP-MS were carried out. Aliquots from an aqueous extract from a textile sample (sample coded as T1-1 in **Table 5.1**), as well as AgNPs (40 and 60 nm)

standards, were directly analysed by spICP-MS (unfiltered assays), and also after filtration (0.22 and 0.45 µm). Results have shown that AgNPs are partially lost during filtration of textile aqueous extracts, mainly when using 0.22 µm syringe filters ($1.67\times10^{7}\pm7.90\times10^{5}$ AgNPs g^{-1} in comparison to $2.00\times10^{7}\pm1.47\times10^{6}$ AgNPs g^{-1} after 0.45 µm filtration, and $2.26\times10^{8}\pm5.10\times10^{6}$AgNPs g^{-1} for unfiltered extracts). Therefore, measured AgNPs concentrations were 14 (0.22 µg filters) and 11 (0.45 µm filters) times lower after filtration. Similar results were obtained when using 40 nm AgNPs standards (AgNPs concentrations were 15 and 12 times lower after 0.22 µm and 0.45 µm filtration, respectively). AgNPs loss was found to be more important for AgNPs of larger size, and experiments carried out using 60 nm AgNPs showed that the AgNPs concentrations were 47 times (0.22 µm filtration) and 37 times (0.45 µm filtration) lower than for unfiltered 60 nm AgNPs standards. The obtained results suggest that the loss of AgNPs during filtration depends on the particle size distribution. Hence, filtration using 0.22 and 0.45 µm filters for fluffs removal is not recommended.

5.4.3.2 AgNPs stability during centrifugation

Experiments based on centrifugation were tested to achieve the elimination of fluffs in textile extracts. AgNPs suspensions (20, 40, and 60 nm) were centrifuged (3900 rpm, 4°C, and 10 min) in triplicate. Untreated (control) and centrifuged AgNPs were analysed by spICP-MS (n=3). The AgNPs concentrations (n=9) obtained are shown in **Figure 5.3**. An ANOVA test (95% confidence interval) elucidated that 20 nm AgNPs concentrations were statistically significant similar [$2.61\times10^{12}\pm4.14\times10^{11}$ and $2.37\times10^{12}\pm4.02\times10^{11}$ NPs L^{-1} for control and centrifuged 20 nm AgNPs standards, respectively]. Nevertheless, there were statistically significant differences between untreated and centrifuged standards when AgNPs with larger nominal diameters were used (40 and 60 nm). The loss of AgNPs during centrifugation increased with increasing AgNPs diameter (**Figure 5.3**). Therefore, centrifugation is not advised as a methodology to remove fluffs in textile extracts.

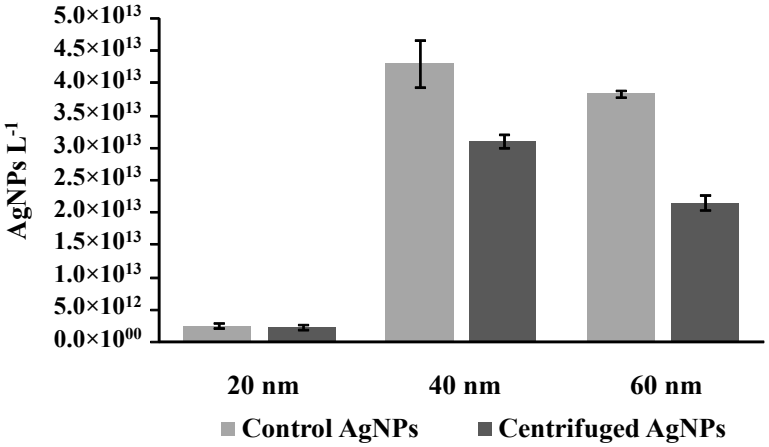

Figure 5.3. Effect of centrifugation (3900 rpm, 4°C, and 10 min) on particle concentration of AgNPs standards (Sigma-Aldrich)

5.4.3.3 AgNPs stability during shaking and filtration (5 µm filters)

Another attempt to remove fluffs was the filtration of AgNPs suspensions using syringe filters with a larger pore size (5 µm). AgNPs suspensions (20, 40, and 60 nm) were subjected in triplicate to mechanical shaking (30 min, 20°C, and 100 rpm) followed by 5 µm filtration, and spICP-MS assessment to test their stability under the whole proposed methodology. The same AgNPs standard solutions were also analysed without any treatment (control AgNPs), and the spICP-MS measurements were carried out in triplicate.

AgNPs concentrations (n=9) for treated and untreated AgNPs are shown in **Table 5.4**. Results concluded that shaking and filtration (5 µm filters) of AgNPs suspensions did not cause the loss of nanoparticles. In addition, AgNPs size distributions were not altered (the AgNPs mean sizes were 22±1, 38±1, and 60±2 nm). Hence, AgNPs were stable using the proposed extraction methodology and filtration (5 µm) of AgNPs suspensions for the removal of fluffs in aqueous extracts from textiles.

Table 5.4. Effect of mechanical shaking (30 min, 20 °C, and 100 rpm) and filtration (syringe filters with 5 µm pore size) on AgNPs concentration of 20, 40, and 60 nm AgNPs standards (NanoComposix)

	AgNPs concentration (AgNPs L^{-1})		
	20 nm	40 nm	60 nm
Control	$8.75\times10^{13} \pm 4.01\times10^{12}$	$3.98\times10^{12} \pm 6.95\times10^{10}$	$4.66\times10^{12} \pm 4.00\times10^{11}$
Shaking+filtration	$8.88\times10^{13} \pm 2.95\times10^{12}$	$4.32\times10^{12} \pm 4.58\times10^{10}$	$4.92\times10^{12} \pm 4.43\times10^{11}$

5.4.4 Validation

The limit of detection (LOD) and the limit of quantification (LOQ) of spICP-MS analysis were calculated in accordance with the $3\sigma/m$ and $10\sigma/m$ criteria, respectively, where σ is the standard deviation of the measurements of eleven blanks (10 mL of ultrapure water subjected to the optimised extraction procedure) by spICP-MS, and m is the mean slope of the ionic Ag calibration (calibration within the 0–5 µg L^{-1} range). Experimental LODs and LOQs were 4.59×10^{4} AgNPs g^{-1} and 1.53×10^{5} AgNPs g^{-1}, respectively, after considering the sample pre-treatment used.

Furthermore, the LOD in size was calculated by applying the 3σ (or 5σ) criterion outlined by Lee et al. [44]. The calculated values were 9.8 and 11.6 nm for 3σ and 5σ criteria, respectively.

The precision of the developed procedure (sample pre-treatment and spICP-MS assessment) was expressed through the relative standard deviation (RSD) after subjecting a textile sample (sample coded as T6-1) to the proposed procedure eleven times. The eleven extracts were further analysed by spICP-MS in triplicate, and the found AgNPs concentration (mean±standard deviation) was $1.91\times10^{8}\pm2.71\times10^{7}$ AgNPs g^{-1}, which implies a RSD value of 14%. Regarding AgNPs size distribution, mean size of 23±1 nm (RSD value of 6%) was obtained. Consequently, the methodology has been therefore to be precise.

The accuracy of spICP-MS measurements was tested by analytical recovery assays. Three aliquots from the same extract from a textile sample containing AgNPs were spiked with AgNPs standards of several nominal diameters (20, 40, or 60 nm). The spiked extracts as well as unspiked extracts (three replicates), and the AgNPs suspensions used for spiking (suspensions at the same AgNPs concentration as those used for spiking experiments) were measured by spICP-MS in triplicate. Therefore, the assay implied nine measurements of each solution (unspiked extracts, extracts spiked with AgNPs of different nominal sizes, and AgNPs solutions of different nominal sizes). Analytical recoveries were calculated as the ratio (×100) of the difference between the AgNPs concentrations of spiked and unspiked extracts, and the concentrations of AgNPs standards used for spiking. Results have shown good accuracy for the spICP-MS measurements because analytical recoveries were close to 100% for all AgNPs sizes (113±5, 102±6, and 106±2 for 20, 40, and 60 nm AgNPs standards, respectively).

5.4.5 Application

The proposed method was applied to seven textiles, three of them (samples coded as T5, T6, and T7) were commercialised as textiles containing nanosilver, and the remaining textiles (T1, T2, T3, and T4) as products containing silver. Subsamples (T1-2, and T6-1 and T6-2) were considered from textiles T1 (cycling sportswear) and T6 (socks) because of the different appearance of fibres. All samples were analysed for total silver (microwave-assisted acid digestion and ICP-MS measurement) and for AgNPs determinations (proposed extraction procedure followed by spICP-MS). **Table 5.5** lists the total silver concentrations determined in textile samples (microwave-assisted acid digestion and ICP-MS measurement) as well as AgNPs concentrations and ionic silver concentrations in aqueous extracts (proposed extraction procedure and spICP-MS analysis); whereas data regarding AgNPs size distribution are given in **Figures 5.4 (a-b)**. **Table 5.5** also shows the silver concentration (and the silver percentage) derived from the assessed AgNPs considering the mean AgNPs concentrations and the mean AgNPs sizes obtained. Assumptions such as the spherical shape and solid nature of all AgNPs have been considered for these theoretical calculations.

Total Ag concentrations varied from 1.3±0.1 (T7) to 10±0.4 (T5) for textiles commercialised as containing nanosilver; whereas, total Ag contents varied from 1.7±0.3 (T1-2) to 36±4 (T4) for textiles reported as containing silver.

In general, AgNPs concentrations in nanosilver textiles are slightly higher than those found in textiles commercialised as containing silver, although the latter has also shown the presence of AgNPs. Regarding size distribution [**Figures 5.4(a-b)**], mean sizes varied from 22±2 nm (T5) to 40±1 nm (T6-2), and were quite close to the most frequent size, which suggests AgNPs size distribution is nearly a normal distribution.

Silver concentrations in textiles derived from the assessed AgNPs (AgNPs concentration and size distribution, considering a spherical shape and solid nature of all AgNPs) were found to be within the 0.0210–13.2 ng g^{-1} ($ng_{silver}\ g_{fabric}^{-1}$) range [**Table 5.5**]. Percentages of nanosilver released in aqueous extracts (percentage of silver derived from extracted AgNPs referred to the total Ag concentration assessed by microwave-assisted acid digestion and ICP-MS) were therefore very low, ranging from 0.001% (T5) to 0.2% (T6-1).

Total silver released was calculated by the addition of ionic silver concentrations and nanosilver concentrations (in mass units) obtained by spICP-MS analysis. Percentage of total silver released varied between 0.3% (fabric T5) and 9% (fabric T6-1) [**Table 5.5**]. Similar results were obtained by Benn et al. [38], who reported that two studied socks released less than 1% of their total silver into water after four washing cycles (agitation at 50 rpm for 24 h). In addition, Nam et al. [40] proved that 90% of total silver remained in cotton fabrics functionalised with AgNPs after ten laundering cycles (laboratory washing machine, 40ºC, 40 rpm, and 45 min).

Furthermore, AgNPs presence in an aqueous extract (fabric T6-1) was confirmed by HRTEM images and energy-dispersive X-ray spectra shown in **Figure 5.5**. Sample T6-1 was selected for its characterisation by electron microscopy owing to it was the extract with the highest concentration of AgNPs released during one washing cycle (**Table 5.5**).

Table 5.5. Silver and AgNPs concentrations in textile products

	ICP-MS	spICP-MS [one cycle of extraction (20°C, 30 min, and 100 rpm)]				
	Total Ag concentration ($\mu g\ g^{-1}$)[a]	AgNPs concentration (NPs g^{-1})[b]	Ionic silver concentration ($\mu g\ g^{-1}$) [b]	Nano Ag concentration ($ng\ g^{-1}$)[c]	Percentage of nano Ag released (%)[d]	Percentage of total Ag released (%)[d]
T1-2	0.489 ± 0.0236	$2.54\times10^{6} \pm 1.92\times10^{5}$	0.034 ± 0.0005	0.245	0.05	7
T2	7.48 ± 0.235	$2.59\times10^{7} \pm 3.35\times10^{6}$	0.25 ± 0.04	1.77	0.02	3
T3	5.83 ± 0.0668	$<LOD_{size}$	---[e]	---[e]	---[e]	---[e]
T4	31.2 ± 1.64	$<LOD_{size}$	---[e]	---[e]	---[e]	---[e]
T5	8.31 ± 0.137	$1.28\times10^{6} \pm 1.58\times10^{5}$	0.028 ± 0.003	0.0713	0.001	0.3
T6-1	6.40 ± 0.466	$1.91\times10^{8} \pm 2.71\times10^{7}$	0.54 ± 0.05	13.2	0.2	9
T6-2	6.02 ± 0.929	$1.22\times10^{7} \pm 1.97\times10^{6}$	0.36 ± 0.05	4.31	0.1	6
T7	1.20 ± 0.171	$2.68\times10^{5} \pm 4.40\times10^{4}$	0.029 ± 0.002	0.0210	0.002	2

(a) Microwave-assisted acid digestion and ICP-MS; (b) Water extraction and spICP-MS; (c) theoretical Ag concentration of AgNPs considering AgNPs concentration and size distribution (water extraction and spICP-MS), assuming a spherical shape of AgNPs; (d) Percentages (%) were referred to total Ag concentration assessed by microwave-assisted acid digestion and ICP-MS; (e) Not assessed

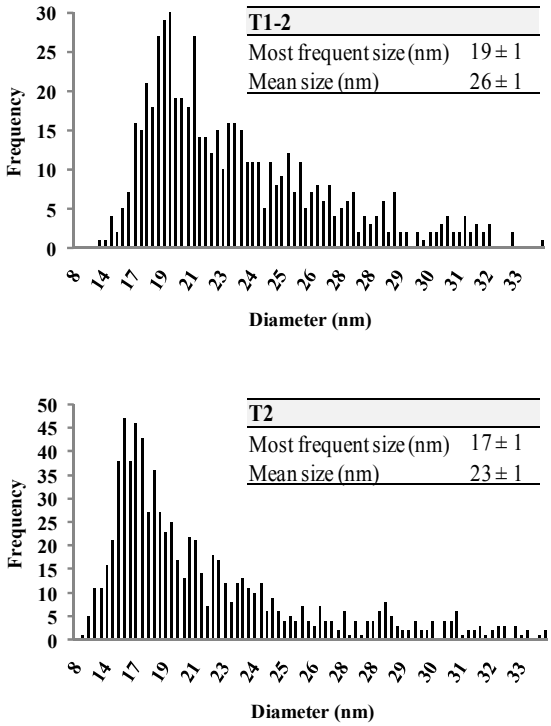

Figure 5.4 (a). Size distribution of AgNPs in textiles containing silver obtained by spICP-MS

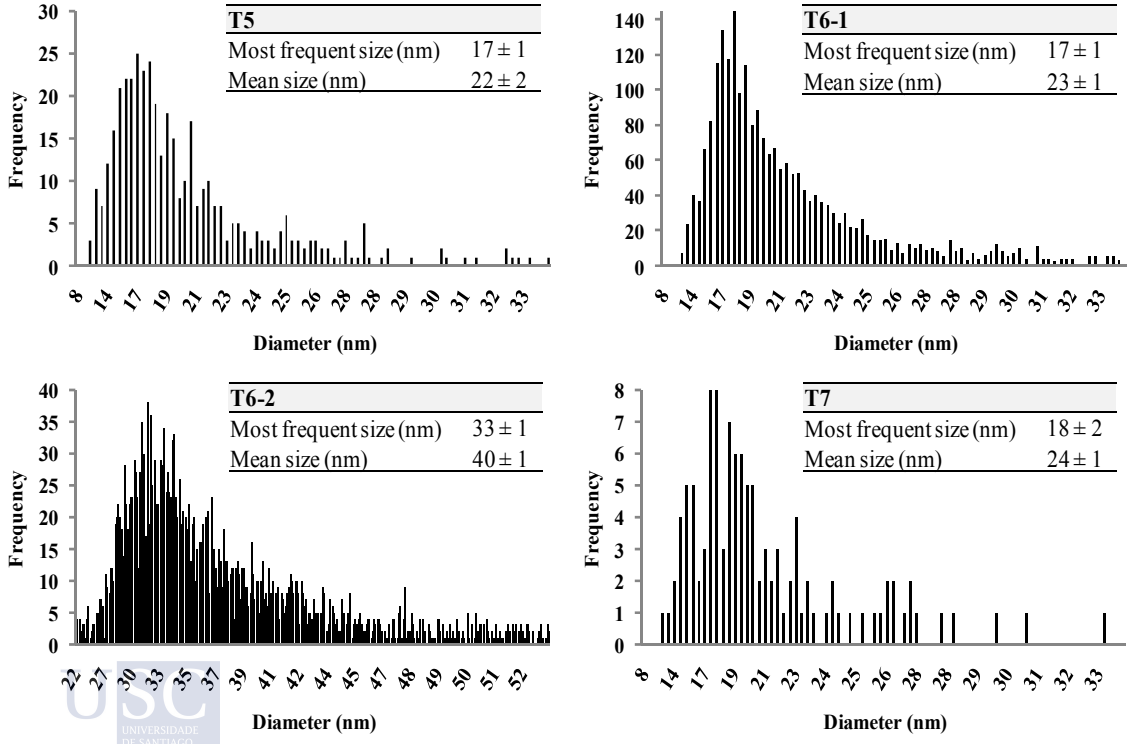

Figure 5.4 (b). Size distribution of AgNPs in textiles containing nanosilver obtained by spICP-MS

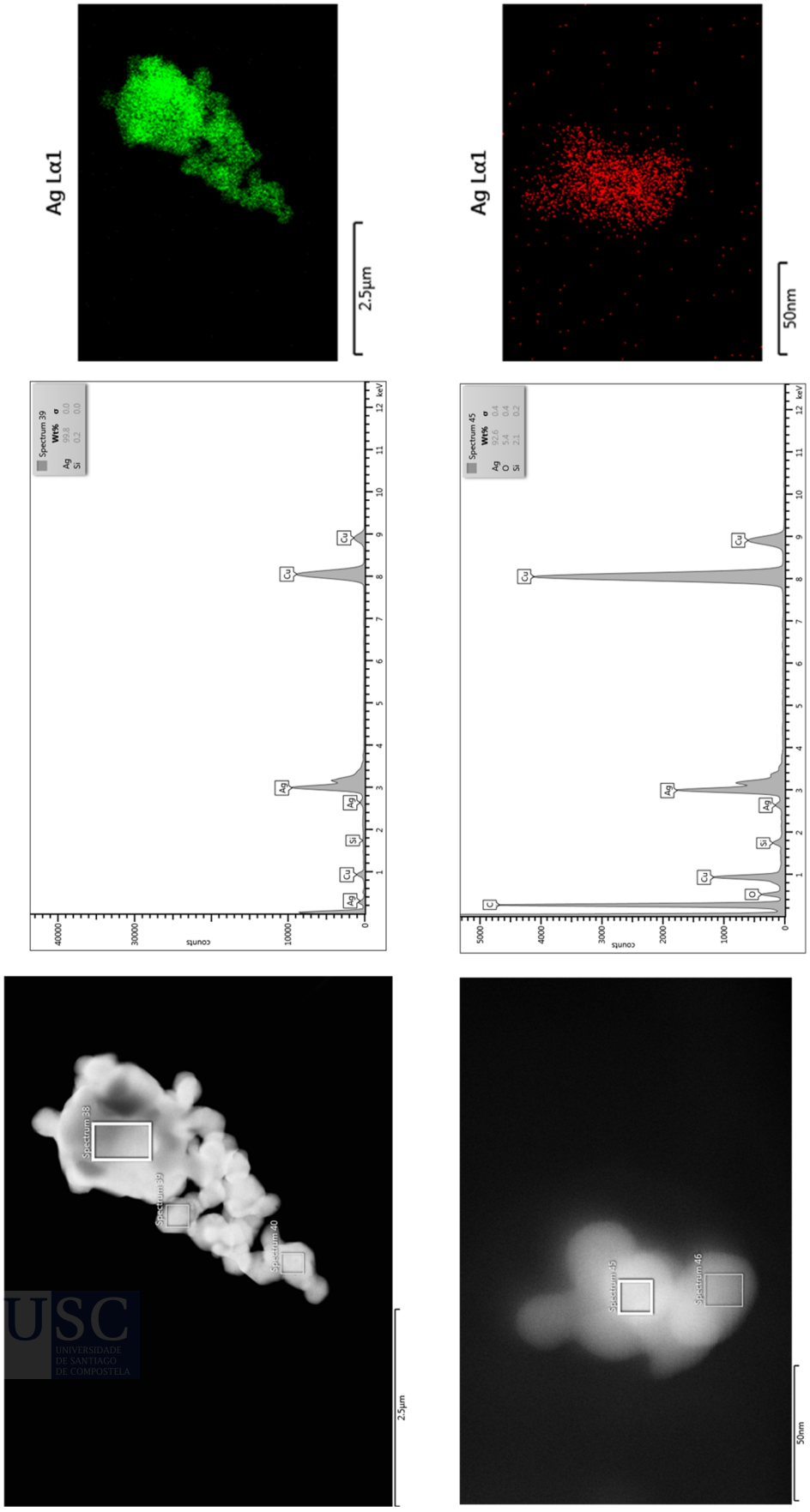

Figure 5.5. HRTEM-EDX analysis of a concentrated and clean aqueous extract from fabric T6-1 after one cycle of extraction

5.4.6 Consecutive extraction cycles from fabrics

Due to the low percentages of silver released in the aqueous extracts from studied fabrics, consecutive extractions were performed using the developed methodology for AgNPs extraction from fabric T5, which released the lowest percentages of nanosilver (0.001%) and total silver (0.3%) of the textiles studied. Six extraction cycles using the optimal extraction conditions (10 mL of water, 30 min, 20°C, and 100 rpm) were performed, and each consecutive extraction was carried out in triplicate, and two blanks were performed for each condition. **Figure 5.6** shows the particle number concentrations of AgNPs measured by spICP-MS in aqueous extracts from textile T5 after subjecting six consecutive extractions. Results indicated a progressive enhancement of extracted AgNPs from fabric T5 with increasing extraction cycle number. This release pattern can be attributed to the fact that AgNPs were strongly integrated into the fibres and their release occurred slowly over several extraction cycles. In this way, Mitrano et al. [28] previously demonstrated that the release rate of AgNPs is lower in fabrics in which NPs are embedded in the fibres than in fabrics modified with NPs on the surface.

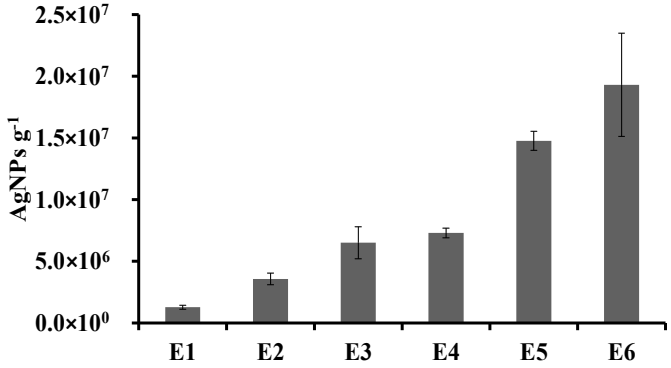

Figure 5.6. Particle number concentrations of AgNPs in aqueous leachates from fabric T5 after subjecting six consecutive extraction cycles using the optimised extraction conditions (the letter "E" followed by a number denotes the extraction number)

5.5 CONCLUSIONS

Mechanical shaking (orbital-horizontal shaking) using ultrapure water as an extractant has been studied as a simple methodology to isolate AgNPs from textile products. spICP-MS operating with a dwell time of 100 µs has offered a rapid analysis for AgNPs quantification (number of AgNPs) and characterisation (AgNPs size distribution) in the aqueous extracts from fabrics.

The developed methodology has been successfully validated and applied to several textiles. However, low percentages of AgNPs were found in the aqueous extracts. Percentages of nanosilver released from studied fabrics varied from 0.001 to 0.2%, and AgNPs mean sizes were found to be within the 22–40 nm range. HRTEM-EDX analysis also confirmed the presence of AgNPs in the extracts.

Furthermore, six consecutive extraction cycles (using the optimised conditions) were applied to the fabric with the lowest silver extraction efficiency. The concentration of AgNPs in the extracts increased steadily as the number of extraction cycles increased. This behaviour could be explained by the fact that AgNPs were well-integrated into fibres.

REFERENCES

[1] M. Rai, A. Yadav, A. Gade, Silver nanoparticles as a new generation of antimicrobials, Biotechnol. Adv. 27 (2009) 76–83, DOI: 10.1016/j.biotechadv.2008.09.002.

[2] K. Wang, J. He, One-Pot Fabrication of Antireflective/Antibacterial Dual-Function Ag NP-Containing Mesoporous Silica Thin Films, ACS Appl. Mater. Interfaces 10 (2018) 11189−11196, DOI: 10.1021/acsami.8b00192.

[3] P. Balashanmugam, M.D. Balakumaran, R. Murugan, K. Dhanapal, P.T. Kalaichelvan, Phytogenic synthesis of silver nanoparticles, optimization and evaluation of *in vitro* antifungal activity against human and plant pathogens, Microbiol. Res. 192 (2016) 52–64, DOI: 10.1016/j.micres.2016.06.004.

[4] T.Q. Huy, N.T.H. Thanh, N.T. Thuy, P.V. Chung, P.N. Hung, A.T. Le, N.T.H. Hanh, Cytotoxicity and antiviral activity of electrochemical-synthesized silver nanoparticles against poliovirus, J. Virol. Methods 241 (2017) 52–57, DOI: 10.1016/j.jviromet.2016.12.015.

[5] K. Chaloupka, Y. Malam, A.M. Seifalian, Nanosilver as a new generation of nanoproduct in biomedical applications, Trends Biotechnol. 28 (2010) 580−588, DOI: 10.1016/j.tibtech.2010.07.006.

[6] K. Venugopal, H.A. Rather, K. Rajagopal, M.P. Shanthi, K. Sheriff, M. Illiyas, R.A. Rather, E. Manikandan, S. Uvarajan, M. Bhaskar, M. Maaza, Synthesis of silver nanoparticles (Ag NPs) for anticancer activities (MCF 7 breast and A549 lung cell lines) of the crude extract of *Syzygium aromaticum*, J. Photochem. Photobiol. B 167 (2017) 282–289, DOI: 10.1016/j.jphotobiol.2016.12.013.

[7] K.A. Homan, M. Souza, R. Truby, G.P. Luke, C. Green, E. Vreeland, S. Emelianov, Silver Nanoplate Contrast Agents for in Vivo Molecular Photoacoustic Imaging, ACS Nano 6 (2012) 641−650, DOI: 10.1021/nn204100n.

[8] S.M. Praveena, K. Karuppiah, L.T.L. Than, Potential of cellulose paper coated with silver nanoparticles: a benign option for emergency drinking water filter, Cellulose 25 (2018) 2647–2658, DOI: 10.1007/s10570-018-1747-x.

[9] K. Ramos, M.M. Gómez-Gómez, C. Cámara, L. Ramos, Silver speciation and characterization of nanoparticles released from plastic food containers by single particle ICPMS, Talanta 151 (2016) 83–90, DOI: 10.1016/j.talanta.2015.12.071.

[10] S. Kokura, O. Handa, T. Takagi, T. Ishikawa, Y. Naito, T. Yoshikawa, Silver nanoparticles as a safe preservative for use in cosmetics, Nanomed.-Nanotechnol. Biol. Med. 6 (2010) 570–574, DOI: 10.1016/j.nano.2009.12.002.

[11] J. Farkas, H. Peter, P. Christian, J.A. Gallego Urrea, M. Hassellöv, J. Tuoriniemi, S. Gustafsson, E. Olsson, K. Hylland, K.V. Thomas, Characterization of the effluent from a nanosilver producing washing machine, Environ. Int. 37 (2011) 1057–1062, DOI: 10.1016/j.envint.2011.03.006.

[12] R. Kaegi, B. Sinnet, S. Zuleeg, H. Hagendorfer, E. Mueller, R. Vonbank, M. Boller, M. Burkhardt, Release of silver nanoparticles from outdoor facades, Environ. Pollut. 158 (2010) 2900–2905, DOI: 10.1016/j.envpol.2010.06.009.

[13] M. Radetić, Functionalization of textile materials with silver nanoparticles, J. Mater. Sci. 48 (2013) 95–107, DOI: 10.1007/s10853-012-6677-7.

[14] W. Feng, T. Huang, L. Gao, X. Yang, W. Deng, R. Zhou, H. Liu, Textile-supported silver nanoparticles as a highly efficient and recyclable heterogeneous catalyst for nitroaromatic reduction at room temperature, RSC Adv. 8 (2018) 6288–6292, DOI: 10.1039/C7RA13257C.

[15] D.Q. Vo, E.W. Shin, J.S. Kim, S. Kim, Low-Temperature Preparation of Highly Conductive Thin Films from Acrylic Acid-Stabilized Silver Nanoparticles Prepared through Ligand Exchange, Langmuir 26 (2010) 17435–17443, DOI: 10.1021/la102627m.

[16] G. Montes-Hernandez, M. Di Girolamo, G. Sarret, S. Bureau, A. Fernandez-Martinez, C. Lelong, E. Eymard Vernain, In Situ Formation of Silver Nanoparticles (Ag-NPs) onto Textile Fibers, ACS Omega 6 (2021) 1316–1327, DOI: 10.1021/acsomega.0c04814.

[17] Q. Xu, R. Li, L. Shen, W. Xu, J. Wang, Q. Jiang, L. Zhang, F. Fu, Y. Fu, X. Liu, Enhancing the surface affinity with silver nano-particles for antibacterial cotton fabric by coating carboxymethyl chitosan and L-cysteine, Appl. Surface Sci. 497 (2019) 143673, DOI: 10.1016/j.apsusc.2019.143673.

[18] R. Dastjerdi, M. Montazer, A review on the application of inorganic nano-structured materials in the modification of textiles: Focus on anti-microbial properties, Colloids Surf. B 79 (2010) 5–18, DOI: 10.1016/j.colsurfb.2010.03.029.

[19] Y.Y. Zhang, Q.B. Xu, F.Y. Fu, X.D. Liu, Durable antimicrobial cotton textiles modified with inorganic nanoparticles, Cellulose 23 (2016) 2791–2808, DOI: 10.1007/s10570-016-1012-0.

[20] F.M. Kelly, J.H. Johnston, Colored and Functional Silver Nanoparticle−Wool Fiber Composites, ACS Appl. Mater. Interfaces 3 (2011) 1083–1092, DOI: 10.1021/am101224v.

[21] B. Tang, M. Zhang, X. Hou, J. Li, L. Sun, X. Wang, Coloration of Cotton Fibers with Anisotropic Silver Nanoparticles, Ind. Eng. Chem. Res. 51 (2012) 12807−12813, DOI: 10.1021/ie3015704.

[22] B. Tang, J. Li, X. Hou, T. Afrin, L. Sun, X. Wang, Colorful and Antibacterial Silk Fiber from Anisotropic Silver Nanoparticles, Ind. Eng. Chem. Res. 52 (2013) 4556–4563, DOI: 10.1021/ie3033872.

[23] H.E. Emam, S. Mowafi, H.M. Mashaly, M. Rehan, Production of antibacterial colored viscose fibers using in situ prepared spherical Ag nanoparticles, Carbohydr. Polym. 110 (2014) 148–155, DOI: 10.1016/j.carbpol.2014.03.082.

[24] B.J. Brüschweiler, C. Merlot, Azo dyes in clothing textiles can be cleaved into a series of mutagenic aromatic amines which are not regulated yet, Regul. Toxicol. Pharmacol. 88 (2017) 214–226, DOI: 10.1016/j.yrtph.2017.06.012.

[25] S. Perera, B. Bhushan, R. Bandara, G. Rajapakse, S. Rajapakse, C. Bandara, Morphological, antimicrobial, durability, and physical properties of untreated and treated textiles using silver-nanoparticles, Colloids Surf. A 436 (2013) 975–989, DOI: 10.1016/j.colsurfa.2013.08.038.

[26] M.E.K. Kraeling, V.D. Topping, Z.M. Keltner, K.R. Belgrave, K.D. Bailey, X. Gao, J.J. Yourick, *In vitro* percutaneous penetration of silver nanoparticles in pig and human skin, Regul. Toxicol. Pharmacol. 95 (2018) 314–322, DOI: 10.1016/j.yrtph.2018.04.006.

[27] F.F. Larese, F. D'Agostin, M. Crosera, G. Adami, N. Renzi, M. Bovenzi, G. Maina, Human skin penetration of silver nanoparticles through intact and damaged skin, Toxicology 255 (2009) 33–37, DOI: 10.1016/j.tox.2008.09.025.

[28] D.M. Mitrano, E. Rimmele, A. Wichser, R. Erni, M. Height, B. Nowack, Presence of Nanoparticles in Wash Water from Conventional Silver and Nano-silver Textiles, ACS Nano 8 (2014) 7208–7219, DOI: 10.1021/nn502228w.

[29] C. Lorenz, L. Windler, N. von Goetz, R.P. Lehmann, M. Schuppler, K. Hungerbühler, M. Heuberger, B. Nowack, Characterization of silver release from commercially available functional (nano)textiles, Chemosphere 89 (2012) 817–824, DOI: 10.1016/j.chemosphere.2012.04.063.

[30] E. Lombi, E. Donner, K.G. Scheckel, R. Sekine, C. Lorenz, N. Von Goetz, B. Nowack, Silver speciation and release in commercial antimicrobial textiles as influenced by washing, Chemosphere 111 (2014) 352–358, DOI: 10.1016/j.chemosphere.2014.03.116.

[31] L. Geranio, M. Heuberger, B. Nowack, The Behavior of Silver Nanotextiles during Washing, Environ. Sci. Technol. 43 (2009) 8113–8118, DOI: 10.1021/es9018332.

[32] R.B. Reed, T. Zaikova, A. Barber, M. Simonich, R. Lankone, M. Marco, K. Hristovski, P. Herckes, L. Passantino, D.H. Fairbrother, R. Tanguay, J.F. Ranville, J.E. Hutchison, P.K. Westerhoff, Potential Environmental Impacts and Antimicrobial Efficacy of Silver- and Nanosilver-Containing Textiles, Environ. Sci. Technol. 50 (2016) 4018–4026, DOI: 10.1021/acs.est.5b06043.

[33] D.M. Mitrano, E. Lombi, Y.A.R. Dasilva, B. Nowack, Unraveling the Complexity in the Aging of Nanoenhanced Textiles: A Comprehensive Sequential Study on the Effects of Sunlight and Washing on Silver Nanoparticles, Environ. Sci. Technol. 50 (2016) 5790–5799, DOI: 10.1021/acs.est.6b01478.

[34] H.E. Pace, N.J. Rogers, C. Jarolimek, V.A. Coleman, C.P. Higgins, J.F. Ranville, Determining Transport Efficiency for the Purpose of Counting and Sizing Nanoparticles via Single Particle Inductively Coupled Plasma Mass Spectrometry, Anal. Chem. 83 (2011) 9361–9369, DOI: 10.1021/ac201952t.

[35] F. Laborda, E. Bolea, J. Jiménez-Lamana, Single Particle Inductively Coupled Plasma Mass Spectrometry: A Powerful Tool for Nanoanalysis, Anal. Chem. 86 (2014) 2270–2278, DOI: 10.1021/ac402980q.

[36] D.M. Mitrano, Y.A.R. Dasilva, B. Nowack, Effect of Variations of Washing Solution Chemistry on Nanomaterial Physicochemical Changes in the Laundry Cycle, Environ. Sci. Technol. 49 (2015) 9665–9673, DOI: 10.1021/acs.est.5b02262.

[37] E. Spielman-Sun, T. Zaikova, T. Dankovich, J. Yun, M. Ryan, J.E. Hutchison, G.V. Lowry, Effect of silver concentration and chemical transformations on release and antibacterial efficacy in silver-containing textiles, NanoImpact 11 (2018) 51–57, DOI: 10.1016/j.impact.2018.02.002.

[38] T.M. Benn, P. Westerhoff, Nanoparticle Silver Released into Water from Commercially Available Sock Fabrics, Environ. Sci. Technol. 42 (2008) 4133–4139, DOI: 10.1021/es7032718.

[39] A. Mackevica, M.E. Olsson, S.F. Hansen, Quantitative characterization of TiO_2 nanoparticle release from textiles by conventional and single particle ICP-MS, J. Nanopart. Res. 20 (2018) 6, DOI: 10.1007/s11051-017-4113-2.

[40] S. Nam, M.B. Hillyer, B.D. Condon, J.S. Lum, M.N. Richards, Q. Zhang, Silver Nanoparticle-Infused Cotton Fiber: Durability and Aqueous Release of Silver in Laundry Water, J. Agric. Food Chem. 68 (2020) 13231–13240, DOI: 10.1021/acs.jafc.9b07531.

[41] J. Łuczak, M. Paszkiewicz, A. Krukowska, A. Malankowska, A. Zaleska-Medynska, Ionic liquids for nano- and microstructures preparation. Part 1: Properties and multifunctional role, Adv. Colloid Interf. Sci. 230 (2016) 13–28, DOI: 10.1016/j.cis.2015.08.006.

[42] G. Clergeaud, R. Genç, M. Ortiz, C.K. O'Sullivan, Liposomal Nanoreactors for the Synthesis of Monodisperse Palladium Nanoparticles Using Glycerol, Langmuir 29 (2013) 15405−15413, DOI: 10.1021/la402892f.

[43] A. Sobhani-Nasab, M. Behpour, Synthesis, characterization, and morphological control of $Eu_2Ti_2O_7$ nanoparticles through green method and its photocatalyst application, J. Mater. Sci. Mater. Electron. 27 (2016) 11946–11951, DOI: 10.1007/s10854-016-5341-4.

[44] S. Lee, X. Bi, R.B. Reed, J.F. Ranville, P. Herckes, P. Westerhoff, Nanoparticle Size Detection Limits by Single Particle ICP-MS for 40 Elements, Environ. Sci. Technol. 48 (2014) 10291–10300, DOI: 10.1021/es502422v.

V. CONCLUSIONS

V. CONCLUSIONS

PART A: DETERMINATION OF TOTAL METAL CONTENT IN MOISTURISERS AND TEXTILES

Chapter 1. Quantification of metals in moisturising creams using microwave-assisted acid digestion and ICP-MS

A mixture of HNO_3 and H_2O_2 has been found adequate to digest regular moisturising creams using microwave energy. Acid digests of moisturisers were analysed by ICP-MS and results showed that ten moisturisers did not comply with the European Regulation 1223/2009 since containing forbidden metals. Furthermore, speciation studies are necessary for three studied creams (tin speciation for two samples and lithium speciation for one sample) to ensure law enforcement. It can only be assured that only one out of fourteen moisturising creams studied fulfilled the European regulation on cosmetic products.

Chapter 2. Metal content in textile and (nano)textile products

The use of complexing agents (HCl and HF) has been found necessary to achieve the complete digestion of textile fibres due to the presence of inorganic NPs and the high titanium contents in the studied fabrics.

Total metal content in textiles has been assessed after microwave-assisted acid digestion (HNO_3, H_2O_2, HF, and HCl) followed by ICP-MS determination. The comparison between the obtained concentrations and the European Regulation 1907/2006 proved that the concentration of lead and arsenic exceeded the maximum allowable concentration in several textile products (1.0 $\mu g\ g^{-1}$). In addition, mercury, which is forbidden in fabrics, was found in three samples. On the other hand, the speciation of chromium in one textile sample is necessary to determine the concentration of chromium (VI) and, therefore, its compliance with the stated regulation (the maximum concentration of hexavalent chromium in textiles is set at 1.0 $\mu g\ g^{-1}$).

PART B: DETERMINATION OF INORGANIC NPS IN MOISTURISERS AND TEXTILES

Chapter 3. Silver nanoparticles assessment in moisturising creams by ultrasound-assisted extraction followed by spICP-MS

AgNPs have been successfully isolated (quantitative extraction) from moisturising creams prescribed for atopic dermatitis by ultrasound assistance using methanol as an extractant. The quantitative extraction of AgNPs in these moisturising creams was possible owing to the absence of mineral components in the formulation (only components such as water, glycerine, glycerine derivates, seed oils, and several organic compounds). Methanolic extracts analysed by spICP-MS showed that AgNPs concentrations were within the 1.83×10^{7}–6.46×10^{9} AgNPs g^{-1} range, and AgNPs mean sizes between 35 and 91 nm.

TEM and SEM-EDX analyses also confirmed the presence of AgNPs in the methanolic extracts from the moisturisers studied.

Chapter 4. spICP-MS assessment of ZnONPs and TiO_2NPs in moisturisers after a tip sonication sample pre-treatment

Acetone was found to be a suitable hydrophilic organic solvent capable of solubilising several moisturising creams with sun protection properties. ZnONPs and TiO_2NPs were assessed in moisturisers using a simple and rapid method based on tip sonication extraction using acetone before spICP-MS analysis.

Nevertheless, the extraction efficiency was highly dependent on the ingredients of the cosmetic formulation and, in several cases, the extraction was non-quantitative (presence of mineral components such as mica and silica). Further improvements in sample pre-treatment are therefore required to avoid the effect of the cosmetic matrix on the extraction process.

Particle number concentrations found in cosmetic extracts varied within the 2.37×10^{11}–5.34×10^{12} ZnONPs g^{-1} and 3.32×10^{11}–1.50×10^{13} TiO_2NPs g^{-1} ranges. In addition, mean sizes were found in the ranges of 86–175 nm (ZnONPs) and 84–145 nm (TiO_2NPs).

In addition, the presence of ZnONPs and TiO_2NPs in extracts from moisturisers was confirmed by HRTEM-EDX analysis.

Chapter 5. spICP-MS characterisation of silver nanoparticles released from textile products

AgNPs have been extracted from fabrics by a simple procedure based on orbital-horizontal shaking under controlled temperature using water as an extractant (10 mL of water, 100 rpm, 20 ºC, and 30 min) before spICP-MS determination.

All studied nanosilver textiles released quantifiable AgNPs contents (2.68×10^{5}–1.91×10^{8} AgNPs g^{-1}). In addition, two out of four textiles modified with silver additives also leached AgNPs ($2.54\times10^{6}\pm1.92\times10^{5}$ and $2.59\times10^{7}\pm3.35\times10^{6}$ AgNPs g^{-1}). The mean sizes of AgNPs in textile extracts were found within the 22–40 nm range. The presence of AgNPs in extracts was also confirmed by HRTEM-EDX analysis.

Nevertheless, the percentage of total silver released from fabrics was very low (0.3–9%) so the extraction was not quantitative, and AgNPs were found to be leached after successive extractions under the optimised conditions. These findings meant that AgNPs were well-integrated into fibres and released slowly from fabrics. More drastic conditions for the extraction, but guaranteeing the integrity of the AgNPs (easily ionised NPs) are needed.

ANNEX I. RESUMO

ANNEX I. RESUMO

A primeira parte desta tese doutoral centrouse na determinación do contido metálico total en cosméticos e produtos téxtiles debido a que varios metais orixinan lesións cutáneas e reaccións alérxicas. Ademais, os metais poden penetrar a través da pel, inducir toxicidade nas células dérmicas, e mesmo chegar ao torrente sanguíneo e acumularse en órganos e tecidos despois da exposición a longo prazo. Debido a isto, a presenza de metais en cosméticos e téxtiles está controlada polos Regulamentos Europeos 1223/2009 e 1907/2006, respectivamente.

Os metais poden estar presentes en produtos de coidado persoal e téxtiles debido a unha contaminación accidental e/ou a unha adición intencionada. Na industria cosmética, os metais empréganse como pigmentos (principalmente en produtos de maquillaxe), filtros ultravioleta inorgánicos, axentes acondicionadores da pel, biocidas, estabilizadores de emulsións, humectantes, opacificantes, entre outros.

Doutra banda, os metais engádense aos tecidos principalmente como colorantes (tintes de complexos metálicos e pigmentos), mentres que outros metais poden aparecer nos tecidos como impurezas debido ao proceso de fabricación. Por exemplo, o antimonio atópase nos téxtiles formados por poliéster debido ao seu uso como catalizador na fabricación de tereftalato de polietileno (PET), o cal é o poliéster máis utilizado na industria téxtil.

Recentemente, a industria cosmética e téxtil incorporou o uso de nanopartículas inorgánicas (NPs) para obter produtos con novas funcionalidades, aumentando así o interese dos consumidores.

Segundo o inventario Nanodatabase, as nanopartículas de prata (AgNPs), as nanopartículas de dióxido de titanio (TiO_2NPs) e as nanopartículas de óxido de zinc (ZnONPs) son as NP inorgánicas máis utilizadas nos produtos manufacturados. Ademais, a partir da información obtida mediante este inventario, a principal vía de exposición dos seres humanos a estas NPs inorgánicas é o contacto dérmico. Así, a segunda parte deste proxecto de tese céntrase na caracterización de AgNPs, TiO_2NPs e ZnONPs en produtos de uso diario que están en contacto directo coa pel, como son cremas hidratantes e os produtos téxtiles.

Estas NPs teñen propiedades antibacterianas, polo que son engadidas a cosméticos e téxtiles como axentes biocidas, evitando así a deterioración dos produtos así como posibles riscos para a saúde derivados do seu uso ou aplicación. Ademais das propiedades antibacterianas, as AgNPs tamén teñen propiedades antiinflamatorias polo que son útiles na fabricación de produtos cosméticos para o tratamento de lesións cutáneas orixinadas por enfermidades tales como a psoriasis, a dermatitis e o acne.

Doutra banda, as TiO_2NPs and ZnONPs ofrecen protección ultravioleta debido a que son compostos semiconductores. Debido a esta propiedade, as TiO_2NPs, e mais recentemente, as ZnONPs son amplamente empregadas na fabricación de cosméticos e téxtiles con factor de protección solar (SPF) debido a que a exposición á radiación ultravioleta orixina queimaduras, fotoenvellecemento, inmunosupresión e incluso carcinoxénese, entre outros efectos tóxicos. Na industria cosmética, o uso de cremas solares inorgánicas está en auxe debido a que as TiO_2NPs e as ZnONPs non producen reacción alérxicas e son fotoestables, ao contrario ca os filtros orgánicos. Non obstante, na superficie das TiO_2NPs e das ZnONPs fórmanse especies reactivas de osíxeno (ROS) [$^{\bullet}O_2^-$, $^{\bullet}OH$ e H_2O_2] baixo a radiación ultravioleta. Debido a que as ROS poden inducir toxicidade nas células dérmicas, as TiO_2NPs e as ZnONPs que se empregan en cosméticos están normalmente recubertas con alumina, hidróxido de aluminio e silica para diminuír a súa

actividade fotocatalítica. A Regulación Europea 1223/2009 controla a presenza de NPs en produtos cosméticos. A adición de NPs a produtos cosméticos debe ser notificada a Comisión Europea seis meses antes da comercialización de produtos modificados. Todos os ingredientes que se atopen na forma nano deben ser indicados claramente na lista de ingredientes seguidos da palabra "nano" en paréntesis. A Regulación 1223/2009 permite o uso das TiO_2NPs e das ZnONPs como filtros ultravioletas, sempre que non excedan a concentración máxima permitida (25% w/w) e teñan as propiedades físicas e químicas establecidas por esta regulación.
En canto a industria téxtil, a actividade fotocatalítica das TiO_2NPs e das ZnONPs evita a decoloración, a formación de cores amarelentos e unha redución da resistencia das fibras xerados pola radiación ultravioleta. Estas NPs son útiles na fabricación de roupa antimanchas pola degradación da materia orgánica debido a xeración de ROS baixo a radiación ultravioleta. Ademais, as AgNPs, as TiO_2NPs e as ZnONPs tamén se engaden as prendas para obter propiedades hidrófobas e antiestáticas, entre outras aplicacións. Porén, a presenza de NPs en produtos téxtiles aínda non está regulada. É importante determinar as NPs inorgánicas en téxtiles debido a que poden ser liberadas durante o seu uso, podendo ser un risco para os humanos. As NPs poden penetrar a través da pel debido ao seu pequeño tamaño. Diversos estudos demostraron que as AgNPs poden penetrar máis alá do *stratum corneum* (capa máis externa da pel e responsable da función de barreira), alcanzando as capas máis profundas da pel, mentres que as TiO_2NPs e as ZnONPs non o fan. A penetración das NPs pode verse afectada polo estado de saúde da pel, incrementándose no caso da pel danada.
Sen embargo, aínda non están dispoñibles metodoloxías estandarizadas para a determinación de NPs en produtos manufacturados. Polo tanto é necesario o desenvolvemento de metodoloxías fiables para a avaliación das propiedades físicas e químicas das NPs (por exemplo, tamaño, forma, estructura cristalina e recubrimento), así como a concentración das NPs (masa e número). A existencia de estratexias nanometrolóxicas é moi importante na análise de produtos cosméticos para asegurar que se cumpre a Regulación 1223/2009.
A etapa crítica na determinación das NPs nas mostras complexas é a etapa de pretratamento da mostra, a cal debe garantir a estabilidade destes analitos. Os disolventes orgánicos e os surfactantes son empregados frecuentemente como extractantes de NPs inorgánicas presentes en cosméticos. Ademais, varios autores usaron unha etapa previa de desgrasado con hexano. En canto á análise de cosméticos, as TiO_2NPs e as ZnONPs contidas en cosméticos foron cuantificadas maioritariamente mediante o acoplamento de técnicas de fraccionamiento de fluxo de campo e técnicas espectrométricas. Porén, a principal limitación destas técnicas híbridas é o largo tempo de análise. Nos últimos anos, varios autores propuxeron o uso da espectrometría de masas con plasma de acoplamento inductivo empregando un modo de detección individualizada de partículas (spICP-MS) para a análise de rutina de mostras cosméticas. Esta técnica presenta vantaxes tales como o corto tempo de análise, a selectividade (diferencia entre o analito disolto e o analito en forma nanoparticulada), e a información proporcionada (concentración en número e distribución en tamaño).
No caso dos produtos téxtiles, a maioría dos estudos dispoñibles simulan a liberación das NPs desde os tecidos durante o lavado da roupa na casa, pero os deterxentes afectan á integridade das NPs, formando novas especies tales como as nanopartículas de cloruro de prata e as nanopartículas de sulfuro de prata. Ademais, os deterxentes que conteñen compostos oxidantes inducen a disolución das NPs. Outros estudos levaron a cabo a incubación dos téxtiles con sudor artificial ou auga. A espectrometría de masas con plasma de acoplamento inductivo (ICP-MS) e a espectrometría de emisión óptica con plasma de acoplamento inductivo (ICP-OES) foron as técnicas analíticas empregadas para a análise dos lixiviados téxtiles.

Estos estudos previos foron tidos en conta á hora de desenvolver metodoloxías para a avaliación das NPs inorgánicas en cremas hidratantes e produtos téxtiles.
Esta tese doutoral está dividida en cinco capítulos: cuantificación de metais en cremas hidratantes empregando dixestión ácida asistida por microondas e ICP-MS (capítulo 1), contido metálico en produtos téxtiles e (nano)téxtiles (capítulo 2), avaliación de nanopartículas de prata en cremas hidratantes mediante unha extracción asistida por ultrasóns seguida de spICP-MS (capítulo 3), avaliación mediante spICP-MS de ZnONPs e TiO_2NPs en cremas hidratantes despois dun pretratamento de mostra empregando sonda de ultrasóns (capítulo 4) e caracterización mediante spICP-MS das nanopartículas de prata liberadas a partir de produtos téxtiles (capítulo 5).

PARTE A: DETERMINACIÓN DO CONTIDO METÁLICO TOTAL EN CREMAS HIDRATANTES E PRODUTOS TÉXTILES

Capítulo 1. Cuantificación de metais en cremas hidratantes empregando dixestión ácida asistida por microondas e ICP-MS

As cremas hidratantes (0.2000 g) foron dixeridas (dixestión ácida asistida por microondas) empregando 3.0 mL de ácido nítrico 69%, 1.0 mL de peróxido de hidróxeno 33% e 4.0 mL de auga ultrapura antes da avaliación do contido metálico total mediante ICP-MS.
A análise mediante ICP-MS foi exacta e precisa (as recuperacións analíticas estaban no rango de 91–110% e as desviación estándar relativas foron inferiores ao 5%). Ademais, os límites de cuantificación obtidos (LOQs) variaron entre 0.00770 (berilio) e 3.37 $\mu g\ g^{-1}$ (aluminio).
O método desenvolto foi aplicado a catorce cremas hidratantes. Varios metais prohibidos pola Regulación Europea 1223/2009 tales como chumbo, mercurio, cadmio, cromio e berilio foron cuantificados en varias cremas hidratantes. Ademais, niquel, cobalto e cromio (orixinan alerxias) tamén se atoparon en varias cremas estudadas.

Capítulo 2. Contido metálico en produtos téxtiles e (nano)téxtiles

A dixestión ácida asistida por microondas foi usada para a descomposición dos produtos téxtiles (0.2000 g) empregando 8.0 mL de ácido nítrico 69%, 0.5 mL de peróxido de hidróxeno 33%, 0.5 mL de ácido clorhídrico 37% e 1.0 mL de ácido fluorhídrico 40% antes da análise mediante ICP-MS.
A exactitude da determinación empregando ICP-MS foi avaliada mediante ensaios da recuperación analítica a diferentes niveles de concentración e os valores obtido variaron entre 90 e 107%, mostrando que as análises con ICP-MS eran exactos. Ademais, as desviacións estándar relativas de once medidas do mesmo dixerido ácido diluído estaban dentro do rango 1–3% para todos os analitos analizados, o que demostrou que a cuantificación empregando esta técnica analítica foi precisa. Os límites de cuantificación (LOQs) variaron entre 0.00427 (berilio) e 6.33 $\mu g\ g^{-1}$ (titanio). O alto valor experimental para o LOQ do titanio foi debido a alta dilución que necesitou para a súa análise.
Metais empregados frecuentemente en tintes de complexos metálicos (cromio, cobre, cobalto, niquel e ferro) ou presentes en pigmentos (bario, zinc, titanio) foron atopados en varios téxtiles estudados.
Metais usados en procesos catalíticos durante o proceso de fabricación dos produtos téxtiles tamén foron cuantificados nos téxtiles analizados. Como un exemplo, o ferro e complexos de manganeso estaban presentes en varios tecidos e a súa presenza pode ser debida a que estos compostos son usados en procesos de branquemento das fibras téxtiles e, como consecuencia,

poden permanecer nas fibras como unha impureza. O antimonio tamén se atopou a altas concentracións (hasta 218 μg g^{-1}) en téxtiles formados por poliéster como unha impureza debido ao uso de compostos de antimonio como catalizadores na fabricación do tereftalato de polietileno (tipo de poliéster máis empregado en produtos téxtiles).
A alta concentración de titanio nos téxtiles estudados (156–6223 μg g^{-1}) pode ser debida a que o titanio é amplamente utilizado na industria téxtil como un colorante branqueador (Ti e TiO_2) e un axente delustrante (TiO_2).
Ultimamente, a adición de NPs inorgánicas é unha práctica común na industria téxtil para obter tecidos con novas funcionalidades. Zinc, titanio ou prata foron cuantificados en nanotéxtiles con factor de protección solar (contiñan ZnONPs ou TiO_2NPs) e con propiedades antibacterianas (contiñan AgNPs).

PARTE B: DETERMINACIÓN DE NPS INORGÁNICAS EN CREMAS HIDRATANTES E TÉXTILES

Capítulo 3. Avaliación de nanopartículas de prata en cremas hidratantes mediante unha extracción asistida por ultrasóns seguida de spICP-MS

As nanopartículas de prata foron extraídas das cremas hidratantes empregando unha extracción asistida por ultrasóns (15 ciclos de tratamento con ultrasóns durante 59 s, seguidos de unha etapa de relaxación de 59 s, aplicando un 60% de amplitude) empregando metanol (20 mL) como extractante antes da determinación mediante spICP-MS.
Estándares de AgNPs comerciais foron sometidos ao proceso desenvolto para avaliar a súa estabilidade. Os resultados das medidas de spICP-MS demostraron que as AgNPs foron estables durante o proceso de ultrasonicación (as concentración e tamaños das AgNPs non variaban en comparación cos estándares que non foran sometidos ao tratamento).
A calibración usada para a avaliación dos tamaños das AgNPs mediante spICP-MS foi levada a cabo mediante estándares iónicos de prata en metanol (dilución 1:40) debido ao efecto matriz. Ademais, os límites de detección e cuantificación (LOD e LOQ) obtidos foron 2.48×10^5 and 8.25×10^5 AgNPs g^{-1}, respectivamente. O LOD teórico calculado en tamaño estaba no rango de 4.5–13.0 nm.
A precisión da metodoloxía completa (extracción asistida por ultrasóns e análise mediante spICP-MS) foi avaliada en base a desviación estándar relativa (RSD) de once extractos metanólicos preparados a partir da mesma crema. Os valores de RSDs foron 5% (concentración das AgNPs), 11% (tamaño máis frecuente das AgNPs) e 7% (tamaño medio das AgNPs), demostrando que a metodoloxía era precisa.
As medidas de spICP-MS tamén foron exactas (as recuperacións analíticas obtidas foron 117±14% para AgNPs de 20 nm, 90±1% para AgNPs de 40 nm, and 109±2% para AgNPs de 60 nm).
Tres cremas hidratantes prescritas para tratar a dermatitis atópica e que contiñan prata (cuantificación previa mediante ICP-MS do contido total de prata despois da dixestión ácida asistida por microondas) foron sometidas á metodoloxía proposta. Os resultados de spICP-MS mostraron concentracións de AgNPs de 1.83×10^7 a 6.46×10^9 AgNPs g^{-1}, e tamaños medios das AgNPs no rango de 35–91 nm. O contido de prata total nos extractos dixeridos determinado mediante ICP-MS (1.4–2352 μg g^{-1}) confirmou que a extracción da prata foi cuantitativa no caso das cremas estudadas. Ademais, o contido de nano-prata nestas cremas variou entre 0.24 e 1.1% da concentración total de prata.

As análises mediante TEM and SEM-EDX confirmaron a presenza de AgNPs nos extractos das cremas hidratantes despois dun tratamento oxidativo empregando peróxido de hidróxeno e ultrasóns (baño de ultrasóns) para eliminar a materia orgánica.

Capítulo 4. Avaliación mediante spICP-MS de ZnONPs e TiO_2NPs en cremas hidratantes despois dun pretratamento de mostra empregando sonda de ultrasóns

A metodoloxía desenvolta baseouse na sonicación empregando unha sonda de ultrasóns en un disolvente orgánico [40 mL de acetona, amplitude do 40% e 5 minutos usando un modo descontinuo (59 s de relaxación despois de 59 s de sonicación)] seguido da avaliación das TiO_2NPs e ZnONPs extraídas mediante spICP-MS.

O titanio pode ser cuantificado sin ser interferido polo calcio (interferencia isobárica con ^{48}Ca) mediante o uso do amoníaco como gas de reacción (RPq=0.2) en instrumentos coa tecnoloxía da celda de reacción dinámica (DRC). O titanio foi cuantificado mediante a monitorización do aducto $^{48}Ti^{14}NH(^{14}NH_3)_4^+$ (*m/z*=131) empregando un fluxo de amoníaco de 1.0 mL min^{-1}.

A cuantificación do zinc no modo estándar (sin gas na celda de colisión/reacción) pode verse obstaculizado debido a que os isótopos ^{64}Zn e ^{66}Zn están interferidos por especies poliatómicas de titanio ($^{48}Ti^{16}O^+$ e $^{50}Ti^{16}O^+$, respectivamente). Porén, a sensibilidade para o zinc no modo DRC foi moi baixa e había unha interferencia na cuantificación do zinc (monitorización dos aductos de zinc con *m/z* 115 e 117) xerada polo titanio incluso a niveles baixos da interferencia (5 µg L^{-1} of Ti) usando as condición de amoníaco óptimas obtidas para o zinc (2.0 mL min^{-1} de amoníaco e un valor de RPq de 0.2).

Finalmente, un estudo de interferencias demostrou que a cuantificación do zinc (monitorización de *m/z*=66) mediante ICP-MS pode levarse a cabo usando o modo estándar en mostras (extractos e cremas dixeridas) que conteñan hasta 500 µg L^{-1} de titanio.

Ademais, suspensións que contiñan TiO_2NPs (50 nm) e ZnONPs (50–80 nm) foron analizadas mediante spICP-MS para así avaliar a posible interferencia das TiO_2NPs na determinación das ZnONPs (isótopo ^{66}Zn, modo estándar). A recuperación analítica das ZnONPs nas suspensións que contiñan ambas NPs foi 99±10%, demostrando que non había interferencia usando esas condicións instrumentais.

En canto a análise mediante spICP-MS, os LODs teóricos en tamaño estiveron nos rangos de 29–35 nm (ZnONPs) e 28–33 nm (TiO_2NPs), mentres que os LODs e LOQs instrumentais foron 1.15×10^3 e 3.82×10^3 ZnONPs mL^{-1}; 1.35×10^3 e 4.50×10^3 TiO_2NPs mL^{-1}, respectivamente.

As porcentaxes de recuperación analítica obtidos foron 119±3 % e 102±12% para as suspensións de TiO_2NPs (50 nm) e ZnONPs (50–80 nm), respectivamente, o que demostrou que as medidas mediante spICP-MS foron exactas.

A precisión de todo o método (extracción e medida) foi avaliada mediante a RSD de once extractos preparados usando as condicións óptimas de extracción. Os valores das RSDs para as concentración e tamaños das TiO_2NPs e das ZnONPs foron inferiores ao 10%, demostrando que a metodoloxía proposta foi repetible.

O método validado foi aplicado a varias cremas hidratantes con factor de protección solar. As eficiencias de extracción estiveron nos rangos de 52–81% e 23–104% para o zinc e o titanio, respectivamente. As baixas eficiencias de extracción obtidas para dúas mostras pode xustificarse debido a que conteñen un alto contido de ingredientes inorgánicos (como por exemplo alumina e mica), os cales poden dificultar a extracción.

As concentracións de partículas obtidas estiveron nos rangos de 2.37×10^{11}–5.34×10^{12} ZnONPs g^{-1} e 3.32×10^{11}–1.50×10^{13} TiO_2NPs g^{-1}, e os tamaños medios variaron nos rangos de 86–175 nm (ZnONPs) e 84–145 nm (TiO_2NPs).

As porcentaxes de NPs nas cremas analizadas chegaron ata o 2.0% (w/w) no caso das TiO_2NPs [0.2–2.0%] e ata o 2.5% (w/w) no caso das ZnONPs [0.4–2.5%].
Finalmente, os extractos cosméticos foron concentrados e limpados (dispositivos de filtración centrífuga Amicon® Ultra-0.5) e analizados mediante HRTEM-EDX, que confirmou a presencia de TiO_2NPs e ZnONPs nas mostras.

Capítulo 5. Caracterización mediante spICP-MS das nanopartículas de prata liberadas a partir de produtos téxtiles

A técnica spICP-MS foi seleccionada como a instrumentación analítica usada para a determinación das AgNPs liberadas de téxtiles debido aos seus baixos límites de detección e á información que proporciona sobre a concentración e a distribución de tamaño das NPs.
As AgNPs foron extraídas dos téxtiles (0.4000 g) empregando auga ultrapura (10 mL) usando axitación mecánica orbital-horizontal (100 rpm, 20°C, 30 min) antes da análise mediante spICP-MS. Despois da extracción, os extractos deben ser filtrados empregando filtros de xeringa (5 μm) para eliminar as pelusas desprendidas polos téxtiles. A estabilidade das AgNPs durante os procesos de extracción e filtración foi comprobada.
Os LODs e LOQs experimentais obtidos foron 4.59×10^4 e 1.53×10^5 AgNPs g^{-1}, respectivamente, mentres que o LOD teórico en tamaño estivo no rango de 9.8–11.6 nm. Os ensaios da recuperación analítica usando estándares de AgNPs de 20 nm, 40 nm e 60 nm variaron entre 102 e 113%, o que demostrou a exactitude da determinación mediante sp-ICP-MS. As RSDs das medidas realizadas mediante spICP-MS de once extractos preparados usando as condicións óptimas foron 14% (concentración das AgNPs) e 6% (tamaño medio das AgNPs), indicando que a metodoloxía (extracción e medida) foi repetible.
A metodoloxía validada foi aplicada a sete téxtiles modicados con aditivos que conteñen prata ou AgNPs. Todos os tecidos modificados con AgNPs liberaron contidos cuantificables de partículas (2.68×10^5–1.91×10^8 AgNPs g^{-1}). Ademais, dous téxtiles modificados con aditivos con prata tamén liberaron AgNPs ($2.54\times10^6\pm1.92\times10^5$ e $2.59\times10^7\pm3.35\times10^6$). Os tamaños medios das AgNPs nas mostras estudadas variaron entre 22±2 nm e 40±1 nm.
A presenza de AgNPs nun extracto da mostra que presentaba a concentración máis alta (medida mediante sp-ICP-MS) foi confirmada mediante a análise con HRTEM-EDX despois da concentración e limpeza do extracto (dispositivos de filtración centrífuga Amicon® Ultra-0.5).
As porcentaxes das AgNPs liberadas nos extractos acuosos calculados como o cociente entre a concentración en masa de prata estimada a partir da concentración en número das AgNPs (spICP-MS) e a concentración total de prata no textil (dixestión ácida asistida por microondas seguida da análise mediante ICP-MS) foron moi baixos, variando entre 0.001 e 0.2%. Doutra banda, a porcentaxe de prata total liberada dos téxtiles variou entre 0.3 e 9%, o que indica que a extracción non foi cuantitativa (ao igual que en otros artículos previamente publicados por outros autores).
Finalmente, o textil que exhibía a porcentaxe de extracción máis baixo foi sometido a varios ciclos consecutivos de extracción empregando as mesmas condicións de extracción (30 min, 20°C, and 100 rpm). O número de AgNPs extraídas foi maior cando se realizaron ciclos consecutivos de extracción. Isto pode ser debido a que as AgNPs están fortemente integradas nas fibras e vanse liberando lentamente durante o lavado do téxtil.

ANNEX II. LIST OF PUBLICATIONS

ANNEX II. LIST OF PUBLICATIONS

- Iria Rujido-Santos, Lucía Naveiro-Seijo, Paloma Herbello-Hermelo, María Carmen Barciela-Alonso, Pilar Bermejo-Barrera, and Antonio Moreda-Piñeiro, Silver nanoparticles assessment in moisturizing creams by ultrasound assisted extraction followed by spICP-MS, Talanta 197 (2019) 530–538, DOI: 10.1016/j.talanta.2019.01.068.
  Impact factor (2019): 5.339.
  Rank by Journal Impact Factor (2019): Analytical Chemistry, 11/86 (Q1).
  Citations: 12.
  Contribution: experimental work and original draft preparation.

- Iria Rujido-Santos, Paloma Herbello-Hermelo, María Carmen Barciela-Alonso, Pilar Bermejo-Barrera, and Antonio Moreda-Piñeiro, Metal Content in Textile and (Nano)Textile Products, Int. J. Environ. Res. Public Health 19 (2022) 944, DOI: 10.3390/ijerph19020944.
  Impact factor (2020): 3.390.
  Rank by Journal Impact Factor (2020): Public, Environmental & Occupational Health, 42/176 (Q1).
  Citations: 0.
  Contribution: experimental work and original draft preparation.

Data obtained from Web of Science (Clarivate Analytics) on April 21st, 2022.

ANNEX III. PERMISSIONS

ANNEX III. PERMISSIONS

FIGURE I.3 (I. INTRODUCTION):

Validation of Gold and Silver Nanoparticle Analysis in Fruit Juices by Single-Particle ICP-MS without Sample Pretreatment

Author: Markus Witzler, Fabian Küllmer, Annika Hirtz, et al
Publication: Journal of Agricultural and Food Chemistry
Publisher: American Chemical Society
Date: May 1, 2016

PERMISSION/LICENSE IS GRANTED FOR YOUR ORDER AT NO CHARGE

This type of permission/license, instead of the standard Terms and Conditions, is sent to you because no fee is being charged for your order. Please note the following:

- Permission is granted for your request in both print and electronic formats, and translations.
- If figures and/or tables were requested, they may be adapted or used in part.
- Please print this page for your records and send a copy of it to your publisher/graduate school.
- Appropriate credit for the requested material should be given as follows: "Reprinted (adapted) with permission from {COMPLETE REFERENCE CITATION}. Copyright {YEAR} American Chemical Society." Insert appropriate information in place of the capitalized words.
- One-time permission is granted only for the use specified in your RightsLink request. No additional uses are granted (such as derivative works or other editions). For any uses, please submit a new request.

If credit is given to another source for the material you requested from RightsLink, permission must be obtained from that source.

CHAPTER 2 (IV. RESULTS AND DISCUSSION):

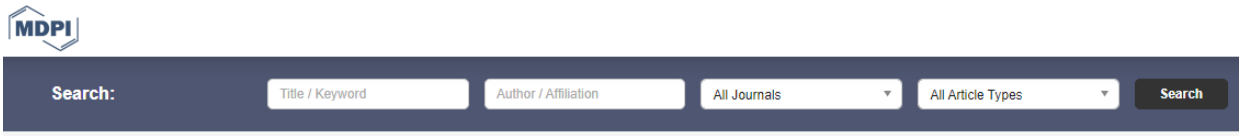

Copyrights

Copyright and Licensing

For all articles published in MDPI journals, copyright is retained by the authors. Articles are licensed under an open access Creative Commons CC BY 4.0 license, meaning that anyone may download and read the paper for free. In addition, the article may be reused and quoted provided that the original published version is cited. These conditions allow for maximum use and exposure of the work, while ensuring that the authors receive proper credit.

In exceptional circumstances articles may be licensed differently. If you have specific condition (such as one linked to funding) that does not allow this license, please mention this to the editorial office of the journal at submission. Exceptions will be granted at the discretion of the publisher.

CHAPTER 3 (IV. RESULTS AND DISCUSSION):

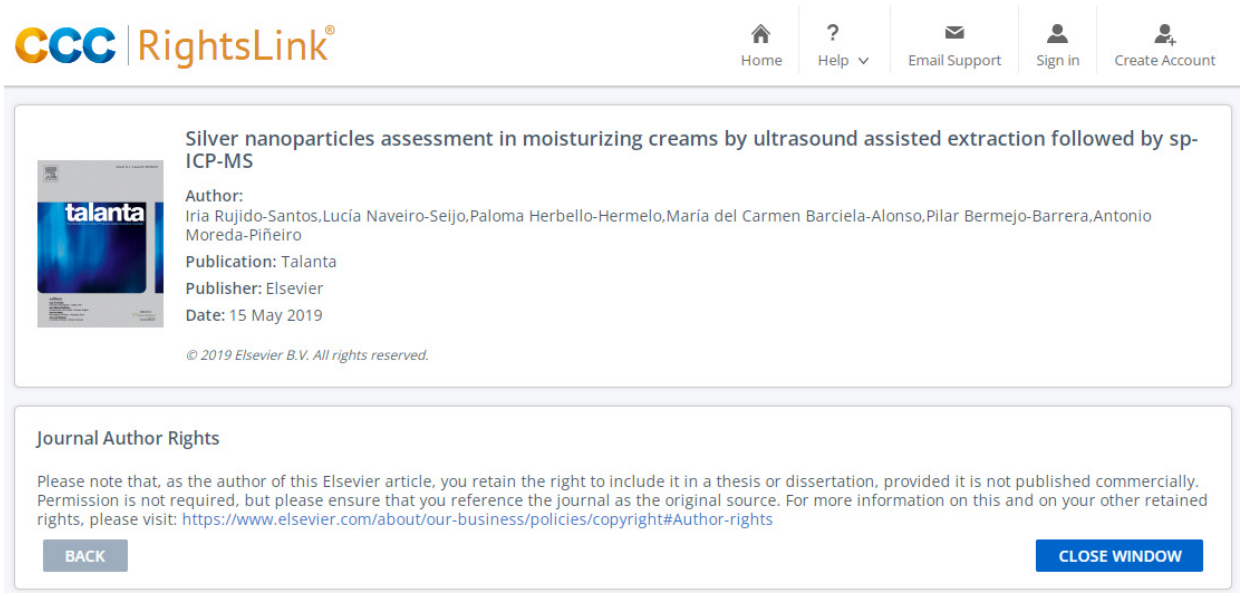

This doctoral thesis focuses on the determination of the total metal content in cosmetics and textile products to verify their compliance with the European Regulations 1223/2009 and 1907/2006, respectively. The methodologies developed are based on microwave-assisted acid digestion of samples followed by inductively coupled plasma mass spectrometry (ICP-MS).

Moreover, strategies for assessing nanoparticles (NPs) in cosmetics and fabrics have also been developed. Inorganic NPs are isolated by ultrasound-assisted extraction (AgNPs, TiO_2NPs, and ZnONPs in moisturisers) or by orbital-horizontal shaking (AgNPs in textiles). Extracts from moisturising creams and fabrics are analysed by ICP-MS in single particle mode (spICP-MS) for determining the concentration and the size distribution of the isolated NPs.